Abstract book

8th MSAT

The 8th International Conference on Materials Science and Technology

December 15-16, 2014
Swissôtel Le Concorde, Bangkok, Thailand

Organized by

MTEC a member of NSTDA

สวทช NSTDA

Co-organized by

CHULA ENGINEERING

CU Science Centennial

THAI TRIBOLOGY ASSOCIATION

8th MSAT

December 15-16, 2014
Swissôtel Le Concorde,
Bangkok, Thailand

8th International Conference on Materials Science and Technology

Disclaimer

This book contains the abstracts of the papers to be presented at the 8th International Conference on Materials Science and Technology (MSAT-8). They reflect the authors' opinions and are published as received after revision by the authors.

The committee assumes no responsibility for the accuracy, completeness or usefulness of the disclosed information.

Committees

Advisory Committees

- Dr. Kopr Kritayakirana — National Science and Technology Development Agency
- Dr. Thaweesak Koanantakool — National Science and Technology Development Agency

Chairman

- Dr. Werasak Udomkichdecha — National Metal and Materials Technology Center

Vice Chairmen

- Dr. Krisda Suchiva — National Metal and Materials Technology Center
- Dr. Pramote Dechaumphai — National Metal and Materials Technology Center
- Assoc. Prof. Siriluck Nivitchanyong — National Metal and Materials Technology Center

International Technical Committees

- Dr. Anthony W. Wren — Alfred University, USA
- Dr. Georgia Papavasiliou — Illinois Institute of Technology, USA

Technical Committees

- Dr. Dumnoensun Pruksakorn — Chiang Mai University
- Dr. Robert Molloy — Chiang Mai University
- Dr. Apirat Theerapapvisetpong — Chulalongkorn University
- Dr. Boonrat Lohwongwatana — Chulalongkorn University
- Dr. Charan Mahatumarat — Chulalongkorn University
- Dr. Duangdao Arj-ong — Chulalongkorn University
- Dr. Dujreutai Pongkao Kashima — Chulalongkorn University
- Dr. Gobboon Lothongkum — Chulalongkorn University
- Dr. Karn Serivalsatit — Chulalongkorn University
- Dr. Natthaphon Raengthon — Chulalongkorn University
- Dr. Nisanart Traiphol — Chulalongkorn University
- Dr. Panyawat Wangyao — Chulalongkorn University
- Dr. Patama Visuttipitukul — Chulalongkorn University
- Dr. Pornnapa Sujaridworakun — Chulalongkorn University
- Dr. Prasonk Sricharoenchai — Chulalongkorn University
- Dr. Rojana Pornprasertsuk — Chulalongkorn University
- Dr. Sirithan Jiemsirilers — Chulalongkorn University
- Dr. Sorada Kanokpanont — Chulalongkorn University
- Dr. Sujarinee Kochawattana — Chulalongkorn University
- Dr. Supatra Jinawath — Chulalongkorn University
- Dr. Thanakorn Wasanapiarnpong — Chulalongkorn University
- Dr. Wantanee Buggakupta — Chulalongkorn University
- Dr. Yuttanant Boonyongmaneerat — Chulalongkorn University

- Dr. Attera Worayingyong	Kasetsart University
- Dr. Singh Intrachooto	Kasetsart University
- Dr. Monrudee Phongaksorn	King Mongkut's University of Technology North Bangkok
- Dr. Nakarin Srisuwan	King Mongkut's University of Technology North Bangkok
- Dr. Pinai Mungsantisuk	King Mongkut's University of Technology North Bangkok
- Dr. Piyorose Promdirek	King Mongkut's University of Technology North Bangkok
- Dr. Rungsima Yeetsorn	King Mongkut's University of Technology North Bangkok
- Dr. Somrerk Chandra-ambhorn	King Mongkut's University of Technology North Bangkok
- Dr. Anak Khantachawana	King Mongkut's University of Technology Thonburi
- Dr. Asa Prateepasen	King Mongkut's University of Technology Thonburi
- Dr. Bovornchok Poopat	King Mongkut's University of Technology Thonburi
- Dr. Chai Jaturapitakkul	King Mongkut's University of Technology Thonburi
- Dr. Chaowalit Limmaneevichitr	King Mongkut's University of Technology Thonburi
- Dr. Navadol Laosiripojana	King Mongkut's University of Technology Thonburi
- Dr. Ittipol Jangchud	King Mongkut's Institute of Technology Ladkrabang
- Dr. Adisak Pattiya	Mahasarakham University
- Dr. Banchong Mahaisavariya	Mahidol University
- Dr. Phornphop Naiyanetr	Mahidol University
- Dr. Ekasit Nisaratanaporn	Metallurgy and Materials Science Research Institute, Chulalongkorn University
- Dr. Nutthita Chuankrerkkul	Metallurgy and Materials Science Research Institute, Chulalongkorn University
- Dr. Suwabun Chirachanchai	Petroleum and Petrochemical College, Chulalongkorn University
- Dr. Jongkol Srithorn	Suranaree University of Technology
- Dr. Pornwasa Wongpanya	Suranaree University of Technology
- Dr. Sirirat Tubsungnoen Rattanachan	Suranaree University of Technology
- Dr. Pratip Vongbandit	Thailand Institute of Scientific and Technological Research
- Dr. Cattaleeya Pattamaprom	Thammasat University
- Assoc. Prof. Chalermwat Tantasavasdi	Thammasat University
- Dr. Pusit Lertwattanaruk	Thammasat University
- Dr. Sappinandana Akamphon	Thammasat University
- Dr. Amnuaysak Chianpairot	National Metal and Materials Technology Center
- Dr. Anucha Wannagon	National Metal and Materials Technology Center
- Dr. Aree Thanaboonsombut	National Metal and Materials Technology Center
- Dr. Chureerat Prahsarn	National Metal and Materials Technology Center
- Dr. Duangduen Atong	National Metal and Materials Technology Center

- Dr. Ekkarut Viyanit	National Metal and Materials Technology Center
- Dr. Jitti Mungkalasiri	National Metal and Materials Technology Center
- Dr. Jomkwun Munnae	National Metal and Materials Technology Center
- Dr. Julathep Kajornchaiyakul	National Metal and Materials Technology Center
- Dr. Naruporn Monmaturapoj	National Metal and Materials Technology Center
- Dr. Nuwong Chollacoop	National Metal and Materials Technology Center
- Dr. Pairote Jittham	National Metal and Materials Technology Center
- Dr. Panadda Sheppard	National Metal and Materials Technology Center
- Dr. Pasaree Laokijcharoen	National Metal and Materials Technology Center
- Dr. Passakorn Tesavibul	National Metal and Materials Technology Center
- Dr. Pitak Laoratanakul	National Metal and Materials Technology Center
- Dr. Samerkhae Jongthammanurak	National Metal and Materials Technology Center
- Dr. Sasawat Mahabunphachai	National Metal and Materials Technology Center
- Dr. Sittha Sukkasi	National Metal and Materials Technology Center
- Dr. Sitthisuntorn Supothina	National Metal and Materials Technology Center
- Dr. Somboon Sahasithiwat	National Metal and Materials Technology Center
- Dr. Somnuk Sirisoonthorn	National Metal and Materials Technology Center
- Dr. Somsak Supasitmongkol	National Metal and Materials Technology Center
- Dr. Sumittra Charojrochkul	National Metal and Materials Technology Center
- Dr. Surapich Loykulnant	National Metal and Materials Technology Center
- Dr. Sutee Olarnrithinun	National Metal and Materials Technology Center
- Dr. Tanakorn Tantanawat	National Metal and Materials Technology Center
- Dr. Thanasat Sooksimuang	National Metal and Materials Technology Center
- Dr. Wanida Janvikul	National Metal and Materials Technology Center
- Dr. Wannee Chinsirikul	National Metal and Materials Technology Center
- Dr. Witchuda Daud	National Metal and Materials Technology Center
- Dr. Worawarit Kobsiriphat	National Metal and Materials Technology Center

Day I December 15, 2014

08:00-09:00	Registration (Foyer Area, 2nd Floor) and Poster Setup			
09:00-09:15	Opening Ceremony (Le Concorde Ballroom, 2nd Floor)			
09:15-10:00	Plenary Lecture 1: 10 Global Materials Science and Engineering Trends by ***Thomas Boellinghaus***			
10:00-10:45	Plenary Lecture 2: New Technology for Carbon Neutral Energy by ***Tatsumi Ishihara***			
10:45-11:00	Break			
Room	**Le Concorde**	**Jamjuree**	**Sakthong**	**Krisana**
Floor	2nd Floor			
Session	Surface Engineering and Heat Treatment	Ceramic-based Materials	Materials for Energy	Polymer-based Materials
11:00-11:30	*Chair:* *Namurata Palsson*	**Photocatalytic Materials** *Chair: Charusporn Mongkolkachit & Pornapa Sujaridworakun*	**Fuel Cells 1** *Chair:* *Sumittra Charojrochkul*	*Chair:* *Wannee Chinsirikul*
	SH-I-01 Thai Auto-parts Trend, Surface Treatment Development and Thai Parker Direction ***Suphot Sukphisarn***	**CM-I-01** Novel Visible-Light-Sensitive Photocatalyt for Indoor Environmental Purification ***Masahiro Miyauchi***	**EN-I-01** Carbon Nanotubes for Chemical Energy Conversion and Storage ***Martin Muhler***	**PM-I-01** Multi-Component Polymer Processing for Novel Applications ***Takeshi Kikutani***
11:30-11:45	**SH-O-01** Evaluation of Surface Roughness of Engineered Wood Composites ***Salim Hiziroglu***	**CM-O-01** Synthesis and Photocatalytic Activity Enhancing for TiO_2 Photocatalyst by Doping with Lanthanum ***Zuhra Zuhra***	**EN-O-01** The Variation of Ternary Catalyst Atomic Ratios (PtRuSn/C and PtRuNi/C) for Ethanol Electro-oxidation in Direct Ethanol Fuel Cell ***Napha Sudachom***	**PM-O-01** Intumescent Coating on Polyester Fabric via Layer-by-Layer Assembly ***Warunee Wattanatanom***
11:45-12:00	**SH-O-02** Comparison Study of TiO_2, Ni-B and Thiourea doped TiO_2 synthesized by Sol-Gel Process at Low Temperature ***Kumthorn Tangwongsirikul***	**CM-O-04** Facile Green Route for the Synthesis of Iron-doped MgO Nanoparticles by Phyllanthus Acidus: Structural, Photoluminescence and Photocatalytic Activity ***Nagaswarupa H. P.***	**EN-O-02** CO Tolerance of Pd-Ni-Sn Electrocatalytic Compositions for Use in Direct Ethanol Fuel Cells ***Sompoch Jongsomjit***	**PM-O-02** Effect of Annealed Temperature on The Preparation of Polypropylene Hollow Fiber Membrane by Melt Spinning and Stretching Method ***Sang Yong Nam***
12:00-12:15		**CM-O-03** The Effects of Solvents on the Solvothermal Synthesis of $BiVO_4$ Photocatalyst Powders ***Nannaphat Thanomsri***		
12:15-13:00	Lunch			

Room	Rachavadee	Patumchard	Ubonchard	Nilubon
Floor	2nd Floor		3rd Floor	
Session	Materials Technology for Environment		Metals, Alloys & Intermetallic Compounds	
11:00-11:30	*Chair:* *Nudjarin Ramungul*		*Chair:* *Chedtha Puncreobutr*	
	EV-I-01 Integrative Design for Sustainable Living ***Chalermwat Tantasavasdi***		**KL-01 (TMETC-8)** High Tensile Strength Steels: State of the Arts in Their Processing and Properties ***Takateru Umeda***	
11:30-11:45	**EV-O-01** Design and Construction Variable Speed Heat Pump for Supply Air Reheat ***Krittamuk Wongprasert***		**MT-I-01** Some Cast Irons are Special ***John Pearce***	
11:45-12:00	**EV-O-02** Response of Bond Strength and Development Length Precast Concrete Using Grouting ***Anis Rosyidah***			
12:00-12:15	**EV-O-03** Production of Woodceramics using Thai Waste Coconut Shell, and their Physical Properties ***Don Kaewdook***			
12:15-13:00		Lunch		

Room	Le Concorde	Jamjuree	Sakthong	Krisana
Floor	2nd Floor			
Session	Surface Engineering and Heat Treatment	Ceramic-based Materials	Materials for Energy	Polymer-based Materials
13:00-13:15	*Chair: Panadda Sheppard*	**Advanced Ceramics/ Processing 1** *Chair: Chatr Panithipongwut*	**Fuel Cells 2** *Chair: Sumittra Charojrochkul*	*Chair: Darunee Aussawasathien & Witchuda Daud*
	SH-O-03 The Effects of O_2:N_2 Gas Ratios on Structural, Optical, Electrical Properties of TiO_xN_y Thin Film deposited by Reactive DC Magnetron Sputtering ***Tanakorn Khumtong***	**CM-I-02** High Emissivity Coating for Energy Saving in Steam Cracking Furnace ***Jaturong Jitputti***	**EN-O-03** Effect of Sr Substituted $La_{2-x}Sr_xNiO_{4\pm\delta}$ (x = 0, 0.2, 0.4, 0.6, and 0.8) on Oxygen Stoichiometry and Oxygen Transport Properties ***Thitirat Inprasit***	**PM-O-03** Effect of Fiber Surface Modification on Properties of Artificial Leather from Leather Fiber Filled Natural Rubber Composites ***Jutaporn Sakmat***
13:15-13:30	**SH-O-04** Microstructure and Immersion Behavior of Plasma Sprayed Bi-Layered Ceramic Coatings ***Sathish Sathish***		**EN-O-04** Improved Conductivity and Phase Stabilization of Sr^{2+} and Ca^{2+} Doped $La_2Mo_2O_9$ ***Pranuda Jivaganont***	**PM-O-04** Characterizations of Silicon Carbide Whisker-Filled in Benzoxazine-Epoxy Shape Memory Polymers ***Chutiwat Likitaporn***
13:30-13:45	**SH-O-05** Use of Scratch Test to Evaluate Cohesive Strength of Mo/NiCrBSi Composite Plasma Sprayed Coating ***Hathaipat Koiprasert***	**CM-O-08** Effects of Water Temperatures on Water-Soluble Binder Removal in Ceramic Materials Fabricated by Powder Injection Moulding ***Wantanee Buggakupta***	**Catalyst & Adsorbent 1** *Chair: Ukrit Sahapatsombut* **EN-O-05** Experimental Investigation and Numerical Determination of Custom Gas Diffusion Layers to Understand Water Transports in PEMFC ***Visarn Lilavivat***	**PM-O-05** Improvement of Structure and Properties of Nanocomposite Foams based on Ethylene-Vinyl Acetate (EVA)/Natural Rubber (NR)/Nanoclay: Effect of NR Addition ***Juthapat Julyanon***
13:45-14:00	**SH-O-06** Investigation of Abrasive Flow Machining on Aluminum 5083 Mold Polishing ***Theerapong Maneepen***	**CM-O-07** Enhancement of Industrial Boiler Efficiency by High Thermal Absorptivity Coating ***Natthawut Nunkaew***	**EN-O-06** Effect of Nitrogen Doping on the Reducibility, Activity and Selectivity of Carbon Nanotube-Supported Iron Catalysts for CO_2 Hydrogenation ***Ly May Chew***	**PM-O-06** Effect of Electric Field on Conductive Network Formation in Polyvinylidene Fluoride/ Carbon Nanotube Composites ***Rungsima Yeetsorn***
14:00-14:15	**SH-O-07** The Effect of Heat Treatment on Fe^{2+}/Fe^{3+} Ratio in Soda-lime Silicate Glass ***Ekarat Meechoowas***	**CM-O-06** The Effect of Rotational Speed on Steel Pipe Lined Fe-WB based Composite Coating by Centrifugal-SHS Process ***Saowanee Singsarothai***	**EN-O-07** Facile Preparation of CuO and Cu_2O Nanoparticles ***Thanyaporn Yotkaew***	**PM-O-07** Photocatalytic Activity and Properties of Nanotitanium Dioxide-filled Natural Rubber in the Presence of Coupling Agents ***Pornsiri Toh-ae***

Room	Rachavadee	Patumchard	Intanin	Ubonchard
Floor	2nd Floor	3rd Floor		
Session	Materials Technology for Environment	Biomedical Materials & Devices	Metals, Alloys & Intermetallic Compounds	Material Reliability
13:00-13:15	*Chair:* *Sittha Sukkasi*	*Chair:* *Robert Molloy*	*Chair:* *Nutthita Chuankrerkkul*	*Chair:* *Amnuaysak Chianpairot & Chedtha Puncreobutr*
13:15-13:30	**EV-I-02** Environmental Nanotechnology: Application of Nanomaterials for Environmental Protection and Pollution Abatement ***Puangrat Kajitvichyanukul***	**BM-I-01** Preferential Orientation of Biological Apatite Crystallites in Bone and Regeneration of Anisotorpic Bony Tissue Surrounding Metal Implants ***Takayoshi Nakano***	**MT-O-01** The Effect of Ag and Sc Alloying Additions to the Casting Microstructure of A356 Automotive Aluminium Alloys ***Phanuphak Seensattayawong*** **MT-O-02** Sintered Frictional Fe-based Materials ***Monnapas Morakotjinda***	**MR-I-01** Strengthening Competitiveness of JFE Steel Corporation through Research and Development (R&D) ***Seishi Tsuyama***
13:30-13:45	**EV-O-04** Wastewater Treatment using TiO_2 Nanoparticles Loaded on Activated Carbon from Soybean Meal ***Voranuch Thongpool***	**BM-O-01** Bleached Shellac as Potential Polymeric Matrix for In Situ Microparticle (ISM) ***Pitsiree Praphanwittaya***	**MT-O-03** Machined Surface Quality of Pre-sintered Hardenable PM Steel ***Thawatchai Khantisitthiporn***	**KL-04 (TMETC-8)** Review on PVD Process Parameters for Specific Application ***Patama Visuttipitukul***
13:45-14:00	**EV-O-05** Effect of TiO_2 Thin Film on Ti Substrate Preparation Techniques on Methylene Blue and Wastewater Degradation via Photoelectrocatalytic Reaction ***Chabaiporn Junin***	**BM-O-02** Biocompatibility and Wound Healing Properties of Silk Fibroin/Chitosan/PVA Dressings ***Pimpon Uttayarat***	**MT-O-04** Sintered Microstructures and Mechanical Properties of Mechanically Alloyed Fe-Cu Powders ***Nattaya Tosangthum***	
14:00-14:15	**EV-O-06** Degradation Behavior of Low Density Polyethylene Bags for Solar Disinfection Application ***Supachai Songngam***	**BM-O-03** Nanofiber Membranes Fabricated from Nang Noi Srisaket 1 Silk Fibroin, Gelatin and Chitosan for Potential used as Barrier Membrane in Guided Tissue/bone Regeneration: Part I Fabrication of the Membranes ***Pornpen Siridamrong***	**MT-O-05** Sintered Frictional SiC-Reinforced Cu-Base Composites ***Jiraporn Damnernsawat***	**Break**

Room	Le Concorde	Jamjuree	Sakthong	Krisana
Floor	2nd Floor			
Session	Surface Engineering and Heat Treatment	Ceramic-based Materials	Materials for Energy	Polymer-based Materials
14:15-14:30	**SH-O-08** Residual Stresses and Fatigue Performance of Modified Mechanical Surface Treated Martensitic Stainless Steel AISI 420 ***Patiphan Juijerm***	**Advanced Ceramics/ Processing 2** *Chair: Wantanee Buggakupta* **CM-O-09** Effect of Preparative Conditions on the Textural Properties of Pure and Metal-Doped γ -Alumina Aerogel and Xerogel ***Abbas Khaleel***	**EN-O-10** The Effect of Doping CaO onto Alumina over Nickel Catalyst in Ethanol Steam Reforming ***Gunt Kranratanasuit***	**PM-O-08** Organomodification of Clay and its Influence on the Thermal, Mechanical and Fire behavior of Clay/Fire additives/ Vinylester Composites ***Vishnu Mahesh K R***
14:30-14:45	**Break**	**CM-O-10** The Effect of Alumina/ Glass Composite Composition on the Adhesion and Strength of A96% Alumina Joint ***Kritkaew Somton***	**EN-O-08** The Effect of 10Ni/10Y_2O_3-Al_2O_3 in Ethanol Stream Reforming (ESR) ***Chanon Pattarangkul***	**Break**
14:45-15:00	*Chair: Sinthu Chanthapan* **SH-O-09** Phase Equilibria of Bi-Se-Sb Thermoelectric Materials at 250 °C ***Hsiung Chih-Chun***	**CM-O-11** Fabrication of Zeolite Na-A and Activated Carbon Composites by Slip Casting Technique for Drinking Water Filtration ***Thanakorn Tepamat***	**EN-O-09** Catalytic Activity of Ethanol Steam Reforming over Ni-Ceria doped Alumina (10Ni/ 10CeO_2-Al_2O_3) ***Phurich Boonngam***	
15:00-15:15	**SH-O-10** Investigation and Characterization of Crystalline ZrN Thin Films deposited by DC Reactive Magnetron Sputtering on Unheated Substrate for Decorative-Coating Applications ***Witthawat Wongpisan***	**Break**	**Break**	*Chair: Atitsa Petchsuk* **PM-O-09** Biaxially-Stretched Poly(lactic) Acid (PLA) and Rubber-Toughened PLA Films:Tensile and Physical Properties ***Lalintip Boonthamjinda***
15:15-15:30	**SH-O-11** Study of the Influence of Thermal Effects on the Tribological Properties of Element Added-DLC Films ***Nutthanun Moolsradoo***	**Electroceramics** *Chair: Natthaphon Raengthon & Rojana Pornprasertsuk* **CM-I-03** Transparent Electrode Material for Organic Light Emitting Diode by Atomic Layer Deposition ***Hyung-Ho Park***	**Catalyst & Adsorbent 2** *Chair: Pimpa Limthongkul* **EN-O-11** Total Energy Requirement for Hydrogen Production Reactor ***Mek Srilomsak***	**PM-O-10** Thermal Properties of Banana Starch Nanocrystals Prepared by Acid Hydrolysis as Reinforcing Filler ***Jittiporn Saeng-On***

Room	Rachavadee	Patumchard	Intanin	Nilubon
Floor	2nd Floor	3rd Floor		
Session	Materials Technology for Environment	Biomedical Materials & Devices	Metals, Alloys & Intermetallic Compounds	Material Reliability
14:15-14:30	**EV-O-07** Material Safety and Integrity of Water-Filled Polyethylene Bags in an Accelerated Weathering Investigation for Applications in Solar Water Disinfection (SODIS) ***Weerawat Terdthaichairat***	**BM-O-05** Synthesis and Preparation of Poly (glycerol sebacate-co-glutamic acid) Scaffold for Bioactive Agent Immobilization ***Tharinee Theerathanagorn***	**MT-O-06** Effects of Cooling Rates and Alloy Compositions on Solidification of Cu-Sn Powders ***Amornsak Rengsomboon***	*Chair: Chaiyasit Banjongprasert & Sompong Srimanosaowapak*
				MR-O-01 Remaining Creep Life Assessment of Service Superheat Tube Boiler ***Pornsak Thasanaraphan***
14:30-14:45	**Break**	**Break**	**Break**	**MR-O-02** Study of the Hydrolytic Resistance of Glass Bottles under a High Fluctuated Weather Condition ***Usuma Naknikham***
14:45-15:00				**MR-O-03** Investigation of Fracture Location in Weldments of T22/T91 Dissimilar Welds ***Salita Petchsang***
15:00-15:15	*Chair: Apinya Panupat*	*Chair: Phornphop Naiyanetr*	*Chair: Pratip Vongbandit*	**MR-O-04** Failure Analysis of a Ductile Iron Roll of Intermediate Rolling Mill Stand ***Saneh Boonrampai***
	EV-I-03 $La_{1-x}A'_xCoO_{3-\delta}$ Perovskite Type Oxides as Catalysts for VOCs Oxidation ***Attera Worayingyong***	**BM-O-13** Three-Dimensional Temperature Field Simulation during Selective Laser Melting Process of Cobalt-Chromium Alloy ***Pongnarin Jiamwatthanachai***	**MT-O-07** Nondestructive Evaluation for Duplex Stainless Steel Tube using Multi-frequencies Remote Field Testing ***Cherdpong Jomdecha***	
15:15:15:30		**BM-O-06** *In Vitro* Resorbability of Three Different Processed Hydroxyapatite ***Faungchat Thammarakcharoen***	**MT-O-08** The Comparison of Acoustic Emission Activities between Material Integrity and Leakage during CNG Cylinder Testing ***Chalermkiat Jirarungsatian***	**MR-O-05** Thermal Fatigue and Creep of Radiant Coil used in High Temperature Application ***Siriwan Ouampan***

Room	Le Concorde	Jamjuree	Sakthong	Krisana
Floor	2nd Floor			
Session	Surface Engineering and Heat Treatment	Ceramic-based Materials	Materials for Energy	Polymer-based Materials
15:30-15:45	**SH-O-12** Dissolution of Y and Al during Plasma Spraying of NiCrAlY ***Panadda Sheppard***	**CM-I-03** (Cont.)	**EN-O-12** Simultaneous Adsorption of Trace Metal and SO_2 using Zeolite Adsorbent during Combustion of Brown Coal ***Asri Gani***	**PM-O-11** Influences of Starch Types on Reactive Dye Removal Efficiency of Eggshell Powder/ Thermoplastic Starch Foam Bio-Composites ***Supitcha Yaisun***
15:45-16:00	**SH-O-13** Post Weld Heat Treatment Cracking in Heat Resistant Alloy ***Kosit Wongpinkaew***	**CM-I-04** Electrical Properties of $Ba(Zr_{0.07}Ti_{0.93})O_3$/ Co Composites ***Gobwute Rujijanagul***	**EN-O-13** Synthesis of Ti-based Icosahedral Quasicrystal Powders by Mechanical Alloying and Their Hydrogen Sorption Properties ***Akito Takasaki***	**PM-O-12** Fabrication and Application of Nanostructures using Gas-assisted Hot Embossing and Self-Assembled Nanospheres ***Rong-Hong Hong***
16:00-16:15			**EN-O-14** Comparison of Pyrolysis of Jatropha Cake with Different Catalysts Using PY-GC/MS ***Sirirak Jariyaphinyo***	
16:15-16:30		**CM-O-12** An Investigation of the Interface Change on Resistive Switching of Manganite Thin Film by Microbeam Spectroscopy ***Hong-Sub Lee***	**EN-O-15** Preparation of Co/ SiO_2-Al_2O_3 Fiber by Electrospinning for Fischer-Tropsch Synthesis ***Natthawan Prasongthum***	
16:30-16:45		**CM-O-13** Synthesis of $BaTiO_3$ Nanoparticles by Varying Capping Agent at Low Temperature ***Wooje Han***	**EN-O-22** Thermoelectric Properties of Au Nanoparticle Incorporated Mesoporous ZnO Composite Thin Film by Using Reverse Micelle Structure ***Min-Hee Hong***	
16:45-17:00		**CM-O-19** Zirconia – Alumina Mixed Aerogel for High Specific Surface Area ***Hae-Noo-Ree Jung***		
17:00-18:00	Break & Poster Session I			
18:30-20:30	Banquet (Four Avenue, 4th Floor)			

Room	Rachavadee	Patumchard	Intanin	Nilubon
Floor	2nd Floor	3rd Floor		
Session	Materials Technology for Environment	Biomedical Materials & Devices	Metals, Alloys & Intermetallic Compounds	Material Reliability
15:30-15:45	**EV-O-08** The Development of Nanofiltration Membrane from Silk Fibroin Protein ***Manitta Aunsiripant***	**BM-O-07** Synthesis and Characterization of Artificial Bone Material using Calcium from a Natural Source ***Poj Chutong***	**MT-O-09** Correlation of Acoustic Emission with Corrosion of Lacquer Coatings on Tin-Free Steel ***Pornsak Srisungsitthisunti***	**MR-O-06** Evaluation of Stress Corrosion Cracking Resistance of Welded Stainless Steels in Ethanol ***Piya Khamsuk***
15:45-16:00	**EV-O-09** Effect of Lignin Acidolysis/ Organosolv System on Lignin-based Polyurethane Foam Properties ***Chularat Sakdaronnarong***	**BM-O-08** Sintered Titanium-Hydroxyapatite Composites as Artificial Bones ***Pongporn Moonchaleanporn***	**MT-O-10** Analysis of Eddy-Current Measurement System for Residual Stress Assessment in Stainless Steel Grade 304 ***Cherdpong Jomdecha***	**MR-O-07** Evaluation of Stress Corrosion Cracking Resistance of Welded Stainless Steels by Accelerated Immersion Tests **Amnuaysak Chianpairot**
16:00-16:15	**EV-O-10** Pomelo (*Citrus maxima*) Peel-Inspired Property for Development of Eco-Friendly Loose-Fill Foam ***Jarawee Looyrach***	**BM-O-09** Prevention of Post-angioplasty Restenosis with MicroRNA-145 nanoparticles-immobilized Coronary Stent in the Rabbit Restenosis Model ***Hui-Lian Che***	**MT-O-11** Influence of Nitrogen in Shielding Gas on Sensitisation of PCGTAW Austenitic Stainless Steels ***Narueporn Vaneesorn***	**MR-O-08** Sulfide Stress Cracking of Welded High Carbon Low Alloy Steel ***Namurata Palsson***
16:15:16:30	**EV-O-11** Organic Based Heat Stabilizers for PVC: A Safer and More Environmentally Friendly Alternative of Lead Compound ***Aran Asawakosinchai***	**BM-O-10** Development of Bacterial Driven Micro Beads for Targeted Anti-cancer Therapy ***Saji Uthaman***		**MR-O-09** Corrosion Evaluation of Zinc-plated Underhood Automotive Fasteners using Salt Spray Test ***Astuty Amrin***
16:30-16:45	**EV-O-12** Method Validation for Determination of Heavy Metals in Plastics by ICP-OES with Reference to EN 13432:2000 Packing Standard ***Panida Muangkasem***	**BM-O-11** *In Vitro* Evaluation of Rifapentine-Loaded PLGA Microparticles for Tuberculosis Inhaled Therapy ***Thaigarajan Parumasivam***		**MR-O-10** Effects of Heat Treatment on Microstructure and Corrosion Resistance of Boronized Austenitic Stainless Steel AISI 304 ***Patcharin Naemjan***
16:45-17:00	**EV-O-13** Efficient PEI-PAN Cellulose Membranes for Copper (II) Ions Determination ***Phitchaya Muensri***			
17:00-18:00	Break & Poster Session I			
18:30-20:30	Banquet (Four Avenue, 4th Floor)			

Poster Sessions

December 15, 17:00-18:00
December 16, 09:45-11:00

2nd Floor, Foyer Area

Ceramic-based Materials
CM-P-01 to CM-P-31
Materials for Energy
EN-P-01 to EN-P-29
Materials Technology for Environment
EV-P-01 to EV-P-17
Polymer-based Materials
PM-P-01 to PM-P-33

Day II December 16, 2014

08:00-09:00	Registration (2nd Floor, Foyer Area)
09:00-09:45	Plenary Lecture 3: Sustainable Use of Materials Rather Than Sustainable Materials. – The Importance of LCA to Assessing Materials Performance by **Tim Grant**
09:45-11:00	Break & Poster Session II

Room	Le Concorde	Jamjuree	Sakthong	Krisana
Floor		2nd Floor		
Session		Ceramic-based Materials	Materials for Energy	Polymer-based Materials
11:00-11:15		**Cement and Construction Materials 1** *Chair: Pitak Laoratanakul & Rojana Pornprasertsuk*	*Chair: Nuwong Chollacoop*	*Chair: Pakorn Opaprakasit*
11:15-11:30		**CM-I-05** Advance Researches on Fibre Reinforced Concrete in Thailand ***Piti Sukontasukkul***	**EN-I-02** (20 min) State of the Art on Advanced Engine Combustion ***Ocktaeck Lim***	**PM-I-02** Organic Light-Emitting Materials based on [5] Helicene Derivatives ***Somboon Sahasithiwat***
			EN-I-03 (20 min) R&D of RE-EV in Ulsan ***Ocktaeck Lim***	

Poster Sessions

3rd Floor, Foyer Area

Biomedical Materials and Devices
BM-P-01 to BM-P-12
Material Reliability
MR-P-01 to MR-P-05
Metals, Alloys and Intermetallic Compounds
MT-P-01 to MT-P-03
Simulation, Design and Manufacturing
SD-P-01 to SD-P-03
Surface Engineering and Heat Treatment
SH-P-01 to SD-P-05

Room	Rachavadee	Patumchard	Intanin	Nilubon
Floor	2nd Floor	3rd Floor		
Session	Materials Technology for Environment	Biomedical Materials & Devices	Metals, Alloys & Intermetallic Compounds	Simulation, Design & Manufacturing
11:00-11:15	*Chair:* *Nongnuch Poolsawad*	*Chair:* *Sorada Kanokpanont*	*Chair:* *Sudsakorn Intidech*	*Chair:* *Chi-na Benyajati*
	EV-O-14 Current Status of Carbon Footprint for Organization in Thailand ***Ruthairat Wisansuwannakorn***	**BM-I-02** New Era of *Aloe vera* as Biomaterial for Tissue Regeneration ***Pasutha Thunyakitpisal***	**MT-O-12** Fe-Sn Intermetallics Synthesized via Mechanical Alloying-Sintering and Mechanical Alloying-Thermal Spraying ***Pinya Meesa-Ard***	**SD-I-01** Considerations in Sheet Metal Forming Simulation ***Suwat Jirathearanat***
11:15-11:30	**EV-O-15** Carbon Footprint and Water Footprint of Refined Sugar in Thailand ***Soottiwan Thamsakon***		**MT-O-13** Synthesis and Characterization of Ni-Co-Si_3N_4 Nanocomposite Coating ***Yusrini Marita***	

Room	Le Concorde	Jamjuree	Sakthong	Krisana
Floor		2nd Floor		
Session		Ceramic-based Materials	Materials for Energy	Polymer-based Materials
11:30-11:45		**CM-O-14** Properties of Sintered Brick Containing Lignite Bottom Ash Substitutions ***Chiraporn Auechalitanukul***	**EN-I-03** (Cont.)	**PM-O-13** Microscopic Configuration of Energy Donor-Acceptor Pairs in Organic Thin Films Studied by Selectively Excited Photoluminescence ***Takaaki Otake***
11:45-12:00		**CM-O-15** Modeling the Influence of Fly Ash on Degree of Hydration and Compressive Strength of Blended Cement Paste ***Nattapong Damrongwiriyanupap***	**EN-I-04** (20 min) Materials Challenge for EV ***Werachet Khan-Ngern***	**PM-O-14** Polycarbonate Track-Etched Membranes by Nuclear Fission Reaction: Preparation and Characterization ***Suwimol Jetawattana***
12:00-13:00		Lunch		

Room	Le Concorde	Jamjuree	Sakthong	Krisana
Floor		2nd Floor		
Session		Ceramic-based Materials	Materials for Energy	Polymer-based Materials
13:00-13:15		**Cement and Construction Materials 2** *Chair: Nisanart Traiphol & Thanakorn Wasanapiarnpong*	**Solar** *Chair: Chanchana Thanachayanont*	*Chair: Pairote Jittham*
		CM-I-06 Binding Phases in Construction Materials ***Kedsarin Pimraksa***	**EN-O-16** Enhanced Electroluminescence of Silicon-rich Oxide/SiO_2 Multilayer Structures Deposited by Hydrogen Ion-beam Assisted Sputtering ***Sheng-Wen Fu***	**PM-O-15** Thermal and Mechanical Properties of Acrylonitrile-butadiene Rubber Modified Polybenzoxazine as Frictional Materials ***Jakkrit Jantaramaha***

Room	Rachavadee	Patumchard	Intanin	Nilubon
Floor	2nd Floor	3rd Floor		
Session	Materials Technology for Environment	Biomedical Materials & Devices	Metals, Alloys & Intermetallic Compounds	Simulation, Design & Manufacturing
11:30-11:45	**EV-O-16** Water Footprint of Polylactic Acid Production from Cassava in Thailand ***Ruethai Trungkavashirakun***	**BM-O-12** Nano-aggregates of Doxorubicin-conjugated Methoxy Poly(ethylene glycol)-b-carboxymethyl Dextran Block Copolymer Nanoparticles and Their Biological Activity ***Hwa Jeong Lee***	**MT-O-14** Composition Dependence of Morphological and Magnetic Properties of $Co_{100-x}Cu_x$ Film Prepared by RF-Sputtering ***Gun Chaloeipote***	**SD-O-01** Multi-scale Multi-physics Modelling of Fusion Welding: Materials, Process, and Mechanisms ***Chinnapat Panwisawas***
11:45-12:00	**EV-O-17** Evaluating Greenhouse Gas Emissions of Ready-mixed Concrete for Construction Industry ***Tassaneewan Chom-in***	**BM-O-04** Synthesis and Fabrication of a Poly (L-lactide-*co*-caprolactone)/Gelatin Blended Scaffold for Use in Articular Cartilage Tissue Engineering ***Wichaya Kalaithong***		**SD-O-02** A Block Algorithm and Its Optimal Block Size for Cholesky Decomposition of Finite Element Matrices in 3D Free Vibration Analysis ***Wassamon Phusakulkajorn***
12:00-12:15	**EV-O-18** Environmental Impact and Potential of Pollution Reduction Options for Foundry Industry: A Case Study of Faucet ***Wanwisa Thanungkano***	Lunch		
12:00-13:00				

Room	Rachavadee	Patumchard	Intanin	Nilubon
Floor	2nd Floor	3rd Floor		
Session			Metals, Alloys & Intermetallic Compounds	Simulation, Design & Manufacturing
13:00-13:15			*Chair: Chakkrist Phongphisutthinan*	*Chair: Somboon Otarawanna*
			MT-O-15 Microstructural and Phase Analysis of Service-exposed Ni-Cr Alloy Turbine Blade ***Nuzul Hazwani Mohamad Hanafi***	**SD-O-03** Effect of Weld Line Formation on Mechanical Properties for 3D-MID Technology ***Supakit Chuaping***

Room	Le Concorde	Jamjuree	Sakthong	Krisana
Floor	2nd Floor			
Session		Ceramic-based Materials	Materials for Energy	Polymer-based Materials
13:15-13:30		**CM-I-06** (Cont.)	**EN-O-17** Two-step Treatment of Electroplated Cu/Sn Bilayers: Impact of Alloying before Sulfurization ***Hui-Ju Chen***	**PM-O-16** Influence of Processing Oil Based on Modified Epoxidized Vegetable Oil with N-Phenyl-*p*-Phenyl-enediamine (PPD) on Extrusion Process Behaviors of Natural Rubber Compounds ***Chalida Moojea-te***
13:30-13:45		**CM-O-16** Fabrication of Fiber Cement Using Tobacco Stalk Pulp from Agricultural Residue ***Thanakorn Wasanapiarnpong***	**EN-O-18** Characterization of TiO_2 Nanotube Arrays Fabricated from Two-Step Anodization ***Marvin L. Samaniego***	**PM-O-17** Effect of Various Extracted Solvents on DPPH Radical Scavenging Activity of Natural Rubber ***Suwimon Siriwong***
13:45-14:00		**CM-O-17** Compressive Strength in Various Submersion Test of Fired Clay Bricks from Chi River Sub-Basin ***Sarunya Promkotra***	**Battery & Thermoelectric** *Chair: Supaporn Wansom* **EN-O-19** Improving the Electro-chemical Performance of SnO_2 Hollow Spheres by Titanium Dioxide Coating ***Songyoot Kaewmala***	**PM-O-18** Properties of Deprotinized Natural Rubber Latex/ Gelatinized Starch Blended Films ***Rungtiwa Waiprib***
14:00-14:15		**Composite Materials** *Chair: Pavadee Aung-kavattana & Sujarinee Kochawattana* **CM-O-18** Microstructure and Properties of Zirconia Toughened Alumina Fabricated by Powder Injection Moulding ***Nutthita Chuankrerkkul***	**EN-O-20** Improvement in Li-Air Batteries using Flow Electrolyte through Electrode Structure Design and Modelling ***Ukrit Sahapatsombut***	**PM-O-19** Fabrication of Novel Polyhydroxybutyrate-co-Hydroxyvalerate (PHBV) Mixed with Natural Rubber Latex ***Karndarthip Kuntanoo***
14:15-14:30		**CM-O-20** Alumina Crucible from Waste of Aluminum Industry ***Watcharee Sornlar***	**EN-O-21** Thermal Effects of Electrical Energy Harvested from a Laminated Piezoelectric Device in Engine Compartment ***Pornrawee Thonapalin***	Break
14:30-14:45	Break			

Room	Rachavadee	Patumchard	Intanin	Nilubon
Floor	2nd Floor		3rd Floor	
Session			Metals, Alloys & Intermetallic Compounds	Simulation, Design & Manufacturing
13:15-13:30			**MT-O-16** Phase Equilibria of Bi-Se-Te Thermoelectric Materials at 250 °C ***Cheng-Lin Tsai***	**SD-O-04** Numerical Simulation of Fluid Mixing in Micro-Mixers ***Suppasit Prasertlarp***
13:30-13:45			**MT-O-17** The Effect of CSL Boundary on Carbon Nanostructure Synthesis ***Panya Kansuwan***	**SD-O-05** Design of Runner and Gating Systems for the Investment Casting of 431 Stainless Steel Netting Hook through Numerical Simulation ***Patrpimol Suwankan***
13:45-14:00			**MT-O-18** Application of the Calphad Method to the Nano-systems Calculation ***Wojciech Gierlotka***	*Chair: Sutee Olarnrithinun*
				SD-O-06 Study of the Fabrication of Microreactor Made of Stainless Steel AISI Type 304 by Using Laser Beam Welding ***Tinna Sorasiri***
14:00-14:15				**SD-O-07** Effect of Vortex Finder, Inlet and Body Diameter of Hydrocyclone on the Separation Efficiency for Crude Palm Oil Industry ***Supachart Pakpooma***
14:15-14:30				**SD-O-08** Influence of Spinning Process Parameters on Spinning Deformation, Force and Surface Roughness ***Thanapat Sangkharat***
14:30-14:45				**SD-O-09** Cost Effective Production of a Permanent Mold Gravity Die Cast A356.0 Aluminum Alloy Motorbike Shock Absorber through Casting Simulation ***Muhammad Saqib***
	Break			

Room	Le Concorde	Jamjuree	Sakthong	Krisana
Floor	2nd Floor			
Session		Ceramic-based Materials		Polymer-based Materials
14:45-15:00		**Geopolymers** *Chair: Apirat Theerapapvisetpong & Anucha Wannagon*		*Chair: Thanasat Sooksimuang*
		CM-I-07 Current Research on Geopolymer Technology ***Sirithan Jiemsirilers***		**PM-O-20** Characterizations of Fluorine-Containing Polybenzoxazine Prepared by Solventless Procedure ***Patcharat Pattharasiriwong***
15:00-15:15				**PM-O-21** Investigation of Synthesis Parameters for Modification of Chitosan with Enrofloxacin ***Saniwan Srithongkham***
15:15:15:30		**CM-O-21** Mechanical Properties and Microstructures of Bottom Ash-Clay Geopolymers under NaOH and KOH Activations ***Sakonwan Hanjitsuwan***		**PM-O-22** Thermo-responsive Biocompatible Membranes Based on Poly (ethylene-co-vinyl alcohol) For Biomolecule Separations ***Sujith Athiyanathil***
15:30-15:45		**CM-O-22** Influence of OPC Replacement and Manufacturing Procedures on the Properties of Self-Cured Geopolymer Cement ***Teewara Suwan***		
15:45-16:00		**CM-O-23** Properties of Steel Fibre Reinforced Geopolymer ***Rachamongkon Wongruk***		
16:00-16:15		**CM-O-24** Effect of Silica to Alumina Ratio on the Compressive Strength of Class C Fly Ash Geopolymer ***Patthamaporn Timakul***		

Sarocha Room, 3rd Floor

Thailand-Japan Polymer Initiative

Time	Topics
08:00–09:00	Registration
09:00–09:15	Opening Ceremony
09:15–10:00	Plenary Lecture 1: 10 Global Materials Science and Engineering Trends by ***Thomas Boellinghaus***
10:00–10:45	Plenary Lecture 2: New Technology for Carbon Neutral Energy by ***Tatsumi Ishihara***
10:45–11:00	Break
11:00–11:25	**TJ-O-01:** Nanomatrix Structure and Viscoelastic Properties of Natural Rubber by ***Dr. Seiichi Kawahara*** Nagaoka University of Technology
11:25–11:50	**TJ-O-02:** Functionalized Magnetic Polymeric Nanoparticles for Bioanalytical Applications by ***Prof. Dr. Pramuan Tangboriboonrat*** Mahidol University
11:50–12:15	**TJ-O-03:** Bromination of Natural Rubber by Anodic Oxidation in Water Process in the Presence of Carbon Dioxide by ***Dr. Yoshimasa Yamamoto*** Tokyo National College of Technology
12:15–13:00	Lunch
13:00–13:25	**TJ-O-04:** Development of Nano-chitosan for Biomedical Applications via Water-based Reaction System by ***Prof. Dr. Suwabun Chirachanchai*** Chulalongkorn University
13:25–13:50	**TJ-O-05:** Controlled Polymerization of Terpene as Renewable Vinyl Monomer for Novel Bio-based Polymers by ***Dr. Kotaro Satoh and Dr. Masami Kamigaito*** Nagoya University
13:50–14:15	**TJ-O-06:** Synthesis of Cyclic Polyesters: The Catalyst Design by ***Dr. Khamphee Phomphrai*** Mahidol University
14:15–14:40	**TJ-O-07:** Synthesis and Properties of Aliphatic Polycarbonates from Epoxides and CO_2 by ***Dr. Koji Nakano*** Tokyo University of Agriculture and Technology
14:40–15:00	Break
15:00–15:25	**TJ-O-08:** Polymer Nanostructures observed by Electron Microscopy by ***Dr. Hiroshi Jinnai*** Kyushu University

Time	Topics
15:25–15:50	**TJ-O-09:** Starch-based Rheology Modifiers in Structuring Health Foods by ***Dr. Asira Fuongfuchat*** National Metal and Materials Technology Center
15:50–16:15	**TJ-O-10:** Effect of Mechanical Instability at Polymer Surface on Cell Adhesion by ***Dr. Keiji Tanaka*** Kyushu University
16:15–16:40	**TJ-O-11:** Polymers for New Generation Solar Cells by ***Dr. Jatuphorn Wootthikanokkharn*** King Mongkut's University of Technology Thonburi
16:40–17:05	**TJ-O-12:** Biobased Furan Polymers with Self-healing Ability and Shape Memory by ***Dr. Naoko Yoshie*** The University of Tokyo
17:05–17:30	**TJ-O-13:** Biodegradable Nanocomposite Blown Films based on Poly(lactic acid) Containing Silver-loaded Kaolinite by ***Dr. Winita Punyodom*** Chiangmai University
17:30–17:55	**TJ-O-14:** Enzymatic Synthesis and Functionalization of Multiphase Cellulose Materials by ***Dr. Takeshi Serizawa*** Tokyo Institute of Technology
17:55–18:20	**TJ-O-15:** Waste to Value - Production of Pectin from Pomelo Peel by ***Dr. Pawadee Methacanon*** National Metal and Materials Technology Center
18:30–20:30	Banquet (Four Avenue, 4th Floor)

Busakorn Room, 3rd Floor

Tribology Technical Session

Time	Topics
09:00–09:15	Opening Ceremony
09:15–10:00	Plenary Lecture 1: 10 Global Materials Science and Engineering Trends by ***Thomas Boellinghaus***
10:00–10:45	Plenary Lecture 2: New Technology for Carbon Neutral Energy by ***Tatsumi Ishihara***
10:45–11:00	Break
11:00–11:05	Opening Speech by ***Assoc. Prof. Siriluck Nivitchanyong*** (TTA President)
11:05–11:10	Introduction of TTA International Academic Advisory Board by ***Prof. Kuniaki Dohda*** (TTA Chair of International Academic Advisory Board)
11:10–12:00	Keynote Lecture: Active Control of Boundary Lubrication by ***Prof. Yonggang Meng, China***
12:00–13:00	Lunch
13:00–13:30	Technical Session 1: TTA and its Role in Mobilizing Thai Industry by ***Dr. Numpon Mahayotsanun*** (TTA Vice President)
13:30–14:15	Technical Session 2: Tribology R&D Activities in Thailand by ***Assoc. Prof. Varunee Premanond*** (TTA Lubrication Division Head)
14:15–14:45	Networking with TTA members and New Members Recruitment
14:45–15:00	Break
15:00–16:00	Forum (in English): Tribology Technology in Thai Manufacturing Industry Chair by Asst. Prof. Numpon Mahayotsanun 1. ***Dr. Hideyuku Kuwahara,*** Thai Parkerizing Co., Ltd. 2. ***Mr. Watcharapol Trisantikul,*** PTT Public Co., Ltd. 3. ***Mr. Takeshi Hashimoto***, Fuji Die 4. A representative from Honda R&D
16:00 – 17:00	TTA Annual Meeting (Invited Only)

CONTENT

PAGE

THE 8th INTERNATIONAL CONFERENCE ON MATERIALS SCIENCE AND TECHNOLOGY

SIMULATION, DESIGN AND MANUFACTURING

THAILAND-JAPAN POLYMER INITIATIVE

PLENARY LECTURES

PL-01

10 Global Materials Science and Engineering Trends

Thomas Boellinghaus and Juergen Lexow

The global challenges of our societies entail important research necessities and perspectives in the field of Materials Science and Engineering (MSE).The world-wide development in this trans-disciplinary area is continuously discussed in the World Materials Research Institutes Forum (WMRIF), the not-for-profit organization of more than 50 independent public research institutes. They will be summarized and continuously updated in the 10 Global MSE Trends. After intensive discussions among the forum members over the last two years, the first set of trends will be released in very due course and can be retrieved from the web-site wmrif.info.

For instance, the materials challenges associated with coverage of the resources for our technical products will gain increasing importance in the near future. This trend includes not only the challenges associated with providing and substitution of the materials resources for sustainable technical products, but vice versa, also the development of sustainable and environmentally compatible technical products for recovering of resources, like scarce elements and minerals, but also potable water. A further trend is based on global energy challenges. For numerous renewable energy applications materials still have to be developed that might withstand the coupled loading during the complete service life of the respective components. Photovoltaic systems at improved efficiency need to be equally adjusted more easily available materials as to climatic challenges including biostability. But, in conventional energy power stations the additional start-up and shut-down cycling as required from intermittent supply of green energy entails risky load spectra in the later stages of the service life. The respective components have not been designed for.

Mobility is a continuous societal demand, on land in the air and on water . It challenges materials both in construction and fueling. Lighter design, ease of manufacturing and recycling and in particular safe operation are on the demand side. This includes the infrastructure, roads, bridges and terminals.

Health and wellbeing in the aging society make demands on biocompatible materials in many applications; be it in implants, artificial limbs or for orthotics. It is in line with light weighting, biocompatibility and integration of electronics.

Another lasting trend in Materials Science and Engineering is the continuous need for improved instrumentation. Modeling requires elaborate and powerful computing science based on valid data. The acquisition of these data requires analytical and mechanical instrumentation that simultaneously and at improved perfection measure materials' characteristics at ever more minute dimensions.

In the lecture at MSAT 2014, the trends will be presented and, exemplarily, some of these will be outlined more detailed.

PL-02

New Technology for Carbon Neutral Energy

Tatsumi Ishihara

[a]*International Institute for Carbon Neutral Energy Research, Kyushu University, Motooka 744, Nishi-ku, Fukuoka, 819-0395, Japan*

* ishihara@cstf.kyushu-u.ac.jp

Keywords: Photocatalyst, Steam electrolyzer, solid oxide reversible cell

At present, climate change is the most serious issues in development of human society and development of low carbon society is strongly required. On the other hand, energy cost gradually increases in the last decay and so more environment compatible as well as highly efficient energy generator is demanded. From these point of view, several carbon neutral energy technologies will be introduced in this talk.

As a renewable energy, solar and wind energy are strongly expected, however, because of fluctuated and low power density, averaging and concentrating electric power is an important for these renewable energy. For this, converting to H_2 as an energy carrier is more promising than storage in battery. Photocatalyst for water splitting can directly convert the solar energy to hydrogen. There are several catalysts proposed as photocatalyst for water splitting, however, visible light was not effectively used for water splitting up to now. In this talk, modification effects of inorganic semiconductor with organic dye will be introduced. In this catalyst, two excitation by photon at two difference frequency is used and achieved the so-called Z-scheme excitation. Figure 1 shows image of the dye modified GaN(ZnO) and H_2, O_2 formation rate in water splitting as a function of wave length of light. This catalyst exhibited high activity to water splitting and H_2 and O_2 formation rate of 59.1 and 21.1 mmol/h $g_{\text{-cat}}$ achieved, respectively under 420 nm light irradiation. On the other hand, low temperature steam electrolysis is another important system for H_2 production with high efficiency. For this technology, by using heat, required electricity became smaller comparing with the normal electrolysis. In this presentation, introduction of steam electrolysis is introduced for solar hydrogen system.

By using $LaGaO_3$ fast oxide ion conductor, high efficiency of electrolysis was achieved and thermal neutral current of 400 mA/cm^2 was achieved at 1073 K when Ni-Fe/La(Sr)Fe(Mn)O_3 composite fuel electrode. On the other hand, this cell is also suitable for reversible operation and in SOFC mode, the maximum power density was as high as 0.6W/cm^2 at 1073 K. Therefore, combination of solar cell with steam electrolyzer gives the highly efficiency solar production system and converting electricity by reversible operation of SOEC is also promising process for carbon neutral energy.

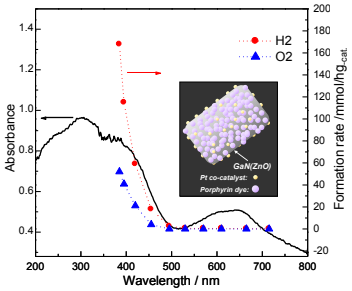

Fig.1 Water splitting activity of RhOx, NiO / Alizarin yellow R / IrO_2-GaN:ZnO catalyst

PL-03

Sustainable Use of Materials Rather Than Sustainable Materials. – The Importance of LCA to Assessing Materials Performance.

Tim Grant
Member of executive of Australian Life Cycle Assessment Society (ALCAS) and Director of Life Cycle Strategies, Australia
tim@lifecycles.com.au

It is recognised that materials contribute significantly to environmental degradation globally. It is logical then to search for alternative materials solutions which reduce the impact of materials on the environment. However materials also provide substantial benefits and utility when they are used, and it is in this context that their environmental impacts should be assessed. Low impact materials can cause substantial environmental impact if used inappropriately. Poor performance or failure of a material can cause flow on effects to other product systems. Similarly high impact materials may reduce environmental impacts through superior performance, durability and recyclability. Life Cycle Assessment (LCA) is an internationally recognised approach to evaluating environmental performance of products systems taking account of all the inputs and outputs from that system, and evaluated per unit of performance, which is referred to in LCA as the functional unit.

A consequential LCA approach is a specific type of LCA which aims to look at all of the significant impacts from changes in material use or product design and is especially important when evaluating the use of wastes and by-products. By-product and co-products are materials produced as a consequence of other material production systems. Waste and by-products are often chosen as alternative materials on the premise that they have little of no environmental impact in production. While it may be appropriate to allocate the impacts of a coproducing system to the primary product, the current uses of the by-products needs to be taken into account. This approach can substantially alter the environmental results for the use of alternative materials. The use of LCA to assess materials and products over their entire life cycle can help use move away from labels such as sustainable materials move towards identification of sustainable material use.

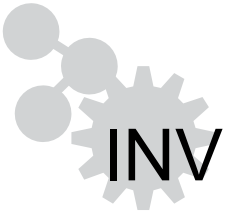

INVITED LECTURES

BM-I-01

Preferential Orientation of Biological Apatite Crystallites in Bone and Regeneration of Anisotorpic Bony Tissue Surrounding Metal Implants

Takayoshi Nakano
Division of Materials & Manufacturing Science, Graduate School of Engineering, Osaka University, 2-1 Yamada-oka, Suita, Osaka 565-0871
nakano@mat.eng.osaka-u.ac.jp

The bone mechanical property depends on both bone quantity and quality corresponding dominantly to bone mineral density (BMD: density of biological apatite) and the integrity of the internal architecture, respectively. BMD is correlated with bone strength, but is not a index accounting for all of bone mechanical properties. Thus, new indeces representing the bone quality have been investigated so far because bone is a well-organized hierarchical composite at various scale levels. It was proposed by the National Institutes of Health in 2000 that bone strength should be represented and analyzed by bone quality as well as bone mass and bone mineral density (BMD). Microstructure organization, bone turnover rate, micro-crack occurrence, and cellular properties are important bone quality parameter candidates. Since BMD refers to the density of BAp, but the crystallographic orientation of BAp crystallites corresponds to the rotated degree of BAp crystallite, these two parameters are independent. In other words, BAp orientation is a possible bone quality parameter. Thus, our group is focusing on the preferential alignment of BAp *c*-axis orientation as a bone quality parameter under normal, pathological, and regenerated bones using the microbeam X-ray diffraction system.

The preferential degree of the BAp *c*-axis strongly depends on the bone position, *in vivo* stress distribution, bone growth, degree of pathology and regeneration, activity of bone cells, gene defect, etc[1-3]. We are challenging to clarify the BAp preferential alignment formation mechanism and to control the degree of BAp orientation by using an anisotropic biomaterial design to develop suitable distribution of the BAp *c*-axis orientation[4-6].

Correlations became clear among *in vivo* stress distribution, anisotropy of the BAp/Col alignment and the mechanical property in the original intact, regenerated and pathological hard tissues including mandible. Since BAp orientation distribution is essential microstructure for exerting mechanical, chemical and biological functions, technique for controlling the BAp orientation should be developed, especially in relation to tissue engineering technique in the lost bone tissue.

Because of the anisotropy of bone microstructure based on the BAp/collagen orientation distribution, development of implants for bone substitute should be considered by structural anisotropy. The Teflon implant with a unidirectional-elongated-through, for example, was implanted so that the elongated pore direction was parallel or perpendicular to the longitudinal axis of rat tibia with one dimensional orientation of BAp *c*-axis. As a result, the degree of calcification and the subsequent orientation of BAp are larger in the elongated pore parallel to the longitudinal axis than those in the pore perpendicular to the axis, indicating that BMD and BAp orientation of the newly formed bone can be controlled by the elongated pore direction closely relating to the anisotropic bone microstructure and principal stress distribution *in vivo*.

We aimed at the following three topics about the preferential alignment of BAp *c*-axis: (1) evaluation of the degree of BAp orientation; (2) control of BAp orientation based on metal

biomaterial design; (3) and clarification of the mechanism for producing the BAp orientation *in vivo* or *in vitro*. In this study, our results regarding these three topics are introduced.

References

[1] T. Nakano, K. Kaibara, Y. Tabata et al.: Unique alignment and texture of biological apatite crystallites in typical calcified tissues analyzed by microbeam X-ray diffractometer system. Bone 31: 479-487, 2002.

[2] T. Nakano, K. Kaibara, T. Ishimoto et al.: Biological apatite (BAp) crystallographic orientation and texture as a new index for assessing the microstructure and function of bone regenerated by tissue engineering. Bone 51: 741–747, 2012.

[3] T. Ishimoto, T. Nakano. Y. Umakoshi, M. Yamamoto, Y. Tabata: Degree of biological apatite c-axis orientation rather than bone mineral density controls mechanical function in bone regenerated using rBMP-2. Journal of Bone and Mineral Research (JBMR) 28: 1170-1179, 2013.

[4] A. Matsugaki, G, Aramoto, T. Nakano: The alignment of MC3T3-E1 osteoblasts on steps of slip traces introduced by dislocation motion. Biomaterials: 7327-7335, 2012.

[5] Y. Noyama, T. Nakano, T. Ishimoto, T. Sakai and H. Yoshikawa: Design and optimization of the oriented groove on the hip implant surface to promote bone microstructure integrity. Bone 52: 659–667, 2013.

[6] A. Matsugaki, N. Fujiwara and T. Nakano: Continuous cyclic stretch induces osteoblast alignment and formation of anisotropic collagen fiber matrix. Acta Biomaterialia 9: 7227–7235, 2013.

BM-I-02

New Era of *Aloe vera* as Biomaterial for Tissue Regeneration

Prof. Dr. Pasutha Thunyakitpisal
Research Unit of Herbal Medicine, Biomaterial and Material for Dental Therapy,
Dental Biomaterials Science Program, Faculty of Dentistry,
Chulalongkorn University, Thailand

Aloe vera has been recognized as a medicinal herb for enhancing skin wound healing. Recently, our group has successfully extracted acemannan, a polysaccharide from *aloe vera* gel. Acemannan contains a unique acetylated D-mannose as a major sugar residue. *In vitro* study, acemannan stimulated proliferation, extracellular matrix synthesis, growth factor secretion, and mineral deposition in primary human gingival fibroblast, pulpal fibroblast, bone marrow stromal cell, and periodontal ligament cell. In animal model, acemannan induced oral wound healing, reparative dentin formation, tooth socket healing , and periodontium regeneration. Clinically, acemannan was effectively in oral aphthous ulcer treatment, reparative dentin formation, and tooth socket healing. The effectiveness of acemannan in reducing ulcer size and pain was superior to that of control, but inferior to that of 0.1% triamcinolone acetonide. Acemannan significantly enhanced new dentin formation to conceal the pulp exposure comparing with $Ca(OH)_2$. Using radiographic evaluation, acemannan accelerated tooth socket healing 3-months after surgical removal of mandibular partial bony impacted third molars. The percentage radiographic density of the socket 3-months post-surgery in the acemannan treated group was significantly higher than that of non-treated control. From our limitation data, acemannan could be natural bioactive material for oral tissue regeneration.

CM-I-01

Novel Visible-Light-Sensitive Photocatalyt for Indoor Environmental Purification

Masahiro MIYAUCHI [a, b,*]

[a] *Graduate School of Science and Engineering, Tokyo Institute of Technology, Meguro-ku, Tokyo, 152-8552, Japan*

[b] *PRESTO, JST, Kawaguchi, Saitama, 332-0012, Japan*

* mmiyauchi@ceram.titech.ac.jp

Keywords: photocatalyst, TiO_2, visible light, environmental purification, anti-pathogen

Efficient visible-light-sensitive photocatalyst has been developed based on the Cu(II) or Fe(III) nanoclusters grafted titanium dioxide (TiO_2). We adopt the two novel concepts for developing the efficient photocatalysts, *i. e.* interfacial charge transfer for visible light absorption and multi-electrons reduction of oxygen molecules.[1-10] When the nanoclusters of Cu(II) or Fe(III) amorphous oxides are grafted onto the TiO_2 surface, electrons in the valence band of TiO_2 can be excited to the surface nanoclusters through the interface under visible light irradiation. Excited holes in the valence band of TiO_2 have strong oxidative activities and can decompose organic contaminants or bacteria, while the electrons in Cu(II) or Fe(III) nanoclusters react with oxygen molecules through the efficient multi-electrons reduction process. The quantum efficiency of our optimized photocatalyst achieves over 90 % under visible light irradiation.[9] The nanoclusters grafted TiO_2 causes efficient photocatalytic oxidation activity and super-hydrophilic conversion even under indoor light illumination like commercial white fluorescent bulb or white light emitting diode (LED). Our photocatalysts exhibited significant air purification, self-cleaning, and anti-pathogenic effects under regular indoor lighting. We have also conducted the field test at hospitals and international airports to confirm the excellent anti-bacterial and deodorization properties of our photocatalysts at indoor building environment.

References,

1 Miyauchi et al. *The Journal of Physical Chemistry C* 114, 16481 (2010).
2 Miyauchi et al. *Journal of the American Chemical Society* 132, 15259 (2010).
3 Miyauchi et al. *Applied Catalysis B: Environmental* 100, 502 (2010).
4 Miyauchi et al. *Langmuir* 26, 796 (2010).
5 Miyauchi et al. *Physical Chemistry Chemical Physics* 13, 14937 (2011).
6 Miyauchi et al. *Chemistry of Materials* 23, 5282 (2011).
7 Miyauchi et al. *ACS Nano* 6, 1609 (2012).
8 Miyauchi et al. *Journal of the American Chemical Society* 135, 10064 (2013).
9 Miyauchi et al. *ACS Nano*, 8, 7229 (2014).
10 Miyauchi et al. *Journal of Materials Chemistry A*, 2, 13571 (2014).

CM-I-02

High Emissivity Coating for Energy Saving in Steam Cracking Furnace

Jaturong Jitputti[1,*], Koichi Fukuda[1], Songsak Klamklang[2]
[1]*Research and Development Center, SCG Chemicals Co.,Ltd., Bangkok, 10800, Thailand*
[2]*Texplore Co.,Ltd., Bangkok, 10800, Thailand*
*jaturojii@scg.co.th

Keywords: Emissivity, Coating, Furnace, Energy Saving

The furnace walls in a steam cracker are lined with refractory, bricks and fiber materials having a relative low emissivity. By applying a "High Emissivity Coating" on the surface of the furnace walls, it is possible to increase the emissivity and thereby improve the thermal efficiency of the furnace box significantly. It was found that applying high-emissivity coating on the furnace walls of steam cracker improves the thermal efficiency of the furnace (~3-6), which resulted in fuel savings, increased production and improved quality in firing and heat treating furnaces. These differences are small, but considering the industrial importance and scale of the steam cracker, significant. In addition, several other secondary benefits, such as increased life of refractory, less NOx emission, etc., are obtained by applying emissivity coating material onto the furnace walls. Recently, high emissivity coating has been applied in several steam crackers with satisfactory results. Moreover, high emissivity coating was also applied to other industrial furnaces and the results are presented.

CM-I-03

Transparent Electrode Material for Organic Light Emitting Diode by Atomic Layer Deposition

Hyung-Ho Park
Department of Materials Science and Engineering, Yonsei University, Korea
hhpark@yonsei.ac.kr

A modified deposition procedure of zinc-metal dopant-oxygen precursor exposure cycle was demonstrated for better distribution of Al-dopants in ZnO (AZO) films by atomic layer deposition (ALD). It was to reduce the formation of nanolaminate thin films that might form with the typically used alternating ZnO and metal oxide deposition procedure. An introduction of a homogeneous AZO buffer layer showed an improvement of the performance of an organic light-emitting diode (OLED) device fabricated on an AZO anode.

Fluorine-doped ZnO (FZO) thin films by ALD was also investigated with home-made fluorine source at a low deposition temperature. The grain growth orientation was found to change significantly as the fluorine concentration was increased due to the characteristics of fluorine doping in the oxygen sites of ZnO. This phenomenon could be explained by a perturbation and passivation effect resulting from the fluorine doping mechanism, with the fluorine anions filling oxygen-related defect sites in the ZnO lattice. We investigated the effect of F-doping-induced texturing of a ZnO surface to enhance the hole injection properties of an OLED device. Conversely, the work functions of the doped ZnO anodes gradually increased with an increase in surface texturing caused by an increase in the amount of exposed (100) planes. Finally, the best OLED performance was obtained for a ZnO anode containing 0.5 at.% F (the work function value for this film was 4.74 eV) in an OLED device composed of a DNTPD/TAPC/ $Bebq_2$:10%-doped RP-411/Bphen/LiF/Al structure.

References

(1) Journal of Vacuum Science & Technology A 28 (2010) 1111.
(2) J. Vac. Sci. Technol. A 31, (2013) 01A101-1.
(3) ACS Applied Materials & Interfaces 5 (2013) 3650.
(4) Journal of Materials Chemistry C 2 (2014) 98.

CM-I-04

Electrical Properties of $Ba(Zr_{0.07}Ti_{0.93})O_3$/ Co Composites

Gobwute Rujijanagul[1,*] Thanatep Phatungthane[1], Parkpoom Jarupoom[2]
(1) Department of Physics and Materials Science, Faculty of Science, Chiang Mai University, Chiang Mai, Thailand
(2) Department of Industrial Engineering, Faculty of Engineering, Rajamangala University of Technology Lanna, Chiang Mai , Thailand
*rujijanagul@yahoo.com

Effects of Co nanoparticles on the magnetic, ferroelectric and dielectric properties of $Ba(Zr_{0.07}Ti_{0.93})O_3$/ Co composites were investigated. The composites were fabricated by a solid-state reaction technique. The additive suppressed grain growth, resulting in an approximately 12-fold decrease in average grain size. M-H hysteresis loops showed an improvement in the magnetic behavior for higher Co content samples plus modified ferroelectric properties. However, the 2 vol. % samples showed the optimum ferroelectric and ferromagnetic properties. Examination of the dielectric spectra showed that the additive promoted a board dielectric – temperature curves with a frequency dispersion. Heterogeneous conduction in the composite was proposed to explain the observed dielectric behavior.

Acknowledgements
This work was supported by the Thailand Research Fund (TRF), the National Research University Project under Thailand's Office of the Higher Education Commission Hands-on Research and Development Project; Rajamangala University of Technology Lanna, and the Faculty of Science, Chiang Mai University.

CM-I-05

Advance Researches on Fibre Reinforced Concrete in Thailand

Piti Sukontasukkul
Department of Civil Engineering, Faculty of Engineering, King Mongkut's University of Technology North Bangkok, Bangkok, Thailand

Key Words: Toughness Enhancement, Fire Resistance, Bulletproof Concrete Panel, Cement Based Sensor, Geopolymer

Concrete is the most use construction material on earth due to its excellent compressive strength, mold-ability and cost effectiveness. However, concrete does have disadvantages on its poor tensile strength and toughness (brittleness). When fibres reinforced concrete (FRC) was first invented, it is aimed mainly to reduce concrete brittleness and provide toughness to concrete. In FRC, small short fibres are uniformed distributed over the body of concrete with main purposes to intercept, slow down and/or even stop crack propagation. However, during the recent years, with several kinds of fibre available in the market and advancements in concrete technology, FRC applications become more than just a toughness enhancement material. In this presentation, advance researches on FRC carried out at KMUTNB Civil Engineering Material laboratory are presented and discussed. Such researches include the application of fibres to enhance fire resistance of concrete, the use of FRC hybridized with rubberized concrete in bulletproof concrete panel, the use of carbon fibre to increase piezoresistivity of concrete in cement based sensor, and the use of FRC technology in Geopolymer concrete.

CM-I-06

Binding Phases in Construction Materials

Kedsarin Pimraksa
Department of Industrial Chemistry, Faculty of Science, Chiang Mai University, Chiang Mai, 50200, Thailand
kedsarin.p@cmu.ac.th

Keywords: binding phase, special cement, high lime based cement, geopolymer

Binding phases in construction materials nowadays tend to be produced in more friendly environmental way because of world-energy crisis and -ecology constraint. The most famous binding materials which have been using since many decades ago are aluminosilicate glassy phases and Portland cement (PC) for fired and unfired products, respectively. Compared with ceramic industry, cement industry suffers the blames of much greater CO_2 emission and higher energy consumption. Therefore, material chemist, ceramist and cement technologist input a huge effort to a search for alternative binders. Special cements viz., high belite and high sulfoaluminate cements are considered to be one of the effective alternatives for PC replacement due to a possibility in a use of industrial wastes such coal ashes and less energy consumption in the production. In addition, very high early strength can be approached dependent on additional gypsum content. High lime based cement, a kind of Roman cement, is in addition reconsidered recently as an effective binder due to the revolution of carbonation solidification obtained by microbial and other chemical activations. Another binder which is expected to play a great role in construction and ceramic industries as a green material in soon future is geopolymeric material, a kind of alkali activated aluminosilicate binder. Geopolymer is considered to be superior to traditional binders in many aspects such as be able to produce various useful phases (zeolite, nepheline syenite, etc.) incorporating with geopolymeric phase using several inorganic wastes as starting materials, able to fabricate into various forms, able to resist to disintegration when is exposed to high temperature dependent on its SiO_2/Al_2O_3 ratio and able to contribute to the conservation of primary resources such energy and raw material. Due to the above mentioned characteristics and properties, geopolymer is, therefore, recognized as “ceramic without firing” which would be highly supportive to the future of world construction materials.

CM-I-07

Current Research on Geopolymer Technology

J. Sirithan[a,b,*], A. Anchalee [a,b] S. Anut[a,b], O. Sujitra[a,b], L. Pitak[c], and T., Parjaree[c]

[a]*Research Unit of Advanced Ceramics, Department of Materials Science, Faculty of Science, Chulalongkorn University, Bangkok, 10330, Thailand*

[b]*National Metal and Materials Technology center, Klong Luang, Phathumthani, 10120, Thailand*

* sirithan.j@chula.ac.th

Keywords: geopolymerization, metakaolin based geopolymer, fly ash based geopolymer.

Geopolymer is an inorganic material with ceramic-like properties involved the chemical reaction of aluminosilicate oxides with alkali silicate solution yielding the amorphous to semi-crystalline 3-D polymeric structure at ambient temperature or slightly above. Geopolymers can be prepared from aluminosilicate materials, therefore any materials composed of silica (SiO_2) and alumina (Al_2O_3) can be used as starting materials for geopolymerization process; for example fly ash, metakaolin, bottom ash, slag, rice husk ash and other industrial wastes. Geopolymer can be synthesized as bulk and porous forms depends on their specified applications. In this sense, geopolymer is one of the optional materials in the future. It reduces the environmental degradation of global warming problems. The use of waste in geopolymer processing is also fits into sustainable economical domain. The main composition is silica and alumina which were decomposed by alkaline solution. Once the alumino-silicate powder is mixed with alkali solution a paste forms and quickly transforms into a hard geopolymer and gained strength. Fly ash based and metakaolin based geopolymer together with various kinds of industrial wastes were synthesized and the synthesis parameters of geopolymerization process were studies. The relation of the amount of alkali solution and ratios of materials used, curing time, curing temperature, and properties of geopolymer was investigated. Properties of geopolymer have been compared to other materials. Possible applications of geopolymer have been proposed.

EN-I-01

Carbon nanotubes for chemical energy conversion and storage

Prof. Dr. Martin Muhler

Laboratory of Industrial Chemistry, Ruhr-University Bochum, 44780 Bochum, Germany

Carbon nanotubes (CNTs) are promising materials for numerous applications because of their unique mechanical, chemical, and electrochemical properties. Various carbon materials such as carbon fibers or carbon cloth can be used as support for the growth of CNTs. As highly effective surface treatments, the localized etching by water vapor and the exposure to nitric acid vapor are used to enhance the number of surface defects. The iron catalyst for the nanotube growth was synthesized by wetting with iron nitrate, by chemical vapor deposition (CVD) of ferrocene, or by electrochemical iron deposition. Carbon nanotubes were subsequently grown on the iron-loaded fibers by pyrolysis of methane or cyclohexane. A highly dispersed, hierarchically structured catalyst support was obtained in this way.

Nitrogen-doped carbon materials have been used as metal-free electrocatalysts in the oxygen reduction reaction (ORR). Some of the N-doped carbon catalysts show remarkable activities in the ORR especially under alkaline conditions, where the activities are often assigned to certain nitrogen groups and surface defects on the carbon surface. To elucidate the electrocatalytic mechanisms, a major challenge is the controlled synthesis of specific nitrogen groups on carbon surfaces. Different methods were employed for the synthesis of nitrogen-doped carbon materials: (a) Catalytic growth of N-doped CNTs from N-containing organic precursors; (b) Post-treatment of oxygen-functionalized CNTs under ammonia atmosphere at elevated temperatures; (c) Post-treatment of oxygen-functionalized CNTs by pyrolyzing N-containing organic precursors at elevated temperatures; (d) Pyrolysis of N-containing polymers. The effect of these methods on the electrocatalytic properties will be discussed.

Fischer-Tropsch synthesis (FTS) is a well-established industrial process for converting synthesis gas derived from coal, natural gas or biomass over iron or cobalt catalysts into mainly linear hydrocarbons exhibiting a broad chain-length distribution. In particular, high synthesis temperatures and Fe-based catalysts are essential for short-chain α-olefins. Fe catalysts supported on active carbon were reported to have a higher activity per unit volume and higher olefin selectivity compared to unsupported catalysts. In my talk, I will report on Fe nanoparticles deposited on oxygen-functionalized CNTs (OCNTs) and on nitrogen-functionalized CNTs (NCNTs). Catalytic testing under industrially relevant conditions was applied to demonstrate the unique properties of OCNTs and NCNTs for the Fe-catalyzed high-temperature FTS. The obtained catalysts showed excellent olefin selectivities, moderate methanation tendency, low growth probabilities and good stabilities. In addition, the Fe/CNT catalysts were applied in CO_2 hydrogenation.

1. S. Kundu, Y. Wang, W. Xia, M. Muhler, *J. Phys. Chem. C.* **2008**, *112*, 16869.
2. W. Xia, C. Jin, S. Kundu, M. Muhler, *Carbon*, **2009**, *47*, 919.
3. S. Kundu, T. Chikka Nagaiah, W. Xia, Y. Wang, S. van Dommele, J. H. Bitter, M. Santa, G. Grundmeier, M. Bron, W. Schuhmann, M. Muhler, *J. Phys. Chem. C.* **2009**, *113*, 14302.
4. S. Kundu, W. Xia, W. Busser, M. Becker, D. Schmidt, M. Havenith, M. Muhler, *Phys. Chem. Chem. Phys.* **2010**, *12*, 4351.
5. C. Jin, T. Nagaiah, W. Xia, B. Spliethoff, S. Wang, M. Bron, W. Schuhmann, M. Muhler, *Nanoscale* **2010,** *2*, 981.
6. W. Xia, J. Masa, M. Bron, W. Schuhmann, M. Muhler, *Electrochem. Commun.* **2011**, *13*, 593.
7. M. Sánchez, P. Chen, T. Reinecke, M. Muhler, W. Xia, *ChemCatChem* **2012**, *4*, 1997.
8. H. J. Schulte, B. Graf, W. Xia, M. Muhler, *ChemCatChem* **2012**, *4*, 350.
9. M. J. Becker, W. Xia, K. Xie, A. Dittmer, K. Voelskow, T. Turek, M. Muhler, *Carbon*, **2013**, *58*, 107.
10. Ly May Chew, P. Kangvansura, H. Ruland, H. J. Schulte, C. Somsen, W. Xia, G. Eggeler, Attera Worayingyong, M. Muhler, *Appl. Catal. A: General* **2014**, *482*, 163.

EV-I-01

Integrative Design for Sustainable Living

Chalermwat Tantasavasdi
Faculty of Architecture and Planning, Thammasat University, Rangsit Campus, Pathum Thani, Thailand
*tchalerm@engr.tu.ac.th

Integrative design represents a holistic architectural design approach that takes various aspects of users' requirements into account along with environmental concerns. In the current and future changing climatic conditions, a number of passive cooling techniques are proved necessary for creating desirable comfort conditions for living. This lecture presents the attempts to create architectural innovations from such approach for the sustainable future, where resources are efficiently utilized while the quality of lives is still maintained.

EV-I-02

Environmental Nanotechnology: Application of Nanomaterials for Environmental Protection and Pollution Abatement

Puangrat Kajitvichyanukul

Director, Center of Excellence on Environmental Research and Innovation,
Faculty of Engineering, Naresuan University, Phitsanulok, Thailand

Nanotechnology is emerging as one of the promising technologies for the environmental protection and pollutant abatement. Many types of nanomaterials have been used for organic and inorganic contaminant removal from water, air, and soil. Currently, many researchers investigate on the synthesis of the novel nanoscale materials and find a way to be used in environmental protection. However, the success of this technology is totally accounted on the properties and reaction mechanism of those invented materials.

To envisage and enhance the application of environmental nanotechnology, this presentation focused on theory, mechanism, and application of the nanomaterials. First, emphasis will be placed on the fundamental properties of nanoparticles that lead to a high performance, success, and failure of those nanoparticles in contaminant removal. Some required properties of nanomaterials for pollutant cleanup can be designed from the synthesis method. The performance of the invented materials can be measured in the lab scale prior to the real application.

Second, the reaction mechanism such as surface adsorption, photocatalytic reaction, and Fenton and photo-Fenton processes occurred during application of nanomaterials for environmental cleaning will be addressed. The examples of existing applications of nanotechnology in the commercial market for clean water, wastewater treatment, and air purification will be given. Many drawbacks and limitations of technology applications such as the required quality of influent or air stream to the reaction unit, the post-treatment requirement, the releasing of nanomaterials to environment, and the cost of technology, are also included.

It is known that the application of nanomaterials in everyday life can cause the releasing of these materials to the environment, and the adverse effect may occur on human health. The last topic of this talk is the nanosafety aspect for the application of nanotechnology. Currently, the safety of nanomaterials mainly assessed on the basis of the pristine substance. The knowledge on the transformation of nanomaterials (NM) is very limited. The nanosafety consideration in applying this technology will base on our works with experts in OECD Working Party on Manufactured Nanomaterials. The precautions in using this technology will be educated and raised to create the sustainability of the nanotechnology for the environment.

EV-I-03

$La_{1-x}A'_xCoO_{3-\delta}$ Perovskite Type Oxides as Catalysts for VOCs Oxidation

Worasarit Sangsui[1], Praewpilin Kangvansura[1], Siritha Asadasuk[2], Attera Worayingyong[1]*

[1]Department of Materials Science, Faculty of Science, Kasetsart University, Bangkok 10900, Thailand

[2]Department of Chemistry, Faculty of Science, Kasetsart University, Bangkok 10900, Thailand

Abstract

$La_{1-x}A'_xCoO_{3-\delta}$ perovskite-type oxides is nonstoichiometry created by substituting the A-site (La) with a bivalent cation (A'=Sr, Ca). For charge balancing, oxygen vacancies form after oxygen desorption resulting structural defects, which are important not only for catalytic activity, but also for oxygen mobility within the perovskites. In the oxidation atmosphere, adsorbed oxygen from the gas phase at different vacant sites leading to charged oxygen adsorption O_2^-, O^-, O^{2-}, play the roles in the catalytic oxidation of volatile organic compounds (VOCs) such as paraffins, and aromatics. Schiff base complex sol-gel method could be used to produce high adsorbed oxygen perovskites type oxides.

Local and electronic structures analyzed by X-ray absorption near edge spectroscopy (XANES) can be used to clarify the high catalytic activity of a perovskte. A bivalent Ca substituted $La_{1-x}Ca_xCoO_{3-\delta}$ (x = 0 - 0.5) perovskites were used as examples. All samples were found to have a rhombohedral structure with *R*-3*c* space group by X-ray diffraction (XRD) and the patterns indicated the cell contraction of $La_{1-x}Ca_xCoO_{3-\delta}$ due to the higher amount of the smaller Ca^{2+} substitution in the La^{3+} sites. Co *K*-edge XANES exhibited the oxidation state of Co as that in the unsubstituted $LaCoO_3$ for all samples. Intensities of Co pre-edge features of all samples indicated distorted octahedral symmetry of Co in the perovskite structures. Transition from low spin to high spin configuration of Co, studied by O *K*-edge XANES, appeared in the samples from x = 0.2. Ca *K*-edge XANES of each sample showed a systematic change in intensities, indicating the changes of calcium local structure in the bivalent substituted $La_{1-x}Ca_xCoO_{3-\delta}$ perovskite. XANES spectral features indicated spin-state transitions of Co^{3+} and oxygen vacancies induced by substitution of La by the bivalent Ca cation.

MR-I-01

Strengthening Competitiveness of JFE Steel Corporation through Research and Development (R&D)

Dr. Seishi Tsuyama
JFE Steel Corporation, Chiba, 260-0835, Japan
s-tsuyama@jfe-steel.co.jp

Keywords: Steel industry, R&D, Technological innovation, Customer satisfaction

Under the corporate philosophy of JFE Steel Corporation, "Contributing to society with the world's most innovative technology", JFE Steel Research Laboratory plots a decisive research and development strategy to enhance the competitiveness of steel industry. By overviewing the numerous technological tasks needing to be solved, the specific action policies are established as follows: 'Innovative processes to improve the quality of products and protect the global environment', 'New products which have the unique and high performances', and 'Basic technologies which support the development of products and processes'. In addition, JFE Research Laboratory takes aim at customers' satisfaction as well as contribution to society.

The representative 'Only one' developments are introduced as follows.

In the field of a sintering process as ion ore pretreatment of iron making, JFE Steel has developed a unique, energy-efficient technology, Super-SINTER® (SINTER: Secondary-fuel Injection Technology for Energy Reduction). The Super-SINTER® is a technology to blow hydrocarbon gases, such as natural gas, into a sinter machine, as a partial alternate for powder coke. The result is greatly enhanced energy efficiency and improved sintered ore quality, which leads to reduce CO_2 emissions in iron making process.

JFE Steel has also developed innovative plate manufacturing technologies incorporated by continuously conducted fundamental research. Among them, Super-OLAC® (OLAC: On-Line Accelerated Cooling) is a revolutionary plate manufacturing technology for high strength, high toughness steel plates with excellent weldability. The Super-OLAC® can realize a high cooling rate substantially equal to the theoretical limit and uniform cooling performance, based on elaborative investigations of heat transfer and boiling phenomena. In addition, JFE has developed the world's first on-line heat treatment process, HOP® (Heat-treatment On-line Process). HOP® is induction heating equipment, installed in plate production line behind the accelerated cooling device, Super-OLAC®. Combination with Super-OLAC® and HOP® has enabled novel metallurgical controlling that cannot be achieved by the conventional TMCP (Thermo Mechanical Control Process). One example of epoch-making products manufactured applying both Super-OLAC® and HOP® is earthquake-resistant linepipe, "JFE-HIPER®". The "JFE-HIPER®" is developed by multi-phase microstructure control with using above mentioned innovative process technology, and won the 2013 R&D 100 Award, presented by the US science and technology publication R&D Magazine. Moreover, JFE steel has some innovative products evolved by R&D activities for automotive use. "JAZ® (JFE Advanced Zinc)" is a steel sheet for

MT-I-01

Some Cast Irons are Special

J.T.H. Pearce.
Panyapiwat Institute of Management (PIM), Nonthaburi, 11120, Thailand.
jthp70@gmail.com

Keywords: alloy cast irons, microstructures, properties, applications.

Most engineers are familiar with the general characteristics and uses of Grey (FC) and Ductile (FCD) Cast Irons especially through their application as vehicle parts such as engine blocks, brake drums and discs, exhaust manifolds and wheel hubs, etc. Less well known are the types of cast irons which are alloyed with elements such as Cr, Ni, Mo, Si, V, Cu, etc. and heat treated, where required, in order to provide special properties such as abrasion, corrosion and heat resistance – these irons are often called the *"Special Cast Irons"*.

This paper reviews the physical metallurgy underlying the control of microstructure and properties in these irons and discusses how service performance depends on correct selection of composition and thermal treatments. The review covers:

- Alloy white irons including Ni-Cr Martensitic White Irons and High Cr Irons which are used for resistance to abrasive & corrosive wear in mining, materials extraction, processing and handling.
- Austenitic Grey and Ductile Irons which are used for resistance to corrosion and heat and also for their physical properties such as low expansion and non-magnetism.
- High Si Ferritic Irons used for heat and corrosion resistance.

Reference is also made to the value of electron microscopy studies in characterizing and understanding the fine scale microstructures in these irons, for example the nature of eutectic, secondary and tempered carbides in High Cr Irons.

PM-I-01

Multi-Component Polymer Processing for Novel Applications

Takeshi Kikutani
Department of Organic and Polymeric Materials, Tokyo Institute of Technology, 2-12-1-S8-32, O-okayama, Meguro-ku, Tokyo 152-8552, Japan
Kikutani.t.aa@m.titech.ac.jp

Keywords: bicomponent spinning, orientation, thermoplastic composites.

In the polymer processing, control of the shape of products as well as control of the high order structure in the products is crucial since the characteristics of polymer products are known to vary significantly depending on their structural parameters such as molecular orientation and crystallinity. In this presentation, utilization of multi-component polymer processing for the better controllability of shape and high order structure will be discussed mainly focusing on the fibers and films of unique functionality.

Optical functionality can be introduced to the polymer products through the control of refractive index and its anisotropy. Interference colored fiber was developed by incorporating the alternating multi-layered structure of two polymers into fiber cross-section. Thickness of each layer was less than 100 nm. Reflective polarizing film (RPF) for the enhancement of the brightness of liquid crystalline display is a typical example for the utilization of multilayered structure with optical anisotropy. We have also tried to produce the RPF by embedding the aligned bicomponent fibers with controlled refractive index anisotropy in the UV cure resin. In this case, good controllability of molecular orientation of sheath and core components in the high-speed melt spinning process was utilized.

Control of molecular orientation also leads to the development of fibers with unique thermal-mechanical characteristics. Highly crimped fibers were produced through melt spinning of side-by-side bicomponent fibers consisting of recycled and virgin poly(ethylene terephthalate), PET. During the pelletizing process of PET flake, polymer was modified through the incorporation of long chain branching. Such modification lead to the enhancement of the strain-hardening behavior. On the other hand, Mutual interaction of two components for the structure development behavior in the melt spinning process was utilized to fabricate sheath-core bicomponent fibers consisting of polyethylene and polypropylene. The fiber, which have a unique characteristics of spontaneous elongation upon annealing, is widely applied for the production of non-woven fabrics of soft touch.

All thermoplastic fiber-reinforced composites can be prepared through the compression molding of sheath-core bicomponent fibers consisting of high melting temperature core and low melting temperature sheath. Composites with structural gradient along the thickness was prepared mimicking the structure of bamboo. Realizing that compression molding of bicomponent fiber is possible if the sheath part is consisting of a crystalline

PM-I-02

Organic Light-Emitting Materials based on [5] Helicene Derivatives

Somboon Sahasithiwat*, Thanasat Sooksimuang, Siriporn Kamtonwong, Waraporn Parnchan and Laongdao Kangkaew

National Metal and Materials Technology Center (MTEC), 114 Thailand Science Park, Paholyothin Rd., Klong Luang, Pathum Thani, 12120, Thailand

*somboons@mtec.or.th

Keywords: Helicene derivative, organic light-emitting diode

A series of new emitters based on a [5]helicene core structure were synthesized and characterized. They were engineered to allow effective internal charge transfer in order to facilitate them to reach high fluorescence quantum yield, Φ_f. Two electron donating groups are attached at position 3 and 12 of a helicene while one or two withdrawing groups are located at position 7 and 8 of a helicene forming a π-shape electron push-pull system. The donor and acceptor groups were varied in order to obtain a variety of compounds. Physical and optical properties of helicenes are affected by their pendant groups. As a result, helicenes that were synthesized possess melting temperature which varies from 265 to 345 ^{o}C. Their band gaps (E_g) are varying from 2.08 to 2.91 eV. Lowest unoccupied molecular orbital (LUMO) energy levels of the compounds are ranging from -2.9 to -3.7 eV and highest occupied molecular orbital (HOMO) energy levels of the compound are ranging from -5.8 to -6.0 eV. The quantum yield as high as 0.96 can be obtained from one of the new compounds. Organic light-emitting diodes using these new compounds as emitting materials were successfully fabricated and characterized.

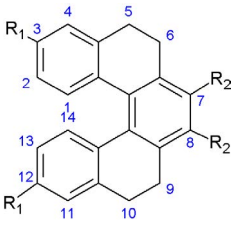

R1 = Donor group; e.g. –OMe, -N(Ph)Me, -N(Ph)$_2$
R2 = Acceptor group; e.g. –CN, -C(=O)-O-C(=O)-, -C(=O)-NR-C(=O)-

SD-I-01

Considerations in Sheet Metal Forming Simulation

Suwat Jirathearanat
National Metal and Materials Technology Center, Thailand Science Park, Pathum Thani, Thailand
suwatj@mtec.or.th

Numerical simulation has undoubtedly become an indispensable tool in sheet metal forming. Finite element analyses are now run routinely in the automotive industry to develop stamping process steps and corresponding dies. With certain simplifications and assumptions adopted in sheet metal forming FE simulation, the calculated results will never completely replace physical die tryouts, but rather drastically reduce lead time spent in die tryouts, leading to near optimized die design. These benefits of FE simulation are evidently diminishing when working with new generations of steel such as Advanced High Strength Steels. Part springback and formability can no longer be predicted as accurately.

This presentation will address the simplifications and assumptions adopted by FEM that might be responsible to theses discrepancies. An emphasis will be put on different material models used in the analyses, including their pros and cons. Also, relevant advancements in material modeling and simulation techniques will be discussed. All these improvements have shown promising results in stamping simulation of AHSS parts.

TTA-I-01

Active Control of Boundary Lubrication

Yonggang Meng[a,*], Xiaoyong Yang[a], Jun Zhang[a]
[a]*State Key Laboratory of Tribology, Tsinghua University, Beijing, 100084, China*
*mengyg@tsinghua.edu.cn

Keywords: Boundary lubrication, Active control, Electrical potential, Ultrasonics.

Interfaces of solid contacts in materials processing and machine elements under severe operation conditions are often lubricated by a thin boundary layer rather than a fluid film. In boundary lubrication, chemical properties of both the contacting solid surfaces and the lubricating media play a vital role in friction and wear. Therefore, most of the researches on boundary lubrication focus on effects of materials and tribochemistry, and not so much attention has been paid to the effects of physical means on boundary lubrication. This article presents some research results of boundary lubrication with the aid of two physical fields. The first approach is to apply an ultrasonic mechanical vibration to the die/workpiece interface in copper wire drawing process under different lubrication conditions. The application of the ultrasonic vibration is helpful for the entraining of lubricant into the diamond die/copper wire contact zone due to intermittent separation between the die conical surface and the wire, and thus resulting in better formation of boundary lubricant film, lower drawing fore and less pick-up scars on the wire surface. The second approach is to apply an external electric field to the contacting surfaces so that the electrical potential of the contacting surface can be shifted from the natural potential (or open circuit potential) to a negative or positive potential within the electrochemical potential window. By changing the electrical potential, the polar components included the lubricant could be attracted to or repelled from the solid surface due to the electrostatic interaction between the charged surface and the polar molecules. In this way, the boundary lubrication can be enhanced or weakened. It has been demonstrated by laboratory tests that such active control of boundary lubrication is possible for water or ester based lubricants with polar additives of surfactants or ionic liquids in a wide range of load condition.

Biomedical Materials and Devices Session

ORAL PRESENTATIONS

BM-O-01

Bleached Shellac as Potential Polymeric Matrix for In Situ Microparticle (ISM)

Pitsiree Praphanwittaya[1, a], Thawatchai Phaechamud[1, b,*]
[1]*Department of Pharmaceutical Technology, Faculty of Pharmacy, Silpakorn University, Nakhon Pathom, 73000 Thailand*
[a] E-mail: barondesperado@hotmail.com, [b] E-mail: thawatchaienator@gmail.com

Keywords: in situ microparticles, non-aqueous

Abstract. Shellac, a biodegradable natural resin purified from insect lac, has been used in several industries especially for a varity of controlled drug delivery systems. Nevertheless, there were negligible researches explored the potential of shellac as in situ microparticles (ISM) applications. This system is an injectable emulsion which can be simply manipulated and comparatively inexpensive. Hence, this can definitely overcome the conventional microparticle. The goal of this study was to primarily utilize shellac to form non-aqueous ISM (shellac-solution dispersed into an external olive oil phase, as oil in oil emulsion) prepared by two-syringe technique and secondly evaluate the obtained non-aqueous ISM in the aspect of emulsifier concentration, type of solvent and emulsion phase ratios on droplet size, and dynamic of microparticle formation. It was discovered that addition of glyceryl monostearate (GMS) as a stabilizer obviously decreased the emulsion droplet size. Moreover, ISM emulsions comprised of 5% w/w GMS in an external phase could form into droplets approximately 65 µm and precipitate in form of microparticles after exposure to phosphate buffer. Furthermore, pyrrolidone was the most appropriate solvent to form massive microparticles with regular shape especially when the ratio of external and internal phases was equal to 7 and 3, respectively. After exposure to phosphate buffer, ISM transformation was occurred. In addition, its droplet size was prone to reduce when the ratio of external phase was higher than 50%. The other finding was that incorporation of doxycycline hyclate had no influence to the amount and size of ISM. Therefore, shellac distinctly exhibited as a potential polymer matrix for ISM formation. Besides, the greater amount of GMS could reduce the size of emulsion droplet and the different volume phase ratio considerably influenced on emulsion size as well as ISM formation. This developed combination between ISM and antibiotic drug will be further investigated as a potential drug delivery system for periodontitis treatment.

BM-O-02

Biocompatibility and Wound Healing Properties of Silk Fibroin/Chitosan/PVA Dressings

Pimpon Uttayarat[a,*], Jarurattana Eamsiri[a], Noppavan Chanunpanich[b,c], Wannee Angkhasirisap[d], Thanee Sukglin[d], Komgrid Charngkaew[e]

[a]*Thailand Institute of Nuclear Technology (Public Organization), Nakhon Nayok, 26120, Thailand*

[b]*Integrated Nanoscience Research Center, King Mongkut's University of Technology North Bangkok, Bangkok, 10800, Thailand*

[c]*Department of Industrial Chemistry, Faculty of Applied Science, King Mongkut's University of Technology North Bangkok, Bangkok, 10800, Thailand*

[d]*National Laboratory Animal Center, Mahidol University, Nakhon Pathom, 73170, Thailand*

[e]*Department of Pathology, Faculty of Medicine Siriraj Hospital, Mahidol University, Bangkok, 10700, Thailand*

*puttayar@alumni.upenn.edu, puttayar@gmail.com

Naturally derived biopolymers such as silk fibroin (SF) protein and chitosan (CS) have attracted considerable attention as potential candidates for various biomedical and biotechnology applications. In this report, SF/CS-based wound dressings were fabricated and evaluated for their mechanical properties, swelling behavior, cytocompatibility and wound healing in rat model. The paste-like solution containing SF, CS and poly(vinyl alcohol) (PVA) were first prepared into films by gamma irradiation at varied PVA concentrations from 20 – 67% (w/w). Films composed of 50% (w/w) PVA (SFCS2PVA) yielded optimal elastic modulus and tensile strength, and exhibited hydrogel properties including the equilibrium degree of swelling of 150% and the remaining gel content of 66.8% after incubation in simulated physiological fluid for 7 days. The *in vitro* cytocompatibility test showed that human dermal fibroblasts could grow and form confluent monolayers in tissue culture media that had been preconditioned with the films. For the *in vivo* evaluation using a full thickness excisional wound model, SFCS2PVA dressings were prepared into 3 different forms; smooth films and patterned films coated with polyvinylidene fluoride (PVDF) nanofibers by gamma irradiation, and sponges by freeze drying technique. All SFCS2PVA dressings were shown to promote would closure similar to the commercial dressing, Tegaderm, within 14 days. Histological results confirmed the near complete epithelialization by day 14 with more than 50% collagen deposition in the dermis by day 5 and low inflammatory responses. Therefore, we have demonstrated that our SFCS2PVA films and sponges are biocompatible and can potentially be applied as dressings for wound healing.

Keywords: silk fibroin, chitosan, gamma irradiation, wound dressings

BM-O-03

Nanofiber Membranes Fabricated from Nang Noi Srisaket 1 Silk Fibroin, Gelatin and Chitosan for Potential used as Barrier Membrane in Guided tissue/bone Regeneration: Part I Fabrication of the Membranes

Pornpen Siridamrong[a,b], Somporn Swasdison[c], Niyom Thamronganansku[d]*

[a] *Department of graduate school, Chulalongkorn University, PhayaThai Road, Phatumwan, Bangkok 10330, Thailand*

[b] *Material Innovation Department, Thailand Institute of Scientific and Technological Research , Khlong Luang, Pathum Thani, 12120, Thailand*

[c] *Department of Oral pathology, Faculty of Dentisty, Chulalongkorn University, PhayaThai Road, Phatumwan, Bangkok 10330, Thailand*

[d] *Department of Prosthodontics, Faculty of Dentisty, Chulalongkorn University, PhayaThai Road, Phatumwan, Bangkok 10330, Thailand*

*E-mail: Niyom@chula.ac.th

Keywords: Electrospinning: Silk fibroin: Gelatin: Chitosan

Barrier membranes are important devices used in directing the growth of new bone in guided tissue/bone regeneration. Different types of membranes prepared from both natural and synthetic materials have recently been used in the treatment of periodontal diseases.
In this study, the nanofiber membranes were fabricated from the mixture of silk fibroin/gelatin/ chitosan at various concentrations of each component in formic acid as solvent. The results demonstrated that when the chitosan content in the mixture increased, the average diameter of the nanofiber decreased and the fiber size distribution was narrow. As the silk fibroin content increased, the tensile strength of the fibers decreased. In addition, at the mixture ratio of silk fibroin (%wt) : gelatin (%wt) : chitosan (vol) =10:20:1, under a high electric field and long electrospinning distance, the fibers were produced as continuous and uniform nonofibers. The formic acid solvent did not affect the electrospinnability or the morphology of the nanofibers. These results, in conjuction with the advantages of biodegradability and antimicrobial effect of these components, indicate that the electrospun nanofibers can be prepared and have the potential to be used as barrier membranes in guided tissue/bone regeneration.

BM-O-04

Synthesis and Fabrication of a Poly(L-lactide-*co*-caprolactone)/Gelatin Blended Scaffold for Use in Articular Cartilage Tissue Engineering

Wichaya Kalaithong[a], Robert Molloy[a,*], Tharinee Theerathanagorn[b]

[a] *Biomedical Polymers Technology Unit, Department of Chemistry, Faculty of Science, Chiang Mai University, Chiang Mai, Thailand 50200*

[b] *National Metal and Materials Technology Center, National Science and Technology Development Agency, Thailand Science Park, Pathum Thani, Thailand 12120*

* Corresponding author, e-mail: robert.m@cmu.ac.th

Keywords: Poly(L-lactide-*co*-caprolactone), gelatin, blend, biodegradable scaffold

Some polymeric fibrous non-woven meshes have been fabricated from solution blends of poly(L-lactide-*co*-caprolactone) (PLC) and gelatin for potential use as biodegradable scaffolds in articular cartilage tissue engineering. PLC statistical copolymers with L:C compositions ranging from 50:50 to 80:20 mol % were synthesized via the bulk ring-opening copolymerization of L-lactide (L) and ε-caprolactone (C) at 120°C for 72 hrs using 0.02 mol % tin(II) octoate, $Sn(Oct)_2$, as the initiator. After purification, the PLC copolymers were obtained in high yield (≥ 95%).

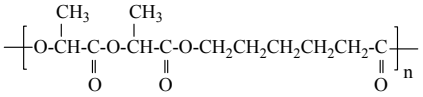

poly(L-lactide-*co*-caprolactone)
PLC

The copolymers were characterized by a combination of analytical techniques, namely: GPC for molecular weight determination, ^{1}H-NMR and ^{13}C-NMR for microstructural analysis, and DSC and TGA for thermal properties. The GPC and DSC results are summarized in the table below.

Copolymer (mol %)	GPC			DSC		
	$M_n \times 10^{-4}$	$M_w \times 10^{-5}$	MWD	T_g (°C)	T_c (°C)	T_m (°C)
PLC 75:25	7.60	1.42	1.87	19.1	98.0	154.3
PLC 80:20	5.84	1.05	1.80	34.5	104.3	159.8
PLC 50:50	7.15	1.46	2.05	-10.0	- *	- *

* The 50:50 copolymer was completely amorphous with no observed T_c or T_m transitions.

In order to make the hydrophobic PLC copolymer more hydrophilic for cell culture, it was solution blended with gelatin using trifluoroethanol (TFE) as the common solvent. Blend solutions were prepared by mixing 10% w/v PLC in TFE with either 10% or 5% w/v gelatin in TFE. The ratio of the two solutions was varied to give PLC:gelatin contents in the final dry blends ranging from 70:30 to 97:3 wt %. Blend solutions were processed using two different techniques: electrospinning and wet spinning. For wet spinning, the non-solvent used was ethanol. Although electrospinning gave a more uniform mesh of nanosized fibres, the non-woven mesh from wet spinning with its much larger pores and less dense network was found to be more suitable in terms of its overall properties as defined by the team of doctors in Chiang Mai University Hospital who are collaborating in this work.

BM-O-05

Synthesis and Preparation of Poly(glycerol sebacate-co-glutamic acid) Scaffold for Bioactive Agent Immobilization

Tharinee Theerathanagorn, Morakot Sakulsombat, Wanida Janvikul*
National Metal and Materials Technology Center, Pathumthani 12120, Thailand
* wanidaj@mtec.or.th

Keywords: poly(glycerol sebacate) (PGS), glutamic acid, scaffold, peptide immobilization

A novel biodegradable and compatible copolymer, poly(glycerol sebacate-co-glutamic acid) (PGS-co-Glu)), was synthesized via stepwise condensation polymerization at 130°C for 24 h under nitrogen atmosphere using different mole ratios of glycerol, sebacic acid and glutamic acid, i.e., 1:1:0.25, 1:1:0.5, and 1:1:0.75. The chemical structure and average molecular weight of the synthesized PGS-co-Glu prepolymers were determined by ^{13}C-NMR spectroscopy and GPC, respectively. The number average molecular weights (M_n) of the prepolymers were found in the range of 1685-3885 g/mol. Highly porous PGS-co-Glu scaffolds were subsequently prepared from the prepolymers by a particle-leaching technique, using NaCl particles as porogen, at 140°C for 16 h. The average pore sizes of the scaffolds were found in the range of 124-135 μm, determined by scanning electron microscopy (SEM). The fabricated porous PGS-co-Glu scaffolds were subjected to low oxygen plasma treatment, to enhance their surface hydrophilicity. The surface wettability of both untreated and plasma-treated PGS-co-Glu scaffolds was evaluated comparatively by water contact angle measurement. The water contact angles on the PGS-co-Glu scaffolds were slightly decreased with an increasing concentration of glutamic acid incorporated and considerably reduced after the plasma treatment. The covalent immobilization of a short-chain red fluorescent-labeled peptide onto the PGS-co-Glu scaffolds was conducted. Greater fluorescent intensities were distinctly observed on the plasma-treated scaffolds, especially ones with higher glutamic acid contents.

BM-O-06

In Vitro Resorbability of Three Different Processed Hydroxyapatite

Faungchat Thammarakcharoen[a], Phee Palanuruksa[b], Jintamai Suwanprateeb[a]*
[a]*National Metal and Materials Technology Center (MTEC),*
114 Paholyothin Road, Klong 1, Klongluang, Pathumthani 12120 Thailand
[b]*Department of Materials Science, Faculty of Science*
Chulalongkorn University, Pathumwan, Bangkok 10330 Thailand
jintamai@mtec.or.th

Keywords: Bone substitutes, Calcium phosphates, Hydroxyapatite, Resorbability.

Hydroxyapatite has been used as bone substitutes in many applications due to its biocompatibility and osteoconductivity. Generally, it is considered to be biostable and shows limited resorption in the body. In some circumstances, resorption of bone substitutes is more desirable since it could accelerate the bone healing process. It is known that processing route is one of the crucial parameters that could affect the properties of materials. Three different processes were employed in this study to fabricate hydroxyapatite samples including low temperature transformation of three-dimensionally printed calcium sulfate (HA1), high temperature sintering of three-dimensionally printed hydroxyapatite (HA2) and high temperature sintering of mold pressed hydroxyapatite (HA3). HA1 was found to contain high porosity and low crystallinity whereas HA2 had high porosity and high crystallinity. HA3 had low porosity, but high crystallinity. *In vitro* resorbability of these samples was studied by submerging all the samples in simulated body fluid (SBF) for 1, 7, 14 and 28 days and determining their phase composition, density change, liquid absorption, ions release and microstructure. It was found that HA1 showed the greatest density loss and liquid absorption followed by HA2 and HA3 respectively. Calcium and phosphorus ions in SBF were observed to decrease with submerging times for HA1 and HA2, but remained constant for HA3. SEM studies showed that new calcium phosphate crystals were found to form on the surface of the HA1 and HA2 samples whereas none was found on HA3. These results suggested that HA1 had the greatest resorbability and calcium phosphate crystals forming ability on its surface followed by HA2 and HA3 respectively. Therefore, porosity and crystallinity of the samples resulting from different processing routes are important factors for *in vitro* resorbability of hydroxyapatite.

BM-O-07

Synthesis and Characterization of Artificial Bone Material using Calcium from a Natural Source

Poj Chutong[1], Nuchthana Poolthong[1], Ruangdaj Tongsri[2]*
[1]Division of materials Technology, School of Energy Environment and Materials, King Mongkut's University of Technology Thonburi, Thailand
[2]Powder Metallurgy Research and Development Unit (PM_RDU), National Metal and Materials Technology Center, 114 Paholyothin, KhlongNueng, KhlongLuang, PathumThani 12120 Thailand Tel: + 662 5646500 Ext. 4702
Email: ruangdt@mtec.or.th

Keywords: Biomaterials, hydroxyapatite, CaO nanoparticles, mechanochemical process.

Hydroxyapatite (HA), with chemical formula of $Ca_{10}(PO_4)_6(OH)_2$,is one of the most popular biomaterials applied as a scaffold or a scaffold component in bone tissue engineering. To synthesize this material using calcium from a natural sourcewill be a good strategy for cost reduction. Waste cockle shells containing abundance of nearly pure calcium carbonate ($CaCO_3$) are ideal source of calcium. In this study, the waste cockle shells were turned to CaO nanoparticles using a simple chemical route. The CaO nanoparticle was used as a starting material to react with calcium hydrogen phosphate ($CaHPO_4$) in the forms of dehydrated and hydratedwith a calcium-to-phosphate (Ca/P) ratio between 1.5-2.0 under a mechanochemical process. Two starting materials were milled for up to 15 hours. The obtained products were characterized by X-ray diffraction technique and scanning electron microscope.The resulting revealed that under the same reaction timethe reaction using the dehydrated $CaHPO_4$ form could produceHA with dehydrated $CaHPO_4$ and the reaction using the hydrated $CaHPO_4.2H_2O$ form could produce HA with β-TCP. The HA yield of the dehydrated $CaHPO_4$ and hydrated $CaHPO_4.2H_2O$ conditions are approximate 71% and 34 % respectively.

BM-O-08

Sintered Titanium-Hydroxyapatite Composites as Artificial Bones

Pongporn Moonchaleanporn[a], Nuchthana Poolthong[a], Ruangdaj Tongsri[b,*]

[a]Division of Materials Technology, School of Energy Environment and Materials, King Mongkut's University of Technology Thonburi, 126 Pracha Uthi, Bang Mod, Thung Khru 10140 Thailand

[b]Powder Metallurgy Research and Development Unit (PM_RDU), National Metal and Materials Technology Center, 114 Paholyothin, Khlong Nueng, Khlong Luang, Pathum Thani 12120 Thailand

Tel: + 662 5646500 Ext. 4702

*Email: ruangdt@mtec.or.th

Keywords: Biomaterials, titanium, hydroxyapatite, artificial bone

The design of engineered bone substitutes takes biocompatibility and mechanical compatibility into account as prerequisite requirements. Titanium (Ti) and hydroxyapatite (HA), with chemical formula of $Ca_{10}(PO_4)_6(OH)_2$, show good biocompatibility and are known as biomaterials. To combine metal powder (Ti) and ceramic powder (HA) as a composite material with mechanical properties comparable to those of natural bones do need strategy. In this work, powder metallurgy process was employed to produce Ti-HA composites, with nominal HA powder contents in the range of 0-100 vol.%. Mixtures of Ti and HA powders were pressed in a rigid die. Sintering was performed in vacuum atmosphere. The as-sintered specimens were tested on biocompatibility in a simulated body fluid (SBF). It was found that processing and materials parameters, including compaction pressure, control the composite microstructures and mechanical properties. Laboratory bone tissue culturing showed that a bone tissue could grow on the artificial bones (sintered Ti-HA composites).

BM-O-09

Prevention of Post-angioplasty Restenosis with MicroRNA-145 nanoparticles-immobilized Coronary Stent in the Rabbit Restenosis Model

Hui-Lian Che[a], HwaJeong Lee[a], Saji Uthaman[a], Won Jong Kim[b] In-Kyu Park[a,*]
[a] *Department of Biomedical Sciences and Center for Biomedical Human Resources (BK-21 Project), Chonnam National University Medical School, Gwangju 501-746, South Korea*
[b] *Center for Self-assembly and Complexicity, Department of Chemistry, Pohang University of Science and Technology, Pohang 790-784, South Korea*
* pik96@chonnam.ac.kr

Keywords: microRNA 145, Disulfide cross-linked low molecular PEI, Hyaluronic acid (HA)-coated stent, Vascular smooth muscle cells

Background: Restenosis is the formation of new blockages at the site of angioplasty or stent placement. In order to avoid this, the suppression of smooth muscle cells near the implanted stent is required. The microRNA 145 is known to be responsible for the cellular proliferation and its enhanced expression has been reported to inhibit the retardation of vascular smooth muscle cell growth specifically.

Objectives: In this study, we developed the microRNA 145 nanoparticles immobilized, hyaluronic acid (HA) coated stent treated restenosis. The disulfide-cross linked low molecular PEI (ssPEI), was used as a gene delivery carrier, because the disulfide bonds are stable in the oxidative extracellular environment but degrade rapidly in the reductive intracellular environment.

Materials & Method: The toxicity of the complex was checked by MTT assay. The miR-145 was labeled with yoyo1 and coated over the stent and the fluorescent microscopy images were obtained. The release from the stent was measured with U V spectrophotometer. The attachment of cells over the microRNA 145 nanoparticles coated stents was observed through TEM. The downstream targeting of the microRNA 145 was checked with western blotting. Balloon injured rabbit model was established to study the effects of microRNA 145 nanoparticle immobilized on the HA-coated stents in vivo by micro CT, immunochemical staining and H&E staining and real time PCR, Northern blot.

Results: MicroRNA 145 nanoparticle immobilized on the HA-coated stent surface exhibited stable binding and localization, followed by time-dependent sustained release for enhanced uptake in neighboring smooth muscle cells. Cellular viability on the nanoparticle-immobilized surface was assessed using A10 vascular smooth muscle cells, and the results revealed that immobilized microRNA 145 nanoparticle exhibited negligible cytotoxicity. MicroRNA 145 nanoparticles immobilized on HA stents were deployed in the balloon-injured external iliac artery in rabbit restenosis model. It was shown that the

microRNA 145 released from the stent suppressed the growth of the smooth muscle at the peri-stent implantation area, resulting in the prevention of restenosis in the post-implantation phase. The qualitative analyses of in-stent restenosis were investigated in rabbit model by micro CT imaging observation. The proliferation status of the vascular tissues located near the microRNA 145 nanoparticles immobilized HA stent was analyzed by immunochemical staining and H&E staining analyses. Moreover, the neo-intima formation over microRNA 145 nanoparticle immobilized HA stent was assessed by elastic fiber staining. Analysis of inflammatory response in vivo was done as inflammatory reaction is a key factor, which could influence in-stent restenosis of polymer coated stents, since we have used HA stent or HA-coated stents with ssPEI carrier with microRNA 145. Enhanced re-endothelialization after implantation of the microRNA 145 nanoparticle coated HA stent was also studied by immunohistochemistry analysis with anti-CD31 antibody. Finally, to identify the molecular mechanism for the reduction in SMC proliferation, which resulted in inhibition of in-stent restenosis, the expression of microRNA 145 and downstream signaling proteins was analyzed by real time PCR and Northern blot in SMC isolated from the treated vasculature.

Conclusion: The miR-145 nanoparticles released from the HA-stent suppressed the growth of the smooth muscle at the peri-stent implantation area, resulting in the prevention of restenosis in the post-implantation phase. Taken together, the implanted microRNA 145-eluting stent mitigated in-stent restenosis efficiently with no side effects and can be considered a successful substitute to the current drug-eluting stent.

BM-O-10

Development of Bacterial Driven Micro Beads for Targeted Anti-cancer Therapy

Saji Uthaman[a], Sunghoon Cho[b], Hwa-Jeong Lee[a], Hui-Lian Che[a] , Sukho Park[b], In-Kyu Park[b*]

[a] *Department of Biomedical Science and BK21 PLUS Center for Creative Biomedical Scientists, Chonnam National University Medical School, 160 Baekseo-ro, Gwangju, 501-746, Republic of Korea*

[b] *School of Mechanical Systems Engineering, Chonnam National University, 77 Yongbong-ro, Gwangju, 500-757, Republic of Korea*

Email: pik96@chonnam.ac.kr

Keywords: Hydrogel, Nanoparticles, Bacteria, Microbead, Targeting

Hydrogels are a unique class of polymeric gels which are three dimensional cross linked hydrophilic networks and one of the most ideal materials for the biomedical application owing to their ability to absorb a large volume of water within in their structure. They also have a highly porous structure which aids in the steady and controlled release of the drug. Our goal is to develop bacterial driven micro-beads which would deliver the drugs inside the tumour and degrade it from inside out. In this work we have developed bacterial driven micro-bead (polyethylene glycol) containing the anti-tumour drug (Paclitaxel) loaded nanoparticles inside as the cargo. In order to have the micro-bead, the tumour targeting capabilities we have attached genetically engineered Salmonella Typhimurium bacteria onto the surface of beads. These bacteria have a dual purpose of both tumor targeting and providing the propulsion force to the micro-beads. This is first of kind of report demonstrating the fabrication of bacteria robot mediated targeted drug delivery system.

BM-O-11

In Vitro Evaluation of Rifapentine-Loaded PLGA Microparticles for Tuberculosis Inhaled Therapy

Thaigarajan Parumasivam[a], Sharon S.Y. Leung[a], Diana Huynh Quan[b], Jamie Triccas[b], Warwick Britton[c], and Hak-Kim Chan[a*]

[a]*Advanced Drug Delivery Group, Faculty of Pharmacy, The University of Sydney, Australia*
[b]*Infectious Diseases and Immunology, Sydney Medical School, Sydney Medical School, The University of Sydney, Australia*
[c]*Tuberculosis Research Program, Centenary Institute, Sydney, Australia*
*E-mail address corresponding author: kim.chan@sydney.edu.au

Keywords: Tuberculosis, Inhalation, Poly (lactic-co-glycolic acid), Rifapentine

Tuberculosis (TB) regiment requires relatively long term oral administration of first-line anti-TB drugs for curing and preventing emergence of drug-resistance. Recently, inhaled administration of drugs encapsulated into micro polymeric particles to the lungs has attracted significant attention, as it offers several advantages compared with local and systemic delivery. These include delivering high drug concentrations to lung tissues, avoiding hepatic first-pass metabolism, prolonging drug residence in the lungs which potentially reduces dosing frequency, as well as targeting alveolar macrophage that harbours tubercle cells proliferation. Poly (lactic-co-glycolic acid) (PLGA) is amongst the most studied microparticulate systems because it (1) is a FDA approved polymer for medical, (2) allows sustained release of the encapsulated drugs to minimize the need for multiple dosing, and (3) is readily phagocyted by alveolar macrophage to enhance macrophage intracellular drug concentration. Nonetheless, limited data are available in the effects of the physiochemical properties of PLGA, such as the monomer (lactide : glycide) ratio and molecular weight, on the aerosol performance. The present study aims to address this knowledge gap. PLGA with a monomer ratio of 50:50, 75:25 and 85:15 and molecular weight ranged 24-240k was studied using rifapentine (RPT) as a model drug. PLGA and RPT were dissolved in acetonitrile at concentrations of 20 mg/ml and 2 mg/ml, respectively. The mixture was spray dried using a B-290 Mini spray-dryer in closed-loop with nitrogen as the drying gas. The particle morphology and size distribution were examined using scanning electron microscopy and laser diffraction respectively. The *in vitro* aerosol performance of the produced powders was assessed using an Osmohaler^{TM} coupled to a next generation impactor (NGI) running at an air flow of 100L/min for 2.4 sec. Macrophage uptake and cytotoxicity profile of these particles were also examined using THP-1 (human monocytic leukemia cell line) and A549 (adenocarcinomic human alveolar basal epithelial cells). All produced particles were spherical with smooth surface and a volume median diameter (D_{50}) was around 2μm (with a span around 2) which is a suitable size for respiratory delivery. The fine particle fraction (FPF_{total}) reached above 55% for all formulations. Apparently, no significant difference was observed in FPF_{total} between all formulations indicating PLGA ratio is not a crucial parameter in PLGA inhalation. Nonetheless, the distribution of drug was found to be a function of monomer ratio, with more drug incorporated on the external surface for particles with higher lactide content. Also, a higher rate of THP-1 phagocytosis was observed for PLGA 85:15 followed by 75:25 and 50:50. Furthermore, cell toxicity analysis indicated PLGA itself does not have any effect on cell viability. Though the monomer ratio and molecular weight did not show any effect in the aerosol performance of particles, the distribution of drugs within the particles was found to be affected by these parameters. This finding may have indirect influence on the controlled release profile of drugs after they are inhaled into the lungs.

BM-O-12

Nano-aggregates of Doxorubicin-conjugated Methoxy poly(ethylene glycol)-b-carboxymethyl Dextran block Copolymer Nanoparticles and their Biological Activity

Sang Joon Lee[a], Hwa Jeong Lee[a], Saji Uthaman[a], Huilian Che[a], In Kyu Park[a], Hyun Chul Lee[b,*]

[a]Department of Biomedical Science and BK21 PLUS Center for Creative Biomedical Scientists, Chonnam National University Medical School, 160 Baekseo-ro, Gwangju, 501-746, Republic of Korea

[b]Department of Microbiology, Chonnam National University Medical School, Gwangju, 501-746, Korea

*Corresponding author. email: hclee@jnu.ac.kr

Keywords: Doxorubicin, Chitosan, Nanoparticle, Cancer cell

Self-aggregation properties of amphiphilic macromolecules accelerates investigation of polymeric drug delivery system as an anticancer drug targeting vehicle. They have several advantages such as small diameter, hydrophilic outershell, and large surfaces compared to traditional drug delivery system. Due to these advantages, core-shell type nanoparticles have small diameters have been considered as an ideal carrier for solid tumor targeting. In this study, we synthesized methoxy poly(ethylene glycol)-grafted carboxymethyl dextran (CMDexPEG) to use as an anticancer drug delivery vehicle. Doxorubicin (DOX) was conjugated to the carboxylic acid of the CMD and fabricated core-shell type nanoparticles. DOX-conjugated CMDexPEG block copolymer formed nanoparticles in water with sizes less than 100 nm. We prepared DOX-resistant CT26 cells by continuous exposure against DOX for a long period. Then, DOX-resistant CT26 cells became were resistant and viability of cells were higher than 80 % at 1.0 μ g/ml of DOX treatment for 2 day. Viability of DOX-sensitive cells was less than 60 % at same concentration. CT26 bearing mice were prepared by implantation of CT26 cells to the back of nude mouse. When tumor diameter was reached to 4~5 mm, DOX or DOX-conjugated CMDexPEG nanoparticles were intravenously injected via tail vein of the mouse. tumor mass was rapidly increased at PBS or empty nanoparticle injection. Otherwise, DOX injection properly inhibited increase of tumor mass compared to PBS and empty nanoparticles. Especially, DOX-conjugated nanoparticles markedly suppressed growth of tumor. These results might be due to that DOX-conjugated nanoparticles improved anticancer drug delivery to the solid tumor and then remained in the tumor tissue. In near infrared (NIR)-dye study, nanoparticles were retained in the tumor tissues for a longer period. We suggest that DOX-conjugated CMDexPEG nanoparticles can be used as a promising candidate for anticancer drug delivery.

BM-O-13

Three-Dimensional Temperature Field Simulation during Selective Laser Melting Process of Cobalt-Chromium Alloy

Pongnarin Jiamwatthanachai[a,*], Sunton Wongsiri[a], Kriskrai Sitthiseripratip[b], Prasert Chalermkanon[b], Marut Wongcumchang[b], Sedthawat Sucharitpwatskul[b], Passakorn Tesavibul[b], Nattapon Chantarapanich[c]

[a]Prince of Songkla Unitversity, Hatyai / Songkla, 90110, Thailand
[b]National Metal and Materials Technology Center, Klongluang / Pathumthani, 12120, Thailand
[c]Kasetsart Unitversity, Sriracha / Chonburi, 20230, Thailand
E-mail address: pongnarinj@gmail.com

Keywords: Temperature Distribution, Finite Element Modeling, Selective Laser Melting, CoCr Alloy

Cobalt chromium alloys ASTM F75 have been used in biomedical applications such as dentistry and orthopedic implants because of their superior properties in corrosion resistance and wear resistance. However, for manufacturing process, the alloy presents low machining-abilities and expensive costs. Selective laser melting (SLM) is an alternative method that was investigated in this research to fabricate three-dimensional parts of the cobalt chromium alloy. The process consists of fusing metallic powders selectively by heat generated from a power laser in a layer by layer fashion. Thus, SLM is a fabrication process, which depends greatly on the variation of temperature. In order to study the distribution of temperature, a three-dimensional transient finite element model has been developed. The effects of processing parameters to the distribution of temperature were evaluated. These parameters included the laser power, the scanning speed and the layer thickness. The simulated results showed the increment of temperature when a higher laser power, a slower scanning speed or a lower layer thickness were applied. The result of the simulation is compared to the result from experimental measurement for verification. The comparison showed that the finite element model is able to be utilized for predicting the variation of temperature in order to facilitate the SLM process.

Biomedical Materials and Devices Session

POSTER PRESENTATIONS

BM-P-01

Growth Factor-Immobilized Polycaprolactone Microspheres as Bioactive Bulking Agent for Soft Tissue Augmentation

Jin Ho Lee[a,*], Tae Ho Kim[a], Se Heang Oh[b]
[a]*Dept. of Advanced Materials, Hannam University, Daejeon 305-811, South Korea*
[b]*Dept. of Nanobiomedical Science, Dankook University, Cheonan 330-714, South Korea*
*jhlee@hnu.kr

Keywords: growth factor, microspheres, bulking agent, soft tissue

Recently, injectable bulking agents are frequently used in soft tissue augmentation. A variety of bulking agents based on natural and synthetic materials have been tried for soft tissue augmentation. In this study, growth factor [basic fibroblast growth factor (bFGF) and/or epidermal growth factor (EGF)]-immobilized polycaprolactone (PCL)/Pluronic F127 microspheres were fabricated to investigate their potential use as an injectable bioactive bulking agent for enhancing soft tissue augmentation. It was expected that the microspheres may stimulate the regeneration of soft tissues by the sustained release of the growth factors as well as provide a bulking effect by the injected volume of the microspheres, and thus allow more effective long-term bulking effect. The PCL/F127 microspheres were fabricated by an isolated particle-melting method, and the growth factors were easily immobilized onto the surfaces of the PCL/F127 microspheres *via* heparin binding. The growth factors immobilized on the microspheres were released with a sustained manner over 4 weeks. From an *in vivo* animal study, it was observed that the mixture of both bFGF-immobilized and EGF-immobilized microspheres lead to effective soft tissue augmentation *[This research was supported by Basic Science Research Program through the National Research Foundation of Korea funded by the Ministry of Science, ICT and future Planning (NRF-2014R1A2A2A04003979)].*

BM-P-02

Peripheral Nerve Regeneration through Asymmetrically Porous Nerve Guide Conduit with Nerve Growth Factor Gradient

Jin Ho Lee[a,*], June Goo Kang[a], Tae Ho Kim[a], Se Heang Oh[b]
[a]*Dept. of Advanced Materials, Hannam University, Daejeon 305-811, South Korea*
[b]*Dept. of Nanobiomedical Science, Dankook University, Cheonan 330-714, South Korea*
*jhlee@hnu.kr

Keywords: nerve guide conduit, nerve growth factor, porous membrane, nerve regeneration

Peripheral nerves function as communication paths between the brain and muscle/organ/skin, and injury to these nerves leads to the severe loss of sensory or motor functions. Although the understanding of nerve regeneration and the development of surgical techniques are rapidly growing, sufficient restoration of damaged nerves still remains a big challenge. Recently, artificial nerve guide conduit (NGC) to bridge the gap between severed peripheral nerve stumps has been demonstrated to be a promising strategy for the treatment of damaged nerves. It is well-known that the nerve regeneration is mediated by gradients of bioactive molecules including nerve growth factor (NGF; chemotaxis). In this study, the NGF gradient NGC was fabricated by rolling an asymmetrically porous polycaprolactone (PCL)/Pluronic F127 membrane with NGF gradient. The NGF loading amount and NGF release profile along the NGF gradient were investigated. The NGF immobilized on the NGC was continuously release up to 28 days, regardless of the NGF concentration. The nerve regeneration behaviours through the NGF gradient NGC were compared to the NGC with uniform NGF immobilization using a SD rat with a 2 cm long sciatic nerve defect. From the animal study, it was recognized that the NGF gradient NGC shows greater nerve regeneration behavior than the uniform NGF group. Based on our findings, it is suggested that the NGC with asymmetrically porous structure and gradient of NGF concentration can be a simple and effective therapeutic technique to accelerate the reinnervation rate and provide sufficient functional recovery of peripheral nerves *[This work was supported by grants of Korea Ministry of Health & Welfare (Grant Nos. A100140 & HI14C0522)]*.

BM-P-03

Simplified Synthesis of Gold Nanoshells from Gold Foil for Medical Applications

Nakadech Youngwilai*, Suttinun Phongtamrug
King Mongkut's University of Technology North Bangkok, Bangkok, 10800, Thailand
*nakadechy@kmutnb.ac.th

Keywords: gold nanoshell, gold foil, photothermal therapy.

The specific aim of this study is to simplify the way to synthesize the Au nanoshells that exhibit properties suitable to be employed in medical applications in terms of the proper core size and shell thickness and the ability to absorb light in the near-IR region, which could be further applied for photothermal treatment of cancer. In this study, gold-coated silica nanoshells were simply prepared via chemical reduction of gold ions extracted from gold foil on to the silica core prepared via sol-gel method using trisodium citrate as a reducing agent and 3-aminopropyltriethoxysilane as a core surface modifier. The synthesized gold nanoshells were characterized by UV-Visible Spectroscopy, Transmission Electron Microscopy (TEM) and Dynamic Light Scattering (DLS) techniques. The synthesized gold nanoshells were found to be well-dispersed and spherical with the average particle size around 150 nm. The gold nanoshells were found to strongly absorb light in the near-IR region (~800 nm), where the photothermal cancer therapy is essentially performed. Effects of preparation variables such as heating rate, concentration, and degree of reduction, on the silica core radius and thickness of the gold shell were also revealed. The information obtained from this study provides useful guidelines to simply prepare gold nanoshells from gold foil and fine tune the synthetic process to obtain the gold nanoshells with the optimum optical and physical properties suitable for medical applications.

BM-P-04

Metrodidazole *In Situ* Forming Eudragit RS Gel Comprising Different Solvents

Jongjan Mahadlek[a,*], Thawatchai Phaechamud[b]

[a]*Pharmaceutical Intelligence Unit Prachote Plengwittaya, Faculty of Pharmacy, Silpakorn University, Nakhon Pathom 73000, Thailand.*

[b]*Department of Pharmaceutical Technology, Faculty of Pharmacy, Silpakorn University, Nakhon Pathom 73000, Thailand*

*jongjan.m@hotmail.com

Keywords: *In situ* forming gel, Eudragit RS, metronidazole, solvents

In situ forming gel by solvent exchange is one of dosage form as drug delivery system for periodontitis treatment. The system was injected into the desired site then transformed by solvent diffuse out and aqueous diffuse in for the drug liberation. Novel *in situ* forming Eudragit RS gels loading 1, 5 and 10%w/w metronidazole were developed using three solvents such as *N*-methyl pyrrolidone (NMP), 2-pyrrolidone and dimethyl sulfoxide (DMSO). Eudragit RS (15-40%w/w) was used as polymer. Their properties were determined including viscosity, rheology, gel formation, syringeability, drug release and antimicrobial activity. The viscosity of the gel systems in all solvents were increased with drug and polymer concentration dependence with Newtonian flow behavior. The transformation into gel of 25, 20 and 20%w/w Eudragit RS in NMP, DMSO and 2-pyrrolidone was initiated in phosphate buffer pH 6.8. The NMP systems exhibited the lowest work of syringeability through 18 G syringe. The work of syringeablity of the NMP system comprising 40%w/w Eudragit RS and 5%w/w metronidazole was 24.54 ± 1.91 N.mm. Drug release from dialysis tube of DMSO systems was slower than that of NMP and 2-pyrrolidone systems, respectively. Antimicrobial activity against *Staphylococcus aureus* of the systems comprising 40%w/w Eudragit RS and 5%w/w metronidazole using 2-pyrrolidone as solvent was greater than that using NMP and DMSO, respectively. The antimicrobial activity was increased as the increased drug amount. Therefore, the solvent type affected the viscosity, gel formation, syringeability, drug release and antimicrobial activity of Eudragit RS systems. These novel developed systems could sustain the drug release and inhibit the bacterial growth hence they were interesting systems for periodontitis treatment.

BM-P-05

Oxidized Regenerated Cellulose/Polycaprolactone Composite for Use as a Synthetic Dura Mater

Thunyanun Theeranattapong [a], Ticomporn Luangwattanawilai [a], Jintamai Suwanprateeb[b], Waraporn Suvannapruk[b], Sorayouth Chumnanvej[c] and Warinkarn Hemstapat[a, *]

[a]*Department of Pharmacology, Faculty of Science, Mahidol University, Bangkok, 10400, Thailand*

[b]*National Metal and Materials Technology Center (MTEC) National Science and Technology Development Agency (NSTDA), Ministry of Science and Technology, Pathumthani, 12120, Thailand*

[c]*Neurosurgery Unit, Surgery Department, Faculty of Medicine, Ramathibodi Hospital, Bangkok, 10400, Thailand*

*E-mail: Warinkarn.hem@mahidol.ac.th

Keywords: synthetic dural substitute, oxidized regenerated cellulose, polycaprolactone

An inadequate dural closure is one of the most challenging problems for neurosurgeons during the surgical procedures. A repair of the dura mater by natural or synthetic materials is often needed. This should satisfy fundamental criteria for example preventing cerebrospinal fluid leakage, exhibiting similar mechanical properties to the natural dura mater and not inducing foreign body reaction or inflammation. Oxidized regenerated cellulose (ORC) and polycaprolactone (PCL) have been extensively used as hemostatic agent and implant in many biomedical applications due to their long term proven safety, biodegradability and biocompatibility. This study investigated the potential of using a combination of ORC and PCL as a novel dural substitute. ORC/PCL composites were prepared by solution infiltration of ORC sheet with PCL solution (Mw ~ 80,000) at various concentrations ranging from 10% to 50% w/w. Characterizations including density, tensile properties, microstructure were then performed. It was found that the density of all formulations did not differ and were in the range of 0.5-0.6 kg m^{-3}. Microstructure of the samples typically comprised a bilayerd structure having a PCL layer on one side and the ORC/PCL mixed layer on another side. Tensile modulus and strength initially decreased with increasing PCL concentration for up to 20% and re-increased again with further increasing PCL concentration. Elongation at break of all formulations was not significantly different. Both physical and mechanical properties of the samples were found to be similar to those of natural human dura mater.

BM-P-06

Preparation of Photopolymerizable PEG-based Hydrogel

Sasithon Phromma[a], Achara Kleawkla[a], Tareerat Lertwimol[b], Tharinee Theerathanagorn[b], Morakot Sakulsombat[b], and Wanida Janvikul[b]*

[a]Department of Chemistry, Faculty of Science, Maejo University, Chiang Mai 50290, Thailand

[b]National Metal and Materials Technology Center, Pathumthani 12120 , Thailand

*wanidaj@mtec.or.th

Keywords: poly(ethylene glycol), hydrogel, photopolymerization

The purpose of this study was to develop photopolymerizable hydrogels to be used as constructs in tissue engineering study. The cross-linked hydrogels were initially prepared from the mixtures of glycidyl methacrylate (GMA), poly(ethylene glycol) (PEG), poly(ethylene glycol) dimethacrylate (PEGDMA) (a crosslinker), and irgacure 819 (a photo-initiator). Each mixture was cured under a halogen lamp (12 V, 75 W, 480 mW/cm^2) to yield flexible hydrogels. The weight ratio of all starting reagents used in the mixtures and curing time were varied in order to optimize the mechanical property of the desired cross-linked hydrogel. The hydrogels prepared by using 3, 6, and 9 min curing times were cut into specimens with the dimension of 1x1x0.4 cm^3 (as shown in Figure 1) and subsequently washed with ethanol and then deionized water to remove any remaining chemical residues. The purified hydrogels were finally freeze-dried. The chemical structure, surface morphology and swelling ability of the hydrogels were determined by FT-IR spectroscopy, scanning electron microscopy (SEM) and a gravimetric method, respectively. The cytotoxicity of the hydrogels was evaluated using a direct contact assay with L929 cells. The results revealed that the prepared hydrogels were non-cytotoxic and possessed good mechanical strength measured by DMA.

Figure 1. Photopolymerized hydrogels (1x1x0.4 cm^3) cured under a halogen lamp for 3 (left), 6 (middle), and 9 (right) min.

BM-P-07

Effect of Surface Charge on Incorporation of Gold Nanoparticles in Poly(*N*-isopropylacrylamide) Nanogels

Phornsawat Baipaywad[a], Soo-Hong Lee[b], In-Kyu Park[c], Won Jong Kim[d], Hansoo Park[a,*]

[a]*School of Integrative Engineering, Chung-Ang University, Seoul, Republic of Korea*
[b]*Department of Biomedical Science, CHA University, Republic of Korea*
[c]*Department of Biomedical Science, Chonnam National University Medical School, Republic of Korea*
[d]*Department of Chemistry, POSTECH, Republic of Korea*
*E-mail: heyshoo@cau.ac.kr

Keywords: Poly(*N*-isopropylacrylamide), Nanogels, Gold Nanoparticles, Surface Charge

Gold nanoparticles (AuNPs) have been widely investigated for various biomedical applications such as biosensors and delivery of genes and proteins. Recently, they were modified with peptides or incorporated with polymers to prohibit aggregation of AuNPs and increase cell penetration, specificity to targets, and stability in aqueous solutions. In this study, poly(*N*-isopropylacrylamide) (PNIPAM) based nanogels were formed by a conventional radical polymerization method. The nanogels containing AuNPs were then prepared through the reduction of $HAuCl_4$ under different pH conditions. In addition, the effect of PNIPAM formulation on the encapsulation of AuNPs using different comonomers was also examined. Transmission electron microscopy (TEM) results confirmed multiple non-aggregated AuNPs in PNIPAM nanogels with positive and neutral surface charges while PNIPAM nanogels with negative surface charges did not have well-disperse AuNPs in the gels. UV-Vis spectra measurements also exhibited different absorption intensity depending on PNIPAM formulations, due to different amount of gold nanoparticles embedded in nanogels.

BM-P-08

Comparison of Reducing Agents for Keratin Extraction from Human Hair

Jitsopa Chaliewsak[a], Sireerat Charuchinda[a,*], Manchumas Prousoontorn[b]

[a]*Department of Materials Science, Faculty of Science, Chulalongkorn University, Bangkok 10330, Thailand*

[b]*Department of Biochemistry, Faculty of Science, Chulalongkorn University, Bangkok 10330, Thailand*

* sireeratc@gmail.com

Keywords: keratin, extraction, reducing agent

Keratins are natural proteins which are insoluble fibrous structure and can be found in hair, feather, nail, horn, hooves and epidermis of animals. Keratins can be classified into 3 types based on their structure which are α-keratin, β-keratin and ɣ-keratin. The α-keratin has α-helix structure and found in mammals. The β-keratin has β-pleated sheet structure which is harder than α-keratin and found in poultry and reptiles. The ɣ-keratin is a matrix protein which has α-keratin and β-keratin embedded to form protein structures. Keratins are insoluble in usual protein solvents and can withstand light, water and weather changes because of disulfide bonds cross-linking between cystine amino acid in their structures. Keratins are commonly used in cosmetics such as hair treatment and biomaterials such as tissue engineering, drug permeation and wound healing because of their biocompatibility, biodegradability, mechanical durability and availability. Furthermore, keratins can be used as flame retardants for cotton fabric. A large amount of keratins remain as wastes from various industries such as poultry feather from food industries and wool from textile industries. Moreover, human hair waste from hair salon is one of keratins wastes because of the increasing number of population. Generally, keratins wastes are used as nitrogenous fertilizer and landfills materials but they can lead to environmental pollution because their high stable structures are difficult to degrade. Therefore, the chemical treatment (keratin extraction) to break disulfide bonds of keratins wastes using reducing agents and to break hydrogen bonds using protein denaturing agents such as urea or thiourea is an effective waste management system of keratins wastes. In this study, three different types of reducing agents having a different number of thiol group and functional group which are mercaptoethanol, thioglycolic acid and 1,2 ethanedithiol were used to break disulfide bonds. In addition, 2.6 M thiourea and 5 M urea with 5% of the above reducing agents were used to extract keratins at 50˚C under atmosphere pressure and various times. The effects of reducing agents and times on keratins yield were investigated. The dry weight yield of keratins and protein yield were determined using an electronic balance and by the colorimetric method of Bradford. The functional group and chemical composition of keratins were characterized using Fourier transform infrared spectroscopy (FTIR). The thermal properties of keratins were investigated using thermal gravimetric analysis (TGA) and differential scanning calorimetry (DSC) for biomaterials application and their processing. Furthermore, the morphological change of hair surface using scanning electron microscope (SEM) was also examined.

BM-P-09

Physical Properties of Xyloglucan/bacterial Cellulose Composite Film Plastized with Glycerol

Pattarapa Jittavisuttiwong[a], Saranyou Oontawee[a], Chanan Phonprapai[a*]
[a]*Department of Biotechnology, Faculty of Science and Technology, Thammasat University (Rangsit Campus), Klong Luang, Pathum Thani, 12121, Thailand*
*chanan@tu.ac.th

Keywords: xyloglucan, bacterial cellulose, glycerol, physical properties

In the past, tamarind seeds were known as food industrial wastes. But, several years ago, their kernels were extracted to obtain the xyloglucan for food, cosmetic, and medical applications. This study aimed to prepare and characterize the xyloglucan (XG) /bacterial cellulose (BC) composite films which were plastized with glycerol (GLY) for cosmetic applications. In the experiments, the controlled condition of the films were prepared by using the solution casting method with varying XG:GLY ratios of 10:90, 20:80, 30:70, 40:60, and 50:50, causing these films had an equivalent controlled weight per area of 225 g/m^2. However, these films were found to be wrinkle which could not be analyzed the physical properties. Thus, each ratio was prepared with the addition of BC to improve their appearance and physical properties. Due to the limitation of mixture volume, BC was firstly dispersed in GLY to decrease the mixture volume. BC contents were varied by following the GLY content, where total weight of the films was increased with the BC content whereas the weight per area of XG:GLY was fixed at 225 g/m^2. The obtained (XG:GLY)-BC films were (10:90)-9%, (20:80)-8%, (30:70)-7%, (40:60)-6% and (50:50)-5% films. Then the prepared films were observed their morphology, and investigated the stickiness using Texture Analyzer. The observation revealed that the BC addition could provide the non-wrinkled films, but the low transparent films could be seen from the BC addition films. To obtain the physical characteristics of the films, stickiness (SN), adhesiveness (AN), and cohesiveness (CN) were measured. The results showed that an increase of GLY and BC could trendily increase SN and CN of the films. The (10:90)-9% film did give the highest SN of 57.64 g and AN of 1.01 g.sec. However, (10:90)-9% and (20:80)-8% films gave an insignificant difference of SN and AN. Meanwhile, (30:70)-7% film was found to give the lowest SN of 10.77 g and AN of 0.21 g.sec. Moreover, the influence of GLY and BC on the decrease of CN was only found on (30:70)-7% film. Thus, it could be concluded that the addition of BC into the films could give the non-wrinkle of the films, and the increase of GLY could provide the high adhesive films that suitable for applying on the skin as a transdermal patch. In the future, the films will be added with the selected herbal extracts in order to provide the desired biological activities such as anti-oxidation, anti-microbes, and anti-melanogenesis to the films.

BM-P-10

Graphene Antenna: Design and Analysis for Implantable Medical Devices

Nateetorn Fugto[a], Suriya Chaisiri[b], Sirinrath Sirivisoot[a]

[a]Biological Engineering, Faculty of Engineering, King Mongkut's University of Technology Thonburi, Thung Khru, Bangkok, 10140, Thailand

[b]Automation Engineering, Department of Instrumentation and Electronic Engineering, Faculty of Engineering, King Mongkut's University of Technology North Bangkok, Bangsue, Bangkok 10800, Thailand

nateetorn.kmutt@mail.kmutt.ac.th, srchsr934@gmail.com, sirinrath.sir@kmutt.ac.th

Keywords: Orthopedic Implant, Nano-patch Antenna, Mathematical Simulation

The implantable antenna, biomedical devices is used as a wireless communication device to send and receive data signal between the implantable circuit inside the human and body and the electronic receiver outside human body. However, implantable antenna design still has many problems including a large size of antenna, biotoxicity of antenna materials to the human tissue caused by metallic material, and the low efficiency of radiation of implantable antennas. This work is a mathematical method to solve these problems. We developed a new design of antenna using mathematical modeling with MATLAB programming. Importantly, graphene was used as a patch antenna since it has an excellent biocompatibility, and titanium, widely used for orthopedic implants, was used as a dielectric substrate to reduce the antenna size. We used an ANSYS software program to simulate our new design antenna in two environments, which are an inside human body and an outside one in order to test the efficiency of antenna radiation. The results in simulation of designed graphene antenna in two environments are still in progress.

BM-P-11

Osteoblast Responses on Graphene Oxide Electrodeposited on Anodized Titanium for Orthopedic Implants

Pacharaporn Tanurat[a,*], Sirinrath Sirivisoot
[a] *Biological Engineering Program , Faculty of Engineering, King Mongkut's University of Technology Thonburi, Bangkok,10140, Thailand*
E-mail phtanurat@gmail.com

Keywords: TiO_2 nanotubes, graphene oxide, orthopedic application, anodization

Using graphene oxide coating on biomaterial surfaces is a great potential for long-term use of orthopedic implants due to its antibacterial property. Anodization is one of many methods that have been used to modify titanium implant surfaces in order to increase osseointegration. In this study, anodized titanium coated with graphene oxide (ATi-GO) was prepared using anodization and electrodeposition of graphene oxide, respectively. Scanning electron microscopy (SEM) and atomic force microscopy (AFM) were used to investigate surface morphologies. Their physiochemical properties were evaluated by energy-dispersive X-ray spectroscopy (EDX), X-ray diffractrometer (XRD) and attenuated total reflection-Fourier transform infrared spectroscopy (FTIR). Furthermore, cell proliferation of pre-osteoblasts (bone-depositing cells) was investigated. The results from ATi-GO, GO coated on titanium (GO-Ti), anodized titanium (ATi), and pure titanium (Ti) were compared and discussed. In addition, enzyme linked immunosorbent assay (ELISA), calcium assays and osteocalcin immunofluorescence analyses will be used to evaluate osteogenic differentiation of the cells.

BM-P-12

The Effect of Calcium on the Corrosion Rate of HA-coated Mg-Ca Alloy

Kwidug Yun[a,*], **Sangwon Park**[a]

[a]*Chonnam National University, Gwangju, 500-757, Republic of Korea*

*ykd@jnu.ac.kr

Keywords: Biodegradable metal, Magnesium, Hydrogen evolution, Corrosion rate.

Magnesium is well known for its good mechanical properties and biocompatibility as biodegradable metal for medical device. However, its high corrosion rate typically limits the use of magnesium in several occasions. Thus, in this article magnesium-based alloys were studied to improved corrosion resistance. Magnesium alloy containing calcium, which is a major component of human bone and essential in chemical signaling with cells, was created, and coating was applied on the surface using sol-gel method. To identify the corrosion properties of a magnesium alloy with calcium coated with hydroxyapatite(HA) in TAS solution were investigated using the hydrogen evolution experiment. As a result, comparing the Mg-0.5 wt.% Ca with Mg-5 wt.% Ca, the hydrogen evolution rate increased with increasing calcium content. With the findings from this study, researches on magnesium alloys containing calcium can be a biodegradable implant material in medical fields.

Ceramic-based Materials Session

ORAL PRESENTATIONS

CM-O-01

Synthesis and Photocatalytic Activity Enhancing for TiO_2 Photocatalyst by Doping with Lanthanum

Zuhra Zuhra*, Komala Pontas and Husni Husin
[a]*Chemical Engineering Department, Engineering Faculty, Syiah Kuala University, Darussalam, Banda Aceh, 23111, Indonesia*
*zuhra74@yahoo.com

Keywords: TiO_2, lanthanum, sol-gel, methylene blue

The La^{3+}-TiO_2 photocatalysts are prepared by doping lanthanum ion into TiO_2 structure developed by sol-gel method. The as-prepared La^{3+}-TiO_2 samples are characterized by X-ray Diffraction (XRD) and Scanning Electron Microscopy (SEM). The results showed that the crystallinity of anatase improved by using La^{3+} doping. The photocatalytic activities of La^{3+}-TiO_2 are examined by methylene blue (MB) aqueous solution under UV light. It is found that the photocatalytic activity of La^{3+}-TiO_2 depend strongly on the doping content of La, and sample La^{3+}-TiO_2 shows the highest photocatalytic activity for the degradation of MB. The photocatalytic activity of La-doped TiO_2 photocatalysts exceeds that of pure TiO_2 photocatalyst with optimum La is kept at 1.2%, due to the sample with good crystallization. La modification is discussed by considering the enhanced particle dispersion, the higher crystallization degree of anatase and the increase of the surface oxygen vacancies and/or defects, which facilitates the adsorption of methylene blue molecules and also inhibits the recombination between photoelectrons and holes, resulting in the higher efficiency of photocatalysis. It was concluded that the enhancement of MB photodegradation using the La^{3+}-TiO_2 catalysts mainly involved in both the improvement of the organic substrate adsorption in catalysts suspension and the enhancement of the separation of electron-hole pairs owing to the presence of Ti^{3+}. Furthermore, it is also found that La^{3+}-TiO_2 catalysts display super structural stabilities during photocatalytic degradation, and it could recover their photocatalytic activity, suggesting a promising utilization of such photocatalyst.

CM-O-03

The Effects of Solvents on the Solvothermal Synthesis of $BiVO_4$ Photocatalyst Powders

Thanomsri N.[a], Mongkolkachit C.[b], Sato T.[c] and Sujaridworakun P.[a,d,*]

[a]*Research Unit of Advanced Ceramics, Department of Materials Science, Faculty of Science, Chulalongkorn University, Bangkok 10330, Thailand*

[b]*National Metal and Materials Technology Center, Klong luang, Pathumthani, 12120, Thailand*

[c]*Institute of Multidisciplinary Research for Advanced Materials (IMRAM), Tohoku University, Sendai 980857, Japan*

[d] *Center of Excellence on Petrochemical and Materials Technology, Chulalongkorn University, Bangkok 10330, Thailand*

* pornapa.s@chula.ac.th

Keywords: bismuth vanadate, solvothermal process, rhodamine B, photocatalyst, ethanol

In this study, the effects of different solvents such as ethanol, ethylene glycol, glycerol on the preparation of $BiVO_4$ via solvothermal process, and the influent of calcination heat treatment were studied. The crystal structure, surface area, morphology and optical properties of the obtained $BiVO_4$ particles were investigated by means of X-ray Diffraction (XRD), Brunauer Emmett Teller method (BET), Scanning electron microscope (SEM) and UV-Vis reflectance spectroscopy (UV-vis DRS), respectively. XRD patterns reveal that all of the obtained $BiVO_4$ samples prepared by solvothrmal at 130^{o}C for 3 h have monoclinic structure. The UV-vis DRS demonstrates that the band gaps of prepared $BiVO_4$ are about 2.28-2.38 eV. The photocatalytic activity was evaluated by photo-degradation of rhodamine B (Rh B) solution under visible light irradiation (λ>420 nm). As the results, the $BiVO_4$ prepared by using ethanol having high surface area showed the highest visible light photocatalytic activity compared to using glycerol and ethylene glycerol, respectively. Furthermore, the photocatalytic activity of $BiVO_4$ prepared by using ethylene glycerol and glycerol could be enhanced by calcination heat treatment at 500^{o}C for 2 h.

CM-O-04

Facile Green Route for the Synthesis of Iron-doped MGO Nanoparticles by Phyllanthus Acidus: Structural, Photoluminescence and Photocatalytic Activity

H. P. Nagaswarupa[a,*], M. R. Anilkumar [a], H. Nagabhushana[b], S. C. Sharma[c], Y. S. Vidya[d], K. S. Anantharaju[e], S. C. Prashantha[a], C. Shivakuamra[c], K. Gurushantha[a] and K R Vishnu Mahesh[f]

[a] *Department of Science, Research center, East West Institute of Technology Bangalore - 560091, Karnataka, India*

[b] *Prof. C.N.R. Rao Centre for Advanced Materials, Tumkur University, Tumkur - 572 103 Karnataka, India*

[c] *Vice Chancellor, Chhattisgarh* Swami Vivekananda Technical University, North Park Avenue, Sector-8, *Bhilai – 490009, Chhattisgarh, India*

[d] *Department of Physics, Lal Bahadur Shastry Government First Grade College Bangalore -560 032, Karnatak, India*

[e] *Solid State and Structural Chemistry Unit, Indian Institute of Science Bangalore - 560 012, Karnatak, India*

[f] *Department of Chemistry, ACS College of Engineering Mysore Road, Bangalore-560074, Karnataka, India*

* nagaswarupa77@gmail.com

Keywords: *Phyllanthus acidus*, Green synthesis, MgO: Fe NPs, Photodecolorization, Photoluminescence

Herein we report for the first time, synthesis of MgO: Fe^{3+} (0.1 – 5mol %) nanoparticles (NPs) by simple and environmental friendly route using *phyllanthus acidus* biomass as a fuel. PXRD, SEM, TEM, FTIR, UV–Visible absorption, photoluminescence (PL) studies were performed to ascertain the formation and characterization of NPs. X- ray diffraction and Rietveld analysis confirmed the cubic crystal system with Space group *Fm-3 m*. The surface morphology of samples show uniform spherical shaped nanoparticles. TEM and SAED studies clearly indicated the formation of high quality cubic nanocrystals. Further, photocatalytic activities of NPs were probed for the decolorization of methylene blue under UVA light irradiation. Enhanced photocatalytic activity was observed for 4 mol % Fe-doped MgO under UVA light irradiation. This can be attributed to effective separation of charge carriers and large red shift in the band gap to visible region. The influence of crystallite size and dopant concentration on the charge carrier trapping -recombination dynamic was investigated and correlated with photoluminescence (PL). The trend of inhibitory effect in the presence of different radical scavengers was $SO_4^{2-} > Cl^- > C_2H_5OH > HCO^{3-} > CO_3^{2-}$. The PL spectra of MgO: Fe^{3+} (0.1 – 5 mol %) with the excitation at 378 nm records the bands at ~ 515 nm ($^4E + {}^4A_1 ({}^4G) \rightarrow {}^6A_1 (6S)$), ~ 620 nm ($^4T_2 ({}^4G) \rightarrow {}^6A_1 (6S)$) and ~ 721 nm ($^4T_1 ({}^4G) \rightarrow {}^6A_1 (6S)$). The visible emission gradually increased with increase in dopant concentration up to 0.5 mol % and then decreased due to the concentration quenching effect. The present study successfully demonstrated bio template green synthesis of MgO: Fe^{3+} NPs with superior photocatalytic and PL properties.

CM-O-06

The Effect of Rotational Speed on Steel Pipe Lined Fe-WB based Composite Coating by Centrifugal-SHS Process

Saowanee Singsarothai[a,b], Vishnu Rachpech[b] and Sutham Niyomwas[a,c,*]
[a]Ceramic and Composite Materials Engineering Research Group (CMERG), Center of Excellence in Materials Engineering (CEME), [b]Department of Mining and Materials Engineering, [c]Department of Mechanical Engineering, Faculty of Engineering, Prince of Songkla University, Hat Yai, Songkhla, Thailand
* sutham.n@psu.ac.th

Keywords: Fe-WB based composite coating, Centrifugal-SHS process.

The Iron-Tungsten boride based composite was coated on the inner surface of steel pipes by centrifugal-self-propagating high-temperature synthesis (centrifugal-SHS) process. The precursors were prepared by a stoichiometric ratio of wolframite mineral ($Fe(Mn)WO_4$), aluminum (Al) and boron oxide (B_2O_3). Phase composition and microstructure of composite coating were investigated by X-ray diffraction (XRD) and scanning electron microscope (SEM). On this study, depending on the rotation speed, the highest rotation speed (2250 rpm) produced highest micro-hardness of the composite (1699 HV).

CM-O-07

Enhancement of Industrial Boiler Efficiency by High Thermal Absorptivity Coating

Natthawut Nunkaew[1,*], Koichi Fukuda[1], Jaturong Jitputti[1] and Songsak Klamklang[2]
[1]Research and Development Center, SCG Chemicals Co.,Ltd., Bangkok, 10800, Thailand
[2]Texplore Co.,Ltd., Bangkok, 10800, Thailand
*natthawn@scg.co.th

Keywords: Coating, Boiler, Thermal absorptivity

Industrial boiler unit is one of major energy-consuming units in a petrochemical plant, supplying steam to other processes for olefin production. In this research, high radiant absorptivity coating was developed and applied onto the surface of boiler (metal) tube in order to enhance absorbed radiation by the tube, resulting in increased energy efficiency of the unit. The result in lab-scale showed that boiler tube coated by high radiant-absorptivity material could absorb the heat more effectively than bare tube. Moreover, this coating material also provides other benefits such as prevention of surface damage from high temperature operation and scale formation on surface, etc.

CM-O-08

Effects of Water Temperatures on Water-Soluble Binder Removal in Ceramic Materials Fabricated by Powder Injection Moulding

Wantanee Buggakupta[1,3*a], Nutthita Chuankrerkkul[2*b] and Juthathep Surawattana[1]

[1]*Department of Materials Science, Faculty of Science, Chulalongkorn University, Bangkok, 10330, Thailand*

[2]*Metallurgy and Materials Science Research Institute, Chulalongkorn University, Bangkok, 10330, Thailand*

[3]*Center of Excellence on Petrochemical and Material Technology, Chulalongkorn University, Bangkok, 10330, Thailand*

* wantanee.b@chula.ac.th

Keyword: powder injection moulding, water-soluble binder, polyethylene glycol, polyvinyl butyral

This work focuses on the debinding conditions of the ceramic materials fabricated by powder injection moulding. Ceramic powder materials, including alumina and alumina-based composites were prepared as feedstocks and mixed with water-soluble polyethylene glycol (PEG) and polyvinyl butyral (PVB). The PEG/PVB binder mixture, with PEG to PVB ratio of 85:15 and powder loading of 44 vol%, were thoroughly mixed and injected into the mould at the temperature of 190 ºC to obtain rod-like specimens. Prior to sintering, the as-injected specimen was then leached in water, the temperature of which was varying from 30 (ambient temperature), 45 to 60 ºC, in order to get rid of PEG and leave the specimens in shape by PVB. The rate of PEG removal according to different water temperatures was investigated. The experimental results suggested that PEG could completely be eliminated by 45 and 60 ºC water without any dimensional disintegration in 5 hours whereas those leached in 30 ºC water showed only 70% PEG removal. Higher water temperatures led to fast PEG removal rate at the beginning and then gradually decreased with elapsed times.

CM-O-09

Effect of Preparative Conditions on the Textural Properties of Pure and Metal-Doped γ-Alumina Aerogel and Xerogel

Abbas Khleel* **and Mohamad Nawaz**
United Arab Emirates University, Al-Ain, UAE
*abbask@uaeu.ac.ae

Keywords: γ-alumina; sol-gel process; textural properties.

Straight forward template-free sol-gel method was employed to prepare highly porous aerogel and xerogel pure and metal-doped γ-Al_2O_3. The gel formation and the textural properties of the calcined powders were strongly dependent on the solvents and the metal ion dopants as well as their concentration. Various solvents including 2-propanol, 1-butanol, 2-butanol, tert-butanol, and toluene were studied for the preparation of γ-Al_2O_3 from alkoxide precursors in the presence as well in the absence of an acid as a gelation catalyst. Mesoporous powders with relatively high surface areas, 350-500 m^2/g, and large total pore volumes, 1.4-2.0 cc/g, were obtained. It was found that higher surface areas and larger pore volumes were obtained in cases where the aluminum precursor was less soluble in the employed solvent. Similar results were also obtained in the presence of the acid catalyst. The unique properties of alumina prepared under these conditions were referred to the presence of colloidal particles of the precursor in the starting solution which acted as templates after hydrolysis in the gel network. The effect of the acid catalyst was referred to its role in enhancing the precursor solubility besides its role in increasing the rate of hydrolysis on the account of the rate of condensation.

Aerogel and xerogel powders of γ-alumina doped with different metal ions including Zn, Ti^{4+}, V^{3+}, Cr^{3+}, Fe^{3+}, Ce^{3+}, Mn^{2+}, and Cu^{2+} were also studied. The gel formation was dependent on the pH of the starting solution and was affected by the type of metal ion dopant as well as its concentration. As an example, the presence of Fe^{3+} or V^{3+} at a molar concentration of 10% in the starting alumina sol precursor significantly enhanced the gel formation process. The particle size, surface area, and porosity were strongly dependent on the preparative conditions and the composition. While the surface areas of xerogel powders were in the range of 200-400 m^2/g, they were as high as 800 m^2/g for γ-alumina-based aerogel powders. In addition, total pore volumes in the range of 2-6 cc/g were obtained for aerogel composites which were composed of interconnected nanoparticles. The metal dopant precursor also played a role in the textural properties of the final product. Metal acetylacetonate (acac) as a dopant precursor was compared with metal nitrate and metal chloride precursors. Employing acac precursors resulted in unique textural and morphological properties. The acac precursor also enhanced resistance to sintering especially at high dopant concentrations and an elevated calcination temperatures.

CM-O-10

The Effect of Alumina/Glass Composite Composition on the Adhesion and Strength of A96% Alumina Joint

Kritkaew Somton[a,*], Mana Rodchom[a], Kannigar Dateraksa[a] and Ryan McCuiston[b]
[a]National Metal and Materials Technology Center, Pathumthani 12120
[b]King Mongkut's University of Technology Thonburi, Bangkok 10140
* kritkaes@mtec.or.th

Keywords: Mullite, Flexural Strength, Alumina, Adhesion

An alumina/glass composite was examined for use as a high-temperature ceramic adhesive for bonding of 96% alumina bodies, with the goal of creating large and/or complex-shaped alumina armor from simple green body shapes. Four compositions of alumina and glass, 90:10, 80:20, 60:40, and 40:60 by wt.% were studied, referred to here as A, B, C, and D, respectively. Rectangular bend bars were produced from compositions A-D by die pressing. Two half-sized bend bars of 96% alumina were bonded together using pastes produced from compositions A-D. The pastes thickness were controlled and were made using PVA binder and water. Sintering of the bars was conducted and the measuring of the sintering behavior was achieved using a dilatometer. A phase analysis of the sintered samples was conducted by XRD. Density and porosity were measured using the Archimedes method. The flexural strengths of the sintered bend bars were measured and the fracture surfaces of the broken bars were examined by SEM. The XRD analysis showed a decrease in the alumina and an increase in mullite as the glass content was increased. The residual porosity of bars produced from compositions A, B, C and D were found to be 10.5, 25.6, 0.2 and 1.0 %, respectively. The minimal porosity of compositions C and D was likely due to the formation of a liquid phase during sintering, due to the excess glass. The dilatometric results found that the onset temperature for sintering shrinkage decreased as the glass content was increased, with composition D having the lowest onset temperature of ~600°C. Such a low onset temperature further indicated the formation of a liquid phase. Composition C was found to have the highest flexural strength of 94 MPa, however the flexural strength of the adhesive joint sample, was only 36 MPa. Composition D had the lowest flexural strength of 43 MPa, but it had the highest flexural strength of the adhesive joint at 61 MPa. The increased adhesive strength of composition D could be due in part to penetration of the excess glass phase into the 96% alumina body. The fracture surfaces of the adhesive joints for compositions A and B were rough and showed separation of the alumina/glass adhesive from the surface of the 96% alumina, which indicated a poor adhesion. However, the fracture surfaces of the adhesive joints of compositions C and D were smoother and showed limited separation of the alumina/glass composite from the 96% alumina, which indicated stronger adhesion. It was concluded that the flexural strength of the pure compositions alone could not be used to reliably predict the adhesive bond strength.

CM-O-11

Fabrication of Zeolite Na-A and Activated Carbon Composites by Slip Casting Technique for Drinking Water Filtration

Thanakorn Tepamat[a], Thanakorn Wasanapiarnpong[a,b]*, Pornapa Sujaridworakul[a,b] and Charusporn Mongkolkachit[c]

[a] *Research Unit of Advanced Ceramics, Department of Materials Science, Faculty of Science, Chulalongkorn University, Bangkok, 10330, Thailand*

[b] *Center of Excellence on Petrochemical and Materials Technology, Bangkok, 10330, Thailand*

[c] *National Metal and Materials Technology Center, Pathum Thani, 12120, Thailand*

*thanakorn.w@chula.ac.th

Keywords: Zeolite Na-A, Activated carbon, Composites, Water filtration, Slip casting

Hybrid composite for drinking water filter aids were prepared by slip casting method. The slip was prepared from the mixture of 17.41% of zeolite Na-A, 17.41% of activated carbon, 0.35% of ZnO nanoparticles, 8.7% of phenolic resin, 0.54% carboxymethyl cellulose and 55.59% of reversed osmosis water. The slip was mixed in a high speed ball mill for 15, 30, 45 and 60 min and was then poured into plaster molds for with 3 hour for hollow casting. The green body was dried and fired at several of firing temperature of 600, 650, 700 and 750 ^{o}C. The composite filter were characterized mechanical strength, morphology, pore diameter and ion exchange ability by three points bending, scanning electron microscopy (SEM), mercury porosimetry and inductive coupled plama-optical emission spectroscopy (ICP-OES), respectively.

CM-O-12

An Investigation of the Interface Change on Resistive Switching of Manganite Thin Film by Microbeam Spectroscopy

Hong-Sub Lee, Tae-Won Lee, Hae-Noo-Ree Jung and Hyung-Ho Park*

Department of Materials Science and Engineering, Yonsei University, Seoul 120-749, Korea

*hhpark@yonsei.ac.kr

Keywords: resistive switching mechanism, perovskite manganite, filament model, interface

Recently, the resistive switching (RS) phenomena in transition metal oxides (TMOs) have received a great deal of attention for next-generation non-volatile memory (NVM) application.[1-3] Among the strong candidates of NVMs, the resistive random access memory (ReRAM) which uses the RS phenomena enables us to realize the highest density integration as a cross point array structure due to metal/insulator/metal (MIM) simple structure.[4] So far, a variety of RS characteristics were observed in MIM structure with TMOs, and various RS mechanisms were suggested as many as the RS characteristics.[2] The phenomenology of observed RS characteristics is currently classified to interface type and filament type.[2] In RS of the filament type, the origin of the mechanism is discussed in terms of a 'filament model', where a thin metallic filament is created by soft dielectric breakdown and then burnt like a fuse. On the other hand, for the RS of interface type, various possible mechanisms have been suggested such as a redox of TE, change of Schottky-like barrier with electrochemical migration, redox of Metal-O-Metal conduction chain, Mott Hubbard metal-insulator transition *etc.*.[2] These mechanisms were proposed following a variety of experimental observations, and the variety characteristics make more difficult to control RS property in device application. So far, in any case of RS mechanism, many studies point out oxygen ions play a key role of RS such as the electrochemical migration and/or redox reaction of oxygen ion at interface between TE and TMOs.[5] Therefore the interface is very important and many studies have tried to observe the interface change as cross section observation by SEM and TEM.[6] In this study, we demonstrated photoelectron microscopy study using mercury top electrode and $Pr_{0.7}Ca_{0.3}MnO_3$ (PCMO) to observe the interface change between TE and TMOs. From the results, this study suggested a new factor and the possibility in RS mechanism of perovskite manganite.

References

(1) Rozenberg, M. J. *Scholarpedia* **2011**, 6(4), 11414.
(2) Waser, R.; Dittmann, R.; Staikov, G.; Szot, K. *Adv. Mater.* **2009**, 21, 2632-2663.
(3) Sawa, A. *Mater. Today* **2008**, 11, 28-36.
(4) Lee, M.-J.; Lee, C. B.; Lee, D.; Lee, S. R.; Chang, M.; Hur, J. H.; Kim, Y.-B.; Kim, C.-J.; Seo, D. H.; Seo, S.; Chung, U.-I.; Yoo, I.-K.; Kim, K. *Nat. Mater.* **2011**, 10, 625-630.
(5) Lee, H. S.; Choi, S. G.; Park, H. H.; Rozenberg, M. J. *Sci. Rep.* **2013**, 3, 1704.
(6) Norpoth, J.; Mildner, S.; Scherff, M.; Hoffmann, J.; Jooss, C. *Nanoscale* **2014**, DOI: 10.1039/c4nr02020k.

CM-O-13

Synthesis of $BaTiO_3$ Nanoparticles by Varying Capping Agent at Low Temperature

Wooje Han, Hong-Sub Lee, Tae-won Lee and Hyung-Ho Park*
Department of Materials Science and Engineering, Yonsei University, 50 Yonsei-ro, Seodaemun-gu, Seoul 120-749, Republic of Korea
* hhpark@yonsei.ac.kr

Keywords: Capping agent, $BaTiO_3$, Nanoparticles.

We present the comparison results of size, morphology, and size distribution between capping agent adopted $BaTiO_3$ nanoparticles and those of unadopted $BaTiO_3$ nanoparticles. $BaTiO_3$ is the most extensively studied ferroelectric material among the perovskite oxides since its high permittivity and ferroelectric properties.[1,2] It is well-known that in perovskite nanoparticles possess, structural and physical properties are strongly dependent on their size, shape, crystallinity, and surface composition.[3-6] We have used oleic acid (OA) or trioctylphosphine oxide (TOPO) for successive capping of $Ti(OH)_6$ with a primary layer. These capping agents make a difference in the size, morphology and particles size distribution of $BaTiO_3$ nanoparticles. We established the synthesis of $BaTiO_3$ nanoparticles at room temperature with modified procedure of *X. Wang et al*.[7] $BaTiO_3$ nanoparticles was synthesized by using barium(II) nitrate, titanium(IV) butoxide and sodium hydroxide as starting material and catalyst, respectively. Adopting capping agent induced an increase in the size of $BaTiO_3$ nanoparticles. $BaTiO_3$ nanoparticles with characteristic morphology were investigated by using Fourier transform infrared spectroscopy, X-ray diffraction, scanning electron microscopy, and particles size analyzer measurement techniques. Through these analyses, the effect of capping agent on the geometrical and compositional characteristics of $BaTiO_3$ nanoparticles has been established.

References

(1) Pithan, C.; Hennings, D.; Waser, R. *Int. J. Appl. Ceram Technol.* **2005**, 2, 1-14
(2) Cross, L. E. *Am. Ceram. Soc. Bull.* **1984**, 63, 586-90
(3) Li, X. *J. Mater. Sci.* **2008**, 19, 271
(4) Lott, J.;Xia, C.; Kosnovsky, L.; Weder, C.; Shan, J. *adv. Mater.* **2009**, 67, 2024
(5) Joshi, U. A.; Yoon, S.; Baik, S.; Lee, J.S. *J. Phys. Chem. B.* **2006**, 110, 12249
(6) Guangeneng,f.; Lizia, H.; Xuenguang, H. *J. Cryst. Growth.* **2005**, 279, 489
(7) Wang, X.; Zhuang, J.; Peng, Q.; Li, Y. *Nature,* **2005**, 437, 121-124

CM-O-14

Properties of Sintered Brick Containing Lignite Bottom Ash Substitutions

Chiraporn Auechalitanukul[a,*], Ryan McCuiston[a], Tarit Prasartseree[a], Pongpat Pungpipat[a] and Smatcha Olaranont[a]

[a]King Mongkut's University of Technology Thonburi (KMUTT), Thung Khru, Bangkok, 10140, Thailand

*chiraporn.aue@kmutt.ac.th

Keywords: Lignite bottom ash, Porous insulating bricks, Thermal properties, Waste utilization

This study examined the feasibility of utilizing lignite bottom ash as a partial substitute for ball clay in an insulating brick composition. Lignite bottom ash is a waste byproduct that is high in alumina and silicates and is therefore a candidate material for replacing aluminosilicate minerals such as clay. The lignite bottom ash powder was obtained from the Mae Moh power plant, Thailand. Small brick specimens were produced by die pressing a mixture of lignite bottom ash, ball clay and aluminum hydroxide. The composition of the mixture contained a fixed amount of aluminum hydroxide, while the lignite bottom ash replaced from 30 to 70% of the ball clay. The pressed samples were sintered at 1300 ºC for 1 hour in air. The density, porosity, strength and thermal properties of the samples were measured. A microstructural analysis of the sintered brick was also performed. It was found that the porosity of the samples increased from 35 to 45% with increased lignite bottom ash content. The modulus of rupture and the thermal conductivity of the bricks were reduced with increased lignite bottom ash content, likely due to the increased amount of porosity. Dilatometric analysis found that the thermal expansion increased with increased amounts of lignite bottom ash, possibly as a result of an increased amount of glassy phase. Despite the high thermal expansion coefficient at high temperature, the feasibility of using lignite bottom ash in the insulating brick composition was demonstrated.

CM-O-15

Modeling the Influence of Fly Ash on Degree of Hydration and Compressive Strength of Blended Cement Paste

Nattapong Damrongwiriyanupap[a,*], Suchart Limkatanyu[b] and Yunping Xi[c]
[a]*University of Phayao, Phayao, 56130, Thailand*
[b]*Prince of Songkla University, Songkla, 90112, Thailand*
[b]*University of Colorado, Boulder, Colorado, 80309, USA*
*natpong_chin@hotmail.com

Keywords: Cement paste, Fly ash, Degree of hydration, Compressive strength.

This article presents the model for predicting the degree of hydration and compressive strength of cement paste containing fly ash. The kinetic hydration model is proposed based on the hydration reaction and pozzolanic activity of Portland cement and aluminosilicate glass phase in fly ash. In addition, the model accounts for the fineness of fly ash. The compressive strength is predicted by the microstructural formation of blended cement paste which is considered mainly on the development of calcium silicate hydrate (C-S-H). The results obtained from the present model are compared to the available test data and a good agreement is observed.

CM-O-16

Fabrication of Fiber Cement Using Tobacco Stalk Pulp from Agricultural Residue

Thanakorn Wasanapiarnpong[a,b,c]*, Siriphan Nilpairach[c] and Krisana Siraleartmukul[c]

[a] *Research Unit of Advance Ceramics, Department of Materials Science, Faculty of Science, Chulalongkorn University, Bangkok 10330, Thailand*

[b] *Center of Excellence on Petrochemical and Materials Technology, Chulalongkorn University, Bangkok 10330, Thailand*

[c] *Local Materials Technology Research Center, Metallurgy and Materials Science Research Institute, Chulalongkorn University, Bangkok 10330, Thailand*

*thanakorn.w@chula.ac.th

Keywords: Fiber cement, Tobacco stalk pulp, Agricultural residue, Reinforcement fiber

The objective of this research is to study the feasibility of using fiber obtained from tobacco stalk as reinforcement fiber in the production of fiber cement through hydrothermal methods. The fiber cement samples are made of the mixtures of 50% of Type I Portland cement, 35% of milled sand, 10% of calcium carbonate powder and 5% of cellulose fiber (eucalyptus pulp and tobacco stalk pulp). This study include the morphological characterization of the fibers and the study of effects that the use of fiber has on the fiber cement suspensions and on the mechanical and physical properties of the final product. The results obtained in the tests confirmed the high potential of the tobacco stalk as a source of fiber for the fabrication of a fiber cement capable of meeting the requirements of demanding applications.

CM-O-17

Compressive Strength in Various Submersion Test of Fired Clay Bricks from Chi River Sub-Basin

Sarunya Promkotra[a,*], Tawiwan Kangsadan[b]
[a]*Department of Geotechnology, Faculty of Technology, Khon Kaen University, Khon Kaen 40002, Thailand*
[b]*Chemical and Process Engineering Program, Department of Mechanical and Process Engineering, The Sirindhorn International Thai-German Graduate School of Engineering (TGGS), King Mongkut's University of Technology North Bangkok (KMUTNB), Bangkok 10800, Thailand*
*sarunya@kku.ac.th

Keywords: fired clay brick, submersion test, compression, Chi River sub-basin

The river sediments from the Chi River basin, including Chi River and Nam Phong River, are valuable to comprehend the brick process, physical and chemical properties which lead to its strength. Study areas cover three different regions in Maha Sarakham, Kalasin and Roi Et provinces nearby six brickyards which are separated in two areas Nam Phong and Chi River area. Mechanical property is referred to compressive strengths of a brick unit and the prism. These compressive strengths of the fired brick unit increase with increasing grain size. Elastic moduli of original fired brick at the ultimate stress and strain corresponding by time in submersion test show that any solutions filled in void or pore can enhance the apparent density of bricks. Thus, fired bricks are capable to resist compressive force than the normal condition. The ratio of modulus in submersion test expressed in the original fired brick to clean water (for 4 hr), acidic saline and saline is 1: 1.1: 1.2: 1.6, respectively. Moreover, prism compressive strength decreases in half related to a fired brick unit. The stress level depends on the fracture plane over particular long space fabricating by manufacturing process. Their impact resistances are significantly distinctive by mineral composition of clay mineral group and silica.

CM-O-18

Microstructure and Properties of Zirconia Toughened Alumina Fabricated by Powder Injection Moulding

Nutthita Chuankrerkkul[a,*], Rattanaporn Charoenkijmongkol[b], Punnapa Somboonthanasarn[b], Chiraporn Auechalitanukul[b] and Ryan C. McCuiston[b]

[a]Metallurgy and Materials Science Research Institute, Chulalongkorn University, Bangkok 10330, Thailand

[b]Department of Tool and Materials Engineering, King Mongkut's University of Technology Thonburi, Bangkok 10140, Thailand

*nutthita.c@chula.ac.th

Keywords: ceramic injection moulding, ZTA ceramic, water soluble binder

The zirconia toughened alumina (ZTA) ceramic has been fabricated by powder injection moulding process. The ZTA ceramic, composed of 80 wt% alumina and 20 wt% zirconia, was mixed with a water-soluble, multi-component binder system. The binder ingredients were polyethylene glycol (PEG), polyvinyl butyral (PVB) and stearic acid (SA). Powder injection moulding was performed with powder loading in range of 48 – 52 vol% using a laboratory-scaled injection moulding machine. Water leaching was used for binder removal prior to sintering at 1650 °C for 2 hour. Microstructure examination of ZTA ceramic revealed that zirconia inhibited alumina grain growth and, therefore, improved mechanical and physical properties of the components. It was found that powder loadings had an influence on density, hardness and strength of the specimens. The flexural strength of 334 MPa and hardness value of 2093 HV could be obtained from components containing 52 vol% of powder loading. The highest sintered density achieved was 97% of the theoretical value.

CM-O-19

Zirconia – Alumina Mixed Aerogel for High Specific Surface Area

Hae-Noo-Ree Jung, Min-Hee Hong, Wooje Han and Hyung-Ho Park*
Department of Materials Science and Engineering, Yonsei University, Seoul 120-749, Republic of Korea
hhpark@yonsei.ac.kr

Keywords: Zirconia aerogel, Alumina aerogel, mixed aerogel, sol-gel, ambient pressure drying.

Aerogel is nano structured and porous material. Due to its high porosity, aerogel has extremely low density and large specific surface area. With large specific surface area and extremely low thermal conductivity, silica aerogel which is one of typical and traditional aerogel, has been studied for catalyst, thermal insulator, and so on. However silica aerogel shows a degradation of pore structure at high temperature. So researchers have studied about non-silica aerogels like zirconia aerogel, alumina aerogel, titania aerogel, etc. Especially, zirconia is suitable for using at high temperature. Usually, aerogel is synthesized via sol-gel processing and through controlling of sol-gel processing parameters, porosity and surface area of aerogel can be changed. But from the difficulty of controlling sol-gel processing parameter in the case of zirconia aerogel, it has been known to be hard to obtain high specific surface area and high porosity with zirconia aerogel. So we introduced mixed aerogel as zirconia-alumina aerogel to maintain nanoporous structure of aerogel to maintain high specific surface area. Because in the case of alumina aerogel, it is easy to control the sol-gel processing parameter and it is easy to obtain an aerogel structure with high specific surface area and high porosity up to 90% for alumina aerogel. For that, in this study, various kinds of processing parameters including precursors were investigated to prepare zirconia-alumina mixed aerogel with high surface area.

References

[1] Bangi, U.K.H., Park, C.-S., Baek, S.b, Park, H.-H., Powder Technology 239 (2013) 314.
[2] Suh, D.J., Park, T.-J., Chem. Mater. 8 (1996) 509.
[3] Ward, D.A., Ko, E.I., Chem. Mater. 5 (1993) 956.
[4] Santos, V., Zeni, M., Bergmann, C.P., Hohemberger, J.M., Rev.Adv.Mater.Sci. 17 (2008) 62.

CM-O-20

Alumina Crucible from Waste of Aluminum Industry

Watcharee Sornlar[a,*], **Pattarawan Choeycharoen and Anucha Wannagon**
National Metal and Materials Technology Center, Pathum Thani 12120
* watcharp@mtec.or.th

Keywords: Alumina crucible, waste, aluminum industry, glass melting

Alumina crucible made from aluminum industrial waste was initially studied for glass melting purpose. The main objective of this work was to reduce or substitute both of alumina powder and alumina crucibles imported from abroad. The crucible formula mainly composed of white calcined powder waste from aluminum factory. Sodium silicate and sodium salts of polycarboxylic acid were used as deflocculant and binder respectively. The crucibles were fabricated by slip casting method and fired at 1600 and 1700^{O}C. The water absorption, bulk density, apparent porosity and 3-point bending strength were investigated after firing at 1600 and 1700^{O}C. It showed 0.18 and 0.06% water absorptions, 3.41 and 3.36 g/cm^{3} bulk densities, 0.61 and 0.20% apparent porosities and 159.84 and 139.11 MPa bending strengths, respectively. The coefficient of thermal expansion between 25-1000^{O}C was 6.9807x10^{-6} /^{O}C. The crucibles passed 3 cycles of 20-200^{O}C thermal shock resistance testing. It was successful to trial used for glass melting at 1450-1500^{O}C without breaking or affecting to the glass component. The estimated cost of the crucible made from this work was 85% cheaper than the commercial crucible. Consequently, this study indicated that the alumina crucible made from industrial waste was compatible with the commercial crucible for glass melting purpose.

CM-O-21

Mechanical Properties and Microstructures of Bottom Ash-clay Geopolymers under NaOH and KOH Activations

Kedsarin Pimraksa[a,*], Sakonwan Hanjitsuwan[b], Wanwisa Saijai[a] and Prinya Chindaprasirt[c]

[a] *Department of Industrial Chemistry, Faculty of Science, Chiang Mai University, Chiang Mai, 50200, Thailand*

[b] *Program of Civil Technology, Faculty of Industrial Technology, Lampang Rajabhat University, Lampang, 52000, Thailand*

[c] *Sustainable Infrastructure Research and Development Center, Faculty of Engineering, Khon Kaen University, Khon Kaen, 40002, Thailand*

* kedsarin.p@cmu.ac.th

Keywords: geopolymer, bottom ash, clay mineral, alkali solution, sodium silicate solution

Bottom ash-clay geopolymers were studied in terms of mechanical properties and microstructures. Bottom ash was obtained from Mae Moh Power Plant (Thailand). Various types of clay viz., kaolin-rich clay, quartz-rich clay and plastic clay, which were locally available, were used individually as starting materials at 20 and 40 wt% in the bottom ash-clay geopolymer mixtures. Alkali solutions, NaOH and KOH were used to activate the system as comparative study. Sodium silicate solution was used as silicate source to achieve the polycondensation at early age. Mechanical properties (compressive strength, water absorption and bulk density at 7 and 28 days curing) were determined. In addition, phase development and microstructures of the bottom ash-clay geopolymers were investigated. Due to the difference in mineralogical compositions of starting clay minerals, the mechanical properties and microstructures were significantly different. Type of alkali solution also played a great role on the product quality.

CM-O-22

Influence of OPC Replacement and Manufacturing Procedures on the Properties of Self-Cured Geopolymer Cement

Teewara Suwan[a,*] and Mizi Fan[a]

[a]*Brunel University, Uxbridge, London, UB8 3PH, United Kingdom*

*teewara.suwan@brunel.ac.uk

Keywords: Ambient curing; Fly ash-based geopolymer; Manufacturing procedures; Self-cured geopolymer

Ordinary Portland Cement (OPC) is an intensive energy consuming product with high greenhouse gas emission along its production process. It has been reported that one ton of cement production emits approximately one ton of carbon- dioxide to the atmosphere. To develop sustainable and environmentally friendly construction materials, Geopolymer cement (GP) has been studying for totally or partially replacing OPC consumption. Geopolymer cement is a binder synthesized from by-products of alumina-silica materials and alkaline activators. Its production starts with the mixing of alkaline solutions and raw starting materials to form homogenous slurry. Heat above ambient temperature is required from 40 to 90°C for 24 to 48 hours, for curing purpose. Afterward, GP will be continually left in room temperature for further curing. As heat curing is one of the vital factors, geopolymer's applications are limited by the size of curing chamber just for producing e.g. bricks or small pre-fabricated components. To achieve more energy conservation and more convenient practical work, there is a challenge to develop GP with its abilities of curing without external source of heat supply as a self-cured geopolymers cement.

This research study presents the development of self-cured fly ash-based geopolymer cementitious systems in ambient conditions: Two approaches, (i) Geopolymer-portland cementing system (GeoPC) and (ii) different manufacturing procedures, have been proposed and investigated. The GeoPC combinations were made from the designation mass of geopolymer paste (GP) and OPC paste. Mass of each material used in GeoPC system, including alkaline solution and water, was calculated individually from the designed GP paste and OPC paste. For synthesis, three different manufacturing procedures were carried out by two typical processes and a new proposed technique called "Just Adding Water (JAW) geopolymer". The investigation were studied with its setting time, internal heat liberation, compressive strength, microstructure (SEM) and functional groups in molecule (FTIR) of the developed cementing system.

It has been found that the replacement of OPC in the GP systems (GeoPC) directly affect in shortening the setting time by the reaction of calcium compound (in OPC) and alkaline activator (in GP). The GeoPC which contained high percentage of OPC had higher heat evolution than those of low percentage of OPC concentration. The compressive strength of GeoPC systems had developed with the time and increased when the percentage of OPC replacement increased. Moreover, the heat generated from OPC-added reaction has also provided positive effect on the curing of geopolymer. The strength was obtained from the formation of coexistence amorphous CSH and semi crystalline structure of geopolymeric gel. For the manufacturing process, those two typical processes provided slightly better strength than the JAW-geopolymer. However, JAW technique clearly generated much more heat and solidification than those two typical processes.

Overall, the alternative heat supply from GeoPC combinations and JAW manufacturing process could provide sufficient heat for the curing regime of GP, indicating potentials of the development of self-curing geopolymer for engineering applications and in-field curing proposes.

CM-O-23

Properties of Steel Fibre Reinforced Geopolymer

Rachamongkon Wongruk[a,*], Smith Songpiriyakij [b] and Piti Sukontasukkul[b]
[1]Graduate Student and Corresponding Author,
King Mongkut's University of Technology North Bangkok, Thailand
[b]Associate Professor,[3]Professor
King Mongkut's University of Technology North Bangkok, Thailand
[*]E-mail: rachamongkon@gmail.com

Keywords: Geopolymer, Steel Fiber, Mechanical Properties, Flexural and Toughness,

In this study, the mechanical properties of steel fibre reinforced geopolymer (SFRG) are investigated. The geopolymer is consisted of fly ash, silica fume and activator solution, sodium silicate and sodium hydroxide. Five mix proportions of fly ash and silica fume are varied to study the effect of fly ash/silica fume ratios. Two curing temperatures are also studied (30°C and 60°C). This experimental series focus mainly on compressive strength, flexural strength and flexural toughness performance of SFRG. Hooked-ends steel fibers are used at 0.5% and 1% by volume fractions. The experiment is carried out based on ASTM C39 for compressive performance (cylindrical specimens) and ASTM C1609 (beam specimens) for flexural performance. The results showed that fiber can significantly enhance the both flexural strength and toughness of geopolymer. The enhancement also increases with the increasing fiber volume fraction.

CM-O-24

Effect of Silica to Alumina Ratio on the Compressive Strength of Class C Fly Ash Geopolymer

P. Timakul[a,*], K. Thanaphatwetphisit [b] and P. Aungkavattana[a]

[a]National Metal and Materials Technology Center, 114 Thailand Science Park, Paholyothin Rd.,Klong 1, Klong Luang, Pathum Thani, 12120, Thailand

[b]Faculty of Liberal Arts and Science, 1 Moo 6, Kamphaeng Saen, Nakhon Pathom, 73140, Thailand

*patthamt@mtec.or.th

Keywords: Geopolymer; Class c fly ash; Silica to alumina ratio; Compressive strength

The effort of reducing the greenhouse gas emission from high temperature firing for construction materials such as portland cement, ceramic products and refractories manufacturing has become a motivation to develop environmental friendly construction materials. An inorganic polymer referred to as "geopolymers" is an alkali-activated alumino-silicate material which possesses excellent physical and chemical properties for wide range of applications in building and construction. In this work, the abundant waste product such as fly ash obtained from Mae Moh power plant of Thailand was employed to prepare geopolymer materials. So far, the studies on fly ash geopolymer has been emphasized on the raw materials derived from class F fly ash (FFA) produced by burning bituminous coals. To date, there have been only a few studies on class C fly ash-based geopolymers. The main difference between class F and class C fly ash is the calcium content which class C contained calcium content more than 10%, whereas both fly ashes contained substantial amount of silica and alumina. This study aims for the development of geopolymers from class C fly ash, and focusing on the effect of silica to alumina ratio on the compressive strength of geopolymer. The class C fly ash wastes from Mae Moh Thailand power plant, which is SiO_2 (30.97%) and Al_2O_3 (17.16%)-rich materials was employed as the main solid part to prepare geopolymers, apart from kaolinite. The combination of sodium hydroxide (NaOH), sodium silicate (Na_2SiO_3) solution, and distilled water as 1:1:4 mass ratios were used as the liquid activator. The curing temperature in the oven was fixed at 75ºC and varied curing time for 24, 48, 72 and 96 hours. Further curing was done at room temperature for 28 days before characterizations. XRD study of synthesized geopolymers showed quartz, kaolinite and muscovite as the main crystalline phases with the alumino-silicate framework illustrating in amorphous structure. Infrared study showed the Al-O-Si and Si-O-Si bonds in all geopolymers samples. The compressive strength of geopolymer increased from 32 to 40 MPa when the ratio of SiO_2 : Al_2O_3 was increased from 2.60 to 2.65. However, the compressive strength was decreased after increasing the SiO_2 : Al_2O_3 ratio from 2.65 to 3.0. The highest compressive strength was found when the SiO_2 : Al_2O_3 ratio was 2.65 with the curing time at 75ºC for 96 h which the samples also possessed high density. It could be concluded that the ratio of SiO_2 : Al_2O_3 and the curing time played an important role to the compressive strength of fly ash based geopolymer.

Ceramic-based Materials Session

POSTER PRESENTATIONS

CM-P-01

The Study of Physical and Thermal Conductivity Properties of Cement Paste with Nanosilica

Pongsak Jittabut[a,*], Prinya Chindaprasirt[b] and Supree. Pinitsoontorn[c]
[a]*Physics and General Science Program, Faculty of Science and Technology, Nakhon Ratchasima Rajabhat University, Nakhon Ratchasima 30000, Thailand*
[b]*Department of Civil Engineering, Faculty of Engineer, Khon Kaen University, Khon Kaen 40002, Thailand*
[c]*Department of Physics, Faculty of Science, Khon Kaen University, Khon Kaen 40002, Thailand*
*pongsak.ey@gmail.com

Keywords: Physical Properties, Thermal Conductivity, Nanosilica, Cement Past

This research article presents the physical and thermal conductivity properties of cement pastes containing nanosilica. The effects of nanosilica particle size and concentration determined by mixing three nanosilica particle sizes of 12, 50 and 150 nm, using nanosilica were of 1-5 wt%. The water to binder ratio of 0.5 was used. The results indicated that the use of nanosilica as an admixture can reduce the thermal conductivity and lowered the bulk density of specimen. The cement paste with nanosilica particle size of 50 nm with 4 wt% nanosilica at the age of 28 day showed the optimized properties. The average thermal conductivity was the lowest at 0.913 W/m-K. The compressive strength was the highest at 51.62 MPa, and the bulk density was 1,806 kg/m^3. The compressive strength increases more than 50% in comparison to the control cement paste. The cement paste with nanosilica have lower unit weight and thermal conductivity than typical control cement paste about 9% and 15%, respectively. The nanosilica mixed cement paste is very interesting for energy saving when used as wall insulating material.

CM-P-02

Morphology and Phase Composition of Sol-gel Derived Aluminum Borate Nanowhiskers

Pat Sooksaen[a, b]*

[a] *Department of Materials Science and Engineering, Faculty of Engineering and Industrial Technology, Silpakorn University, Nakhon Pathom 73000 Thailand*

[b] *Center of Excellence for Petroleum, Petrochemicals and Advanced Materials, Chulalongkorn University, Bangkok, 10330, Thailand*

* pat@su.ac.th

Keywords: aluminum borate, nanowhiskers, sol-gel, morphology, spectroscopy

A sol–gel synthesis route was used to grow aluminium borate nanowhiskers with varying aspect ratio. Calcination was carried out at 850 and 1100°C for 4 and 32 hours, respectively. The morphology of aluminum borate ($Al_4B_2O_9$ and $Al_{18}B_4O_{33}$) nanowhiskers could be controlled by varying the aluminum to boron (Al:B) molar ratio in the sol–gel derived precursors. Sintering temperature and time also affected the phase composition and size of the nanowhiskers. Citric acid was also added in the sol–gel derived precursors as a surface stabilizer for obtaining uniform nanostructures. Fine nanowhiskers were obtained by the calcination at 850°C, whereas higher heat treatment temperature of 1100°C led to thicker and longer nanowhiskers and becoming rod-like crystals. The morphology and phase composition were investigated by field emission scanning electron microscope and x-ray diffraction. Chemical bond vibrations in the synthesized nanowhiskers were investigated by Fourier-transform infrared spectroscopy. The frequencies at which there were absorptions of infrared radiation were correlated directly to bonds within the substances.

References

[1] J. Wang, J. Sha, Q. Yang, Y. Wang, D. Yang., Materials Research Bulletin, 40, 1551–1557 (2005)

[2] J. Wang, G. Ning, X. Yang, Z. Gan, , H. Liu, and Y. Lin, Materials Letters, 62, 1208–1211 (2008)

[3] X. Tao, X. Wang and X. Li, Nano Letters, 7-10, 3172-3176 (2007)

[4] Y. Cheng, H. Xia, C. Shuguang, B. Tang, Physica B 404, 1230-1234 (2009)

[5] Z.X. Hou, Journal of Non-Cryst Solids 536, 201-207 (2010)

CM-P-03

Surface Modification of Zinc Oxide Nanoparticles using Polyethylene Glycol under Microwave Radiation

Pat Sooksaen [a, b*], Anutra Keawpimol [a], Piyavan Deeniam [a] and Panumart Boonkum [a]
[a] *Department of Materials Science and Engineering, Faculty of Engineering and Industrial Technology, Silpakorn University, Nakhon Pathom 73000 Thailand*
[b] *Center of Excellence for Petroleum, Petrochemicals and Advanced Materials, Chulalongkorn University, Bangkok, 10330, Thailand*
* pat@su.ac.th

Keywords: zinc oxide, microwave, nanostructures, polyethylene glycol, photo-catalyst

Zinc oxide (ZnO) is semiconductor with band gap energy of ~3.3 eV. ZnO can be used in many applications such as sensors, solar cells and electro-optical devices. The properties are strongly dependent on its structure, including the morphology, aspect ratio, size and orientation. Microwave heating has been successfully used for fast synthesis of many nanostructured materials due to the charged particles vibrating in the electric field form nuclei and grow in the temperature gradient.
This study investigated the effect of polyethylene glycol (PEG), with molecular weight of 1500 and 4000, on the formation of zinc oxide nanostructures synthesized by microwave radiation. Microwave heating was carried out at 2.45 GHz between 320 and 640 watts with 5s/15s on/off step time. The precursors used were $Zn(NO_3)_2.6H_2O$, NaOH and PEG. Microwave radiation generates heat to activate the formation of ZnO nanoparticles where the morphology can be controlled by the addition of PEG, time and heating power. The formation of wurtzite structure of ZnO was confirmed by X-ray diffraction. Morphology was investigated by a scanning electron microscope. PEG acted as acted as a structure-directing agent or chelating agent resulting in the formation of rod-like crystals. These nanostructures are different to those synthesized without the addition of PEG where flower-like crystals are observed. The average size of ZnO nanocrystals increased with increasing microwave power as well as increasing PEG addition in precursor solution.

References

Z. Zhu, D. Yang, H. Liu, Advanced Powder Technology, 22, 493–497 (2011)
T. Thongtem, A. Phuruangrat, S. Thongtem, Ceramics International, 36, 257–262 (2010)
Y. Ni, S. Yang, J. Hong, P. Zhen, Y. Zhou, D. Chu, Scripta Materialia, 59, 127–130 (2008)
T. Krishnakumar, R. Jayaprakash, N. Pinna, V.N. Singh, B.R. Mehta, A.R. Phani, Materials Letters, 63, 242–245 (2009)
M.G. Ma, Y.J. Zhu, G.F. Cheng, Y.H. Huang, Materials Letters, 62, 507–510 (2008)

CM-P-04

Homogeneous Precipitation Synthesis and Sintering of Magnesium Aluminate Spinel Nanoparticles

Karn Serivalsatit[a,*], Thanataon Pornpatdetaudom[a], Adison Saelee[a], Sarut Teerasoradech[a]

[a]*Research Unit of Advanced ceramics, Department of Materials Science, Faculty of Science, Chulalongkorn University, Pathumwan, Bangkok, 10330, Thailand*

*E-mail address : karn.s@chula.ac.th

Keywords: $MgAl_2O_4$, Nanoparticles, Homogeneous precipitation, Sintering

A wide application of magnesium aluminate spinel powder has attracted a number of studies concerning the preparation of magnesium aluminate spinel powder. In this study, a precursor for magnesium aluminate spinel was synthesized by a homogeneous precipitation method using urea as a precipitant. The precursor and calcined powder were characterized by X-ray diffractometry, Fourier transform infrared spectroscopy, scanning electron microscopy, and transmission electron microscopy. After precipitation, the precursor was magnesium aluminium hydrate carbonate compound. By calcining, the precursor decomposed to MgO and an amorphous phase after calcining at 600°C. The formation of magnesium aluminate spinel via a reaction between MgO and the amorphous phase was observed after calcining over 800°C. The equiaxed magnesium aluminate spinel nanoparticles with particle size of 10-30 nm were obtained after calcining at 1100°C for 2 hours. Sinterability of the obtained magnesium aluminate spinel nanoparticles was also investigated by sintering compacts of magnesium aluminate spinel nanoparticles in the temperature interval of 1300-1650°C. Sintering temperature of 1600°C allowed the fabrication of dense magnesium aluminate spinel ceramics with relative density over 95%

CM-P-05

Utilization of Glass Cutting Sludge and Sanitary Ware Sludge in Ceramic Pressed Bodies

Apirat Theerapapvisetpong[a,*] and Siriphan Nilpairach[b]
[a]Research Unit of Advanced ceramics, Department of Materials Science, Faculty of Science, Chulalongkorn University, Bangkok 10330, Thailand
[b]Metallurgy and Materials Science Research Institute, Chulalongkorn University, Bangkok 10330, Thailand
*apirat.t@chula.ac.th

Keywords: Soda lime glass, Stoneware, Low firing ceramic, Sintering aid.

Ceramic manufacturers are finding the way to decrease firing temperature and recover their wastes in order to keep production costs down. In this study earthenware ceramic bodies were prepared by adding a soda-lime glass grinding effluent powder (dried sludge) as a fluxing agent at 0–50 wt.% into either sanitary ware sludge powder (from a sanitary ware manufacturing process) or fresh pottery clay from Ang-thong, Thailand. The dried and pressed mixtures were fired at 1100, 1125 and 1150 °C and tested for the firing shrinkage, modulus of rupture, water absorption and bulk density. The formed product microstructure was observed by the scanning electron microscopy, and the phase composition was characterized by X-ray diffractometer. The results revealed that the best condition for adding the glass powder in Ang-thang pottery clay was the inclusion of 10 wt.% soda-lime glass effluent powder in the pottery clay. Its flexural strength increased from 51.25 MPa to 93.40 MPa after firing at 1125 °C with the water absorption of 0.42 wt.% and the firing shrinkage of 10.25 %. The optimum firing temperature and soda-lime glass content in sanitary ware sludge were 1150 °C and 20 wt.%, respectively. Its flexural strength increased from 103.16 MPa to 118.16 MPa with the water absorption of 0.52 wt.% and the firing shrinkage of 13.67 %. The results illustrated the potential to use soda-lime glass cutting sludge and sanitary ware sludge as raw materials for earthenware ceramic body.

CM-P-06

Effect of Precipitant Solution pH on Morphology and Chemical Composition of Magnesium Aluminate Spinel Nanoparticles

Karn Serivalsatit[a,*], Adison Saelee[a], Sarut Teerasoradech[a], Thanataon Pornpatdetaudom[a]

[a]*Research Unit of Advanced ceramics, Department of Materials Science, Faculty of Science, Chulalongkorn University, Pathumwan, Bangkok, 10330, Thailand*

*E-mail address : karn.s@chula.ac.th

Keywords: $MgAl_2O_4$, Nanoparticles, Precipitation, pH

Precipitation method is a promising route for preparation of nanoparticles because of its advantages such as the relatively simple synthetic route, low cost, and ease of mass production. The precipitant solution pH is one of the significant factors that impacts physical and chemical characteristics of the nanoparticles. In this study, magnesium aluminate spinel ($MgAl_2O_4$) nanoparticles were synthesized by co-precipitation method. Different pH value of ammonium bicarbonate ($(NH_4)HCO_3$) solution was used as precipitants. The precipitate precursors were characterized by x-ray diffractometry, scanning electron microscopy, and energy dispersive spectroscopy. The result showed that the pH value of the precipitant solution had a significant effect on morphology and chemical composition of $MgAl_2O_4$ nanoparticles. The precipitate precursor prepared from precipitant pH of 7.7 had equiaxed shape. As the pH of the precipitate solution increased, the aspect ratio of the precipitate precursors increased. Rod-like particles were observed for the precipitate precursor prepared from precipitant pH of 10. The $MgAl_2O_4$ nanoparticles were obtained by calcining the precipitate precursor at 1100 °C for 2 hours. The $MgAl_2O_4$ nanoparticles with Al_2O_3/MgO molar ratio ranging from 2.68 to 1.07 were successfully prepared by varying the pH of the precipitant solution ranging from 7.7 to 10.

CM-P-07

Influence of Carbon Nanotubes on Photocatalytic Activities of Thermal Sprayed Titanium Dioxide Nanocomposite Powders

Phuangphaga Daram[a], Wiradej Thongsuwan[a,b], Sukanda Jiansirisomboon[a,b,*]
[a]*Department of Physics and Materials Science, Faculty of Science, Chiangmai University/ Chiangmai, 50200, Thailand*
[b]*Materials Science Reseach Center, Faculty of Science, Chiangmai University/ Chiangmai, 50200, Thailand*
*E-mail sukanda.jian@cmu.ac.th

Keywords: Titanium dioxide, Carbon nanotube, Thermal spray, Photocatalytic activities, Nanocomposite, Coating.

This research aims to produce TiO_2-based nanocomposite powder by growing of CNTs on the surface of micron-sized TiO_2 particles using a chemical vapor deposition (CVD) technique. This nanocomposite powder will be further used as feedstock powder to build up as a coating using a thermal spray technique. This coating is expected to have better photocatalytic efficiency over that of pure TiO_2 coating. For nanocomposite powder preparation, anatase-phase of TiO_2 powder with particle size in a range of 25 – 45 µm was used as a starting powder. The powder was placed in a CVD apparatus under ethanol atmosphere as a carbon source. The best CNTs growing condition was found to be 750°C for 60 min. The stating powder and as-synthesized nanocomposite powders were characterized by scanning electron microscopy, X-ray diffractometry, Raman spectroscopy and UV-vis spectroscopy. The results showed that CNTs were successfully grown in situ on the surface of TiO_2 particles. The UV light photocatalytic activities were examined based on a degradation of methylene blue (MB). The degradation efficiency of the TiO_2/CNTs nanocomposite powder was found to be higher than that of pure TiO_2 powder. From this result it is expected that the thermal sprayed coating made from this nanocomposite powder would be likely to provide appropriated coating for further applied in water pollution treatment.

CM-P-08

Application of Statistical Analysis in the Powder Injection Molding (PIM) of Mullite

Parinya Chakartnarodom[a,d], Nuntaporn Kongkajun[b,*], Nutthita Chuankrerkkul[c,*]
[a]*Department of Materials Engineering, Faculty of Engineering, Kasetsart University, Chatuchak, Bangkok, 10900, Thailand*
[b]*Department of Physic, Faculty of Science and Technology, Thammasat University, Klong Luang, Prathumthani, 12121, Thailand*
[c]*Metallurgy and Materials Science Research Institute, Chulalongkorn University, Patumwan, Bangkok, 10330, Thailand*
[d]*Materials Innovation Center, Faculty of Engineering, Kasetsart University, Chatuchak, Bangkok, 10900, Thailand*
* n-kongkj@tu.ac.th and nutthita.c@chula.ac.th (corresponding author)

Keywords: powder injection molding, statistical analysis, flexural strength, density

In this work, statistical analysis methods, including linear regression and statistical hypothesis testing, were used to study the flexural strength and density of the specimens formed from mullite powder by powder injection molding (PIM). The feedstock for PIM consist of mullite powder and the composite binder consisting of 78 wt% polyethylene glycol (PEG), 20 wt% polyvinyl butyral (PVB), and 2 wt% steric acid (SA). The small lab scale powder injection molding machine was used in this work. By using this machine, the possible feedstock compositions, which can be injection molded, were 50, 52, or 54 vol% mullite. After molding, PEG in the green product was removed prior to sintering by soaking the specimens in the water for 24 hours while PVB and SA were removed during sintering. The sintering temperatures were 1300 or 1400 ^{o}C. From the statistical analysis at significance level of 0.05, the specimens sintered at 1400 ^{o}C have higher average flexural strength and density than the specimens sintered at 1300 ^{o}C. In addition, the density of the sintered specimens has the positive linear correlation with the volume percent of mullite in the feedstock used in this work.

CM-P-09

The Use of Bottom Ash from Mae Moh Power Plant and Waste Glass in Ceramic Glaze Composition

Benya Cherdhirunkorn[a*], Chanapa Panthong[a], Rarintorn Darunpong[a] and Pratch Kittipongpattana[b]
[a]*Materials Science Program, Department of Physics, Faculty of Science and Technology, Thammasat University, Klong Laung, Patum Thani, 12120, Thailand*
[b]*Electricity Generating Authority of Thailand, Mae Moh, Lampang, 52220, Thailand*
*benya@tu.ac.th

Keywords: bottom ash, ceramic glaze

In this work, experiments have been carried out to evaluate the utilization of bottom ash (by-product of Mae Moh power plant, Lampang, Thailand) as a raw material in the ceramic glaze composition. The bottom ash was mixed with a commercial transparent glaze powder and ground waste glass (soda-lime glass). The bottom ash was used to replace the transparent glaze powder in a proportion of up to 100% in weight. The chemical compositions of the bottom ash, transparent glaze and waste glass were investigated using XRF technique. The major compositions of the bottom ash are silica (SiO_2), alumina (Al_2O_3), calcite (CaO) and iron oxide (Fe_2O_3), which could possibly be a suitable raw material for ceramic glaze. The bottom ash modified glaze was applied on calcined stoneware biscuits, and were then sintered at the temperature of 1200, 1250 and 1300ºC for 1 hour. Effects of the bottom ash on the color, glossiness, hardness, phase structure and microstructure of the glaze were investigated. The iron oxide in the bottom ash composition gave rise to the green to dark brown colors of the bottom ash glaze fired at high temperature. It was found that the glossiness and fusibility of the glaze decreased with the higher content of bottom ash. Optical microscope revealed the development of needle liked shape crystals in the bottom ash glaze. In this study, waste glass was also used as an additional raw material to encourage the fusibility of the bottom ash glaze. The surface hardness of all glazes determined by the Mohs scale were between 6–7.

CM-P-10

The Effects of Water Removal Process on the Properties of Magnesium Aluminate Spinel Nanopowders Synthesized by Co-precipitation Method

Sarut Teerasoradech[a] and Karn Serivalsatit[a,*]

[a]*Department of Materials Science, Faculty of Science, Chulalongkorn University, Pathumwan, Bangkok, 10330, Thailand*

*Email address: Karn.s@chula.ac.th

Keywords: $MgAl_2O_4$, Precipitation, Water Removal Process

Magnesium aluminate spinel ($MgAl_2O_4$) or spinel ceramics have been widely used in engineering fields due to its attractive properties, such as high mechanical strength, good optical properties, and high refractoriness. Precipitation is one of the most common technique for preparing spinel nanopowders because it offers many advantages including low cost, simple method, and ease of mass production. However, severe agglomeration usually takes place during water removal process, i.e. washing and drying. These hard agglomerates deteriorate sinterability of nanopowders. In this study, spinel nanopowders were prepared by co-precipitation. The remaining water in the precipitate precursor was removed by freeze drying or washing the precipitate precursor with organic solvents, i.e. ethanol and acetone-toluene-acetone. Conventional drying process was also performed for comparison. The characteristics of the obtained spinel nanopowders were investigated by X-ray Diffraction (XRD), Scanning electron microscopy (SEM), Transmission electron microscopy (TEM), Brunauer–Emmett–Teller (BET) method. The results showed that the water removal process did not have any significant effects on phases of dried precursors and calcined powders. However, washing the precipitate precursor with organic solvent is the most effective process to prepare spinel nanopowders with low degree of agglomeration. Whereas, removing water by conventional drying process led to the formation of hard agglomerates. Furthermore, the effects of water removal process on sinterability of the spinel nanopowders were also reported.

CM-P-11

Fabrication and Properties of ZrO_2(1.5Y)-25mol% Al_2O_3 Powder Injection Moulding Feedstock using Pulsed Electric-Current Pressure Sintering

Nutthita Chuankrerkkul[a,*], Koki Sasai[b] and Ken Hirota[b]
[a]Metallurgy and Materials Science Research Institute, Chulalongkorn University, Bangkok 10330, Thailand
[b]Faculty of Science and Engineering, Doshisha University, Kyotanabe, Kyoto 610-0321, Japan
*nutthita.c@chula.ac.th

Keywords: zirconia, alumina, pulsed electric-current pressure sintering, polyethylene glycol

Powder of ZrO_2(1.5Y)-25mol%Al_2O_3 was used as starting materials for fabrication of powder injection moulding feedstock prior to densification using pulsed electric current pressure sintering (PECPS). The binder system employed in this study composed of polyethylene glycol (PEG) and polyvinyl butyral (PVB). A variety of processing parameters have been investigated, including powder and binder ratio, binder removal condition as well as sintering profile. After systematically optimizing of the process, it has been found that density of 97.7 % of the theoretical value could be achieved from specimens containing 35vol% powder loading and sintered by PECPS apparatus at 1350ºC under pressure of 60 MPa for 10 min in Ar atmosphere. The hardness (H_v) and fracture toughness (K_{IC}) values of the specimens are 12.6 GPa and 12.8 MPa.$m^{1/2}$, respectively. Phase analysis was carried out with XRD and microstructure of fracture surface of sintered specimens was observed using SEM.

CM-P-12

Preparation and Characterization of Clays from Different Areas in Ban Bo Suak, Nan province, Thailand

Usanee Malee[a,b]*, Sakdiphon Thiansem[c]

[a]*Department of Physics and Materials Science, Faculty of Science, Chiang Mai University, Chiang Mai 50200, Thailand.*

[b]*Science and Technology, Chiang Mai Rajabhat University, Chiang Mai 50200, Thailand.*

[c]*Department of Industrial Chemistry, Faculty of Science, Chiang Mai University, Chiang Mai 50200, Thailand.*

* umclay2014@gmail.com

Keywords: Clay, Nan pottery, Iron oxides, quartz

The scientific process was applied for explanation of the characterization and physical properties of the clays close to the ancient Nan kiln site. These clays were obtained from JQA, FQB, PQC and NQD. X-ray diffraction (XRD) and X-ray fluorescence (XRF) techniques were determined the chemical composition and phase transformation before and after fired at 1250 ºC. XRD pattern indicated that quartz was the majority of phase in all ancient clays. This quartz structure was transformed depending on firing temperatures in the range of 800-1250 ºC. XRF result was confirmed that all clays had main SiO_2 (>80 wt. %) that formed in quartz structure. High Fe_2O_3 (>1.6 wt.%) related to the red-dark tone color. The maximum Fe_2O_3 content was obtained in PQC clays, so it had dark tone color. Therefore, the highest densification was investigated in PQC clay because it had high fluxing agent of Fe_2O_3 during sintering mechanism. Besides, the firing resistance found that these clays could be fired up to 1280 ºC without wrapping behavior, while FQB clay had the highest of firing resistance due to the maximum quartz content.

CM-P-13

Preparation and Properties of PSZTM Ceramics with Different Method

Arjin Boonruang*, Piyalak Ngernchuklin, Saengdoen Daungdaw, Nestchanok Yongpraderm, Chalermchai Jeerapan and Chutima Eamchotchawalit
Thailand Institute of Scientific and Technological Research, Technopolis, Klong Luang, Pathum Thani, 12120, Thailand
* arjin@tistr.or.th

Keywords: Solid State Reaction, Piezoelectric coefficient, Mechanical Quality Factor, Planar Coupling Coefficient.

The PSZTM ceramics from $Pb_{0.94}Sr_{0.06}(Zr_{0.52}Ti_{0.48})O_3$ doped with 0.1 mol% Mn were prepared by a solid state reaction and then conventional sintering process. Two different methods were used to calculate the amount of Mn-dopant into PSZT powder. One was calculated rely on B-site precursor represented by *B* method. The other was computed based on the amount of calcined PSZT called *C* method. This study was to investigate the effect of the two different calculating formulations of Mn doped PSZT ceramics calculated by B and C methods on phase formation, microstructure, physical and electrical properties. The results were observed that phase identification showed the formation of perovskite structure in both cases. Besides, the mechanical quality factor (Q_m) of the PSZTM ceramics derived from *B* method was two times higher than those from *C* method. Nevertheless, the dielectric constant (K), piezoelectric coefficient (d_{33}) and planar coupling coefficient (k_p) of the PSZTM ceramics from *B* method were slightly lower than those of derived from *C* method. This could be drawn the conclusion that PSZTM with 0.1 mol% Mn prepared by *B* method can be used as hard-type piezoelectric material.

CM-P-14

Fabrication of Lead-free $Li_{0.06}(K_{0.5},Na_{0.5})_{0.94}NbO_3$ Piezoelectric Nanofiber by Electrospinning

Supattra Wongsaenmai[a,*], Santi Maensiri and Rattikorn Yimnirun

[a]*Program in Materials Science, Faculty of Science, Maejo University, Sansai, Chiang Mai, 50290, Thailand*

[b]*School of Physics, Institute of Science, Suranaree University of Technology, Nakhon Ratchasima,30000, Thailand*

*wongsaenmai@yahoo.com

Keywords: Lead-free; Nanofiber; Sol-Gel; Electrospinning

In this work, $Li_{0.06}(K_{0.5},Na_{0.5})_{0.94}NbO_3$ nanofibers were synthesized by electrospinning utilizing sol–gel precursors. The electrospun polymer-ceramic composite fibers were heat treated to yield perovskite $Li_{0.06}(K_{0.5},Na_{0.5})_{0.94}NbO_3$ fibers after calcined at 600 ºC for 2 h. The morphology, microstructure and crystal structure were investigated by SEM and XRD. Typical fiber diameter was between 80 and 95 nm with the length over 0.1 mm. It has been found that the single phase tetragonal structure was obtained at temperature of 800ºC. The morphology of the nanofibers were influenced by the calcination temperature.

CM-P-15

The Influence of Feeding Rate, Inlet Temperature, and Atomization Pressure on the Particle Size of Spray Dried Alumina Granules

Mana Rodchom[a,*], Kritkaew Somton[a], Kannigar Dateraksa[a] and Ryan McCuiston[b]
[a]*National Metal and Materials Technology Center, Pathum Thani 12120*
[b]*King Mongkut's University of Technology Thonburi, Bangkok 10140*
* Manar@mtec.or.th

Keywords: Spray Drying, Particle Size, Atomization Pressure, Alumina Granules

This research studied the effect of varying spray drying parameters on the resulting particle size of alumina granules. The variable parameters in the study were the slurry feeding rate (400-1200 ml/min), the inlet air temperature (200-300 ºC) and the nozzle atomization pressure (2.5-5.5 bar). A two-fluid nozzle type spray dryer was used for the experiments. An aqueous alumina slurry with a solids content of 55 to 60% was produced by ball milling. The particle size of the slurry and the granule sizes after spray drying were measured using a Malvern Mastersizer 2000. The microstructure and cross-sectional morphology of the granules were analyzed by optical microscopy. The produced granules had more spherical shape than hollow shape. The average particle size of the slurry before spray drying was less than 1 micron. The average granule sizes ranged from approximately 25 to 115 microns for the 63 spray drying experiments that were performed. It was found that the average granule size was increased as the inlet temperature and feeding rate were increased, while the atomization pressure was decreased. Though, the average granule size appeared to be the most sensitive to the atomization pressure followed by either the inlet temperature or feeding rate. Possible explanations for the observed trends will be discussed.

CM-P-16

Effect of Processing Temperature on Physical Properties of SnO_2-based Nanostructure Synthesized by Hydrothermal Process

Wuttichai Sinornate[a,*], Wanichaya Mekprasart[a] and Wisanu Pecharapa[a,b]

[a]College of Nanotechnology, King Mongkut's Institute of Technology Ladkrabang, Bangkok 10520, Thailand

[b]ThEP Center, CHE, 328 Si Ayutthaya Rd., Bangkok 10400, Thailand Tel. +6623298000 ext. 3117, Fax. +6623298265

E-mail: kan1479@gmail.com

Keywords : Hydrothermal process, Physical properties, Tin oxide

SnO_2-based nanostructures were synthesized via hydrothermal process by varying process temperature starting from solution of tin chloride and catyltrimethyl ammonium bromine (CTAB) for reducing agent. The hydrothermal temperature was conducted in range of 100 to 120 °C and its effect on significant properties of the products were investigated. The physical properties, its morphology and chemical bonding of hydrothermally synthesized SnO_2 nanostructure were characterized by X-ray diffraction spectra (XRD) scanning electron microscopy (SEM), and Raman spectroscopy. Preliminary results suggest that, as-synthesized nano-sized SnO_2 structures and phase transform are highly affected by the hydrothermal temperature. The enhancement in their crystallinity and good formation of SnO_2 nanostructure are obtained by the increase in processing temperature resulting from sufficient heat energy during the hydrothermal process.

CM-P-17

Synthesis of $BiVO_4$ Photocatalyst Powders by Microwave-assisted Hydro/solvothermal Process

Sujaridworakun P.[a,b,*], Thanomsri N.[a], Wu X.[c] and Sato T.[c]
[a]*Research Unit of Advanced Ceramics, Department of Materials Science, Faculty of Science, Chulalongkorn University, Bangkok 10330, Thailand*
[b] *Center of Excellence on Petrochemical and Materials Technology, Chulalongkorn University, Bangkok 10330, Thailand*
[c]*Institute of Multidisciplinary Research for Advanced Materials (IMRAM), Tohoku University, Sendai 980857, Japan*
*E-mail: pornapa.s@chula.ac.th

Keywords: bismuth vanadate, microwave synthesis, solvothermal, visible-light responsive photocatalyst

In this work, the pure monoclinic $BiVO_4$ powders were prepared by microwave-assisted hydro/solvothermal process using $Bi(NO_3)$ and $NaVO_4$ as precursors. The effects of synthesis conditions on the phase formation, particles size and surface area of the resultant products were characterized by X-ray diffraction (XRD), scanning electron microscopy (SEM), transmission electron microscopy and BET surface area analysis. It was found that synthesis pH played a significant influence on the phase formation of $BiVO_4$. The increasing in microwave irradiation time and temperature enhanced the crystallization of pure monoclinic $BiVO_4$. Moreover, $BiVO_4$ powder obtained from solvothermal synthesis had smaller particle with higher surface area than that obtained from hydrothermal. As the results, it was obtained that the pure monoclinic $BiVO_4$ powder with surface area in range of 3-10 m^2/g could be prepared by microwave-assisted hydro/solvothermal process at pH about 5 and temperature at 170-200^oC for 10-30 min.

CM-P-18

Influences of Inhibitor and Firing Temperature on Efflorescence Reduction of Clay Products

Sunisa Jindasuwan[a,*], Pim Chakornnipit[a] and Sitthisuntorn Supothina[b,*]
[a]*Department of Industrial Chemistry, Faculty of Applied Science, King Mongkut's University of Technology North Bangkok, Bangkok, 10800 Thailand*
[b]*National Metal and Materials Technology Center, 114 Thailand Science Park, Paholyothin Rd., Pathumthani 12120 Thailand*
*sunisaj@gmail.com

Keywords: Efflorescence; Clay products; Firing temperature; Barium carbonate

For ceramic industry, efflorescence is undesirable and cannot be completely eliminated. The efflorescence mostly appears as white and thin foggy salts deposited on the surface of porous ceramic body. The presence of soluble sulfate compounds in the raw materials is mostly certain to cause the efflorescence. In this research, the removal of sulfate ions in clay ceramic was studied and the sulfate ions were immobilized by forming a water-insoluble compound. The sulfate ions in raw materials and fired products were extracted by distilled water, and the concentration was determined by using UV-visible spectroscopy at wavelength 420 nm following the ASTM C 380-03 standard. Three sources of raw materials from Tambon Suan Phung, Ratchaburi, Tambon Mae Win and Mae Ta, Chiang Mai, were investigated. The sulfate concentrations were 253.17, 185.81 and 145.14 ppm, respectively. Thus, the highest sulfate concentration of Tambon Suan Phung, Ratchaburi was selected for further study on the effect of inhibitor and firing temperature on efflorescence inhibition. To reduce solubility of the sulfate, three kinds of inhibitor, *i.e.* barium chloride, barium carbonate and barium hydroxide, were added into the raw material from Tambon Suan Phung at various concentrations, *i.e.* 0.5, 1.0, 1.5 and 2.0 wt.% and homogeneously mixed by ball milling followed by the addition of distilled water to prepare clay slip. The clay products were mold casted to 1 x 1 x 3 inch^3 in size. Then, they were fired at 800, 900 and 1000 C. The results showed that the addition of barium carbonate at 2 wt.%, which is the highest amount employed in this study, and firing temperature of 900 C resulted in least sulfate leaching due to the formation of water-insoluble barium sulfate. To perform a field test, the fired samples with and without the addition of barium carbonate were immersed in water for 4 months. The efflorescence was observed on the sample without barium carbonate within the 1st month. In contrast, with the addition of barium carbonate, no efflorescence was observed after testing for 4 months.

CM-P-19

Electromechanical Displacement of Soft/Hard PZT Bi-layer Composite Actuator

Piyalak Ngernchuklin[a,*], Jungho Ryu[b], Arjin Boonruang[a], Sittichai Kanchanasutha[a] and Pracha Laoauyporn[a]

[a] *Materials Innovation, Thailand institute of scientific and technological research (TISTR), Klong Luang, Pathum Thani, 12120, Thailand*

[b] *Functional Ceramics Group - Korea Institute of Materials Science, 797 Changwondaero, Seongsan-gu, Changwon, Gyeongnam, 642-831, Korea*

*piyalak@tistr.or.th

Keywords: soft PZT, hard PZT, bi-layer composite, actuator

Lead Zirconate Titanate (PZT) is a well-known piezoelectric material which has been widely used for transducer, sensor and actuator applications. According to the compositional modifications near morphotropic phase boundary, PZTs can be classified into two types, soft PZT and hard PZT, which are distinguished by the piezoelectric properties. Therefore, the combination effect of the strain-E-field response of soft/hard PZT composite actuator has been much interested to be observed. In this study, soft and hard PZT powders were co-pressed into bi-layer disks with various ratios of soft PZT powder, ranging from 0-100 vol. % (with 10 % increments) and then co-sintering. Due to the shrinkage difference of the two layers, the bi-layer composites with various dome heights were obtained. Moreover, it was shown that the constrained layer either soft PZT or hard PZT affected to the dome geometry, the strain-E-field response and displacement hysteresis loop. The purpose of this study was to investigate the electromechanical properties and actuation performance of such bi-layer composite actuators and to compare with the soft and hard PZT single layer counterparts.

CM-P-20

Forming of Zeolite Composite Substrate Coated with Titania for Photocatalyst Decomposition of Organic Compound

Khemmakorn Gomonsirisuk[a,b] , Thanakorn Wasanapiarnpong[a,b*]

[a] *Research Unite of Advanced Ceramics, Department of Materials Science, Faculty of Science, Chulalongkorn University, Bangkok, Thailand*

[b] *Center of Excellence on Petrochemical and Materials Technology, Chulalongkorn University, Bangkok, Thailand*

*thanakorn.w@chula.ac.th

Keywords: Zeolite, Photocatalyst, TiO_2, Activated carbon, Waste water treatment

Organic contaminated waste waters from petrochemical industries can be removed by adsorbent and photocatalyst. In this work, the degradation rate of phenol have been studied at different ratios of Activated carbon/Na-A zeolite/TiO_2 photocatalyst composite materials which are easily to be fabricated into tubular shape by extrusion method. In addition, the foam-inserted composite can be floated on the surface of waste water for the higher phocatalyst activity. While the composite is the low cost adsorbent with high absorption and high ion exchange properties. In order to optimize the efficiency of material, the various ratios of Activated carbon/Na-A zeolite (3/1, 1/1 and 1/3) and amount of coated TiO_2 on the specimen was studied by UV/Vis spectrophotometer which related to phenol concentration. Moreover the various amount of phenolic resins (10, 20, 30, 40 and 50%) at different reduction firing temperatures (600 and 650 ^oC) with soaking time of 1, 2 and 3 hours affected to the compressive strength of samples. For the characterization, XRD is used to characterize the phase and SEM is used to provide the morphology of the prepared composite materials.

CM-P-21

Fabrication of Porous Hollow Cylinder Activated Carbon-Zeolite Substrate

Nithiwach Nawaukkaratharnant[a], Thanakorn Wasanapiarnpong[a,b,*], Pornapa Sujaridworakul[a,b], Charusporn Mongkolkachit[c]

[a] Research Unit of Advanced Ceramics, Department of Materials Science, Faculty of Science, Chulalongkorn University, Bangkok, 10330, Thailand
[b] Center of Excellence on Petrochemical and Materials Technology, Bangkok, 10330, Thailand
[c] National Metal and Materials Technology Center, Pathum Thani, 12120, Thailand
*thanakorn.w@chula.ac.th

Keywords: Porous, Hollow Cylinder, Activated Carbon, Zeolite.

Activated carbon, zeolite and titanium dioxide are wildly used for removing the organic compounds in waste water. Although, these materials exhibit high performance (in powder form), reclaiming of these materials from the waste water treatment system is still hard. The objective of this study is to fabricate hollow cylinder activated carbon-zeolite samples which were used as a porous substrate. Various percentages of activated carbon and zeolite NaA were mixed with special binder to form dough before extruded to be hollow cylinder shape. The samples were dried at room temperature for 24 hours and at 60°C for 6 hours. The hollow cylinder samples were cut into 2.5 cm long before fired at different temperature and soaking time. The result showed that the strength of the fired samples decreased with the amount of zeolite NaA increased. Moreover, the XRD patterns of samples showed crystallinity of zeolite slightly decreased with firing temperature increased. The physical properties and microstructure will be discussed.

CM-P-22

Effect of Rice Husk and Rice Husk Ash on Properties of Lightweight Clay Bricks

Sutas Janbuala* **and Thanakorn Wasanapiarnpong**
Department of Materials Science, Faculty of Science, Chulalongkorn University, Bangkok,10300 Thailand
*sutas_jan@dusit.ac.th

Keywords: Lightweight ceramics, Clay bricks, Rice husk, Rice husk ash

The objective of this study is to investigate the effect of rice husk and rice husk ash with has the difference chemical composition and organic matter on porosity and properties of lightweight clay brick ceramics. Comparative adding between rice husk and rice husk ash were varied by 10, 20, 30, 40 % by weight. The results showed that more adding of rice husk and rice husk ash increase porosity and water absorption, while decrease bulk density. Porosity and water absorption is maximized when the rice husk is added at 40 %. The clay brick ceramics with 10, 20 and 30 % of rice husk or rice husk ash addition showed the required density and compressive strength followed the industrial standard of lightweight brick. The addition with 10 % of rice husk showed the best properties as 1.20 g/cm^3 of bulk density and 4.5 MPa of compressive strength with 36.57 % of porosity. Whereas, the 10 % addition of rice husk ash showed 1.28 g/cm^3 of bulk density and 5.97 MPa with 37.27 % of porosity. Moreover, microstructure are also investigated and discussed.

CM-P-23

Effect of Sintering Additive and Pyrolysis Temperature on Porous Silicon Carbide Ceramic

Chalermkwan Makornpan[a,b], **Charusporn Mongkolkachit**[c], **Suda Wanakitti**[c], **Thanakorn Wasanapiarnpong**[a,b,d*]

[a] *Research Unite of Advanced Ceramics, Department of Materials Science, Faculty of Science, Chulalongkorn University, Bangkok, Thailand*

[b] *Center of Excellence on Petrochemical and Materials Technology, Chulalongkorn University, Bangkok, Thailand*

[c] *National Metal and Materials Technology Center, Khlong Luang, Pathum Thani, Thailand*

[d] *Local Materials Technology Development Center, Metallurgy and Materials Science Research Institute, Chulalongkorn University*

*thanakorn.w@chula.ac.th

Keywords: Silicon Carbide, Pyrolysis, Rice Husk, In-situ Reaction Bonding

Rice husk was used as a raw material to fabricate silicon carbide (SiC) ceramics. Carbothermal reduction was used together with in-situ reaction bonding as the preparation method. Rice husk was carbonized at the temperature around 700 ^{o}C in an incineration furnace. Carbonized rice husk was ground and treated with hydrochloric acid solution. After grinding, the sample powders were mixed with silicon metal powder and sintering additives (alumina (Al_2O_3) and magnesia (MgO)). The mixed powders were pressed and then pyrolyzed at various temperatures and pyrolysis patterns in argon atmosphere. Silicon carbide, as the main crystalline phase, was obtained in all pyrolized samples. Cristobalite was found together with silicon carbide in the samples which pyrolized only lower than 1500 ^{o}C. Amount of silicon carbide particle was increased at higher pyrolysis temperature while silicon carbide whisker was decreased. Weight loss, shrinkage and porosity of the pyrolized samples were investigated. Weight loss and shrinkage of the samples increased when increasing pyrolysis temperature while porosity decreased.

CM-P-24

Dispersion Stability of Silicate Powder in Water

Siriporn Larpkiattaworn [a*], Wasana Khongwong [a], Siriporn Tong-On[a], Chutima Eamchotechawalit [a] and Chaiwat Vorapeboonpong[b]

[a]Thailand Institute of Scientific and Technological Research (TISTR), Pathumthani,12120 Thailand

[b]Metropolitan Waterworks Authority, Bangkok, 10210 Thailand

* siriporn@tistr.or.th

Keywords: particle suspension, silicate powder, Zeta potential, turbidity

The objective of this study is to investigate the particle suspension stability of silicate powder which are bentonite, micro silica (Micro-SiO_2), nano-silica (Nano-SiO_2), and drinking water treatment sludge (DWTS). The main dispersion characteristic are related to particle size, and dispersion force. The representative samples of bentonite, micro-SiO_2, nano-SiO_2, and DWTS were dispersed at the same solid content in water. The particle size distribution and chemical composition of samples were analyzed. The suspended samples were measured for Zeta potential at the controlled pH value. Furthermore, turbidity of suspended samples were investigated at various sedimenting time. The results indicated that nano-SiO_2 has the highest Zeta potential value at pH 8-12. The stability of particle dispersion could be implied from turbidity of suspension at various sedimenting time. Bentonite suspension performed more stability than other samples for longer time. However, stability of SiO_2 and DWTS particles can be improved by adding dispersion agent in the suspension to create repulsive force from the charge on the particle surface.

CM-P-25

High Porous Zinc Oxide Nanosheets Prepared by a Simple Dipped Coating Method

Theerapong Santhaveesuk*, Chamaiporn Tongpeang, Phongwit Muangnum and Siriwimon Pommek
Physics Program, Faculty of Science and Technology, Pibulsongkram Rajabhat University, Phitsanuloke, 65000, Thailand
*s_theerapong@yahoo.co.th

Keywords: Nanosheets, Porous structure, Dipped coating, ZnO

In this study, high porous Zinc oxide nanosheets were successfully synthesized using a simple dipped coating method. Commercial glass slides were cleaned and used as substrate; and 0.1 M Zinc nitrate solution was used as starting material. The dipped cycle was varied to be 1, 2, 5, and 10 times using bared glass substrate as a control sample. After dipped coating in Zinc nitrate solution, the glass substrate was heated at 150°C for 10 min for each dipped cycle. The dipped coating glass substrates were calcined at 350, 400, 450 and 500°C for 2 hr; and theirs characteristics were investigated. It was observed that the synthesized product exhibited a sheet-like structure with high number of a very small pore, growing perpendicular with the glass substrate. The high porous ZnO nanosheets showed the hexagonal-wurtzite structure similar to the JCPDs standard file, with a good crystallinity of single crystal. In should be note that the crystalline size decreased with the increasing of calcined temperature. The film thickness was increased as the increasing of the dipped cycle; however, the morphology and the chemical composition of the porous ZnO nanosheets were not changed with the heating temperature. Moreover, optical energy band gap of porous ZnO nanosheets was also carried out. It was calculated to be 3.33 - 3.35 eV. The high porous ZnO nanosheets might be apply for many electronic applications.

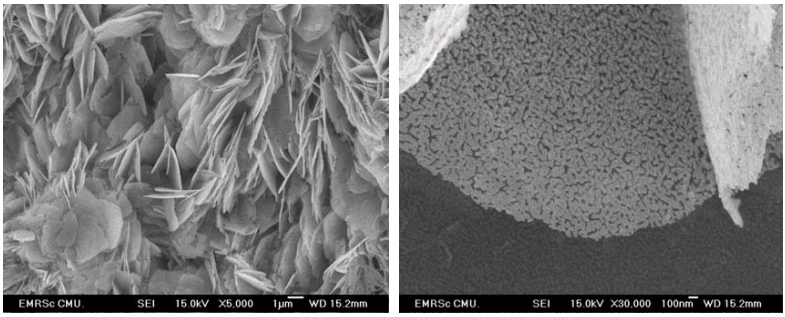

Fig.1 show the porous ZnO nanosheets with different magnification,
(a) 2 cycles dipped and calcined at 400°C and (b) 5 cycles dipped and calcined at 500°C.

CM-P-26

Effect of Firing Temperature and Mo Doping on Properties of Solar-Reflective $Sm_2Ce_2O_7$ Yellow Pigment

Mantana Suwan, Pantip Sakchaikul, Sorachon Yoriya and Sitthisuntorn Supothina*

National Metal and Materials Technology Center, 114 Thailand Science Park, Paholyothin Rd., Klong Luang, Pathumthani, 12120, Thailand

*sitthis@mtec.or.th

Keywords: Cool pigment; Solar-reflective pigment; Near-infrared; Yellow pigment

It has been well realized that a white pigment has highest solar reflectance while a dark pigment has lowest reflectance. However, the white pigment is not well accepted for an outdoor paint. It is thus the aim of this study to develop a non-white pigment focusing on the yellow pigment with the targeted reflectance of at least 60%. The pigment was synthesized from raw materials consisting of the Sm_2O_3 and the CeO_2 in the presence of the $(NH_4)_6Mo_7O_{24}$ employed for the Mo doping. The raw materials were wet milled in acetone for 6 h to acheive a homogeneous slurry followed by calcination at 1100, 1300 and 1500 ºC for 6 h. Then, the fired product was ground and sieved through a 325-mesh. The effect of the Mo doping was investigated by adding 10, 15, 20, 25 and 30 wt.% $(NH_4)_6Mo_7O_{24}$. XRD analysis of the undoped product revealed the presence of $Sm_2Ce_2O_7$ at 1300 ºC along with the unreacted Sm_2O_3 and CeO_2, and revealed the complete reaction at 1500 ºC. The addition of $(NH_4)_6Mo_7O_{24}$ resulted in the formation of $Sm_2Ce_{2-x}Mo_xO_7$, where x = 0.02, 0.03, 0.04 and 0.05 depending on the amount of the dopant employed. The doping also significantly affected the product's color; it turned from ivory white to yellow with increasing dopant content up to 20 wt.% and became dark yellow afterward. Increasing firing temperature from 1100 to 1500 ºC led to brigther yellow, and the decrease of band-gap energy from 2.88 to 2.62 eV due to the substitution of Mo^{6+} for Ce^{4+}. At the optimum synthesis condition, *i.e*. 20 wt.% doping and 1500 ºC firing temperature, the product was most yellowish and had 69.2 % near-infrared reflectance.

CM-P-27

Effect of Crystallinity of Hydroxyapatite Nanoparticles Prepared from Bovine Bone on Adsorption of Ammonium Gas

Thonnisorn Choochaisangrat[a], Teerasak Powduang[a], Neeranut Kuanchertchoo[b], and Dujreutai Pongkao Kashima[a,*]
[a]*Research Uunit of Advanced Ceramics, Department of Materials Science, Faculty of Science, Chulalongkorn University, Pathumwan, Bangkok 10330, Thailand.*
[b]*Department of Materials Technology, Faculty of Science, Ramkamhaeng University, Huamark, Bangkapi, Bangkok 10240, Thailand.*
* dujreutai@gmail.com

Keywords: Crystallinity, Hydroxyapatite, Bovine Bone, Ammonium Gas Adsorbent

The adsorption of ammonium gas on nanoparticle hydroxyapatite (HA) prepared from bovine bone was investigated. Hydroxyapatite acts as good adsorbent for positive charge containing gas. In this study, bovine bone was cleaned, calcined at 700 °C for 4 hr and subsequently ground. The ground bovine bone powder was the starting material for synthesize of nanoparticle hydroxyapatite (HA) via precipitation. As-precipitated HA nanoparticles were filtered, washed and finally calcined at 500, 600, and 700°C. Phase analyses were performed by x-ray diffraction (XRD) and the result showed that the higher the calcined temperature, the higher the degree of crystallinity. The result of ammonium gas adsorption indicated that as-precipitated HA with low crystallinity displayed better adsorption activity to ammonium gas than calcined HA with high crystallinity.

CM-P-28

Development of Durability against Water of Waste-based Gypsum Bodies due to Steel Ladle Furnace Slag and Roofing Tile Sludge

Wantanee Buggakupta[1,2*], Pinsiri Umponpararat[1] and Withaya Panpa[3]

[1]*Department of Materials Science, Faculty of Science, Chulalongkorn University, Bangkok, 10330, Thailand*

[2]*Center of Excellence on Petrochemical and Materials Technology, Chulalongkorn University, Bangkok, 10330, Thailand*

[3] *Faculty of Industrial Technology, Thepsatri Rajabhat University, Lopburi 15000, Thailand*

* wantanee.b@chula.ac.th

Keyword: industrial wastes, FGD gypsum, water durability, ladle furnace slag

Gypsum bodies can be made from natural sources as minerals, as well as synthetic sources, in the form of industrial wastes like phosphogypsum and flue-gas desulphurization gypsum (FGD gypsum). Regardless of gypsum's originality, all gypsum bodies still have low strength and poor water resistance. This work proposes the improvement of water resistance along with strength and physical nature of the FGD-based gypsum mix according to the addition of steel ladle furnace slag. The gypsum matrix contained up to 75 wt% FGD gypsum and cements in order to gain strength an early stage. Various combinations of slag and sludge were added into the mixture, in total of 15 wt%. The ingredients were them thoroughly mixed and cast into cubes and cured at room temperature for 7, 14 and 28 days. Phase content, mechanical strength and microstructure of the gypsum bodies were characterized. Durability of the introduced waste-bearing-gypsum was determined by wet-dry cycles, followed by compressive test. Resistance against water in particular was also reported. Experimental results showed that gypsum with a high slag to sludge ratio provided higher strength and lower water absorption after 28 days. Durability in water was enhanced compared to ones without slag and sludge. Weight loss after immersion in water also slightly decreased with increasing slag and sludge ratio.

CM-P-29

Phase Formation of Cu and Zn Doped Nickel Maganite Ceramics by Sol-Gel Autocombustion Method

Tanawadee Dechakupt[a,*], Piyalak Ngernchuklin[b], Sakunthip Sutharuk[a] and Juthamad Seacheu[a]

[a]Department of Industrial Chemistry, Faculty of Applied Science, King Mongkut's University of Technology North Bangkok, 10800, Thailand

[b]Materials Innovation Department, Thailand Institute Scientific and Technological Research, Pathum Thani, 12120, Thailand

* twadee@gmail.com

Keywords: Nickel manganite, sol-gel autocombustion, phase formation

Phase formation and microstructure of $NiMn_2O_4$ and $NiMn_{1.4-x}Zn_{0.6}Cu_xO_4$ (x=0, 0.2, 0.4, 0.6) ceramics synthesized by sol-gel autocombustion were investigated. X-ray diffraction shows that as-burnt powders consist of second phases such as NiO, CuO and ZnO as a result of incomplete combustion. After calcined at 850°C, high crystallinity of cubic spinel structured powders was obtained. However, NiO and CuO were found in $NiMn_{1.4-x}Zn_{0.6}Cu_xO_4$ powders when $x \geq 0.4$, indicating phase separation from spinel structure. After ceramic fabrication and sintering at 1150°C, it was revealed that tetragonal spinel structure transforms into cubic structure when the amount of copper increases. ZnO was present in low Cu compositions and disappeared in high ($x \geq 0.4$) compositions. Scanning electron microscopy shows that $NiMn_2O_4$ and $NiMn_{1.4-x}Zn_{0.6}Cu_xO_4$ ceramics, when x = 0 and 0.2, have equiaxed grains. Grain size increased as the amount of Cu increased. Separation of high Cu phases along with porosity was clearly observed in $NiMn_{1.4-x}Zn_{0.6}Cu_xO_4$ ceramics when $x \geq 0.6$.

CM-P-30

Influence of Alkaline Concentration on Physical Properties of Porous Geopolymer using Silica Fume as Foaming Agent

S. Anut[a,b,*], J. Sirithan[a,b] and L. Pitak[c]

[a]Research Unit of Advanced Ceramics, Department of Materials Science, Faculty of Science, Chulalongkorn University, Bangkok, 10330, Thailand

[b]Center of Excellence on Petrochemical and Materials Technology, Chulalongkorn University, Bangkok, 10330, Thailand

[c]National Metal and Materials Technology Center, Klong Luang, Phathum Thani, 10120, Thailand

*Sirithan.j@chula.ac.th

Keywords: Porous geopolymer, thermal conductivity, dehydroxylated kaolin.

Porous geopolymer could be synthesized by using dehydroxylated kaolin and silica fume as foaming agent. Silica fume has motivation to use as additive. Free silicon contained inside silica fume is oxidized with alkaline solution. This reaction released hydrogen gas which generated porosity. The foams morphology were estimated as function of silica fume contents and alkaline concentration. To get homogenous geopolymer paste, the raw materials were mixed by high speed ball mill then poured to polypropylene cylinders mold after that cured at 70 degree celcius for 6 hours. The samples were further cured at room temperature for 3, 7, and 14 days. During the synthesis process, the complex reaction would occur such as polycondensation and oxidation. These reactions affect to chemical and physical properties of porous sample. The porous geopolymer samples were characterized by XRD, compressive strength, FT-IR, microstructure and thermal properties. Porous geopolymer that had NaOH content of 10 molality give high volume expansion (34%) and compressive strength of 17.74 MPa.

CM-P-31

Composition-Microstructure-Property Relationships in $BaTiO_3$ with Mg Addition

Oratai Jongprateep*, Tunchanoke Khongnakhon, Jednupong Palomas
Department of Materials Engineering, Faculty of Engineering, Kasetsart University, 50 Ngamwongwan, Ladyao, Chatuchak, Bangkok, 10900, Thailand
*fengotj@ku.ac.th

Keywords: Barium titanate, combustion synthesis, ceramic processing, dielectric properties

High dielectric constant is one of the main requirements for materials used in fabrication of high energy density capacitors. Enhancement of dielectric constant can be achieved through incorporation of proper elements into dielectric materials. Nevertheless, excessive quantities of additives often lead to secondary phase formation, which often degrades dielectric properties in the materials. This study aims at examining relationships among additive quantities, secondary phase formation, microstructure, and dielectric properties of $BaTiO_3$ with 20, 30 and 40 at% Mg. Solution combustion technique was employed in synthesis of pure and Mg-doped $BaTiO_3$ powders, which were subsequently pressed and sintered at 1350°C. Chemical composition analysis revealed that single phase was observed in undoped $BaTiO_3$ and in $BaTiO_3$ doped at 20 at% Mg. On the contrary, secondary phases were detected in samples with 30 and 40 at% Mg. Grain refinement was observed in samples with 20 at% Mg, while grain coarsening was evident in samples with higher Mg concentrations. Dielectric measurements indicated that dielectric constants of single-phase $BaTiO_3$ increased by more than 3-fold with addition of 20 at% Mg. Dielectric constant, however, significantly decreased in the samples with secondary phases, specifically $BaTiO_3$ with 40 at% Mg addition. Experimental results revealed that the highest dielectric constant was obtained in $BaTiO_3$ samples with 20 at% Mg, which might be attributed to the absence of a secondary phase and grain refinement.

Materials for Energy Session

ORAL PRESENTATIONS

EN-O-01

The Variation of Ternary Catalyst Atomic Ratios (PtRuSn/C and PtRuNi/C) for Ethanol Electrooxidation in Direct Ethanol Fuel Cell

Napha sudachom[a, b], Chompunuch Warakulwit[c, d] and Paweena Parpainainar[a, b, c, *]
[a]*Department of Chemical Engineering, Faculty of Engineering,*
[b] *National Center of Excellence for Petroleum, Petrochemicals and Advance Material, ,*
[c] *Center for Advanced Studies in Nanotechnology, Applications in Chemical Food and Agricultural Industries,*
[d]*Department of Physical Chemistry, Kasetsart University, 50 Ngamwongwan Road, Ladyao, Jatujak, Bangkok, 1090, Thailand*
* fengpwn@ku.ac.th

Keywords: Ternary catalyst, Tri-metallic catalyst, Atomic ratios, Direct ethanol fuel cell.

The studying of the different metal atomic ratios on carbon support (Vulcan XC-72R) for ethanol electrooxidation reaction were investigated by synthesizing of the ternary catalysts (PtRuSn/C and PtRuNi/C) in various atomic ratios (75:20:5, 75:15:10, 75:10:15, 75:5:20). All catalysts were prepared via the Polyol process which the ethylene glycol was used as both solvent and reducing agent. The atomic ratios of the metals on carbon support were confirmed by EDX-SEM. Cyclic Voltammetry was used to investigate the electrocatalytic activity of the catalysts. It was found that the addition of Sn and Ni improved the current density of ethanol electrooxidation reaction. The PtRuSn/C (75:10:15) catalyst showed the highest maximum current density of 3.25 mA/cm^2 in comparison to all catalysts. However, the PtRuNi/C (75:5:20) catalyst exhibited the maximum current density of 2.66 mA/cm^2 which was the maximum current density for PtRuNi/C catalysts. The peak potential of PtRuSn/C catalysts was still lower than the PtRuNi/C catalysts except only PtRuNi/C (75:5:20) catalyst that appeared at the same peak potential (0.6848 V) as PtRuSn/C (75:15:10) and PtRuSn/C (75:20:5). The three highest forward anodic peak current density (I_F) to the reverse anodic peak current density (I_R) ratio were PtRuSn/C (75:15:10), PtRuNi/C (75:15:10) and PtRuNi/C (75:10:15) which were 1.03, 1.01 and 0.99, respectively. This was due to the addition of Sn facilitated the C-C bond breaking in molecule of ethanol and the CO tolerance at lower potential while adding Ni facilitated the CO tolerance and the stability. The high CO tolerance were also found from the medium content of the second metal (Ru) and the third metal (Sn and Ni) with the proper atomic ratio.

EN-O-02

CO Tolerance of Pd-Ni-Sn Electrocatalytic Compositions for Use in Direct Ethanol Fuel Cells

Sompoch Jongsomjit[a], Korakot Sombatmankhong[b,*], Paweena Prapainainar[c,d,e]

[a]Interdisciplinary Graduate Program in Advanced and Sustainable Environmental Engineering (International Program), Faculty of Engineering, Kasetsart University, Bangkok 10900, Thailand

[b]National Metal and Materials Technology Center, 114 Thailand Science Park, Phahonyothin Rd., Khlong Nueng, Khlong Luang, Pathum Thani 12120, Thailand

[c]National Center of Excellence for Petroleum, Petrochemicals and Advance Material, Department of Chemical Engineering, Faculty of Engineering, Kasetsart University, Bangkok 10900, Thailand

[d]Center for Advanced Studies in Nanotechnology Applications in Chemical Food and Agricultural Industries, Kasetsart University, Bangkok 10900, Thailand

[e]Department of Chemistry and NanoTech Center for Nanoscale Materials Design for Green Nanotechnology, Kasetsart University, Bangkok 10900, Thailand

*E-mail: Korakots@mtec.or.th

Keywords: Sodium Borohydride Reduction, CO Tolerance, Direct Ethanol Fuel Cells.

The direct ethanol fuel cell (DEFC) is suffered with electrode poisoning which is a result of strongly adsorbed CO intermediate on the catalyst surface at low operating temperature. Consequently, the present work developed non-noble metals which are durable to the presence of CO contaminant in the system. The sodium borohydride reduction method was used to prepare non-noble catalysts for use in direct ethanol fuel cells. Various compositions of Pd-Ni-Sn electrocatalysts were impregnated on carbon black (Vulcan XC72-R) powder. Twenty percent of palladium by weight was exploited as a based metal catalyst whereas the quantity of nickel and/or tin metal promoters were varied to define the suitable catalyst composition with excellent CO tolerance and high performance for ethanol oxidation reaction. The metal weight ratio of the as-prepared catalysts were 20%Pd/C, 20%Pd20%Ni/C, 20%Pd20%Sn/C, 20%Pd15%Ni5%Sn/C, 20%Pd10%-Ni10%Sn/C and 20%Pd5%Ni15%Sn/C. The X-ray diffraction (XRD) was employed to confirm the presence of Pd peak, $Ni(OH)_2$ peak and SnO_2 peak with respect to the Pd content, Ni content and Sn content catalysts respectively. The oxidation number of Pd, Ni and Sn in 20%Pd10%Ni10%Sn/C ternary catalyst was investigated by X-ray photoelectron spectroscopy (XPS). Apart from the metal forms of Pd^0, Sn^0 and Ni^0, oxides of those metals were also obtained including PdO, SnO_2, NiO, $Ni(OH)_2$ and NiOOH. However, the as-prepared catalysts were primarily composed of Pd^0, $Ni(OH)_2$ and SnO_2. Additionally, CO tolerance of those electrocatalysts was studied via CO stripping test in a mixture of 1M KOH and 1M ethanol. It was found that 20%Pd15%Ni5Sn/C ternary catalytic system exhibited the lowest onset potential of -0.525 V and the highest peak current of 41.71 mA cm^{-2} with the largest peak area of 6.74 mC, indicating the more favourable CO oxidation when compared to those of the binary catalytic system and the based metal catalyst.

EN-O-03

Effect of Sr Substituted $La_{2-x}Sr_xNiO_{4\pm\delta}$ (x = 0, 0.2, 0.4, 0.6, and 0.8) on Oxygen Stoichiometry and Oxygen Transport Properties

Thitirat Inprasit[a], Sujitra Wongkasemjit[a,b], Stephen J. Skinner[c], Mónica Burriel[c,1] and Pimpa Limthongkul[d,*]

[a]*The Petroleum and Petrochemical College, Chulalongkorn University, Bangkok, 10130, Thailand*

[b]*Center of Excellence for Petroleum, Petrochemicals, and Advanced Materials, Chulalongkorn University, Bangkok 10330, Thailand*

[c]*Department of Materials, Imperial College London, Exhibition Road, London, SW7 2AZ, UK*

[d]*National Metal and Materials Technology Center, National Science and Development Agency, 114 Thailand Science Park, Paholyothin Road, Klong 1, Klong Luang, Pathum Thani, 12120, Thailand*

[1]*present address: Catalonia Institute for Energy Research (IREC), Department of Advanced Materials for Energy, Jardins de les Dones de Negre 1, 2nd floor, 08930-Sant Adriá del Besòs, Barcelona, Spain*

*pimpal@mtec.or.th

Keywords: Oxygen content, Oxygen diffusion, Ruddlesden-Popper, Sr substitution on Lanthanum nickelate.

Ruddlesden–Popper type oxides, $La_{2-x}Sr_xNiO_{4\pm\delta}$, have attracted considerable attention as alternative cathode materials for intermediate–temperature solid oxide fuel cells (IT–SOFC) due to their interesting transport properties and adequate thermal expansion coefficient that match with those of the other cell components. Stoichiometry, phase and oxygen diffusion properties of $La_{2-x}Sr_xNiO_{4\pm\delta}$ with x = 0.2, 0.4, 0.6, and 0.8 were investigated in this study. The compounds were prepared via a sol-gel method. Iodometric titration and thermogravimetric analysis were used to determine the oxygen non-stoichiometry. Over the entire compositional range the samples exhibited the I4/mmm tetragonal structure and were in the hyperstoichiometric form with the minimum value δ = 0.14 at x = 0.4. Mixed effects between reduction of oxygen excess and increasing valence of Ni were found as charge compensation mechanisms; the former dominated at a low level of substitution, $x < 0.4$, while the latter dominated at higher levels of Sr ($0.4 < x < 0.8$). Oxygen tracer diffusion (D*) and surface exchange coefficients (k*) of the polycrystalline samples were determined by the oxygen isotopic exchange experiment over the temperature range of 550–800°C. Tracer diffusivity was found to follow an increasing trend with increasing oxygen content. Consequently the highest diffusion coefficient was found for the minimum amount of Sr substitution, x = 0.2, continuously decreasing with x until x = 0.6. An unusual increase in D* was observed when the Sr content increased up to x = 0.8. Among the Sr substituted compositions studied, $La_{1.2}Sr_{0.8}NiO_{4\pm\delta}$ was found to exhibit good oxygen diffusivity and a matching thermal expansion coefficient with typical SOFC electrolytes while exhibiting the highest total conductivity.

EN-O-04

Improved Conductivity and Phase Stabilization of Sr^{2+} and Ca^{2+} doped $La_2Mo_2O_9$

Pranuda Jivaganont[a,*], Pimpa Limthongkul[a], Sumittra Charojrojkul[a]

[a]*National Metal and Materials Technology Center, Klong Luang / Pathumthani, 12120, Thailand*

*pranudj@mtec.or.th

Keywords: Lanthalum molybdate; $La_2Mo_2O_9$; SOFC; oxide conductor.

The new fast oxide-ion conductors from $La_2Mo_2O_9$ family, firstly introduced in year 2000, has received attention by intermediate temperature SOFCs research field due to its higher ionic conductivity than the current typical SOFCs electrolyte, i.e. yttria-stabilized zirconia (YSZ). While the replacement was aimed for the operating temperature of 400-600°C, the material indeed possesses the phase transition between the low temperature α- $La_2Mo_2O_9$ and the high temperature β- $La_2Mo_2O_9$ at 560-580°C. The α- form is found to exhibit one magnitude lower in conductivity, therefore several studies have attempted to stabilize the β-form upon lowering the temperature by doping with lower aliovalent atom on the cationic site. However, effects of doping on conductivity reported in literatures are still in debate. In addition, high densification, which is the key property for electrolyte, is hard to achieve via simple fabrication methods. In this study, we have succeeded in forming pure $La_2Mo_2O_9$ phase of up to 93% densification via the relatively simple steps. The undoped, Sr^{2+}-doped and Ca^{2+}-doped (doping content varied from 0.05-0.2 mol) $La_2Mo_2O_9$ powder were prepared via a solid state reaction at 800°C. Pressed pellets were sintered at 950 and 1000°C for 4 h. Sintered pellets were characterized by X-ray diffraction, scanning electron microscope and AC impedance spectroscopy. High temperature β-phase could be stabilized at room temperature with Sr^{2+} doping of 0.1 mol sintered at 1000°C without the presence of a foreign phase. Completed β-phase stabilization was not observed with Ca^{2+} doping. Moreover, $CaMoO_4$ was found for all conditions. Larger grain size was observed upon the substitution regardless of the sintering temperature. Sr^{2+} 0.1 mol doped $La_2Mo_2O_9$ sintered at 1000°C exhibits the conductivity of 3.0×10^{-4} S cm^{-1} at 450°C, which is the highest among the chosen conditions and the same substitution content reported in literatures.

EN-O-05

Experimental Investigation and Numerical Determination of Custom Gas Diffusion Layers to Understand Water Transports in PEMFC

Visarn Lilavivat[a,b], Shimpalee Shimpalee[b,*], Cortney Mittelsteadt[c] and Hui Xu[c]
[a]National Metal and Materials Technology Center (MTEC)
114 Thailand Science Park, Paholyothin Rd., Klong 1, Klong Luang, Pathumthani 12120, Thailand
[b]Department of Chemical Engineering,
University of South Carolina, Columbia, SC 29208, USA
[c]Giner Electrochemical Systems, LLC.
89 Rumford Avenues, Newton, MA 0246, USA
*shimpale@cec.sc.edu

Keywords: Gas diffusion layer, micro porous layer, PEMFC, water management

The various type of custom gas diffusion layer (GDL) for proton exchange membrane fuel cells (PEMFCs) was studied. These GDLs have two different micro porous layers (MPL) and a carbon substrate. The effect of different MPL in the GDL on fuel cell performance is investigated. The gas diffusion layer (GDL) is one of the vital components of PEMFCs that has a variety of functions significant for their overall performance and durability. It was discovered that the liquid water distribution was strongly dependent on the hydrophilicity of GDL. The performance of fuel cell was measured in-situ with different GDLs on several operating conditions. The pore morphology of the GDLs as well as pore size distribution of the GDLs including the MPL was determined. The data of pore size distribution including the relationship of tortuosity and porosity were used as the model parameters. Water distribution in GDLs of PEMFCs was reported by computational fluid dynamic (CFD) modeling. The CFD prediction of current density distribution and gas/water transports in PEMFC will be used to understand the effect of these new designs of GDL.

EN-O-06

Effect Of Nitrogen Doping On The Reducibility, Activity And Selectivity of Carbon Nanotube-Supported Iron Catalysts For CO_2 Hydrogenation

Ly May Chew[a,*], Praewpilin Kangvansura[b], Holger Ruland[a], Wei Xia[a], Attera Worayingyong[b], Martin Muhler[a]

a. Laboratory of Industrial Chemistry, Ruhr-University Bochum, 44780 Bochum, Germany.

b. Faculty of Science, Kasetsart University, Bangkok 10903, Thailand.

*lymay.chew@techem.rub.de

Keywords: CO_2 hydrogenation, iron oxide-based catalyst, reducibility, XANES

Introduction: Rising concentrations of CO_2 have a huge impact on the environment resulting in an increase in the global temperature. In addition, depletion in crude oil resources and the continuous increase of its price have raised the research interest in CO_2 hydrogenation. CO_2 hydrogenation to hydrocarbons is a modification of Fischer-Tropsch synthesis (FTS), where CO_2 is used as reactant instead of CO. Recently, carbon nanotubes (CNTs) have been claimed as a promising support for catalysts used in FTS, because CNTs have a large outer surface area and are able to increase the dispersion of the catalytically active nanoparticles. Hence, this work describes CO_2 hydrogenation to short-chain hydrocarbons over iron nanoparticles supported on oxygen- and nitrogen-functionalized CNTs (OCNTs and NCNTs). Silica was used as reference support for comparison with the CNT supports.

Experimental: Multi-walled CNTs with inner diameters of 20-50 nm from Applied Sciences lnc. (Ohio) were subjected to nitric acid vapour treatment at 200°C for 24 h to create OCNTs. The OCNTs were treated at 400°C for 6 h in flowing ammonia (10 vol% NH_3 in He, 25 sccm) to obtain NCNTs. The supports (OCNTs, NCNTs and SiO_2) were added to the aqueous solution of ammonium ferric citrate to achieve a 40 wt% Fe loading. The mixture was dried at 50°C overnight and calcination of the mixture was carried out in air at 300°C for 90 min. CO_2 hydrogenation experiments were conducted in a fixed-bed U-tube reactor. The catalyst was first reduced in pure H_2 at 380°C and atmospheric pressure for 5 h. Subsequently, the hydrogenation reaction was performed at 360°C and 25 bar using a mixture of 22.5% CO_2, 67.5% H_2 and 10% Ar at a total flow rate of 50 L g^{-1} h^{-1}. Online gas analysis was performed with a GC-TCD-FID allowing us to close the carbon balance.

Results and discussion: H_2 TPR and *in situ* XANES results revealed that iron oxide nanoparticles on NCNTs were easier to reduce compared to those on OCNTs indicating that the nitrogen species on CNTs are able to promote the reduction of iron oxide. Iron oxide nanoparticles on SiO_2 were more difficult to reduce than those on CNTs demonstrating that the interaction between iron oxide and silica was substantially stronger than the interaction between iron oxide and CNTs. The iron phases present in all three catalysts before reaction were found to be a mixture of Fe_2O_3 and Fe_3O_4 by XRD measurements. After CO_2 hydrogenation for 60 h at 360°C and 25 bar, the dominant iron phases on all three catalysts were found to be Fe_5C_2 and Fe_3O_4. The catalytic activity of both Fe/OCNT and Fe/NCNT catalysts was almost twofold higher than that of Fe/SiO_2. The low activity of Fe/SiO_2 catalyst points to unfavorable strong metal-support interactions preventing full reduction and carbidization. For all three catalysts, CO_2 was converted into C_1-C_5 products with CO and methane as major products. The CNT-supported iron catalysts were significantly more active and selective to short-chain olefins in the range from C_2-C_5.

EN-O-07

Facile Preparation of CuO and Cu_2O Nanoparticles

Thanyaporn Yotkaew, Rungtip Krataitong, Warangkana Anuchitolarn, Pennapa Muthitamongkol and Ruangdaj Tongsri*
Powder Metallurgy Research and Development Unit, National Metal and Materials Technology Center 114 Paholyothin Road, Khlong Nueng, Khlong Luang, Pathum Thani 12120 Thailand
* ruangdt@mtec.or.th

Keywords: CuO, Cu_2O, nanocrystals, synthesis, characterization.

Nanoparticles of copper oxides (CuO and Cu_2O) are important inorganic semiconductors. The CuO and Cu_2O have bandgap values of 1.85 eV and 2.21 eV, respectively. These oxides show promising applications including gas sensor, catalyst, magnetic storage medium, thermoelectric material, photo-thermal and photo conductive materials, superconductor, solar cell and anode material for Li ion battery. Because of the promising applications given above, the CuO and Cu_2O nanoparticles were prepared by an environmentally benign facile route. In the synthesis route, glacial acetic acid was employed to react with pure Cu powder to form $Cu(CH_3CO_2)_2$ intermediate. After purification, the intermediate was reacted with NaOH via a solid-state route to form CuO nanoparticles. Reduction of CuO nanoparticles under the conditions consisting of an extremely low O_2 partial pressure and elevated temperatures resulted in a mixture of CuO and Cu_2O nanoparticles. Under a certain elevated temperature, metal Cu nanoparticles were obtained. The intermediate and end products of the synthesized materials and the reduced powders were confirmed by Fourier transform infrared spectroscopy, scanning electron microscopy, transmission electron microscopy and X-ray diffraction technique.

EN-O-08

The Effect of 10Ni/10Y_2O_3-Al_2O_3 in Ethanol Stream Reforming (ESR)

Chanon Pattaraangkul[a,*], Phurich Boonngam[a], Gunt Kranratanasuit[a], Sumittra Charojrochkul[b] and Pisanu Toochinda[a]

[a] *Sirindhorn International Institute of Technology (SIIT), Khlong Luang, Pathum Thani, 12121, Thailand*

[b] *National Metal and Materials Technology Center (MTEC), Khlong Luang, Pathum Thani, 12120, Thailand*

*bird_mask@hotmail.com

Keywords: Ethanol Steam Reforming (ESR), Nickel doped Yttrium-Alumina, catalyst support

The Nickel catalyst is an active catalyst for ethanol steam reforming (ESR), but it also suffers from coke formation. Yttrium has a transition state of 3+ similar to aluminum and the size of the atom is slightly bigger than aluminum. Therefore, Y_2O_3 could be easily replaced into the structure of Al_2O_3. Literature reports that Y_2O_3 can reduce coke formation without alternating the charge of the support structure. Yttria doped alumina support is studied for the catalytic activity for ESR. This work focuses on the different methods of preparation of the catalysts supports to replace Al atom by Y to see the different effect in physical properties and catalyst activities. The two types of preparation method used were wetness impregnation and sol-gel both with thermal treatment. The catalysts were characterized by X-ray diffraction (XRD), X-ray fluorescent (XRF), specific surface area by BET method, and scanning electron microscopy (SEM). The comparison between the performance of10Ni/10Y_2O_3-Al_2O_3 and 10Ni/Al_2O_3in the production of hydrogen from ESR will be further discussed.

EN-O-09

Catalytic Activity of Ethanol Steam Reforming over Ni-Ceria Doped Alumina (10Ni/10CeO_2-Al_2O_3)

Phurich Boonngam[a,*], Gunt Kranratanasuit[a], Chanon Pattaraangkul[a], Sumittra Charojrochkul[b] and Pisanu Toochinda[a]

[a] *Sirindhorn International Institute of Technology (SIIT), Khlong Luang, Pathum Thani, 12121, Thailand*

[b] *National Metal and Materials Technology Center (MTEC), Khlong Luang, Pathum Thani, 12120, Thailand*

*perfect1mperfection@live.com

Keywords: Ethanol Steam Reforming (ESR), Nickel doped Ceria-Alumina, Catalyst Support

The catalytic activity of Nickel catalysts on doped ceria-alumina support was studied for the hydrogen production from ethanol steam reforming (ESR). ESR suffers from coke formation on the catalysts under prolonged reaction. Cerium oxide was chosen because of its ability to reduce the acidity of the support and coke formation as well as ceria's oxygen vacancy property. The acid support can induce coking via dehydration reaction and thus needs to be prevented in order to maintain catalytic activity of the catalysts. The aim of this work is to investigate the effect of replacing Al^{2+} in Al_2O_3 with Ce^{4+} in the catalyst supports by two preparation methods, wetness impregnation and sol-gel with thermal treatment. The supports were compared in their physical properties and reaction activity of ESR with the catalyst composition of 10%Ni/10%CeO_2-Al_2O_3 calcined at 600-1300°C. The catalysts were characterized using X-ray diffraction (XRD), X-ray fluorescent (XRF), specific surface area by BET method, and scanning electron microscopy (SEM). The hydrogen production performance of the catalysts from ESR will be further discussed.

EN-O-10

The Effect of Doping CaO onto Alumina over Nickel Catalyst in Ethanol Steam Reforming

Gunt Kranratanasuit[a,*], Phurich Boonngam[a], Chanon Pattaraangkul[a], Sumittra Charojrochkul[b] and Pisanu Toochinda[a]

[a]*Sirindhorn International Institute of Technology (SIIT), Khlong Luang, Pathum Thani, 12121, Thailand*

[b]*National Metal and Materials Technology Center (MTEC), Khlong Luang, Pathum Thani, 12120, Thailand*

[*]gunt255@hotmail.com

Keywords: Ethanol Steam Reforming (ESR), Calcium Oxide doped Alumina over Nickel Catalyst, Catalyst Support

Ni/Al_2O_3 and Ni/CaO doped Al_2O_3were studied in catalytic activity for ethanol steam reforming (ESR). Two support preparation methods, wetness impregnation and sol-gel methods followed by thermal treatment, were investigated to identify their physical and catalytic properties. The properties of supports can be alternated by the replacement of Al^{3+} in Al_2O_3 by Ca^{2+} to change the structure of the supports. ESR catalysts suffer from deactivation by coking after a long use. To overcome this problem, Ca^{2+} was introduced to lower the acidity of support which can reduce the coke formation. The basic property and the alkalinity of CaO are to promote the dehydrogenation reaction instead of the dehydration reaction to produce acetaldehyde which can further undergo steam reforming again to produce additional hydrogen. The characterization techniques include X-ray diffraction (XRD), specific surface area by BET method, X-ray fluorescence (XRF), and scanning electron microscopy (SEM), were conducted to identify Ca^{2+} in the support, crystal structure and morphology of the support as well as the catalyst surface area. The size of CaO may also affect the ethanol steam reforming which will be investigated. Ni/Al_2O_3 was produced as a reference to compare with $Ni/CaO\text{-}Al_2O_3$ in coke formation observation.

EN-O-11

Total Energy Requirement for Hydrogen Production Reactor

Mek Srilomsak[a,*], Sumittra Charochrojkul[b], Jarruwat Charoensuk[c], Thanathon Sesuk[b], Waroht Aungkharuengrattana[d]

[a]*Automotive Engineering program, International College, King Mongkut's Institute of Technology Ladkrabang, Bangkok 10530, Thailand*

[b]*National Metal and Materials Technology Center (MTEC), Pathum Thani 12120, Thailand*

[c]*Department Mechanical Engineering, Faculty of Engineering, King Mongkut's Institute of Technology Ladkrabang, Ladkrabang, Bangkok 10530, Thailand.*

[d]*Department of Mechanical Engineering Technology, College of Industrial Technology, King Mongkut's University of Technology North Bangkok, Bangkok 10800, Thailand*

*micksrilomsak@gmail.com

Keywords: Porous media combustion, LPG consumption, Ethanol steam reforming, and Hydrogen production.

In the Hydrogen production reactor, combustion of LPG was used as a heat source for ethanol steam reforming. For such purpose, the operating temperature was required to be around 700-900ºC along the entire height of the reactor. Various types of porous media materials were used as a heat transfer media, those were: 25mm ceramic saddles, random size Bio-filter media from Ecocera of MTEC, and 20x20x20 mm^3 ceramic foam. The objective of this study was to obtain the practical amount of total energy input, and compare with theoretical calculation which can achieve the required temperature of Ethanol steam reforming hydrogen production. From the experiment, 4.60 kW of energy was needed to fulfill the requirement of the reactor, while only 2.65 kW was expected from theoretical calculation. Most of energy loss was due mainly to: 1.) heat loss at the top of the reactor where the metal part was directly exposed to the environment, 2.) a large amount of energy loss at stack and, 3.) insufficient mixing at the early stage of combustion at the bottom of the furnace as noticed by high CO concentration in flue gas. The Porous media material has significant effect on temperature distribution and energy consumption. The results show that the use of ceramic saddles as porous media consume more energy than the ceramic foam and the Bio-filter media mixed with ceramic saddles during the start-up period of the reactor.

EN-O-12

Simultaneous Adsorption of Trace Metal and SO_2 using Zeolite Adsorbent during Combustion of Brown Coal

Asri Gani[a,*], Mahidin[a] and Khairil[b]

[a]*Chemical Engineering Department, Engineering Faculty, Syiah Kuala University, Banda Aceh, Aceh Province, 23111, Indonesia*

[b]*Mechanical Engineering Department, Engineering Faculty, Syiah Kuala University, Banda Aceh, Aceh Province, 23111, Indonesia*

*asri.gani@che.unsyiah.ac.id

Keywords: Brown coal, trace element, SO_2, emission, adsorption, zeolite.

The demand for cheap energy has made many industries turned to coal as alternative energy source. The large deposit of brown coal in Indonesia make its use economically viable eventough it has low energy content compare to sub bituminous or bituminous coal. Unfortunately coal processing to produce energy particularly combustion processes create emissions in the form of trace elements and SO_2 , which are dangerous pollutants for health. Natural adsorbent zeolite is used to adsorb trace element components and SO_2 simultaneously to reduce the negative effect of brown coal combustion. This research observed the efficiency level of trace element adsorption such as Cd, Hg, Pb and SO_2 gas by zeolite during coal combustion. Thirty minutes combustions with various temperature and adsorbent ratio toward coal in bricket form were conducted. The analysis towards trace metal in bottom ash such as Cd, Pb were conducted using *Atomic Absorbtion Spectroscopy* (AAS) while analysis on merkuri was conducted using mercury analyzer. SO_2 emission analysis was done using idustrial gas combustion and emission analyzer. The results show that trace metal and SO_2 adsorption efficiency by zeolite increases as the adsorbent ratio and temperature increase. High volatility level of Hg metal really influences the adsorption efficiency. It increase along with the temperature increase. Zeolite performance tend to decrease at temperature 800^oC because it started the desorption process. Optimum adsorbent capacity for Hg adsorption is obtained at 2% ratio and at 4% and 6% ratio for Pb and Cd respectively.

EN-O-13

Synthesis of Ti-based Icosahedral Quasicrystal Powders by Mechanical Alloying and Their Hydrogen Sorption Properties

Akito Takasaki[a,*] **and Konrad Świerczek**[b]
[a]*Shibaura Institute of Technology, Tokyo, 135-8548, Japan*
[b]*AGH University of Science and Technology, Krakow, 30-059, Poland*
*takasaki@sic.shibaura-it.ac.jp

Keywords: Quasicrystal, Mechanical alloying, Hydrogen, Ti-Zr-Ni

Icosahedral quasicrystals (i) phases have a new type of translational long-range order, noncrystallographic rotational symmetry, and presumably contain more tetrahedral interstitial sites than normal crystals [1], which may exhibit better physical properties for hydrogen storage applications if some atoms of the i-phase have adequate chemical affinities with hydrogen. Since a report on production of a stable Ti-based i-phase produced by a melt spinning [2], we have attempted to produce the i-phase by mechanical alloying (MA), and to study their hydrogen sorption properties [3-6]. In this report, we would summarize and update our studies on synthesis of the i-phase powders by MA and their hydrogenation. As the starting materials, Ti, Zr and Ni elemental powders, whose chemical compositions were varied, were poured in stainless steel vials with some stainless steel balls in an argon gas atmosphere, and mechanical alloyed and annealed subsequently. An adequate annealing after MA in a vacuum caused the formation of the i-phase with a Ti_2Ni type crystal phases. The amount of the i-phase was dependent on annealing temperature and the chemical compositions. The maximum hydrogen storage capacity at a high pressure of hydrogen gas obtained were almost 60 at.%. The details of the results on microstructural observation by TEM, hydrogen sorption properties measured by Sieverts' type apparatus, high-pressure vessel with a pressure transducer and quadrupole mass analyzer will be presented at the conference.

References

[1] P.C. Gibbons, K.F. Kelton, Z.M. Stadnik (Ed.),in Physical Properties of Quasicrystals, Springer, 1999, p. 403
[2] K.F. Kelton, W.J. Kim, R.M. Stroud, Applied Phys. Lett., 70 (1997), 3230
[3] A. Takasaki, C.H. Han, Y. Furuya, K.F. Kelton, Phil. Mag. Lett. 82 (2002), 353.
[4] A. Takasaki, V. T. Huett, K.F. Kelton, Mater. Trans., 43 (2002), 2165.
[5] A. Takasaki, K.F. Kelton, J. Alloys Comps 347 (2002), 295.
[6] A. Takasaki, K.F. Kelton, Intl. J. Hydrogen Energy 31 (2006), 183.

EN-O-14

Comparison of Pyrolysis of Jatropha Cake with Different Catalysts Using PY-GC/MS

Sirirak Jariyaphinyo [a], Siriporn Larpkiattaworn [b], Orapin Chienthavorn [a*]

[a]*Department of Chemistry and the Center of Excellence for Innovation in Chemistry, Faculty of Science, Kasetsart University, Bangkok,10903 Thailand*

[b]*Thailand Institute of Scientific and Technological Research (TISTR), Pathumthani,12120 Thailand*

*E-mail address: fsciopc@ku.ac.th

Keywords: jatropha cake, zeolite, separation, pyrolysis-GC-MS.

In this work, effect of different zeolite catalysts that react with jatropha cake residue to give pyrolysed products was studied. The products were separated and characterised by using pyrolysis gas chromatography-mass spectrometry (PY-GC/MS). A 0.004 g of jatropha sample was put into the capsule sample holder of the pyrolysis-GC-MS instrument and the pyrolysis was performed at 500°C. In this work two separate experiments were carried out. In the first experiment the catalysts were Modernite zeolite (30 mol/mol ratio of SiO_2/Al_2O_3), Beta zeolite (37 mol/mol ratio of SiO_2/Al_2O_3) and Al_2O_3/Pd. Each catalyst was mixed with jatropha cake with a ratio of 1:1 by weight. The jatropha cake pyrolysed with Modernite zeolite gave the highest amount of aromatic hydrocarbons and the lowest amount of fatty acids than the products obtained from the other zeolites. In the second experiment, the amount of Modernite zeolite was optimised for maximum production of aromatic hydrocarbon. The jatropha cake was mixed with an increasing ratio of Modernite zeolite of 1:2, 1:3 and 1:5 by weight. Improving the ratio of the zeolite increased the amount of aliphatic hydrocarbon and N-heterocycle, but the yield of aromatic hydrocarbon slightly changed, while the yield of phenol and oxygenated components significant decreased. To study the interrelation effect between two catalysts to the pyrolysis of jatropha cake, Modernite zeolite and Al_2O_3/Pd, were mixed with different ratios of 1:1, 2:1 and 3:1 by weight, and the jatropha cake was pyrolysed with the mixed catalyst at the ratio of 1:1. Increasing the ratio of Modernite zeolite in the mixed catalyst gave similar effect to those without Al_2O_3/Pd, except that the phenol component in the product reduced. To obtain the highest yield of desirable components, namely aromatic and aliphatic hydrocarbons, Modernite zeolite was proved to be the most suitable catalyst with the ratio of 1:5 by weight.

EN-O-15

Preparation of Co/SiO_2-Al_2O_3 Fiber by Electrospinning for Fischer-Tropsch Synthesis

Natthawan Prasongthum[a*], **Prasert Reubroycharoen**[b,c]
[a]*Program for Petrochemical and Polymer Science, Faculty of Science, Chulalongkorn University, Bangkok,, 10330, Thailand*
[b]*Department of Chemical Technology, Faculty of Science, Chulalongkorn University, Bangkok, 10330, Thailand*
[c]*Center of Excellence on Petrochemical and Materials Technology, Chulalongkorn University Research Building, Bangkok 10330, Thailand*
*Natthawan_takon@yahoo.com

Keywords: Fischer-Tropsch Synthesis, Co/SiO_2-Al_2O_3 fiber, Electrospinning

The SiO_2-Al_2O_3 fiber composites had been successfully prepared by the combination technique of electrospinning and sol-gel method. The effects of Al_2O_3 contents (1, 2, 3, 4 and 5%wt) on fiber diameter and morphology were investigated by SEM. It was observed that alumina content significantly influenced the average diameter of fiber which increased by increasing the alumina content. The prepared fibers were used as a support for cobalt (Co)-based catalysts for Fischer–Tropsch synthesis. The Fischer–Tropsch synthesis performances over the fiber and porous catalysts were carried out in a fixed bed reactor. The results showed that the fibers catalyst was easily reduced when comparing the porous catalyst. It was found that the fiber catalyst showed the activity at the same level of the porous catalyst, but its advantage was the lower water gas shift reaction which produced less CO_2 than the porous catalyst. The CO conversion was 59.62% with the fiber catalyst and 52.80% with the porous catalyst under the same experimental condition. The fiber catalyst gave the maximum methane selectivity of 96.08% compared to the porous catalyst (85.63%).

EN-O-16

Enhanced Electroluminescence of Silicon-rich Oxide/SiO_2 Multilayer Structures Deposited by Hydrogen Ion-beam Assisted Sputtering

Sheng-Wen Fu (Presenter)[a,*], Shao-Ping Chen[a], Hui-Ju Chen[a], Chuan-Feng Shih[a]

[a]*National Cheng Kung University, Tainan City, 70101, Taiwan*

*E-mail: shengwen1031@gmail.com

Keywords: LED, silicon-rich oxide, photoluminescence, electroluminescence, HIBAS

Recently, the silicon-rich oxide (SRO)/SiO_2 multilayer structures have drawn a great attention owing to their potential optoelectronic applications, especially for the visible light emitting devices (LED). In this study, we prepared SRO/SiO_2 multilayers by hydrogen ion-beam assisted sputtering (HIBAS) with different hydrogen anode voltage (70V and 116V) for the LED application. The property of the prepared samples was determined by Fourier transform infra-red (FTIR), X-ray photoelectron spectroscopy (XPS), Transmission electron microscope (TEM,), photoluminescence (PL) and electroluminescence (EL) analysis.

Firstly, the FTIR spectra showed the absorption peak at 883 cm^{-1} specific to Si-H bond was only detected in HIBAS prepared SRO/SiO_2 films. The result confirmed the hydrogen incorporated into the films through the process of hydrogen ion bombardment.

Secondly, XPS was carried out to analyze the size-dependent Si 2*p* core-level. Gaussian-Lorentzian line shapes were used to fit the states of Si^{0+}, Si^{1+}, Si^{2+}, Si^{3+} and Si^{4+}. For hydrogen anode voltage at 70 V, the result showed the intensity of Si suboxides of Si^{2+} and Si^{3+} obviously increased, meaning the generation of the Si nanoclusters with the size smaller than 2 nm (approved by TEM images). On the other hand, for hydrogen anode voltage at 116 V, the Si suboxides contribution slightly descended and the states of Si^{0+} and Si^{4+} ascended, that demonstrated the size of the Si-clusters increased as the phase separation of SRO into Si and SiO_2 from the nanoclusters assembling.

Thirdly, the PL intensity for HIBAS treated SRO/SiO_2 films was stronger than that without HIBAS. The enhancement of the PL intensity was due to the radiative recombination included of the Si nanocluster, E' center and non-bridging oxygen hole center (NBOHC). In addition, E' center and NBOHC are oxygen-related defects at the interface between the Si nanoclusters and SiO_2 matrix. The HIBAS not only improve the formation of the Si nanoclusters but also fabricate the E' center and NBOHC.

Finally, the EL intensity largely enhanced for HIBAS prepared devices compared to that without the ion-beam assisting. Through the plot of Arrhenius Fowler-Nordheim, the ratio of the injection barrier height in SRO/SiO_2 multilayers were 4.44 (without HIBAS), 6.50 (HIBAS, 70 V) and 9.67 (HIBAS, 116 V). We attributed the high EL intensity to the high injection barrier which effectively confined the charge carriers in Si nanoclusters to improve the radiative recombination rate (E' center and NBOHC).

In conclusion, we approve the HIBAS effectively improve the SRO/SiO_2 based LED, where the intensity of EL was 15 times higher than the conventional devices at the same operated power.

EN-O-17

Two-step Treatment of Electroplated Cu/Sn Bilayers: Impact of Alloying before Sulfurization

Hui-Ju Chen (Presenter)[a,*], Sheng-Wen Fu[a], Chuan-Feng Shih[a]
[a]*National Cheng Kung University, Tainan City, , 70101, Taiwan*
*E-mail address: shoula92a28@outlook.com

Keywords: CZTS, CTS, sulfurization, electroplating

$Cu(In,Ga)Se_2$ (CIGS) solar cells have proved the reliability in practical application with record efficiency of 20.3%. However, the commercialization is limited by the scarce and expensive elements of In, Ga and Se. Recently, new absorber compound $Cu_2ZnSn(S,Se)_4$ (CZTS) has been regarded as a promising alternative owing to its earth abundant and environmentally friendly constituents. Research of the CZTS solar cells has been reported with the efficiency of 11.1%. However, since the number of elements in the compound increases, the process to achieve single phase become critical and uncontrolled. New kinds of In-free Cu chalcogenides, other potential p-type absorber semiconductor Cu_2SnS_3 (CTS) with fewer elements and less complex than CZTS. Based on the perspective, the CTS compound has drawn the attention for application in solar cells now.

In this work, electroplating was used for depositing Cu/Sn metallic precursors. The process is of particular interest due to the advantages of the low-cost and large-area deposition. The Cu and Sn layers were sequentially electrodeposited in the order of Mo/Cu/Sn at room temperature. Cu layer was firstly plated onto the Mo-coated soda lime glass substrate in an aqueous solution containing copper sulfate (0.02 M) and trisodium citrate (0.085 M). Then, Sn layer was deposited onto Cu layer using acidic bath of tin sulfate (0.022 M) and trisodium citrate (0.12 M). Trisodium citrate was added as the complexing agent. The sulfuric acid was used to adjust the pH value nearly 4.5 to 5.0. After the deposition, the precursors were rinsed in de-ionized water and dried under flowing nitrogen, followed by the heat treatment.

The study focused on the sulfurization of the CTS synthesis. Two different sulfurization processes were produced and compared: (a) one-step sulfurization and (b) two-step sulfurization (TSS). The one-step prepared samples were performed by conventional sulfurization method in a tubular furnace. Sulfurization of Cu/Sn precursors occurred when the temperature was higher than the melting point of sulfur (~120 °C). In the TSS approach, the precursors were alloyed first before the sulfurization. The property of the prepared samples was determined by morphological, compositional and optical analysis. The study of crystal structure was carried out using x-ray diffraction. The morphology and the composition of the CTS thin films were characterized by scanning electron microscopy and energy dispersive spectroscopy. Raman and photoluminescence analysis were performed at room temperature using 532 nm He-Cd Laser. Time-of-flight secondary ion mass spectrometer provides the detailed elemental distribution after the alloy process and sulfurization. In the conclusion, the TSS process improved the CTS thin films, yielding uniform, large and dense grains without the cracks and the secondary phases included of CuS, $Cu_{2-x}S$ and SnS. Furthermore, it also demonstrated that TSS enhanced the CTS solar cells with the high power conversion efficiency.

EN-O-18

Characterization of TiO_2 Nanotube Arrays Fabricated from Two-Step Anodization

Marvin L. Samaniego[a,*], Kim Katrina P. Rivera[b], Jeffrey Jon dG. Venezuela[b]

[a] *Department of Engineering Science, University of the Philippines, 4031 Los Baños, Laguna, Philippines*

[b] *Department of Mining, Metallurgical, and Materials Engineering, University of the Philippines, 1101 Diliman, Quezon City, Philippines*

*mlsamaniego@uplb.edu.ph

Keywords: Anodization, Titanium dioxide, Nanotube arrays, Photocurrent response.

In this study, the fabrication of titanium dioxide (TiO_2) nanotube arrays was carried out via two-step anodization of titanium foil in 0.80% NH_4F in ethylene glycol electrolyte. The anodization voltage in all experiments was 55V. First anodization was done for 30 min while the final anodization was done for 90 min. Post production annealing was performed at 400° C for 2 h and at 500° C for 3 h. The grown nanotubes were characterized by obtaining the surface morphology and crystalline phases using field-emission scanning electron microscopy (FESEM) and X-ray diffraction (XRD) analysis, respectively. Highly ordered TiO_2 nanotube arrays were observed from the SEM images. Larger pore openings and thinner tube walls were observed from the TiO_2 annealed at 500° C for 3 h as compared to the TiO_2 annealed at 400° C for 2 h. Crystalline TiO_2 was present as anatase and rutile in the XRD patterns. Unannealed TiO_2 consisted mostly of amorphous TiO_2 whereas TiO_2 annealed at 500° C for 3 h exhibited a combination of anatase and rutile. The photoelectrochemical behavior was investigated by measuring the induced photocurrent response in a beaker-type cell connected to a three-electrode system under ultraviolet (UV) radiation. Dark current corresponds to measurements taken when UV irradiation was turned off. Photocurrent measurements show that irradiation with UV light induces current flow and charge activity in all TiO_2 nanotubes. Net charge is an important quantity in measuring analytical signals in photoelectrochemical experiments and its value is dependent on the maximum current. In this experiment, all photocurrent measurements were larger than the dark current measurements, confirming the photoelectrochemical properties of the prepared TiO_2 nanotube arrays.

EN-O-19

Improving the Electrochemical Performance of SnO_2 Hollow Spheres by Titanium Dioxide Coating

Songyoot Kaewmala[a], Pimpa Limthongkul[b*] and Nonglak Meethong[a,c]
[a]*Li-ion Battery Research Group, Materials Science and Nanotechnology Program, Faculty of Science, Khon Kaen University, Khon Kaen, 40002, Thailand.*
[b]*National Metal and Materials Technology Center, National Science and Technology Development Agency, Pathumthani, 12120, Thailand*
[c]*Department of Physics, Faculty of Science, KhonKaen University, KhonKaen, 40002, Thailand*
E-mail:songyootkaewmala@gmail.com

Keywords: anode materials for Li-ion batteries, Sn-based anodes, coating

Tin dioxide (SnO_2) have attracted considerable attention as an anode material for lithium ion batteries owing to its high theoretical capacity of 781 mAh/g compared with graphite (372 mAh/g). However, SnO_2 material experiences very large volume changes (up to 300 Vol. %) during lithium insertion and extraction processes, which causes crumbling and cracking of electrode leading to poor cyclic performance and large irreversible capacity. Creating SnO_2 with special structure such as hollow sphere is an effective strategy to reduce the volume expansion, but the capacity decreases rapidly in 20 cycles. To circumvent the problem, SnO_2 hollow spheres were coated by other materials such as carbon and TiO_2. This research demonstrates that dimensional confinement of SnO_2 hollow spheres by TiO_2 coating limits the volume expansion during charge/discharge processes and leads to the improved cyclic performance and decreasing of irreversible capacity.

EN-O-20

Improvement in Li-air Batteries using Flow Electrolyte through Electrode Structure Design and Modelling

Ukrit Sahapatsombut[a,*], Hua Cheng[b], Keith Scott[b]
[a]*National Metal and Materials Technology Center (MTEC), 114 Thailand Science Park, Paholyothin Rd., Klong Luang, Pathumthani 12120, Thailand*
[b]*School of Chemical Engineering and Advanced Materials, Newcastle University, Merz Court, Newcastle upon Tyne NE1 7RU, UK*
*ukrits@mtec.or.th

Keywords: Li-air battery, Macro-homogeneous model, Solid products, Flow battery.

The development of high performance and light weight energy storages has recently focused on the rechargeable lithium-air batteries (Li-air) due to their high energy density, theoretically up to 11,400 Wh kg^{-1}. However, the performance and energy efficiency of non-aqueous Li-air batteries is deteriorated by the solid product formation (Li_2O_2 and Li_2CO_3) during battery operation. To overcome this problem, the promising structure of a Li-air flow battery model with an electrolyte recycling unit has been developed to continuously deliver the discharge capacity and provided high power density as shown in Figure 1. A micro-macro homogeneous mathematical model is developed for a rechargeable Li-air battery using a concentrated binary electrolyte theory. The active materials are a pure lithium metal as the anode electrode and porous carbons are used as the cathode. The electrolyte contains 1 M $LiPF_6$ dissolved organic solvent. The dynamic behaviour of the porous cathode is determined by a numerical solution of the combined continuity, transport and kinetics equations. The new developed structure of a Li-air flow battery integrated with an electrochemical reaction unit and an electrolyte recycling unit can continuously deliver the discharge capacity from inexhaustible oxygen supplied from the recycling unit (more than 2000 mAh g_{carbon}^{-1} compared with the Li-air system without an electrolyte recycling unit provided only 700 mAh g_{carbon}^{-1}). This could be a promising alternative battery structure for the advanced energy storage device.

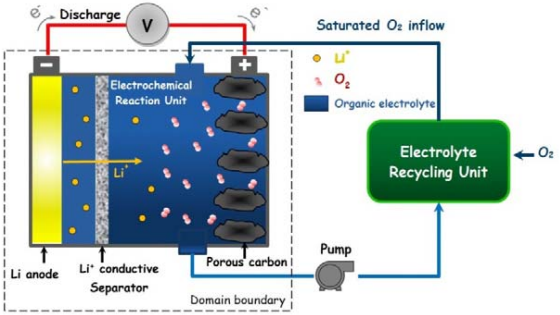

Figure 1: Schematic representation of the developed Li-air flow battery with electrochemical reaction unit and electrolyte recycling unit.

EN-O-21

Thermal Effects of Electrical Energy Harvested from a Laminated Piezoelectric Device in Engine Compartment

P. Thonapalin[a,*], S. Aimmanee[a], P. Laoratanakul[b]

[a]*Department of Mechanical Engineering, Faculty of Engineering, King Mongkut's University of Technology Thonburi, 126 Pracha Uthit Road, Bang Mod, Thung Khru, Bangkok 10140, Thailand*

[b] *National Metal and Materials Technology Center, National Science and Technology Development Agency, 114 Paholyotin Road, Klong 1, Khlong Luang, Pathumtani 12120, Thailand*

*[a]carboncopy_@hotmail.com, [a]sontipee.aim@kmutt.ac.th, [b]pitakl@mtec.or.th

Keywords: Energy Harvesting, Piezoelectric Material, THUNDER, Automotive Technology

For these recent years, piezoelectric energy harvesting has been a very popular research topic. Piezoelectric materials are used to harvest wasted mechanical energy from ambient environment and supply electrical energy via their electromechanical coupling properties. However, there has been no research which explicitly studies the influence of environmental factors on the performance of energy harvesting from the piezoelectric materials in automotive applications, especially in the engine compartment where temperature is varied with engine operating conditions. The main purpose of this research was to investigate thermal effects on electrical energy harvested from a laminated piezoelectric device in engine compartment. In this research THin Layer UNimorph Ferroelectric DrivER (THUNDER), a type of laminated piezoelectric devices, was studied. Three configurations of THUNDER devices i.e. 6R, 7R, and 8R were tested. The investigation of thermal effect on the performance of the devices while operating in temperature range of 25^{o}C – 80^{o}C with 20^{o}C increments was performed. THUNDER devices were driven mechanically by using a cam-lever mechanism to generate dynamic displacement. The frequency for testing all three configurations of THUNDER devices was controlled in the range of 5-80 Hz by rotary motion of a motor, which was directly connected to a cam. The displacement inputs, however, were different from type to type. The pressing displacements of 6R were 0.4, 1.0 and 1.6 mm; for 7R the displacements were 0.4, 1.0, 1.6, 2.2 and 2.8 mm while the displacement of 8R was only 0.4 mm. The experimental results exhibit energy harvesting performance depending on temperature changes. The results can be used as a basis for future design of a new piezoelectric device used in automobiles.

EN-O-22

Thermoelectric Properties of Au Nanoparticle Incorporated Mesoporous ZnO Composite Thin Film by Using Reverse Micelle Structure

Min-Hee Hong, Wooje Han, Hong-Sub Lee, Hyung-Ho Park*
Department of Materials Science and Engineering, Yonsei University, Seoul 120-749, Republic of Korea
*hhpark@yonsei.ac.kr

Keywords: reverse micelle, mesoporous, thermoelectric, one-pot synthesis.

In thermoelectric device, low thermal conductivity and high electrical conductivity are essential [1]. In this work, ordered mesoporous structure was applied to decrease the thermal conductivity of ZnO to enhance the thermoelectric property [2-4]. However an introduction of ordered mesoporous structure also causes a decrease in the electrical conductivity of materials. Then in this work, to increase the electrical conductivity of ordered mesoporous ZnO without a collapse of pore structure, Au nanoparticles were incorporated in mesoporous ZnO thin film. Au nanoparticle incorporated mesoporous ZnO composite thin films were synthesized by simple one pot process with reverse micelle structure. As Au precursor has hydrophilic ligand, reverse micelle structure could help to form Au nanoparticle into the pore structure [5]. Because part of pore structure is filled with Au nanoparticles, overall porosity of ZnO composite thin film was decreased. Nevertheless, pore arrangement wasn`t collapsed because Au nanoparticles were uniformly distributed in the pore structure, and thermal conductivity was not increased. Finally, Au nanoparticles incorporated mesoporous ZnO composite thin film showed an enhanced thermoelectric property due to decreased thermal conductivity from ordered mesoporous structure and increased electrical property from incorporated Au nanoparticles.

References

[1] E. Altenkirch, Phys. Z. 10 (1909) 560.
[2] C.J. Brinker, Y. Lu, A. Sellinger, H. Fan, Adv. Mater. 11 (1999) 579.
[3] D. Grosso, F. Cagnol, G.J. de A.A. Soler-Illia, E.L. Crepaldi, H. Amenitsch, A. Brunet-Bruneau, A. Bourgeois, C. Sanchez, Adv. Funct. Mater. 14 (2004) 309.
[4] G. J. Snyder, M. Christensen, E. Nishibori, T. Caillat, B.B. Iversen, Nature Materials 3 (2004) 458.,
[5] Y.H. Jang, S.Y. Yang, Y.J. Jang, C. Park, J.K. Kim, D.H. Kim, Chem. Eur. J. 17 (2011) 2068.

Materials for Energy Session

POSTER PRESENTATIONS

EN-P-01

A Facile Synthesis of Nanorods of ZnO/Graphene Oxide Composites with Enhanced Photocatalytic Activity

Jiaqian Qin (Presenter)[a,*], Nutsakun Kittiwattanothai[b], Yanan Xue[c], Pongsakorn Kongsittikul[d] , Xinyu Zhang[c], Nadnudda Rodthongkum[a], Sarintorn Limpanart[a]

[a]*Metallurgy and Materials Science Research Institute, Chulalongkorn University, Bangkok,10330, Thailand*

[b]*Department of Physics, King Mongkut's University of Technology Thonburi, Bangkok, 10140, Thailand*

[c]*State Key Laboratory of Metastable Materials Science and Technology, Yanshan University, Qinhuangdao 066004, P.R. China*

[d]*Department of Petrochemicals and Polymer Science, Chulalongkorn University, Bangkok,10330, Thailand*

*E-mail address jiaqianqin@gmail.com, jiaqian.q@chula.ac.th

Keywords: Photocatalyst, ZnO, Graphene oxide

In our previous work, we have successfully synthesized the ZnO nanorods with good photocatalytic activity. The photocatalytic studies showed that as-synthesized ZnO nanorods have good photocatalytic performance, and the photocatalytic activity increased with aspect ratio increasing. However, the major limiting factor in the application of ZnO in the degradation of the photogenerated electron-hole pairs. This leads to the poor rate of electrons and holes reaching the interface between semiconductor and water, where the degradation is inherent to occur. This problem can be addressed by coupling of two semiconductors possessing suitable energy levels for their corresponding conduction and valence bands. The coupling of a large band gap semiconductor with a small band gap semiconductor of a more negative CB level can result in the injection of e_{cb}- from the small band gap semiconductor to the large band gap semiconductor, which is helpful for electron-hole separation. Besides strengthening charge separation by isolating electrons and holes in two distinct semiconductors, it also allows the extension of the absorption threshold of light to a lower energy level. Therefore, the use of composite semiconductors for organic dyes degradation is feasible under visible light illumination. Here, we introduce the graphene oxide to ZnO nanorods as the substrate for further enhancing its photocatlytic performance. Graphene-ZnO nanorods composites were successfully synthesized by a facile room-temperature approach using the colloidal coagulation effect. The samples are characterized by using x-ray diffraction, scanning and transmission electron microscopy. The photodegradation of methylene blue (MB) has been investigated in the presence of composites. It is observed that the photocatalytic performance could be enhanced by adding graphene oxide.

EN-P-02

Confined Growth of WO_3 for High Performance Electrochromism

Sangeeta Adhikari* and Debasish Sarkar
Department of Ceramic Engineering, National Institute of Technology, Rourkela-769008, Odisha, India
* adhikari.sangeeta8@gmail.com

Keywords: WO_3, Nanostructures, TEM, Electrochromism

Nanostructuring has emerged as one of the best tools to unlock the full potential. Tungsten trioxide semiconductor is one of the fundamental functional materials due to its versatile application in devices such as gas sensors, solar cells and smart windows. Control of the metal oxide dimension can tune the electrical and optical properties for modern device application. Morphology management is a challenge to investigate the ultimate performance. In this paper, self assembled nanostructures are favorably grown using different structure directing agents through co-precipitation and hydrothermal techniques. Confined growth of four different tungsten trioxide (WO_3) nanopowders with two different crystal structures has been carried. The monoclinic spherical and rod-like WO_3 nanostructures are obtained by acid precipitation method using CTAB for WO_3 nanorod synthesis. WO_3 nanocuboids and nanofibers are synthesized hydrothermally using HBF_4 and NaCl as structure directing agents to attain monoclinic and hexagonal crystal phases, respectively. Similar band gap energy is observed for all morphologies at visible wavelength. Phase and morphology has been confirmed through XRD, TEM and FESEM imaging methods. Morphology formation mechanism through different directing agents is also studied. A simple dip coated WO_3/ITO fabricated electrode has been used as reference electrode to carry out the electrochemical measurements. Hexagonal nanofiber WO_3/ITO electrode exhibits high current density with fast optical switching characteristics showing high coloration efficiency with respect to other monoclinic nanostructures. The evaluated properties suggest the plausible use of WO_3 nanofibers for high efficient electrochromic device.

References:

[1] H. Zheng, J. Ou, M. S. Strano, R. B. Kaner, A. Mitchell and K. K. Zadeh, Adv. Funct. Mater., 2011, 21, 2175.
[2] S. Adhikari and D. Sarkar, RSC Advances, 2014, 4, 20145.
[3] S. Adhikari and D. Sarkar, Electrochim. Acta, 2014, 138, 115.

EN-P-03

Characterization and Catalytic Activity Studies of Lanthanum Oxide Catalyst for Biodiesel Production

Dussadee Rattanaphra*and Jatechan Channuie
Research and Development Division, Thailand Institute of Nuclear Technology, Phathumtani, 12120, Thailand
*drattanapha@yahoo.com

Keywords: Lanthanum oxide catalyst, Characterization, Catalytic activity, Biodiesel

Lanthanum-EDTA solution obtained from decomposition of monazite ore by alkali method and using ion exchange technique as purification process was used as raw material to prepare lanthanum oxide (La_2O_3) catalyst. This catalyst was synthesized by oxalate precipitation method. Effect of calcination temperature (500, 600, 800, 900 and 1000 ^oC) on structure and properties of La_2O_3 catalyst was studied. The obtained catalyst was characterized by X-ray diffraction (XRD), Brunauer-Emmett-Teller (BET) method, Thermogravimetric analysis (TGA) and Scanning electron microscope (SEM). The result showed that the prepared catalyst was very fine. The average crystalline size of La_2O_3 catalyst was about 63.35 nm. The catalyst was used to catalyze the transesterification of palm oil with methanol to biodiesel production. It was found that the fatty acid methyl ester (biodiesel) content of 96.7% was obtained under the conditions: molar ratio of methanol to oil of 30:1, catalyst loading of 10 wt%, reaction temperature of 200 ^oC, reaction pressure of 39 bar and stirring rate of 600 rpm for 5 h.

EN-P-04

Response of PVDF Energy Harvester on Wind Speed

Prissana Rakbamrung[a,*], Chainuson Kasagepongsan[b], Nantakan Muensit[c]
[a]*Faculty of Education, Suratthani Rajabhat University, Surat Thani, 84100, Thailand*
[b]*Faculty of Science and Technology, Suratthani Rajabhat University, Surat Thani, 84100,Thailand*
[c]*Center of Excellence in Nanotechnology for Energy, Department of Physics, Faculty of Science, Prince of Songkla University, Hat Yai, Songkhla, 84100, Thailand*
* prisana_sru@hotmail.co.th

Keywords: Energy harvesting, Piezoelectricity, Poly(vinylidene fluoride), Wind energy.

This work was interested in extracting wind energy with PVDF for utilizing in low power electronic devices. We, therefore, designed and constructed an experimental set up similar to hoot for laminar flow generating. We focused on the effect of wind speed and active area on voltage response of PVDF film. Thus, the voltage response of PVDF on wind speed over the range of 0 – 5.3 m/s with PVDF area of 4, 6, 8, 10 and 12 cm^2 was evaluated under no load condition. Based on the experimental results, the highest peak voltage output of about 175 volt was obviously observed from PVDF dimension of 1cm×12 cm×28 μm at wind speed of 1.6 m/s. Voltage declined with increasing of wind speed from 1.6 to 5.3. We noted that generated voltage depended significantly upon film flowing (PVDF deformation) rather than that of mechanical force (wind speed) impact on PVDF surface. This work also suggest that it should be possible to transform wind energy generated from electrical fan or hoot into conveniently use form of electrical energy that can be stored and supply for power electrical devices.

EN-P-05

Figures of Merit of Low-Cost $CuAl_{0.9}Fe_{0.1}O_2$ Thermoelectric Material Prepared at Different Solid State Reaction Sintering Temperatures

Aparporn Sakulkalavek[a,*], Rungnapa Thonglamul[a] and Rachsak Sakdanuphab[b]
[a]*Faculty of Science, King Mongkut's Institute of Technology Ladkrabang Chalongkrung Rd. LadkrabangBangkok 10520, THAILAND*
[b] *College of Data Storage Innovation, King Mongkut's Institute of Technology Ladkrabang Chalongkrung Rd. LadkrabangBangkok 10520, THAILAND*
*ksaparpo@kmitl.ac.th

Keywords: $CuAlO_2$, delafossite , thermoelectric material, ZT

In this study, we investigated a $CuAl_{0.9}Fe_{0.1}O_2$ compound prepared at two different sintering temperatures in order to find out the effect of sintering temperature on the compound's figure of merit of thermoelectric properties. The thermoelectric $CuAl_{0.9}Fe_{0.1}O_2$ compound was prepared from high purity grade Cu_2O, Al_2O_3 and Fe_2O_3 powders. The mixture of these powders were ground and then pressed with uniaxial pressure into pellets. The pellets obtained were sintered in the air at 1423 K and 1473 K. X-ray diffraction (XRD) patterns showed a single phase of $CuAl_{0.9}Fe_{0.1}O_2$ with rhombohedral structure, along with a trace of CuO second phase. Moreover, the XRD peaks of the sample sintered at 1423 K indicated that more Fe^{3+} atoms replaced Al^{3+} atoms in this sample than they did in the sample sintered at 1473 K. The average grain size of the $CuAl_{0.9}Fe_{0.1}O_2$ compound prepared increased with increasing sintering temperature, whereas its mean pore size and porosity decreased with increasing sintering temperature. The dispersed small pores markedly decreased the thermal conductivity of the compound, while the Fe^{3+} substitution of Al^{3+} increased its electrical conductivity. The highest dimensionless figure of merit (ZT) found was 0.021 at 973 K in the $CuAl_{0.9}Fe_{0.1}O_2$ sample sintered at 1423 K. Our findings show that this low-cost material with a reasonable figure of merit is a good candidate for thermoelectric applications at high-temperature.

EN-P-06

Utilization of Waste Shells as an Environmentally Friendly Catalyst for Synthesis of Biodiesel

Achanai Buasri[a,b,*], Teera Sriboonraung[a], Kittika Ruangnam[a], Pattarapon Imsombati[a], Vorrada Loryuenyong[a,b]

[a]*Department of Materials Science and Engineering, Faculty of Engineering and Industrial Technology, Silpakorn University, Nakhon Pathom, 73000, Thailand*

[b]*National Center of Excellence for Petroleum, Petrochemicals, and Advanced Materials, Chulalongkorn University, Bangkok, 10330, Thailand*

*E-mail address achanai130@gmail.com

Keywords: biodiesel, waste shells, microwave irradiation, transesterification.

Calcium oxide (CaO) is one of the most promising heterogeneous alkali catalysts since it is cheap, abundantly available in nature, and some of the sources of this compound are renewable (waste material consisting of $CaCO_3$). In this study, the waste shells were used as the raw materials for CaO catalyst. The calcination of bio-waste was conducted at 900 °C for 2 h. The raw material and the resulting CaO catalyst were characterized using X-ray diffraction (XRD), X-ray fluorescence (XRF), scanning electron microscopy (SEM) and the Brunauer-Emmett-Teller (BET) method. The effects of reaction variables such as reaction time, microwave power, methanol/oil molar ratio, and catalyst loading on the yield of biodiesel were investigated by gas chromatograph-mass spectrometry (GC-MS). From the experimental results, it was found that the CaO catalysts derived from waste material showed good catalytic activity (the conversion of oil of nearly 93%, a very similar catalytic activity with laboratory CaO) and had high potential to be used as biodiesel production catalysts in transesterification of *Jatropha Curcas* oil with methanol.

EN-P-07

Hydroxyapatite (HAp) Derived from Pork Bone as a Renewable Catalyst for Biodiesel Production via Microwave Irradiation

Achanai Buasri[a,b,*], Thaweethong Inkaew[a], Laorrut Kodephun[a], Wipada Yenying[a], Vorrada Loryuenyong[a,b]

[a]*Department of Materials Science and Engineering, Faculty of Engineering and Industrial Technology, Silpakorn University, Nakhon Pathom, 73000, Thailand*

[b]*National Center of Excellence for Petroleum, Petrochemicals, and Advanced Materials, Chulalongkorn University, Bangkok, 10330, Thailand*

*E-mail address achanai130@gmail.com

Keywords: biodiesel, microwave irradiation, pork bone, transesterification.

The use of waste materials for producing biodiesel via transesterification has been of recent interest. In this study, the pork bone was used as the raw materials for hydroxyapatite (HAp) catalyst. The calcination of animal bone was conducted at 900 °C for 2 h. The raw material and the resulting heterogeneous catalyst were characterized using X-ray diffraction (XRD), X-ray fluorescence (XRF), scanning electron microscopy (SEM) and the Brunauer-Emmett-Teller (BET) method. The effects of reaction time, microwave power, methanol/oil molar ratio, catalyst loading and reusability of catalyst were systematically investigated. The optimum conditions, which yielded a conversion of oil of nearly 94%, were reaction time 5 min and microwave power 800 W. The results indicated that the HAp catalysts derived from pork bone showed good reusability and had high potential to be used as biodiesel production catalysts under microwave-assisted transesterification of *Jatropha Curcas* oil with methanol.

EN-P-08

Preparation of Uranium Oxides by Thermal Decomposition of Uranium Extracted from Monazite Ore

Uthaiwan Injarean[a,*] and Pipat Pichestapong[a]

[a]*Thailand Institute of Nuclear Technology, Chatuchak, Bangkok, 10900, Thailand*

*uthaiwan42@yahoo.com

Keywords: uranium oxides, monazite ore, solvent extraction, ammonium diuranate

Monazite ore in the tailings of tin mines in the South of Thailand was found to contain 0.20 - 0.67% of uranium in the form of phosphate compound. This uranium can be chemically extracted from the ore and thermally converted to uranium oxides to be used for the production of membrane microfilter by nuclear track-etching technique. In this work, uranium separated from monazite ore was purified by solvent extraction using 5% tributyl phosphate in kerosene as the extractant. The purified uranium in nitrate solution was precipitated with ammonium hydroxide to form ammonium diuranate. Then, the uranium compound was calcined to uranium oxides at temperatures 400 - 800°C. The structure of obtained uranium oxides were determined by XRD. At 400°C, uranium was converted to yellow-orange powder of uranium trioxide (UO_3) and black-green powder of triuranium octoxide (U_3O_8) started to form at temperature 600°C. The conversion of uranium trioxide to uranium dioxide (UO_2) in a reducing atmosphere of hydrogen was also studied.

EN-P-09

From Waste Mollusk Shells to Thermoelectric Materials

Pennapa Muthitamongkol, Thanyaporn Yotkaew, Nattaya Tosanthum, Bralee Chayasombat, Chanchana Thanachayanont and Ruangdaj Tongsri*
National Metal and Materials Technology Center, 114 Paholyothin Road, Khlong Nueng, Khlong Luang, Pathum Thani 12120 Thailand
*ruangdt@mtec.or.th

Keywords: Mollusk shells, calcium oxide nanoparticles, $Ca_9Co_{12}O_{28}$ phase, thermoelectric material.

Waste shells of three mollusks, including *Anadara granosa*, *Paphia undulata*, *Perna viridis*, were employed to produce calcium oxide nanoparticles using a simple chemical route. The shells of *Anadara granosa* provided the best yield of calcium oxide nanoparticles, which were used to synthesize a high-temperature oxide thermoelectric material.Two synthesis routes with different starting materials and heat treatment steps were emloyed for preparing the oxide thermoelectric material. The synthesis route using calcium oxide nanoparticles, compared with the other using a commercial calcium carbonate, provided benefit of reduced processing time. Characterization of the synthesized thermoelectric materials revealed that $Ca_9Co_{12}O_{28}$ was the main phase. The $Ca_9Co_{12}O_{28}$ phase showed modulated structure characteristics, as evidenced by its X-ray diffraction pattern and electron diffraction by transmission electron microscopy. Measurement results of electrictal conductivity, Seebeck coefficient and thermal conductivity suggested that the synthesized material showed promising thermoelectical properties.

EN-P-10

Investigation of Fuel Pellet Properties from Agricultural Residues

Wassachol Wattana*, Wrawat Sompasong, Nattawut Onpakdee, and Apichat Dangsangtong

[a]*King Mongkut's Institute of Technology Ladkrabang, Prince of Chumphon Campus, Pathiu, Chumphon, 86160, Thailand*

*kwwassac@kmitl.ac.th

Keywords: Fuel Pellet, Betel nut husk, Agricultural residue, Microstructure.

The Betel nut husks, residues from agricultural plantation, were introduced for a renewable energy source. The size of husks was reduced to below 4 mm and then compressed in a single pelletization unit. The effect of die temperature (90°C, 120°C and 150°C) and compressive pressure (90, 120 and 150 MPa) on densification characteristics (particle and bulk density) and physical quality according to fuel pellet standard was investigated. Moreover, the changes in pellet microstructure at different production conditions were examined. The results of the study showed that all properties investigated fell within the range of fuel pellet standard except the ash content. The die temperature and compressive pressure lead to a difference in pellet structure. The best production condition was found to be at 120°C and 90 MPa for die temperature and compressive pressure, respectively.

EN-P-11

Cu/ZnO Catalysts for Enhancing the Methanol Selectivity in Fischer-Tropsch Synthesis

Passakorn Kongkinka[1,a], Kittima Chatrewongwan[1,b], Patraporn Saiwattanasuk[1,c], Pinsuda Viravathana[1,2,d,*]

[1]*Department of Chemistry, Faculty of Science, Kasetsart University, Bangkok 10900, Thailand*
[2]*Center of Advanced Studies in Tropical Natural Resources, National Research University, Kasetsart University, Bangkok 10900, Thailand*
[a]madeaw_watchap@hotmail.com, [b]fscikmc@ku.ac.th, [c]fsciprss@ku.ac.th,
[d,*]fscipdv@ku.ac.th

Keywords: methanol, syngas, bimetal, Fischer-Tropsch synthesis

Cu/ZnO catalysts were studied to enhance the methanol selectivity in Fischer-Tropsch synthesis (FTS). By knowing that the methanol production from syngas (CO/H_2) accelerated the crystallization of Cu and ZnO and led to the deactivation of the catalysts, a small amount of iron added to the catalyst could improve the catalyst stability by suppressing the crystallization of Cu and ZnO. The promotional effects of iron on the textural properties, reduction behavior, and structural changes of the Cu-based FTS catalysts were investigated by X-ray diffraction (XRD), X-ray absorption near edge structure (XANES), and extended X-ray absorption fine structure (EXAFS). Their catalytic activity was measured at 10 bar and 190°C with H_2/CO ratio of 2 and the FTS products were analyzed by GC. The product distribution was presented in terms of methanol, C_1, C_2-C_4, and C_{5+} selectivity.

EN-P-12

High Performance Calcium Hydroxide Catalyst from Waste Green-mussel Shell for Biodiesel Production

Korakot Niyomsat, Duangamol Tungasmita and Numpon Insin*
Department of Chemistry, Faculty of Science, Chulalongkorn University, Bangkok, 10330, Thailand
*Numpon.I@chula.ac.th

Keywords: biodiesel, green-mussel shell, transesterification

An economical cost and environmentally friendly catalyst derived from waste Green-mussel shell was utilized for transesterification reaction in biodiesel production. The catalytic activity of high-performance calcium hydroxide ($Ca(OH)_2$) catalyst from waste Green-mussel shell was studied in the transesterification reaction of plam oil using 6.5:1 methanol to oil molar ratio at 64°C with 3 wt.% $Ca(OH)_2$. The $CaCO_3$, CaO and $Ca(OH)_2$ catalysts were characterized using X-ray powder diffraction (XRD), Fourier transform infrared spectroscopy (FTIR), scanning electron microscope (SEM) and Brunauer-Emmett-Teller (BET) surface area analysis. The conversion of triglyceride from palm oil to biodiesel was determined using Proton nuclear magnetic resonance (^{1}H-NMR). The experiment results showed that 88.89% conversion of biodiesel was obtained after the reaction for 0.5 h at agitation speed of 700 rpm, and the maximum biodiesel conversion of 99.50% was achieved when the reaction was carried out for 2 h. Furthermore, the prepared $Ca(OH)_2$ catalyst was able to be reused for more than three cycles without significant deterioration in its activity, and the biodiesel conversion was maintained above 96.62%.

EN-P-13

Electrochemical Fabrication of Cu_2O Photocathode for Photoelectrochemical Hydrogen Evolution Reaction

Pattranit Thongthep [a], Somporn Moonmangmee[b], Chatchai Ponchio [a,*]
[a] *Department of Chemistry, Faculty of Science and Technology, Rajamangala University of Technology Thanyaburi, Thanyaburi, Phathumtani 12110, Thailand*
[b] *Bioscience Department, Thailand Institute of Scientific and Technological Research, Khlong Luang, Pathum Thani. 12120, Thailand*
*chatchai@rmutt.ac.th

Keywords: Photoelectrochemical, Hydrogen evolution, Cu_2O photocathode.

In this study, we can fabricate Cu_2O on F-doped SnO_2 coated glass (FTO) substrates as photocathode for hydrogen evolution reaction by electro-deposition techniques. Cyclic voltammetry as a new deposition methods was studied to fabricate Cu_2O photocathode in a mixed solution of $Cu(NO_3)_2$ and KNO_3 under condition of low temperature and without pH value adjustment. Amperometry as a previous method was used to compare for Cu_2O electrode fabrication under situation of pH adjustment and higher temperature condition. A photocurrent from hydrogen evolution reaction was performed by keep potential at -0.2 V in 0.1 M Na_2SO_4 under visible irradiation comparing with both fabricated method. The Cu_2O photocathode from cyclic voltammetry deposition method presents photoelectrocatalytic activity higher than that of amperometry deposition method with the optimum conditions. This electro-deposition technique represents the excellent method with simple, fast and low cost of Cu_2O photocathode fabrication for photoelectrochemical hydrogen evolution reaction.

EN-P-14

Cu/ZnO Nanoparticles Prepared By Ultrasonic Spray Pyrolysis Using Different Precursors

Panjit Saepun and Prasert Reubroycharoen *

Department of Chemical Technology, Faculty of science, Chulalongkorn University, Bangkok 10330, Thailand

Center of Excellence on Petrochemical and Materials Technology, Chulalongkorn University Research Building, Bangkok 10330, Thailand

*prasert.r@chula.ac.th

Keywords: Cu/ZnO catalysts, deactivation, LPG synthesis, ultrasonic spray pyrolysis.

Synthesis gas to liquefied petroleum gas (LPG) was carried out by Cu-ZnO composite β-type zeolite catalyst. The ultrasonic spray pyrolysis (USP) method has been applied to directly prepare particle of Cu-ZnO catalyst from different precursors at various temperature under air with continuous process. Precursor solutions containing nitrate, acetate, sulphate and chloride of copper and zinc were atomized by ultrasonic, passed through pyrolysis reactor and converted to oxide compounds of copper and zinc. The size and shape of particle depended on the type of precursors and different the reaction temperatures. The crystallite size grew by increasing the temperature when use of nitrate and acetate solution but the crystal size was decreased when use of sulphate and chloride and found that the particles are spherical with mixed large and small size. The USP presented efficient catalyst preparation technique for controlling atomic ratio with nearly desired ratio. The surface morphology, particle size, composition surface area and crystalline structure of Cu/ZnO catalysts were characterized by scanning electron microscopy (SEM), X-ray diffraction (XRD), energy dispersive X-ray spectrometer (EDX) , temperature-programmed reduction(TPR) and nitrogen adsorption-desorption (BET), respectively. The Cu-ZnO catalyst was tested the catalytic activity for LPG production by physical mixing with β-type zeolite which the reaction in the fixed-bed reactor under the low temperature (260°C) and pressure at 3 MPa, syngas flow rate of 20 ml/min (H_2/CO/CO_2/Ar = 60/32/5/3 by mole), 0.25g of Cu-ZnO/β-type zeolite catalyst. The experimental results indicated that the deactivation of Cu-ZnO catalysts was rather rapid where the sintering of copper has been considered as a main reason for the deactivation.

EN-P-15
Spherical Cu/ZnO Catalyst by Ultrasonic Spray Pyrolysis For LPG Production

Sudarat Chaiwatyothin, Prasert Reubroycharoen, Tharapong Vitidsant*
Department of Chemical Technology, Faculty of science, Chulalongkorn University, Bangkok 10330, Thailand
Center of Excellence on Petrochemical and Materials Technology, Chulalongkorn University Research Building, Bangkok 10330, Thailand
*Tharapong.v@chula.ac.th

Keywords: Ultrasonic spray pyrolysis, Cu/ZnO, LPG.

Synthesis of nano Cu/ZnO catalyst by ultrasonic spray pyrolysis (USP) for LPG production was examined. Hollow spherical particles were obtained using an aqueous solution of $Cu(NO_3)_3.6H_2O$ and $Zn(NO_3)_3.3H_2O$ at different concentration of 0.05, 0.1 and 0.5 molar under the pyrolysis temperature of 600, 700 and 800 °C. Mists of the solution were generated from the starting solution with ultrasonic vibrators at frequency of ~1.7 MHz. The physicochemical properties of catalysts were characterized by X-ray diffraction, temperature-programmed reduction, scanning electron microscope, nitrogen adsorption-desorption, and energy dispersive X-ray spectrometer. The results showed that increasing in precursor concentration resulted in a large particle and particles size distributed in a range of 448-1209 nm. Particles prepared at pyrolysis temperature 700°C exhibited homogeneous in size and shape compared to other temperature. The catalytic activity of nano Cu/ZnO-Pd-β catalysts was performed in a fixed-bed reactor for synthesizing LPG. The reaction took place at 260°C, 3.0 MPa, and the ratio of $H_2/CO = 2/1$. All the products from the reactor were in gaseous state, and analyzed by on-line gas chromatography. The results showed that %CO conversion was high but decreased rapidly with increasing reaction time. Cu/ZnO catalyst prepared by co-precipitation gave higher %CO conversion than that prepared by ultrasonic spray pyrolysis. Moreover, hydrocarbon product distribution for Cu/ZnO catalyst produced at concentration 0.1 M 700 °C by ultrasonic spray pyrolysis gave the highest LPG selectivity.

EN-P-16

LPG Synthesis Over Cu/ZnO-ZSM-5 Catalyst Prepared by Ultrasonic Spray Pyrolysis and Hydrothermal Synthesis

Narumon Thonkhaw, Prsert Reubroycharoen and Tharapong Vitidsant*
Department of Chemical Technology, Faculty of Science Chulalongkorn University, Bangkok, 10330, Thailand
Center of Excellence on Petrochemicals and Materials Technology, Chulalongkorn University, Bangkok, 10330, Thailand
*Tharapong.v@chula.ac.th

Keywords: ZSM-5/CuZno catalyst, Hydrothemal synthesis, syngas.

Chemical mixture of Cu/ZnO and ZSM-5 was prepared by ultrasonic spray pyrolysis and hydrothermal synthesis. The Cu/ZnO catalysts were prepared in the first step by ultrasonic spray pyrolysis of copper/zinc nitrate solution at 700°C. Then, the catalyst was transfer to the hydrothermal synthesis of zeolite to obtain the chemical mixture Cu/ZnO and ZSM-5 catalyst. The chemical mixture catalysts were characterized by scanning electron microscopy (SEM), X-ray diffraction (XRD), nitrogen adsorption-desorption (BET), and energy dispersive X-ray spectrometer. Both SEM and XRD results showed that the crystallinity and particle size of the synthesized zeolite increase with increasing crystallization time .During this 24 h period the relative crystallinity of ZSM-5 increased when the crystallization temperature was increased. Also, the crystallization temperature had a strong effect on crystallinity and morphology; a highly crystalline ZSM-5 zeolite was synthesized at 180°C. However, the intensity of Cu/ZnO from XRD peak was decreased after 6 h mixed in hydrothermal process. The catalytic performance test with synthesis of liquefied petroleum gas (LPG) from syngas was investigated over Cu/ZnO-ZSM-5 in fixed bed reactor. The operating condition for the formation of C3-C4 hydrocarbons were identified by optimizing syngas flow rate and reaction temperature as well as feed partial pressure, 20 ml/min, > 260°C, and > 3 MPa. LPG fractional hydrocarbon could be formed selectively from methanol, DME or a mixed feed. Selectivity towards LPG hydrocarbon increased when the crystallization temperature was increased but co conversion decreased rapid. Due to the poisoning of acid site by water molecule on the zeolite effect to catalyst deactivated in reaction process.

EN-P-17

Preparation of H_2 Separation Membrane from Palladium Deposition on Porous Alumina Support Using Agar

Kowit Lertwittayanon[1,2*], **Wirote Youravong**[2,3]
[1]*Department of Materials Science and Technology, Faculty of Science, Prince of Songkla University, Hat Yai, Songkhla, Thailand, 90110*
[2]*Membrane Science and Technology Research Center (MSTRC), Prince of Songkla University, Hat Yai, Songkhla, Thailand, 90110*
[3]*Department of Food Technology, Faculty of Agro-Industry, Prince of Songkla University, Hat Yai, Songkhla, Thailand, 90110*
*Kowit.l@psu.ac.th

Keywords: Palladium membrane; Hydrogen separation; Deposition; Agar

A preparation of Pd/porous Al_2O_3 composite membrane through agar-assisted deposition was studied for using in H_2 separation. The agar-assisted Pd deposition offered simple and green preparation compared with the typical method of electroless plating. The effect of agar amounts (0.25–1.00wt%) on the microstructure of Pd layer were investigated using XRD, SEM, TGA and XPS. The deposited samples were calcined at 600°C to burnout agar and then reduced in H_2 atmosphere to obtain Pd metal layer. TGA results revealed the increases in the weight loss percentage with increasing agar. XRD patterns of the calcined samples showed the existence of PdS and Al_2O_3. The SEM microstructures of Pd layer confirmed that the agar content resulted in crack in Pd layer. After the H_2 reduction of membrane containing 0.25wt% agar, XPS result displayed the existence of C, Pd, S, O, Na and Al.

EN-P-18

Effect of Gallium Loading on Reducibility and Dispersion of Copper-based Catalyst

Parncheewa Udomsap*, Somsak Supasitmongkol
National Metal and Materials Technology Center, Klong Luang, Pathumthani, 12120, Thailand
*E-mail address parncheu@mtec.or.th

Keywords: Copper dispersion, TPR, Dissociative Nitrous (N_2O) adsorption, Gallium loading.

The effect of gallium-promoted copper-based catalysts has been investigated in connection with the characteristic of the active copper phase. CuO-ZnO-Ga_2O_3 catalysts with different gallium loadings were prepared using oxalate co-precipitation method. The effects of gallium loading on the properties of catalysts were studied by means of X-ray diffraction (XRD), Transmission Electron Microscopy (TEM) and Temperature-Programmed Reduction (TPR). The dispersion and metal area of copper were also determined by Dissociative Nitrous (N_2O) adsorption technique conducted on a Metal dispersion analyzer (BELCAT). The TPR profiles showed that the presence of two different reduction regions in the CuO-ZnO catalysts can be attributed to the reduction of highly dispersed copper oxide species (reduction at 246 ^oC) and bulk-like CuO (reduction at above 390 ^oC). By contrast, the only low-temperature reduction peak was presented in the TPR profiles after the Ga_2O_3 loading is higher than 4 wt%. With the same molar ratio (Cu/Zn = 2:1), the reducibility of CuO-ZnO-Ga_2O_3 was found to be more facile than CuO-ZnO due to the lower copper oxide crystallite sizes of gallium-promoted catalysts. Higher Ga_2O_3 loadings resulted in an increase in both copper dispersion and metal surface area of all the catalysts studied in good agreement with the reduction behaviors in the TPR profiles, although all the gallium-promoted catalysts were slightly different for the reducibility.

EN-P-19

Removal of Hydrogen Sulfide from Gas Streams in a Single Packed Column System

Kiatkong Suwannakij*, Sedthawatt Sucharitpwatskul, Vises Layluck and Somsak Supasitmongkol
National Metal and Materials Technology Center, Klong Luang, Pathum Thani, 12120, Thailand
* kiatkons@mtec.or.th

Keywords: Hydrogen sulfide (H_2S), Biogas, purification, Water scrubbing, CFD simulations

Biogas from anaerobic digestion of biological wastes is a renewable energy resource. It has been used to provide heat, shaft power and electricity. The presence of hydrogen sulfide (H_2S) in biogas has a toxic and corrosive to most equipment such as piping, boilers and power-generating machine. Reducing H_2S content needs to be considered in practical application before utilizing biogas. In this work, H_2S absorption by water in a packed column was experimentally investigated to determine technical feasibility of a water scrubbing system designed for small-scale biogas production. The influence of many parameters on absorption characteristics such as packing media, liquid spray nozzles, gas vane inlet, liquid to gas flow rate (L/G) ratios were considered. A computational fluid dynamic (CFD) analysis of gas flow through the column was also presented. The CFD simulations showed that the entrance direction of the gas in vane inlet affects superficial velocity and pressure loss of the flowing gas momentum inside column. At the same superficial gas velocity, pressure loss was significantly less for the tangential gas inlet when compared with the perpendicular gas inlet. The tangential gas inlet showed a better H_2S removal efficiency than the perpendicular inlet due to uniform gas flow distribution. The higher biogas flow rate had negative impact to contacting efficiency and mass transfer of liquid and gas phase. The optimum operating condition of the single packed column are 0.6 of L/G ratio, 6 l/min biogas and 135 cm of packing height in the absorption column to get the highest H_2S removal efficiency 74%.

EN-P-20

Effective Channel Width and Length Ratio in Water-Gated Organic Field-Effect Transistors

Kroekchai Inpor[a]*, Pollawat Prisawong[b], Werapon Kamonkhantikul[b], Seeroong Prichanont[b], Chanchana Thanachayanont[a]

[a]National Metal and Materials Technology Center (MTEC) 114 Thailand Science Park (TSP), Phahonyothin Road, Khlong Nueng, Khlong Luang, Pathum Thani 12120, Thailand.

[b]Chulalongkorn University 254 Phayathai Road, Pathumwan, Bangkok 10330, Thailand.

*kroekchi@mtec.or.th

Keywords: Organic Transistors, Field-effect Transistors, Semiconductor polymer

Organic field effect transistors (OFET) are widely utilized in alternative disposable electronic devices. These devices provide fabrication simplicity, low-cost, fast, and adequate sensitivity. A water-gated organic field-effect transistors (OFETs) are promising for detection of chemical species in water. The device was reported to operate under low-voltage as low-energy consumption device. In this investigation, Poly(3-hexylthiophene) (P3HT) was used as the semiconducting layer in the water-gated organic field-effect transistors. Drain and source electrode materials were deposited by the thermal evaporation of gold. Deionized water droplet was applied the dielectric layer for our devices. In this study, the effects of channel width and length ratio on electrical characteristics of the semiconducting layers were investigated. It was found that the increasing channel width and length ratio improved the electrical performance of the water-gated OFETs. However, at short-channel lengths, the OFETs no longer saturate due to space charge limiting current effects.

EN-P-21

Development of Electrospray Technique Used for Electrode Preparation in Proton Exchange Membranes Fuel Cells (PEMFCs)

Natthika Chingthamai[a], Phanwadee Phomprasert[a], Anonpit Koedkul[a], Weerachai Glaithin[a], Korakot Sombatmankhong[b, *], Yossapong Laoonual[a]
[a]Combustion and Engines Research Laboratory
Department of Mechanical Engineering, Faculty of Engineering,
King Mongkut's University of Technology Thonburi,
126 Pracha Uthit Road, Bangmod, Thung Khru, Bangkok, 10140, Thailand
[b]Electrochemical Materials and System Laboratory,
National Metal and Materials Technology Center (MTEC), 114 Thailand Science Park,
Phahonyothin Road, Khlong Nueng, Pathum Thani 12120, Thailand
*E-mail: korakots@mtec.or.th

Keywords: Electrospray, Electrocatalyst Deposition, Proton Exchange Membranes Fuel Cell

Electrospray technique is a novel method used to produce well-dispersed and uniformly distributed catalyst layers on carbon substrates in the process of electrode fabrication in proton exchange membrane fuel cell (PEMFC). As a result, the catalyst loading can be lowered while the utilization level can be maintained. In this research work, catalyst suspension was initially prepared by mixing carbon black, nafion solution and isopropanol at different compositions. Next, the catalyst ink was deposited on carbon substrates using electrospray technique. In order to generate cone-jet mode during electrospinning process, the applied potential and flow rate were varied in a range of 6.6-7.8 kV and 0.1-1.1 ml/hr respectively. The particle size distribution obtained from the electrospray technique was examined using scanning electron microscopy (SEM) which was also compared with that of electrode prepared by conventional painting method. It was found that the average particle size obtained by electrospray was 2.023 μm which was 4-fold smaller than the electrode prepared by painting method (i.e. 8.903 μm). Moreover, the average thickness of electrocatalyst layer was 65.6 μm with standard deviation of 4.038 μm using the electrospray technique which was lower than that of the electrocatalyst layer obtained by painting technique (i.e. 67.7 μm with standard deviation of 7.142 μm). This indicated the smooth electrode surface fabricated by electrospray technique. Consequently, the electrospray deposition demonstrated to be a promising tool for the production of high quality catalyst layers with an increase in the utilization of catalysts and in cell performance.

EN-P-22

Electrostatic Spray Deposition of Y-doped $BaZrO_3$ Thin Films on Porous Anodes for Protonic Ceramic Fuel Cell Application

Rojana Pornprasertsuk[a,b*], Thanaporn Yoomanthamma[a,b] and Kittichai Somroop[a,c]

[a]*Research Unit of Advanced Ceramics, Department of Materials Science, Faculty of Science, Chulalongkorn University, Bangkok, 10330, Thailand*

[b]*Center of Excellence on Petrochemical and Materials Technology, Chulalongkorn University, Bangkok 10330, Thailand*

[c]*Viptel Co.,Ltd., Rayong, 21000, Thailand*

*rojana.p@chula.ac.th

Keywords: barium zirconate, thin film, electrostatic spray deposition, protonic ceramic fuel cell

This research focused on the fabrication of yttrium-doped barium zirconate (BYZ) thin films on 60 wt% NiO- 40 wt% BYZ anodes by electrostatic spray deposition (ESD) technique. The effects of precursor preparation and ESD conditions (i.e. type of precursor, type of solvent, flow rate, applied voltage, substrate temperature and nozzle-to-substrate distance) on the thin film microstructure were systematically studied and optimized to achieve the dense BYZ films on the porous anode substrates. After sintering at 1100-1500 °C, the microstructure and phase analysis of BYZ films was performed using scanning electron microscopy (SEM) and X-ray diffraction (XRD) techniques. The optimum parameters were thus summarized as followed: (i) using $Ba(C_2H_3O_2)_2$, $Y(C_2H_3O_2)_3{\cdot}4H_2O$ and $Zr(C_5H_7O_2)_4$ as precursors, (ii) dissolving 0.05 mol/L of precursors in the solvent mixture of deionized water and butyl carbitol (at the volume ratio of 50:50), (iii) mixing the solution at 50°C for 1 h, (iv) electrospraying at the applied voltage of 10 kV, the substrate temperature of 230 °C, the nozzle-to-substrate distance of 8 cm and the flow rate of 2.8 mL/h. Since the dense BYZ films could not be achieved on the bare NiO-BYZ anode substrates, the anode functional layers (AFLs) with lower mass fractions of NiO:BYZ at 10:90, 30:70 and 50:50 was co-pressed on top of NiO-BYZ anode substrates. The heating rate, sintering temperature and anode microstructure were further adjusted to reduce the porosity and crack formation on the BYZ films. The results will then be analyzed and reported.

EN-P-23

Effect of Sputtering Power on Morphological, Structural and Optical Properties of Al-Doped Zinc Oxide Film

P. Boonprakom[a] and W. Rattanasakulthong[a,*]
[a]*Department of Physics, Faculty of Science, Kasetsart University,50 Ngam Wong Wan Ladyaow, Chatuchak, Bangkok, 10900,Thailand*
* fsciwrr@ku.ac.th

Keywords: ZnO:Al film, Sputtering power, RF sputtering, Optical transmission

Transparent Conductive Al-doped Zinc Oxide (ZnO:Al) films with different sputtering powers were prepared on glass substrate by RF sputtering technique. Two main peaks of the hexagonal wurtzite structure in the (002) and (004) direction were observed in all deposited ZnO:Al films. Intensity of these peaks was increased with the increase of sputtering power. Moreover, surface roughness tended to increase with increasing sputtering power whereas electrical resistance was decreased with increasing sputtering power. The ZnO:Al film deposited at 150 and 200 W showed the maximum optical transmittance over 80% in visible wavelength range. All results confirm that sputtering power directly affects the film thickness because the higher sputtering power gives rise to the higher deposition rate, surface morphology of deposited films was depended sputtering power and optical properties is indirectly affected by the power of deposition process.

EN-P-24

Effect of Bi_2O_3 on Thermal Properties of Barium-free Glass-Ceramic sealant in the CaO-MgO-B_2O_3-Al_2O_3-SiO_2 System

Pornchanok Lawita[a], Apirat Theerapapvisetpong[a], Sirithan Jiemsirilers[a,*]

[a] *Research Unit of Advanced Ceramics, Department of Materials Science, Faculty of Science, Chulalongkorn University, Bangkok, 10330, Thailand*

*sirithan.j@chula.ac.th

Keywords: SOFC, Sealant, Glass-ceramics, Barium-free

Barium-free glass-ceramic sealants for the planar solid oxide fuel cell (pSOFC) have attracted considerable attention to avoid the crystallization of the high-CTE $BaCrO_4$; reaction product at the interface between barium-containing glass-ceramic sealants and Crofer22 APU interconnect, which decreases the long-term mechanical stability of the sealant. In this study, Barium-free glass-ceramic sealants in the CaO-MgO-B_2O_3-Al_2O_3-SiO_2 system with varying amounts of Bi_2O_3 from 0 to 10 wt. % were prepared by conventional melting and their thermal properties were investigated. The glass transition temperature (T_g), dilatometric softening temperature, and coefficient of thermal expansion (CTE) were determined by dilatometer. The T_g, onset of crystallization (T_x) and Crystallization temperature (T_c) were obtained from DSC/TG. Results of Phase analysis by X–ray diffraction of glasses after thermal treatment at 900 ºC for 2 h indicated that the major phase of all glasses was diopside ($MgCaSi_2O_6$) and minor phases were åkermanite ($Ca_2MgSi_2O_7$) and forsterite (Mg_2SiO_4). The T_g of the fabricated glasses tended to decrease with increasing Bi_2O_3 content while the CTE of glasses increased after the thermal treatment and was in the range of requirement for SOFC sealant.

EN-P-25

Materials Selection and Design for Ethanol Steam Reforming Reactor

Thanathon Sesuk[a*], Jarruwat Charoensuk[b], Sumittra Charojrochkul[a,]
[a] *National Metal and Materials Technology Center (MTEC), 114 Paholyothin Road, Klong 1, Klongluang, Pathumthani 12120, Thailand*
[b]*Department of Mechanical Engineering, Faculty of Engineering, King Mongkut's Institute of Technology Ladkrabang, Bangkok 10520, Thailand*
*thanaths@mtec.or.th

Keywords : Hydrogen production, steam reforming, Bioethanol, reactor

Hydrogen is considered as a clean energy carrier based on renewable energy sources for the future. One of the most promising hydrogen production methods is based on bioethanol because of its relatively high hydrogen content, availability, low production cost, simple system and safe handling, transportation, storage and non-toxic. In this work, a design of hydrogen production process using bioethanol reforming was studied at a pilot scale. A system of hydrogen production from bioethanol consists of three main parts: reactor, furnace and boiler. The reactor was designed to submerge in a porous media with operating temperature around 900˚C. The furnace contains a combustion zone and air/fuel distributor which provides equal distribution of air/fuel to the combustion zone. In addition, a boiler is used to convert liquid bioethanol to vapor before transferring to the reactor. All of these components are operated at high temperature, which need to be resistant to thermal stresses. The materials are selected based on design consideration, notably strength, corrosion resistance and thermal stability. Correct selection of materials are essential to ensure safety and economy in production, operation, reaction and heat loss. There are several sources of materials challenges related to this system. In making a choice, it is necessary to consider materials availability with the suitable property requirement for the specific application i.e. a reactor, furnace shell, tube, insulation. This new design system can generate hydrogen on a long term basis and in the future can be upscaled to a commercial plant level.

EN-P-26

Physical and Optical Properties of Indium Oxide:Tin Nanoparticles Synthesized by Co-precipitation Method

J. Kanoksinwuttipong [a,*], W. Pecharapa [b,c], R. Noonuruk [b] and W. Techitdheera[a]

[a] *School of Physics, Faculty of Science, King Mongkut's Institute of Technology Ladkrabang, Bangkok 10520, Thailand*

[b] *College of Nanotechnology, King Mongkut's Institute of Technology Ladkrabang, Bangkok 10520, Thailand*

[c] *ThEP Center, CHE, 328 Si Ayutthaya Rd., Bangkok 10400, Thailand*

* newrxzero@gmail.com

Keywords: ITO nanoparticle, co-precipitation, diffused reflection spectroscopy.

Indium oxide:tin nanoparticles were synthesized by co-precipitation method using $InCl_3$ and $SnCl_4 \cdot 5H_2O$ as starting precursor with different molar ratios of Sn:In. Thermal properties of the precursor was analyzed by thermogravimetry and derivative thermogravimetry. Meanwhile, crystalline structure, optical properties and chemical bonding of Indium oxide:tin nanoparticles were characterized by X-ray diffraction (XRD), diffused reflection spectroscopy and Raman spectroscopy, respectively. The size, shape and microstructure of the particles were observed by field emission scanning electron microscope and chemical composition was investigated by energy dispersive X-ray spectrophotometer (EDS). The XRD results show that the crystallinity of as-synthesized powders was initially amorphous phase. After annealed at 400 °C for 2 h, a single phase ITO powder with 10% (mol%) SnO_2 was obtained.The particle size of the ITO nanoparticles is 20-25 nm. EDS shows (6 mol% and 10 mol%) Sn in respect to In in In_2O_3 structure, which is consistent with the initial stoichiometric proportion. Moreover, the color of indium oxide:tin nanopowders after heat treatment changed from white to yellow due to the substitution of oxygen vacancies in the sample. After calcination, the Raman peak intensities significantly decreased with increasing amount of Sn loading. This phenomenon indicates that ion substitution may occur during the synthesis process. It is also noticed that the optical reflectance of the sample has observable change with increasing Sn loading.

EN-P-27

Visible Light Driven Photocatalytic Hydrogen Evolution by La and C Co-doped $NaTaO_3$ Photocatalyst

Husni Husin[a,*], Mahidin[a] and Zuhra[a], Fikri Hasfita[b]
[a]*Chemical Engineering Department, Engineering Faculty, Syiah Kuala University, Darussalam, Banda Aceh, 23111, Indonesia*
[b]*Chemical Engineering Department, Engineering Faculty, Malikussaleh University, Lhoekseumawe, Aceh Utara, 24300, Indonesia*
*husni_husin2002@yahoo.com

Keywords: La-C-$NaTaO_3$, photocatalyst, sol-gel, hydrogen.

Lanthanum and carbon co-doped $NaTaO_3$ photocatalyst (La-C-$NaTaO_3$) catalyst are successfully synthesized at calcination temperature of 700 ^oC via sol-gel route using a sucrose as carbon source. Effects of carbon contents on the crystal, shape, optical absorption response and activity of hydrogen production of the sample are evaluated. The crystal of La-C-$NaTaO_3$ is characterized by XRD analysis. The results show that the XRD pattern of the La C co-doped $NaTaO_3$ is found to be crystalline phase with monoclinic structure. From the analysis of SEM images, the particle size of the prepared powder is about 40-200 nm. The optical response is examined by diffuse reflectance spectra (DRS). It is depicted that the absorption edge of La-C-$NaTaO_3$ crystalline shift to lower wavelength. The extension to the visible light absorption edge became drastic with increasing carbon content in the sample. The photocatalytic activity of La-C-$NaTaO_3$ is examined from water-methanol aqueous solution under visible light irradiation. It is found that the photocatalytic activity of La-C-$NaTaO_3$ depend strongly on the doping content of C, and sample La-C-$NaTaO_3$ shows the highest photocatalytic activity for the water reduction. The optimum amounts of carbon to maximize the hydrogen evolution rate is to be 2.5 mol %. The La-C-$NaTaO_3$ catalyst has high activity of H_2 evolution (40.0 μmol h^{-1}) and long time stability under visible-light irradiation, suggesting a promising utilization of such photocatalyst. La C co-doped $NaTaO_3$ photocatalyst can be developed further in order to produce hydrogen as a green energy.

EN-P-28

Analysis of Ion Transport Behavior of the Ion Exchange Membrane by Molecular Dynamic Simulation

Sang Yong Nam[a,*], Deuk Ju Kim[a], Chi Hoon Park[b]

[a]Department of Materials Engineering and Convergence Technology, Engineering Research Institute, Gyeongsang National University, Jinju, 660-701, Korea

[2]Department of Energy Engineering, Gyeongnam National University of Science and Technology, Jinju, Korea

*walden@gnu.ac.kr (Sang Yong Nam)

Keywords: MDS, ion exchange capacity, membrane.

We investigated dynamics of hydronium ions and methanol molecules in hydrated SPAES and blend membranes using molecular dynamics simulations with the COMPASS force field. In addition to calculating diffusion coefficients as a function of hydration level, we made and tested the amorphous cell with determined the composition of H_2O molecules and H_3O^+ obtained from experimental. Water and methanol diffusion coefficients are considerably smaller at lower hydration levels and room temperature. The diffusion coefficient of Water and methanol molecules increases with increasing hydration level and is in good agreement with experiment. Analysis of pair correlation functions supports the experimental observation of membrane performance upon hydration as well the increase in water and methanol diffusion with increasing water contents

EN-P-29

Alternative Utilization of Oil Palm Empty Fruit Brunch

[a,*]Chom-in Tassaneewan, Thamsakon Soottiwan[a], Wenunun Pechda[b] , Pinyo Waraporn[b]
[a]National Metal and Materials Technology Center (MTEC), National Science and Technology Development Pathumthani, 12120, Thailand
* tassanc@mtec.or.th

Keywords: EFB, biogas, energy, Greenhouse Gas.

Palm oil is very importance vegetable oil that can be found in many products from foods to non-food. Thailand is the one of most importance producer in the world, the palm mill industry in Thailand have total milling capacity almost 2000 tonne fresh fruit branch (FFB) per hour, one tonne of fresh fruit bunches (FFB) produces about 0.22 tonne empty fruit bunches (EFB). This means 400 tonne of EFB can be produce in every hour of milling. Palm milling industry attempt to utilized EFB more than dump to landfill as the normal way to treat this waste.

This paper show the environmental impact from utilize EFB as fertilizer supplement and energy source by using alternative method that using 2 step of combination process; composting and anaerobic digestion. By collecting data from pilot scale of aerobic composter, 15 tonne of EFB will be composted for 3 months before sent to anaerobic fermenting system that provide methane to gas engine for generated electricity. Data has been analyzed by using life cycle assessment concept, method CML baseline 2000. The result show that the combination process of EFB utilization have low environmental impact than just only used as fertilizer supplement for oil palm because of energy surplus from methane.

Materials Technology for Environment Session

ORAL PRESENTATIONS

EV-O-01

Design and Construction of Variable Speed Heat Pump for Supply Air Reheat

Krittamuk Wongprasert*, Tul Manewattana
Department of Mechanical Engineering, Faculty of Engineering, Chulalongkorn University, Pathumwan, Bangkok, 10330, Thailand
*w_krittamuk@hotmail.com

Keywords: heat pump, supply air reheat, variable speed drive

Fresh air supply to air conditioned space sometime needs to be reheated to suit room required conditions. In the past, electric heater, steam or hot water coil are mostly used for this purpose even though they are not energy efficient. Nowadays heat pump is a more favorable means to do this reheating with better control and more energy efficient. However, a constant speed compressor for heat pump is still a common choice for today technology.
Nowadays, variable speed drive compressors technology has been improved significantly. Applying this technology to heat pump for reheat could further improve energy efficiency of a system. This study focus on the design and construction of heat pump using variable speed drive compressor for supply air reheat. Main equipment of system are consisted of evaporator coil, condenser coil, electronic expansion valve, variable speed drive compressor and a direct digital control for a system. Variable speed drive of a compressor will be controlled to generate heat at the condenser exactly as required by the supply air temperature. Cooling effect from evaporator is just a byproduct from heat pump. It is not a control parameter. However it can help bringing down the dew point of the supply air a little further.
After the unit was constructed, the unit has been tested for performance at 10 ºC supply air dew point. Results show that the variable speed heat pump could save about 50% on energy saving when compared with air heater and 15% more when compared to constant speed heat pump. Disadvantage of this system is a more complex DDC control and high cost for construction.

EV-O-02

Response of Bond Strength and Development Length Precast Concrete Using Grouting

Rosyidah, Anis[a,*], Fahimmudin, Fauzri [a], Sucita, I Ketut[a] and Sari and Chintya[b]
[a]*Politechnic State of Jakarta, Depok, 16425, Indonesia*
[b]*Graduate Politechnic State of Jakarta, Depok, 16425, Indonesia*
*anis.rosyidah@gmail.com

Keywords: Precast Concrete, Bond Strength and Development Length.

The connection is needed in reinforced precast concrete construction to link the precast elements. In general, the connection uses reinforcing steel embedded into precast concrete. The requirements in reinforced concrete construction is a bond between concrete and reinforcing steel, so that if the concrete structure is loaded it will not slip between concrete and reinforcing steel, with a condition the development length and bar's diameter are covered. The epoxy used in this research was Sikagrout 215 as a grouting to make a good bond. This paper conducted by software simulation approach, based on finite element method to compare the laboratory investigations as well as to provide a valuable supplement to the previous research. ABAQUS program was used to determine the behavior of the structure because it could represent and find out the response of reinforced concrete connections. This model was divided by 2 (two) steps. The first step was to find out the bond strength between reinforced concrete using epoxy, then compared with monolith reinforced concrete specimen without epoxy. The result of the first step was 5,2 MPa for monolith reinforced concrete specimen and 6,52 MPa for reinforced concrete using epoxy. The results indicated that the ratio between bond strength of reinforced concrete using epoxy was 0,94 compared with previous research, from the first step results was found the required development length was 200 mm. The second step was to investigate the stress failure from the models. The models were defined into 4 development length categories. The development lengths were used 120 mm (<40%ld), 160 mm (<20%ld), 200 mm (=ld), 260 mm (>30%ld) for monolith and sikagrout 215 reinforced concrete. There were two types failure of reinforced concrete, which were yielding and collapsed at reinforcing steel. The results revealed that the analysis of ABAQUS output were well matched with the previous research in the laboratory.

EV-O-03

Production of Woodceramics using Thai Waste Coconut Shell, and their Physical Properties

Don Kaewdook[a,*], Masahiro Ookawa[a], Kie Sato[b], Akito Takasaki[b] and Toshihiro Okabe[c]

[a]*Graduate School of Engineering and Science, Shibaura Institute of Technology, Tokyo, 135-8548, Japan*

[b]*Department of Engineering Science and Mechanics, Shibaura Institute of Technology, Tokyo, 135-8548, Japan*

[c]*Industrial Research Institute, Aomori Prefecture Industrial Technology Research Center, 030-0142, Japan*

*na12102@shibaura-it.ac.jp

Keywords: Woodceramics, Coconut Shell, Glassy carbon, Compressive strength.

New woodceramics (WCMs) were developed by carbonizing waste of coconut shell (charcoal powder) with phenolic resin under vacuum atmosphere for economy and waste control, which was driven by an increase of environmental concerns in Thailand. In this study, we have investigated the characteristics of new functional carbon materials consisted of waste coconut shell charcoal using technology for WCMs developed in Japan. The samples were made from coconut shell charcoal powder mixed with phenolic resin with various ratio (50:40, 60:40, 70:30 and 80:20). The powder mixtures were poured in a mold and hot pressed for 10 min. at a pressure of 10 MPa and a temperature of 453 K, and then carbonized at various carbonizing temperatures (673, 873, 1073 and 1273 K) to produce WCMs. The characteristics of the WCMs samples have been investigated by X-Ray diffraction (XRD) and scanning electron microscope with energy dispersive X-ray spectroscopy (SEM/EDX). Experimental results showed that the graphite (002) X-ray diffraction peak become stronger with increasing carbonizing temperature. With increasing carbonizing temperature, more volatiles of phenol resin changed to glassy carbon, then increasing mesopores and macropores in the WCMs. The volume density of WCMs decreased depending on amount of resin added and carbonizing temperature. The impact toughness and compressive strength were slightly increased with the increase carbonizing temperature. The physical and mechanical properties, such as electric conductivity, impact strength, bending strength and compressive strength were also investigated. Some industrial application will be discussed and proposed.

EV-O-04

Wastewater Treatment using TiO_2 Nanoparticles Loaded on Activated Carbon from Soybean Meal

Voranuch Thongpool[a,*], Naris Barnthip[a] and Danai Saetan[b]

[a] Division of Physics, Faculty of Science and Technology, Rajamangala University of Technology Thanyaburi, Pathum Thani 12110, Thailand

[b]Udomvittaya School, Thanyaburi, Pathum Thani 12110, Thailand

* nuchphysics@gmail.com

Keywords: Activated carbon, TiO2 nanoparticles, Soybean meal, Wastewater

In this study, activated carbon from soybean meal was prepared by physical activation. Prepared activated carbon was loaded with TiO2 nanoparticles by sol-gel method. The effect of ratio between activated carbon and TiO2 nanoparticles was investigated. The prepared TiO2 nanoparticles loaded on activated carbon (TAC) was applied to remove methylene blue (MB) from aqueous solution adsorption experiment. The results showed that, the MB could be removed from aqueous solution. MB removal efficiency increased with increasing the amount of TiO2. The reduction of chemical oxygen demand (COD) of wastewater from noodle processing plant in Pathumthani province was also studied. The maximum percentage reduction of COD was 41.62%.

EV-O-05

Effect of TiO_2 Thin Film on Ti Substrate Preparation Techniques on Methylene Blue and Wastewater Degradation via Photoelectrocatalytic Reaction

Chabaiporn Junin[a,*] and Chanchana Thanachayanont[a],
[a]National Metal and Materials Technology Center, 114 Thailand Science Park, Paholyothin Rd., Klong 1, Klong Luang, Pathum Thani, 12120, Thailand
*chabaij@mtec.or.th

Keywords: TiO_2 film, Titanium substrate, Photoelectrocatalysis, Wastewater treatment

Titanium dioxide, TiO_2, has been widely applied to energy (solar cells, fuel cells and batteries) and environmental (photocatalysis) applications due to its stability and biocompatibility. Phase, morphology and crystallite sizes have been identified as important parameters in controlling functional properties. For examples, anatase phase of TiO_2 has been shown to be more photocatalytically active than the thermodynamically stable rutile phase and preform better in Dye-Sensitized Solar Cells. Degussa P25 (75% anatase and 25% rutile) has been known to outperform both pure anatase and rutile phases. In this study, TiO_2 thin films on Ti substrates (TiO_2/Ti) were prepared by sol-gel method, using titanium (IV) isoproproxide (TTIP) with isopropanol as precursor. Effects of coating techniques, i.e. dip- and spray- coating, were investigated by x-ray diffractometer (XRD), atomic force microscopy (AFM) and scanning electron microscope (SEM) in order to study phase, morphology and crystal structure. Films prepared by both techniques went through the same heat treatment procedure. Photoelectrocatalytic activities of the TiO_2 films were tested with methylene blue and using UV-VIS spectrophotometer to observe degradation. It was found that the TiO_2 films prepared by dip coating technique resulted in mixed anatase:rutile phases. On the other hand, pure anatase phase was obtained for the TiO_2 films prepared by spray coating. The pure anatase TiO_2 films were found to have higher photoelectrocatalytic activity than the mixed-phase films. Then, TiO_2/Ti prepared by spray coating was chosen to treat real wastewaters, i.e.wastewater from public use (Kaotao reservoir), industrial wastewater (Doitung, Metrofiber company). The result showed that this film via photoelectrocatalytic activity can decrease chemical oxygen demand (COD) which represent organic degradation in wastewater. However, effect of apply voltage in photoelectrocatalytic reaction was still further investigated.

EV-O-06

Degradation Behavior of Low Density Polyethylene Bags for Solar Disinfection Application

Supachai Songngam, Tipawan Fhulua, Panida Muangkasem, Saisamorn Khunhom, Sittha Sukkasi and Supamas Danwittayakul*

National Metal and Materials Technology Center, 114 Thailand Science Park, Klong1, Klong Luang, Pathum Thani, 12120, Thailand

** supamasd@mtec.or.th*

Keywords: solar disinfection; SODIS; LDPE, degradation

Solar water disinfection (SODIS) is a simple procedure to disinfect drinking water. This technique is locally sustainable where there is abundant sunlight. In this research, SODIS reactor was designed as a set of two layers of low density polyethylene (LDPE) bags. The outer bag was directly exposed to the sunlight while the inner one was filled with the contaminated water. The black plastic board was inserted in between two bags in order to enhance the light absorbability. The SODIS was conducted for 8 hours per day and the fresh contaminated water was replenished every day. LDPE bags were collected after the SODIS process every week up to 12 weeks. The solar photo-degradation of LDPE bag was then analyzed using FTIR spectroscopy, UV/VIS spectrophotometer, differential scanning calorimeter (DSC) and tensile strength tester. It was found that LDPE could be gradually degraded under the sunlight that can be attributed to the photo-oxidation reaction leading to the reduction of both transparencies and tensile strengths. In addition, the leaching of organic compounds was examined using gas chromatography-mass spectrometer (GCMS). In this work, we will report the reliability of using LDPE bags for the SODIS process.

EV-O-07

Material Safety and Integrity of Water-Filled Polyethylene Bags in an Accelerated Weathering Investigation for Applications in Solar Water Disinfection (SODIS)

Weerawat Terdthaichairat[a], Ratchatee Techapiesancharoenkij[a,b], Apirat Laobuthee[a,b], Supamas Danwittayakul[c], Sittha Sukkasi[c,*]

[a]*Department of Materials Engineering, Faculty of Engineering, Kasetsart University, Chatuchak, Bangkok, 10900, Thailand*

[b]*Materials Innovation Center, Faculty of Engineering, Kasetsart University, Chatuchak, Bangkok, 10900, Thailand*

[c]*National Metal and Materials Technology Center (MTEC), Khlong Luang, Pathum Thani, 12120, Thailand*

*sitthas@mtec.or.th

Keywords: Point-of-Use Drinking-Water Treatment, Polymer Degradation and Leaching, PE, SODIS containers.

Solar Water Disinfection (SODIS) is a simple and low-cost point-of-use method for drinking-water treatment. The method simply involves filling water into a clear container, typically a PET bottle, and exposing it to direct sunlight for 6 hours (on a sunny day, or 2 days under cloudy skies). The UV radiation and heat in the sunlight can inactivate pathogens in the water, which are a major cause of diarrheal diseases that kill over 2.4 million people per year, most of whom are children under the age of 5. Despite their common use as SODIS containers, PET bottles have limitations in terms of shape and ratio of radiation-exposed area to water volume, which can negatively affect transportability and disinfection effectiveness, respectively. There have been some attempts to overcome those limitations with alternative materials and designs. One recent design uses food-safe, resealable PE bags and achieves a breakthrough in disinfection performance and improved portability, while maintaining the affordability of the SODIS method.

Few studies have elucidated the durability and safety of PE bags as SODIS containers for SODIS applications. The objective of this study is to investigate the potential of PE bags as SODIS containers, with respect to material safety, durability, and performance. The SODIS application of the PE bags was simulated in an accelerated weathering tester (QUV), using UV-A 340 lamps operated at 1.35 W/m^2 (ASTM G154) and controlled temperature of 70°C, for time periods calculated to be equivalent to 1-6 weeks in actual sunlight. The water samples from the exposed bags were analyzed by GC-MS to measure the amounts of leached plastic additives. The exposed bags themselves were characterized by three techniques: UV- Vis spectrometry for UV absorption, FT-IR for possible functional-group changes due to UV degradation, and tensile-strength measurement (ASTM D882) for mechanical integrity. The UV-Vis results showed that the UV transmittance, mostly in the UV-B region, of the bags decreased with increasing UV exposure. The FT-IR results showed a slight increase in C=O peaks (1715 cm^{-1}), particularly observable in the bags exposed for 3 weeks or longer. From the mechanical testing, an apparent decrease in the elongation at break from 818% (at the beginning) to 21% (after 6 weeks) corresponded to the long UV exposure. A significant degree of mechanical degradation was evident during 2 to 4 weeks of UV exposure. The results and analyses from this study can provide insights into the feasibility of PE as an alternative material for SODIS containers and potentially be useful for future designs of SODIS containers to improve the disinfection and durability performances.

EV-O-08

The Development of Nanofiltration Membrane from Silk Fibroin Protein

Manitta Aunsiripant, Bovornlak Oonkhanond* *Department of Chemical Engineering, Faculty of Engineering, Mahidol University, Nakornpathom, 73170, Thailand*
*E-mail address: bovornlak.oon@mahidol.ac.th

Keywords: Silk Fibroin Membrane, Permeability's Constant, Nanofiltration

The silk fibroin protein has been widely studies for various applications including medicine, tissue engineering, agricultural. Due to the excellent chemical and mechanical properties of silk proteins, silk fibroin can be processed in several forms for each application. However, the utilization of silk fibroin is still under investigation. Therefore, this research was conducted in order to develop the use of silk fibroin as a membrane for separation process. The separation performance of membranes is usually described in terms of flux and the permeability constant or permeance. However, the permeability of a membrane can be affected by various factors such as membrane thickness, salt concentration across the membrane, type of transport molecules. The experiments are carried out by evaluation of the permeability constant of ethanol, sodium chloride, potassium chloride and glucose across prepared silk fibroin membranes. First, silk fibroin membrane was prepared by eliminate sericin protein as degumming process. Usually, the degumming process could be prepared by two different methods. The first method is boiling in water under a sterilize condition by using an autoclave. Another, silk are boiled using sodium carbonate solution. After that, the fibroin core protein was dissolved in calcium chloride solution follows by using dialysis cellulose membrane for salt removal. The fibroin protein solution was then casted on a plastic plate to form silk fibroin membrane under the controlled environment such as temperature and moisture. Also, silk fibroin membranes were prepared with varying the ratio of salt addition in solution-casting process. The ratio of salt addition has a range from 0.01% to 1% (w/v) in order to investigate porous of membrane that gave effect to the diffusion properties. The results show that the preparing of silk fibroin by using sodium carbonate in degumming process gave the better physical properties to casting membranes than the other method. Moreover, the addition of salt show that the concentration of 0.3% leading to the highest diffusion coefficient. The silk fibroin membrane evaluations the permeability of ethanol, sodium chloride, potassium chloride were 10^{-8} m/s, otherwise glucose was 10^{-11} m/s. Due to the very small membrane area, the permeate flow was very low. Although, the diffusion of tested solutes are occurred on the membrane the diffusion rate of glucose solution is very low compared to that of ethanol and salts. Therefore, the developed silk fibroin membranes could be used as the nanofiltration membranes which beneficial to monovalent ion removal with low energy consumption.

EV-O-09

Effect of Lignin Acidolysis/Organosolv System on Lignin-based Polyurethane Foam Properties

Chularat Sakdaronnarong[a,*] and Navadol Laosiripojana[b]
[a]*Department of Chemical Engineering, Faculty of Engineering, Mahidol University, Putthamonthon, Nakorn Pathom 73170 Thailand*
[b]*The Joint Graduate School of Energy and Environment (JGSEE), King Mongkut's University of Technology Thonburi, Tungkru, Bangkok 10140 Thailand*
*chularat.sak@mahidol.ac.th

Keywords: Sugarcane bagasse, Simultaneous lignin fractionation and acidolysis, Liquefied lignin, Lignin-based polyurethane

Sugarcane bagasse was subjected to acidolysis reaction in the presence of various organic solvents in order to combine both lignin fractionation and lignin acidolysis processes. Lignin solubility that influenced the lignin-based polyurethane foam properties was presumed to increase after acidolysis process. In the present study, the reaction was performed at 140 C and 170 C for 2 h when sulfuric acid was used as catalyst. The organic solvents in the study included ethanolamine, ethylene glycol, amyl alcohol, ethanol, glycerol, butanol, dimethylformamide and bromobenzene. The results showed that the suitable solvent and temperature significantly enhanced the yield of lignin fractionation from sugarcane bagasse. Simultaneously, acidolysis reaction took place indicated by an increase of hydroxyl groups in lignin molecules. Lignin-based polyurethane foam that contained lignin from simultaneous fractionation and acidolysis reactions of sugarcane bagasse having better physical and mechanical properties compared with liquefied commercial lignin. This energy-efficient lignin fractionation is a powerful process to apply for cellulosic ethanol production in which polysaccharides are separated for ethanol production and lignin in black liquor is able to use for lignin-based polyurethane production.

EV-O-10

Pomelo (*Citrus maxima*) Peel-Inspired Property for Development of Eco- Friendly Loose-Fill Foam

Jarawee Looyrach[a], Pawadee Methacanon[b,*], Chaiwut Gamonpilas[b], Porntip Lekpittaya[c], Amornrat Lertworasirikul[c]

[a]*Interdisciplinary Graduate Program in Advanced and Sustainable Environmental Engineering, Faculty of Engineering, Kasetsart University, Bangkok, 10900 Thailand*

[b]*National Metal and Materials Technology Center, 114 Paholyothin Rd., Klong 1, Klong Luang, Pathumthani 12120 Thailand*

[c]*Department of Materials Engineering, Faculty of Engineering, Kasetsart University, Bangkok, 10900 Thailand*

*E-mail address: pawadeem@mtec.or.th

Traditionally, expanded polystyrene (EPS) is used for loose-fill packaging foam, which provides cushioning, protection, and stabilisation of articles packaged for shipping. The volume of this foam used in packaging is enormous. However, it has been widely criticised for several reasons in environmental issues such as solid waste disposal and harmful blowing agents. Currently, bio-based foams are utilised as alternative material and many efforts have been made to use agricultural commodities as raw materials for manufacturing loose-fill packaging foam. In nature, pomelo peel possesses excellent damping behaviour, preventing fruit pulp damage when dropping from trees. In this study, physical and mechanical properties of pomelo peels from three varieties, namely Kao-nampueng, Thong-dee, and Kao-pan, were extensively investigated for future development of eco-friendly packaging foam. Results showed that pomelo peel accounted for 44-51% of its fruit weight and contained high moisture content of 73-80% w/w. The peel thickness, consisting of albedo (white sponge) and flavedo (green peel), was approximately 20-35 mm. The albedo accounted for 90-95% of the total thickness. Thereby, it served functionally as an energy absorbing layer. Among the studied varieties, Thong-dee possessed the highest thickness, followed by Kao-numpueng and Kao-pan, respectively. Cell structure and pore size of the pomelo peel was also examined using environmental scanning electron microscope (ESEM). The images revealed an open cell foam structure with a gradient of pore size. Fine pores were observed near the outer surface. They became more open and large with increasing distance from the outer surface. The average pore size was measured as approximately 151 μm. For mechanical properties, cylinder-shape samples with diameter of 20 mm were uni-axially compressed at constant speed of 5 mm/min. Compressive stress-strain curves were plotted and the Young's modulus was approximated from the initial slope (up to 5% strain). It was found that linear elasticity was obeyed at low strain but the stress increased sharply with increasing stain. Unlike other foams, no plateau region was observed. The absence of this region implies that there was no cell collapse within foam structure. Young's moduli of samples with and without flavedo were calculated as around 185-340 kPa and 110-230 kPa, respectively, whose of samples with flavedo tended to be slightly higher. Moreover, the most important property of packaging foam is the ability to absorb energy. The onset strain of densification (OSD) defined as the strain at the maximum energy absorption efficiency was consequently determined according to method of Thielen *et al*. (2013). The OSD of samples with and without flavedo from three pomelo varieties was calculated as approximately 60-70%, which is in good agreement with the results conducted by Thielen *et al*. (2013). Finally, viscoelastic behaviour of pomelo peels was also investigated. Understanding about their structure- property relationship could be used as a concept for designing a high energy absorption material.

Keywords: pomelo peel, environmentally friendly foam, mechanical properties, microstructure

Reference: Thielen, M., Schmitt, C.N.Z., Eckert, S., Speck, T. & Seidel, R. (2013). *Bioinspiration & Biomimetics*, 8(2), 025001

EV-O-11

Organic Based Heat Stabilizers for PVC: A Safer and More Environmentally Friendly Alternative of Lead Compound

Aran Asawakosinchai[a], Chanchira Jubsilp[b] and Sarawut Rimdusit[a,*]
[a]Polymer Engineering Laboratory, Department of Chemical Engineering, Faculty of Engineering, Chulalongkorn University, Bangkok, 10330, THAILAND.
[b]Department of Chemical Engineering, Faculty of Engineering, Srinakharinwirot University, Bangkok, 10110, THAILAND.
*sarawut.r@chula.ac.th

Keywords: Poly(vinyl chloride), Heat stabilizer, Organic based heat stabilizer, Uracil derivatives

Organic based stabilizers have been considered as a new technology providing environmentally friendly heat stabilizer for PVC pipe production to substitute conventional lead stabilizer as well as calcium zinc stabilizer. In this research, PVC samples stabilized with 5 types of heat stabilizers i.e. 1) commercial lead stabilizer, 2) commercial calcium zinc stabilizer, 3) commercial organic based stabilizer (OBS), 4) 1,3-dimetyl-6-aminouracil (DAU) and 5) eugenol, were investigated. PVC dry-blend was prepared by mixing PVC resin with 3 phr of each heat stabilizer in a high speed mixer. The obtained PVC dry-blend was processed by two-roll mills with 0.125 mm gap at temperatures of 180ºC for 3 minutes to yield a homogeneous sample. The obtained sample was pressed into sheet by compression molder at 180ºC and pressure of 150 bars for 30 s. For reprocessing ability test, the samples were cut into small pieces and then reprocessed by two-roll mills and compressed again at the same condition. From dynamic mechanical analysis, storage modulus at room temperature of PVC stabilized with DAU was found to provide the highest value among those stabilizers. Glass transition temperature of the PVC stabilized with all types of heat stabilizers was determined to be approximately 99°C except the value of about 89ºC in eugenol stabilized PVC. Furthermore, PVC stabilized with commercial lead, calcium zinc stabilizer and commercial OBS could be reprocessed up to at least 5 cycles. Whereas, PVC stabilized with DAU was found to be able to withstand the processing cycle up to 4 cycles. Additionally, PVC stabilized with DAU showed the most outstanding short term thermal stability and can maintain its original color for at least up to 4 processing cycles. Finally, repeated processing of PVC stabilized with each type of heat stabilizers showed negligible effect on mechanical properties for at least up to 3 processing cycles. From the above results, it is evident that DAU showed high potential use as a safe and effective organic based heat stabilizer for PVC to substitute traditional lead or calcium zinc compounds.

EV-O-12

Method Validation for Determination of Heavy Metals in Plastics by ICP-OES with Reference to EN 13432:2000 Packing Standard

Panida Muangkasem*, Phitchaya Muensri and Aree Thanaboonsombut
National Metal and Materials Technology Center, 114 Thailand Science Park, Klong1, Klong Luang, Pathum Thani, 12120, Thailand
* panidm@mtec.or.th

Keywords: heavy metals, validation, plastic packaging, ICP-OES

The aim of this study is to validate the method of the heavy metal determination in plastic samples. Plastic samples must be digested prior to the analysis using inductively coupled plasma-optical emission spectrometry (ICP-OES) with reference to EN 13432 packaging standard. The concentrations of 10 elements, Zn, Cu, Ni, Cd, Pb, Hg, Cr, Mo, As and Se, were selected to be analyzed based on the standard. First, plastic samples were digested by a microwave digester with various digestion conditions until clear sample solutions were obtained. The sample solutions were then analyzed the amount of elemental concentrations by ICP-OES. Linearity, limit of detection, accuracy and repeatability, were taken into account to verify the method. The linearity of calibration curves were found to be acceptable with correlation coefficients higher than 0.999. Recovery test by spiking method at three concentration levels of such elements were found to be in the range of 80 to 120%.

EV-O-13

Efficient PEI-PAN Cellulose Membranes for Copper (II) Ions Determination

Phitchaya Muensri and Supamas Danwittayakul*
National Metal and Materials Technology Center, 114 Thailand Science Park, Paholyothin Rd., Klong 1, Klong Luang, Pathum Thani, 12120, Thailand.
* supamasd@mtec.or.th

Keywords: Copper (II), Polyacrylonitrile, Polyethylenimine, Determination

Abstract: Polyethylenimine (PEI)- Polyacrylonitrile (PAN) functionalized cellulose membranes were sequentially functionalized on cellulose membrane via electrostatic self-assembly interaction. PAN was firstly coated on cellulose membrane by filtration technique, followed by PEI surface functionalization. The functionalized membranes were then characterized by UV-VIS spectrophotometer, scanning electron microscope (SEM) and Fourier transform infrared spectroscope (FTIR). Cu(II) ions was detected by filtering 50 mL of Cu(II) aqueous solution through the cellulose membrane at pH 7. Optical spectra of the PEI-PAN and Cu(II)-PEI-PAN membranes were investigated by UV-Visible spectroscopy. The addition of Cu(II) ions resulting to the change in spectrum of Cu(II) detected membrane at 650 nm with respect to the formation of blue cuprammonium complex. Limit of detection of this method was found to be 0.27 mg/L. Repeatability of the method was determined by detecting Cu(II) ions in water at the concentration of 0.5 and 1 mg/L and the results were found to have a good precision with the recovery not over than 110%. The PAN-PEI functionalized cellulose membrane were selectively with copper(II) ions at pH 7 that can be detected by naked eye and has potential for detection in waste water samples.

EV-O-14

Current Status of Carbon Footprint for Organization in Thailand

Ruthairat Wisansuwannakorn, Athiwatr Jirajariyavech* and Jitti Mungkalasiri
National Metal and Materials Technology Center, 114 Thailand Science Park, Paholyothin Rd., Klong Nueng, Klong Luang, Pathum Thani 12120, Thailand
* athiwatj@mtec.or.th

Keywords: Carbon Footprint, Organization, CFO

At present, the carbon footprint of product (CFP) is well known in industrial sector in Thailand. However, the other carbon footprint assessment should be encouraged to evaluate greenhouse gases emitted from all activities done by organizations, called "Carbon Footprint for Organization or CFO". CFO is defined as the quantity of greenhouse gases emitted in tonnes of carbon dioxide equivalent from organizational activities such as fuel combustion, electricity use, waste management and transportation. The scope of emission sources can be classified into 3 categories: scope 1- direct emissions, scope 2 - energy indirect emissions and scope 3 - other indirect emissions. The first CFO project in Thailand (pilot project), was launched on 2011, has collaborated between the Thailand Greenhouse Gas Management Organization (Public Organization) (TGO), with the National Science and Technology Development Agency (NSTDA) and other ten pilot organizations from the government sector, the private sector, and academic institutions. The NSTDA is the pilot organization in the CFO project while National Metal and Materials Technology Center (MTEC) is a co-host of the project. Furthermore, on 2013, the second phase CFO project was implemented on the same collaboration (TGO & MTEC/NSTDA), however focusing on industrial organizations. The Thailand carbon footprint guideline and methodology, that were applied from international methodology (i.e. ISO 14064-1 (2006), ISO 14064-3 (2006), ISO 14065 (2006), WBCSD & WRI (2004), etc.), the Thai carbon footprint technical committees and the Thai verification system were the outcomes of the collaboration project. In addition, the twenty six industrial organizations were approved the CFO label by TGO, especially industrial organization on food & agriculture sector, materials sector and electronic sector, respectively.

EV-O-15

Carbon Footprint and Water Footprint of Refined Sugar in Thailand

Soottiwan Thamsakon[a], Prakaytham Suksatit[a] and Seksan Papong[a,*]
[a] Life Cycle Assessment Lab, National Metal and Materials Technology Center, Thailand Science Park, Pathum Thani, Thailand
** seksanp@mtec.or.th*

Keywords: Carbon Footprint, Water Footprint, Refined Sugar

Sugar is an importance agriculture product that is in the third of highest exported value of Thai agricultural products. Thailand is one of the largest sugar exporters in the world. Because the sugarcane areas have increased rapidly in Thailand, the contribution of greenhouse gas emissions from the sugarcane production especially the sugarcane harvest system is an issue of national concern. In addition, the expansion of sugarcane planting areas, it results in the increase of the competition of water use. This study aims to assess water footprint (WF) and carbon footprint (CF) of refined sugar in Thailand. The system boundary considered the sugarcane cultivation and harvesting, sugar milling, and related transport. The functional unit was 1 kg of refined sugar. The WF in cultivation stage was calculated by using CROPWAT model. The sugar milling and transportation stages were estimated based on the draft international standard on WF assessment (ISO 14046). The CF calculation was followed for the Thailand's carbon footprint assessment guideline. The results show that the total CF of refined sugar was 355 g CO_2eq./kg sugar, while the WF was 0.896 m^3, 0.016 m^3, and 0.343 m^3 for the green, blue, and gray components, respectively. This analysis found that at the sugarcane cultivation stage has accumulated 65% of the total CF and 71.4% of the green component of WF while it accumulated only 1.3% of total blue WF component and 27.3% of the gray WF component. This study also found that carbon and water footprints were significantly high in the farming stage. The CF was mainly from the use of chemical fertilizer and leaf burning in the fields. Therefore, the water management and fertilizer application management in cultivation stage will be reducing water and carbon footprint in agricultural stage.

EV-O-16

Water Footprint of Polylactic Acid Production from Cassava in Thailand

Ruethai Trungkavashirakun[a], Seksan Papong [a,*], Prakaytham Suksatit[a] and Soottiwan Thamsakon[a]

[a] Life Cycle Assessment Lab, National Metal and Materials Technology Center, Thailand Science Park, Pathum Thani, Thailand

** seksanp@mtec.or.th*

Keywords: Water Footprint, PLA, Cassava, Starch

Since Thailand has abundant biomass resources, there are great potentials to convert these resources to eco-friendly products such as bioplastics. Cassava is the important economy crop of Thailand. Initiated as the National Innovation Agency (NIA) bioplastic master plan, cassava was selected as a potential resource to produce the biopolymer especially polylactic acid (PLA) in Thailand for value added creation and alternative to conventional plastics. From these aspects should be to increase the production of biopolymer. When the needs of biomass increase, it results in the increase of the competition of water use. Cultivation of biomass sources to substitute fossil plastics has a large influence on the demand for more freshwater resources in the future. This study aims to assess water footprint of bioplastic production from cassava in Thailand, based on the water footprint (WF) concept methodology. The system boundary covered cultivation and harvesting, cassava starch production, glucose production, and biopolymer production. The functional unit was 1 tonne of PLA production. The WF in cultivation stage was calculated by using CROPWAT model. For industrial stages were estimated based on the draft international standard on WF assessment (ISO 14046). The result found that total WF of PLA resin was 2,922 m^3 per ton. It is consisted of green, blue and grey WF of 51%, 35% and 14%, respectively. Approximately 50% of the total WF of PLA is used to cultivate crops and is green WF. For industrial stages was consumed the direct blue WF around 25% whereas the indirect blue WF around 10%. However, this study focused only the volumetric WF indicator does not directly provide information on the actual water impact of bioplastic. Further works on impact assessment need be carried out to complete the water footprint assessment.

EV-O-17

Evaluating Greenhouse Gas Emissions of Ready-mixed Concrete for Construction Industry

Tassaneewan Chom-in[a], Seksan Papong[a,*], Soottiwan Thamsakon[a], Kittipoj Datchaneekul[a]

[a]Life Cycle Assessment Lab, National Metal and Materials Technology Center, Thailand Science Park, Pathumthani, 12120

** Corresponding author: seksanp@mtec.or.th*

Keywords: Ready-Mixed Concrete, Compressive Strength, Business-to-Business, Greenhouse Gas.

Ready-mix concrete (RMC) is a material formed by mixing cement, aggregate like sand, gravel and crushed stone, and water, with or without the incorporation of additives and recycled materials like fly ashes, slag, etc. RMC can be found at construction sites whole the country. An expansion of construction industry is exciting consumption of RMC since these structures require concrete that is of uniformly high quality. However, the concrete industry has also cause large burden on the environment due to the air emissions by the production of cement. This study aims to assess the greenhouse gas (GHG) emissions of RMC products with compressive strength of 240 kg/cm^2 (240 KSC) and 280 kg/cm^2 (280 KSC). The system boundary covered raw materials acquisition, RMC production, and transportation. The functional unit was 1 m^3 of RMC product. The GHG evaluation methodology was followed for the Thailand's carbon footprint assessment guideline. The result shown that total GHGs emissions of RMC model 240 KSC and 280 KSC were 260 and 272 kg CO_2eq per m^3, respectively. Approximately 90% of total GHG emissions are from the raw materials acquisition due to the production of cement while 9% come from transportation. The potential option in order to reduce GHG emissions and its associated cost–effectiveness is the reducing embodied emissions by increasing fly ash content in RMC. The results indicate that significant GHG emission reductions are possible, replacement of 30% cement with fly ash in RMC can be reduce 15% of total GHG emissions.

EV-O-18

Environmental Impact and Potential of Pollution Reduction Options for Foundry Industry: A Case Study of Faucet

Wanwisa Thanungkano[a], Ruthairat Wisansuwannakorn[a], Rungnapa Tongpool[a], Jitti Mungkalasiri[a,*]

[a]National Metal and Materials Technology Center, Klong Luang / Pathumthani, 12120, Thailand

*Corresponding author: jitti.mungkalasiri@nstda.or.th

Keywords: Environmental impact, Pollution reduction, Foundry industry

Over the last decades, industrial sectors confront with environmental issues and aiming to reduce the environmental impact of the industrial activities. The foundry industry remains one of the pollution generated sectors. Thus, the objective of this work is to study the environmental impacts and options to reduce emissions due to the faucet production, using life cycle assessment (LCA) methodology. The primary data from a manufacture was collected as the foreground data of this study, covered five unit processes: foundry, turning, polishing, plating and assembly. The impact assessment method via ReCiPe Midpoint (H) was used to evaluate the impact categories of climate change, metal depletion and human toxicity. The result shows that all impact categories are dominated by foundry unit process. Therefore, the sub-unit processes of foundry were classified and examined to find out the hot spot of the production. It was found that the two sub-unit processes, melting and die casting, contribute more than 80% of environmental impact of the foundry unit process, in all impact categories. In the case study, the various alternative methods for reducing environmental impacts were considered, such as alternative input materials, production process modifications and new process technologies. The reduction of the amount of scrap rate, the production process modification, was proposed to improve the environmental impacts of this case. Not only the internal recycled materials but also the amount of direct pollutants released by the plant process was reduced.

Materials Technology for Environment Session

POSTER PRESENTATIONS

EV-P-01

Arsenic(III) and Chromiumr(VI) Removal from Water by Zirconium Oxide Ethylenediamine Adipate Hybrid Material and its Mathematical Modeling

S. Mandal[a*], S.S Mahapatra[b] and R. K. Patel[a]
[a] *Department of Chemistry, National Institute of Technology, Rourkela, Odisha, 769008, India*
[b] *Department of Mechanical Engineering, National Institute of Technology, Rourkela, 769008, Odisha, India*
*sandipmandal9@gmail.com

Keywords: Zirconium, Arsenic, TEM, hybrid material

The present research work emphases on the predictive method for the removal of As(III) and Cr(VI) from water using a ZEDA hybrid material. The material was synthesized by sol-gel method and characterized by HR-TEM, SAD, EDS, Fe-SEM, XRD, BET, TGA-DSC and HG-AAS. Batch and column adsorption experiments were conducted as function of different variable parameters like adsorbent dose, solution pH, contact time, temperature, competitive ions, bed height and flow rate. The maximum removal percentage at an optimal condition of pH 6.5 and dose =1.2 mg/L for As(III) and optimal condition of pH 5.5 and dose =1.4 mg/L for Cr (VI) has been observed to be 97% and 91%, respectively with contact time of 40 minutes, temperature 60 ºC and initial concentration of 5 mg/L. The adsorption data are best fitted with the pseudo-second-order kinetic model and Langmuir isotherm model with correlation value (R^2) > 0.98. The removal phenomenon being a non linear complex chemical process, for the purpose a predictive model was used to predict removal percentage without resorting to costly experimental efforts. The data series of batch and column adsorption experiments are used for prediction purpose using Adaptive Neuro-Fuzzy Inference System (ANFIS). The accuracy of the model is checked by correlation coefficient (R^2), absolute relative percentage error (AARE), mean squared error (MSE). Comparison of experimental and prediction results shows that the model can predict satisfactorily the removal efficiency (R^2> 0.94) with reasonable accuracy at training and testing of batch and column studies.

EV-P-02

Photocatalytic Degradation of Phenol by Impure $BiFeO_3$ under Visible Light Irradiation

Katnanipa Wanchai
Department of Chemistry, Faculty of Science and Technology, Phranakhon Si Ayutthaya Rajabhat University, Phranakhon Si Ayutthaya, 13000, Thailand
katnanipa@gmail.com

Keywords: Photocatalytic, Impure $BiFeO_3$, degradation, phenol, visible light

Impure $BiFeO_3$ as a visible light photocatalyst for phenol degradation was synthesized via solid state method by using Bi_2O_3 and Fe_2O_3 as a starting material and calcined at 600 to 900ºC for 5 h. The products were characterized by XRD SEM/EDS and BET. The majority phase of all samples was rhombohedrally distorted perovskite-type $BiFeO_3$ with impurity phase ($B_2Fe_4O_9$, $Bi_{25}FeO_{40}$ and Bi_2O_3) except calcined at 600ºC. Photocatalytic activity of phenol (5 mg/L) was studied in the impure $BiFeO_3$ illuminated with 200 w fluorescence lamps. The efficiency of photodegradation process has been observed to be strongly depended on catalyst amount and initial pH value of phenol solution. The experimental results indicated that the catalyst was calcined at 800ºC shows the highest activity, the optimal catalyst loading of 0.5 g/L and pH value were obtained to be a neutral pH range.

EV-P-03

Study of Photodegradable Recycle Polyethylene by an Addition of Poly(Ethylene Oxide) Microcapsule Containing TiO_2

Napatchon Intarakumnerd[a,*] **and Tawat Soitong**[a]
Program of Material Science, Faculty of Science, Maejo University, Chiang Mai, Thailand
*napatchon19@gmail.com

Keywords: Recycle polyethylene, Titanium dioxide, Photo degradable, Poly(ethylene oxide)

In this study of photo-degradable recycle polyethylene (rPE) an addition of poly(ethylene oxide)(PEO) microcapsule containing TiO2 to rPE was performed. Composite of rPE/TiO2 and rPE/PEO/TiO_2 were prepared with 1.0 and 2.0 wt% of TiO2 and 1-10 of PEO. The mixture of components was performed using a two roll mills and forming a thin film using a compression molding. Adsorbed H2O in the PEO phase and the TiO2 photocatalytically reacted, and a hydroxyl radical, which initiated the PEO degradation, was produced. The degraded PEO produced an acid and an aldehyde, which were able to facilitate PE degradation. The addition of the PEO/TiO2 microcapsule brought about the facilitative effect of the PE degradation. The photocatalytic degradation behavior of rPE/PEO/TiO_2 nano-composite film under UV light irradiation was investigated and compared with those of the rPE/TiO_2 film and the rPE/PEO, with the aid of Fourier Transform Infrared (FT-IR), UV-Vis spectroscopy, scanning electron microscopy (SEM), weight loss monitoring, and X-ray diffraction spectra (XRD).

EV-P-04

Sol-gel Synthesis and Characterization of Barium Orthotitanate Powders

Supattra Wongsaenmai[a,*]

[a]*Program in Materials Science, Faculty of Science, Maejo University, Sansai, Chiang Mai, 50290, Thailand*

*wongsaenmai@yahoo.com

Keywords: Carbon Absorption; Barium Orthotitanate; Sol-Gel

Environmental issues due to emissions of pollutants from combustion of fossil fuels have become global problems, including air toxics and greenhouse gases. The use of fossil fuels for energy contributes to a number of environmental problems globally. The increase in atmospheric CO_2 is attributable to burning fossil fuels. Various separation technologies were considered for the purpose of CO_2 recovery from flue gases. Among them, for practical application, chemical absorption using amine solutions, for which some pilot plants, have been started. However, these method although the reaction is possible at room temperature, the absorbed CO_2 is hard to isolate with low energy consumption. Barium orthotitanate (Ba_2TiO_4) was considered as a CO_2 absorbent because its relatively high temperature of 600°C. In this work, a simple aqueous sol-gel route has been refined to prepare barium orthotitanate (Ba_2TiO_4) powders. The precursor gel was intermediate calcined at 600 ºC, and the final synthesis products were characterized by x-ray diffraction technique (XRD) and scanning electron microscopy (SEM). It has been found that the single phase monoclinic structure was obtained at temperature of 1000ºC. The efficiency of carbon dioxide absorption of barium orthotitanate was measurement.

EV-P-05

High Density Polyethylene Catalyst Waste as a Filler in Papermaking

Wantanee Buggakupta[1,3*], Somporn Chaiarrekij[2], Kuntinee Suvannakich[2], Auchuta Niravittanon[2] and Thawanrat Apisampinvong[2]
[1]Department of Materials Science, Faculty of Science, Chulalongkorn University, Bangkok, 10330, Thailand
[2]Department of Image and Printing Technology, Faculty of Science, Chulalongkorn University, Bangkok, 10330, Thailand
[3]Center of Excellence on Petrochemical and Materials Technology, Chulalongkorn University, Bangkok, 10330, Thailand
*wantanee.b@chula.ac.th

Keyword: high density polyethylene, catalyst waste, filler, paper

The study observes the use of a waste derived from high density polyethylene (HDPE) catalyst production as fillers in papermaking. The replacement of the industrial waste to two common fillers; calcium carbonate and clay, are of interest. The waste is in the form of white slurry containing very fine particulates, the composition of which is a compound of titanium dioxide, calcium oxide and alumina, along with a small amount of chlorides. As-received HDPE waste of 0-30 wt% was added into a mixture of pulp stock to make handsheets. Cationic polyacrylamide was employed as a retention aid. The obtained handsheet samples were then dried and their properties were characterized and also compared with the handsheets holding carbonate and clay. Such properties included both physical and mechanical one, i.e. grammage, porosity, whiteness, opacity, smoothness, tear strength and tensile index. The experimental results showed that the as-received industrial waste gave comparable outcomes to carbonate and clay. The improvement of the handsheet properties with the HDPE catalyst waste were reported and discussed.

EV-P-06

Use of Chitosan as a Dye Adsorption in Dyeing Bagasse Fiber Process

Sudarat Phungphai[a,*], Nantana Jiratumnukul[a]

[a,*]*Faculty of Science, Chulalongkorn University, Patumwan , Bangkok, 10330,Thailand*

[a]*Faculty of Science, Chulalongkorn University, Patumwan , Bangkok, 10330,Thailand*

*E-mail address slam_somjai@hotmail.com

[a]E-mail address nantanaj@gmail.com

Keywords: chitosan, bagasse fiber, dye adsorption, paper sheet

In recent years, the development of biodegradable materials from renewable natural resources has received increasing attention. In Thailand, bagasse fiber is an extremely abundance waste product from sugar production. Bagasse fiber has increased interest due to environmentally friendly and high fiber content. However, bagasse fiber is colorless and difficult for dyeing process. Chitosan which derived from chitin is a biopolymer that performed higher adsorption capacity of dye. In this work, chitosan was used to improve dye adsorption and color strength on bagasse fiber. Bagasse pulp dispersion that consist of bagasse fiber in water were mixing with chitosan and dye. Bagasse dispersion were obtained. The paper sheet from bagasse dispersion were process in according with TAPPI T 250 standard. Physical and mechanical properties of the paper sheet with and without chitosan were investigated. From the hereby study, the result showed that chitosan increase dye adsorption of bagasse fiber.

EV-P-07

Gas-sensing Properties of Pt-V_2O_5 Thin Films for Ethanol Detection

Viruntachar Kruefu[a,*], Pusit Pookmanee[b], Anurat Wisitsoraat[c] and Sukon Phanichphant[d]
[a]*Program in Materials Science, Faculty of Science, Maejo University, Chiang Mai 50290, Thailand*
[b]*Program in Chemistry, Faculty of Science, Maejo University, Chiang Mai 50290, Thailand*
[c]*National Electronics and Computer Technology Center, Pathum Thani 12120, Thailand*
[d]*Nanoscience Research Laboratory, Department of Chemistry, Faculty of Science, Chiang Mai University, Chiang Mai 50200, Thailand*
[*]v_viruntachar@hotmail.com,

Keywords: Vanadium pentoxide, Platinum, Ethanol, Gas sensor

Vanadium pentoxide (V_2O_5) nanoparticles have been investigated for monitoring ethanol (C_2H_5OH) at ppm levels in air. A one-step flame spray pyrolysis (FSP) process has been applied for the synthesis of vanadium pentoxide (V_2O_5) and platinum-loaded vanadium pentoxide (Pt-V_2O_5) nanoparticles. The samples have been studied to characterize their morphological and microstructural properties by X-ray diffraction and transmission electron microscopy investigations. Pt addition to V_2O_5 samples were verified by energy dispersive X-ray spectrometry mode. The specific surface area of the nanoparticles was measured by nitrogen adsorption. The application of the produced nanoparticles in sensitive and selective ethanol resistive sensor has been demonstrated. Pt-V_2O_5 has shown higher response toward ethanol at ppm concentrations compared to unloaded samples.

EV-P-08

Characterization of Hen and Duck Eggshells for Waste Utilization

Pennapa Muthitamongkol[a*], Utaiwan Watcharosin[a], Kriangkai Supanpong[a], Sarmart Nutsai[a] and Nuttawan Pramanpol[b]

[a]National Metal and Materials Technology Center, Patum Thani, 12120, Thailand

[b]Synchrotron Light Research Institute (Public Organization), Nakhon Ratchasima, 30000, Thailand

*pennapm@mtec.or.th

Keywords: eggshell, characterization, waste utilization.

Over 11,100 million eggs has been consumed in the recent year in Thailand, resulting in large amounts of eggshell wastes which could contribute to environmental burdens. Although, waste eggshells have been used in many aspects to add their value, the characterization of hen and duck eggshells have not been yet reported, comparatively. Thus, this work aims to examine the comparative studies of hen and duck eggshells using different techniques. Waste hen and duck eggshells collected from a canteen were washed using tap water, air-dried and ground, prior to the following investigations. The chemical compositions of the hen and duck eggshells has been observed using X-ray fluorescence. X-ray diffraction of eggshell powders shows they both consist of calcium carbonate and the thermogravimetric analysis of eggshells also confirms their major constitution of calcium carbonate. However, the hen eggshell has greater specific surface area than the duck eggshell. These preliminary studies of different eggshells have demonstrated that the hen and duck eggshells have similar and different characteristics. Further investigation of the eggshells are underway for practical implication of waste utilization.

EV-P-09

Antibacterial Activity of *P. aeroginosa* Bacteria by Ni-doping Titaniumdioxide Thin Film on Glass Fiber Roving

Kornkanok Uboncholakat[a,*], Lek Sikong[b] and Prachit Khongratana[c]
[a]*Department of Physics, Faculty of Science, Thaksin University (TSU), Pattalung, Thailand.*
[b]*Department of Mining and Materials Engineering, Faculty of Engineering, Prince of Songkla University (PSU), Songkhla, Thailand.*
[c]*Department of Physics, Faculty of Science, Thaksin University (TSU), Songkhla, Thailand.*

[*]Corresponding Author: kornkanok.ubon@yahoo.co.th

Keywords: Ni-doped TiO_2, Antibacterial, Photocatalytic, Air purification

The Ni doped TiO_2 films were prepared by sol-gel method and coated on glass fiber roving for air purification. TiO_2 composite films were characterized by x-ray diffraction (XRD), scanning electron microscopy (SEM), energy dispersive x-ray spectroscopy (EDS), transmission electron microscopy (TEM), atomic force microscopy (AFM) and scanning electron microscopy (DRS). Disinfection efficiency against *P. aeruginosa* was investigated. From experimental study, it was found that nickel oxide was formed in Ni doped TiO_2 and Ni making porous structure on TiO_2 thin films. The disinfection efficiency against *P. aeruginosa* of the TiO_2 films it was found that Ni-doped TiO_2 higher than TiO_2 un-doping irradiation under UV and fluorescence light. Especially, TiO_2-1Ni was highest antibacterial efficiency irradiation under fluorescence light.

EV-P-10

Development of a GCMS Procedure for Determination of Organic Substances Migrating from Low Density Polyethylene Bags into Drinking Water

Tipawan Fhulua, Supachai Songngam, Panida Muangkasem, Saisamorn Khunhom, Sittha Sukkasi and Supamas Danwittayakul*

National Metal and Materials Technology Center, 114 Thailand Science Park, Klong1, Klong Luang, Pathum Thani, 12120, Thailand

* supamasd@mtec.or.th

Keywords: liquid-liquid extraction, leaching, organic substances

The purposes of this study were to investigate the method of liquid-liquid extraction and identify of chemicals leaching from low density polyethylene (LDPE) bag into water during the solar disinfection. Leaching of organic substances occurred from deterioration time of LDPE bags under the sunlight and the organic compounds migrated to water. Using 2-napthal was surrogate internal standards, in order to confirm method of extraction in the laboratory study. The extraction protocol was firstly extracted the organic compounds from water into chloroform for several cycles, followed by evaporated by gently flow of an ultra-high purity nitrogen gas. Identification of chemical extraction was performed on the by GC coupled with a mass spectrometry detector (GC-MS). The recovery percentage of the surrogate increased from 45 to 106% with an increase of extraction cycles from 2 to 7 cycles, respectively. The linearity, repeatability and method of detection limit (MDL) will be reported.

EV-P-11

Synthesis of Polyaniline – Chitosan Membrane from Paddy Field Crab-Shell Chitosan and its Adsorption Efficiency for Chromium(VI), Lead(II), and Manganese(II)

Ratana Sananmuang [a,b,*] **and Jirawat Boonpoung** [a]
[a]*Department of Chemistry, Faculty of Science, Naresuan University, Phitsanulok, 65000, Thailand*
[b]*Center of Excellence for Petroleum, Petrochemical and Advanced Materials, Naresuan University, Phitsanulok, 65000, Thailand*
* ratanas@nu.ac.th

Keywords: Polyaniline–Chitosan membrane, heavy metals, adsorption

The aims of this investigation were to synthesize Polyaniline – Chitosan membrane and to study the adsorption efficiency of membrane for heavy metals including Cr(VI), Pb(II), and Mn(II) using Batch technique. The SEM, FTIR, and FAAS were used for characterization and analysis. The results revealed that the tensile strength and elongation of this membrane were 0.0319 kN/mm^2 and 15.52 %, respectively. The optimum pH for adsorption of Cr(VI), Pb(II), and Mn(II) were 2, 3.5, and 3,respectively. For adsorption isotherm study, it was found that the adsorption model for Cr(VI) and Mn(II) was fit to Langmuir model, while those of Pb(II) was Freundlich model. These findings could be applied for heavy metal removal in some solutions.

EV-P-12

The Effect of Composition and Particle Size of Rice Husk Ash and Sludge from Textile Wastewater Treatment on the Portland Cement-base Solidification

Piya Gosalvitr[a], Penjit Srinophakun[a], Premrudee Kanchanapiya[b]* and Supamas Danwittayakul[b]
[a]Faculty of Engineering, Kasetsart University, Ngam Wong Wan Rd, Ladyaow, Chatuchak,Bangkok, 10900, Thailand.
[b]National Metal and Materials Technology Center, Paholyothin Rd., Klong 1, Klong Luang, Pathum Thani, 12120, Thailand.
* premrudk@mtec.or.th

Keywords : Solidification , Textile wastewater , Rice husk ash, Textile sludge

Waste from textile wastewater treatment consist of heavy metals that toxic to the environment. Solidification is an alternative method to manage these pollutants. The objective of this research is to study the properties of solidification using ordinary Portland cement (OPC) type I mixed with rice husk ash (RHA) and textile sludge obtained from wastewater treatment unit of local textile entrepreneur in central and northeast parts of Thailand. The effects of composition ratio and particle size of RHA in solidification on physical and chemical properties of mortar were investigated. The experiments were conducted by replacing cement in mortar by RHA at 10, 20 and 30 % by weight and textile sludge at 5% by weight. Three sets of particle size distribution of RHA were varied. The ratio of fine sand to binder in mortar was controlled at 1:2.75 while the ratio of water to binder was varied based on the water requirements conforming to flow value at 110 ± 5%. The samples were cured up to 60 days before being tested. The properties of mortar such as compressive strength, setting time, leachability were investigated.

EV-P-13

Treatment of Textile Dyeing Wastewater by Electrocoagulation

Phutthamon Chantes[a], Chalor Jarusutthirak[b], Premrudee Kanchanapiya[c] and Supamas Danwittayakul[c]*

[a]*Faculty of Engineering, Kasetsart University, Ngam Wong Wan Rd, Ladyaow, Chatuchak, Bangkok, 10900, Thailand.*

[b]*Faculty of Environment, Kasetsart University, Ngam Wong Wan Rd, Ladyaow, Chatuchak, Bangkok, 10900, Thailand.*

[c]*National Metal and Materials Technology Center, Paholyothin Rd., Klong 1, Klong Luang, Pathum Thani, 12120, Thailand.*

* supamasd@mtec.or.th

Keyword: Electrocoagulation, Textile wastewater, Treatment

Industrial wastewater discharged into the environment has been a serious and crucial problem, especially the wastewater from textile industry. It is one of the most harmful wastewaters due to their dark color, high COD and biotoxicity. Technologies for wastewater treatment have become essential to reduce such pollutants over the last couple decades. Electrocoagulation is a technically easy, convenient and quick process that use an electric field to neutralize the surface charges of contaminants in wastewater leading to coagulation and sedimentation. In this work, we will report the effects of parameters such as electrode materials, current density, inter electrode distance and electrocoagulation time, etc., on the removal of reactive dyes from Batik dyeing wastewater. In addition, electrical energy consumption, electrode consumption and operating cost at optimum condition will be discussed.

EV-P-14

Natural Kaolin-Carbon Nanocomposite for Roof Insulation Material

Apiluck Eiad-ua[1]*, Nipawan Chaleiwchalard[2] and Nawin Viriya-empikul[3]

[1]College of Nanotechnology, King Mongkut's Institute of Technology Ladkrabang, Ladkrabang, Bangkok 10520, Thailand

[2]Civil Engineering, Faculty of Engineering, Kasetsart University Kamphaeng Saen Campus, Nakhon Pathom 73140, Thailand

[3]Nanotechnology Center, National Science Technology Development Agency, Klongluang, Pathumni 12120, Thailand

* keapiluc@kmitl.ac.th

Keywords: Kaolin, Carbon, Nanocomposite, Roof Insulation

Roof insulation material was successfully fabricated from natural kaolin-carbon nanocomposite. In this study, kaolin obtained from natural resource and carbon obtained from typha angustifolia flower via hydrothermal method. Effect of composite ratio between kaolin and carbon were discussed. The current research studies a new advanced material with super properties based on the powder of kaolin-carbon nanocomposite. This new material can produce sustainable and low cost and addition to enivironmentally green performance. The efficiency of this nanocomposite material is very high for Insulation, fracture resistance, thermal stability, impermeability for gas and water, hardness, etc. This research introduces it as a new nanocomposite material for roof insulation.

EV-P-15

Efficient Colorimetric Method for Nickel (II) Ions Determination using Dimethylglyoxime

Phakjira Khamlajan[a], Jenjira Thongrung[a], Amornrat Wongklom[a] and Supamas Danwittayakul[b]*

[a]Science Faculty, Ubon Ratchathani Rajabhat University, Nai-Muang, Muang, Ubon Ratchathani, 34000, Thailand.

[b]National Metal and Materials Technology Center, 114 Thailand Science Park, Paholyothin Rd., Klong 1, Klong Luang, Pathum Thani, 12120, Thailand.

*supamasd@mtec.or.th

Keywords: Ni(II), Dimethylglyoxime, Determination, colorimetric method

The instrumentalless technique to determine Ni(II) ions in wastewaters was developed using dimethylglyoxime (DMG). When trace amounts of Ni(II) ions was added to the colorless DMG aqueous solution, Ni(II) could react with DMG to form solid particles of reddish-pink complex (Ni(II)-DMG). By filtration technique, the Ni(II)-DMG particles could be extracted on the filter paper. Intensity of reddish-pink color depends on Ni(II) concentrations in the water. By this technique, Ni(II) ions in test water can be determined by comparing to the color chart of known concentrations of Ni(II) ions after detection process. In this work, we will report the effects of pH of the test solution on size and shape of the Ni(II)-DMG complex particles. Linearity, repeatability, limit of detection of the test method will be reported.

EV-P-16

Eco-Friendly Dyeing Textiles with Neem Herb for Multifunctional Fabrics. Part 1: Extraction Standardization

Heba Mansour*, Hanan Bukhari and Khadijah Qashgari
Fashion Design Depart.,Faculty of Art and Design, King Abdul-Aziz University, Jeddah, KSA
* hfmansour@kau.edu.sa

Keywords: Environmental technology, Neem extraction, solvents, natural dyes.

Owing to the growing concerns about the eco-system and the increasing awareness of toxicity and health hazards problems of synthetic dyes, an interest in returning back to natural dyes has increased. Therefore, their extraction process and optimizing its variables, have technical and commercial importance on cost and color yield for dyeing cost. The first current part of this study deals on identifying the most appropriate leaching solvent for neem pigments to produce an optimum concentrated extract with high extraction capacity, avoiding any loss in the color quality and time consuming. This has been carried out using distilled water and different concentrations of water-acetone and water ethanol mixtures at different temperatures, pH values and time intervals. Data observed that the optimum extraction condition was achieved with 50% (v/v) acetone, 18% (w/v) neem amount at pH 9 at 70oC for 60 min where 50% (v/v) water- acetone exhibited 60 % absorbance percentage compared to (31 and 9) % of 40% (v/v) water-ethanol and water respectively. The absorbance values are influenced by the properties of solvents such as, the dipole moment, dielectric constant, and refractive index values. Alkaline extraction at pH 9 for 60 min at 70oC gave the highest diffusion coefficients of color component. FTIR analysis investigated the presence of quercetin (flavonoid) compounds in neem extract which have antibacterial and antifungal properties giving chance to be applied for antimicrobial textile dyeing in the second part of this study.

EV-P-17

Adsorptive Removal of Methylene Blue from Aqueous Solution by Bamboo and Macadamia Nut Shells Charcoals Activated with Different Chemicals

Chabaiporn Jun-in[a], Samerkhae Jongthammanurak[a,*] and Anna Simsen[b]
[a]*National Metal and Materials Technology Center, 114 Thailand Science Park, Phahonyothin Rd., Klong 1, Klong Luang, Pathum Thani, 12120, Thailand*
[b]*Faculty of Science, Khon Kaen University, Khon Kaen, 40002, Thailand*
*samerkhj@mtec.or.th

Keywords: Biochar, Chemical activation, Adsorbent characterization

Activated carbon with high specific surface area is an effective adsorbent of dye from aqueous solution. The production of activated carbon was feasible using chemical or thermo-chemical activation processes on biomass-based charcoals. In this study, bamboo-derived and macadamia nut shell-derived charcoals were used as starting materials for the chemical activation at room temperature using potassium dioxide (KOH), potassium permanganate ($KMnO_4$), and nitric acid (HNO_3) solutions, and for the thermo-chemical process using KOH solution. The characteristics of the adsorbents were characterized by X-Ray Diffractions (XRD), Scanning Electron Microscopy (SEM), Fourier-transform infrared spectroscopy (FTIR). The adsorbents were assessed for their ability to adsorb methylene blue from aqueous solution. Langmuir, Freundlich, Redlich-Peterson model isotherms were applied for the analysis of the adsorption data.

Material Reliability Session

ORAL PRESENTATIONS

MR-O-01

Remaining Creep Life Assessment of Service Superheat Tube Boiler

P. Thasanaraphan [a,*], P. Thapnuy[a], D. Ounpanich[a] and P. Vongbandit[a]
[a] *Thailand Institute of Scientific and Technological Research, Pathumthani, 12120, Thailand*
*pornsak@tistr.or.th

Keywords: Remaining life assessment; creep; damage mechanism; primary superheat tube.

The demand of remaining life assessment of the boilers arises from technical, economic, and legal reasons. Creep is major damage mechanism of primary superheat tube boiler during prolong operation at high temperature and pressure in a water tube boiler. This paper presents the calculation method for the remaining life assessment due to creep damage. The service-exposed primary superheat tube made of 2.25Cr-1Mo steels. During scheduled inspection, wall thickness measurement, metallographic investigation by replica technique, design data and operating condition were used to estimate the remaining life in the form of creep damage accumulation rate calculated from life fraction using Larson-Miller Parameter. The results indicate that the primary superheat tubes satisfy in extension service life. By attaining an accurate and timely discussion of the results, the engineer can manage the maintenance and inspection schedule for the critical part in the boiler.

MR-O-02

Study of the Hydrolytic Resistance of Glass Bottles under a High Fluctuated Weather Condition

Usuma Naknikham*, Suwannee Thepbutdee, Tepiwan Jitwatcharakomol, Kanit Tapasa
Department of Science Service, Ratchathewi, Bangkok 10400, Thailand
* usuma@dss.go.th

Keywords: Leaching, Glass container, Weathering, Corrosion

The occurrence of corrosion on glass surfaces results from the reaction between sodium in glass surfaces and water in the atmosphere under a certain condition. This reaction is promoted at high difference of humidity and temperature between a daytime and a nighttime especially in a rainy season. Glass surface treatments, for example by solutions, can improve the hydrolytic resistance. In the previous study, it was found that using 5wt% of alum gave the best effect to increase this property. The aim of this study was to examine the effect of closed and unclosed glass bottles during storage in a warehouse to the hydrolytic resistance. After treatment by 5wt% of alum, the amount of Na leached from the inner surfaces of glass bottles under simulated condition was determined. The weathering chamber was used to simulate the condition of a rainy season in Thailand with conditions set up and run in cycle. At first, the condition under the relative humidity (RH) value of 60 at 32°C was run for 12 hours, and then followed by RH of 80 at 25°C for 12 hours. The cycle was continued in the period of 8, 14, 21, 28, 53 days. After that the quantity of leached Na which is the conversion of hydrolytic property was analyzed by Flame-Atomic Absorption Spectrometry (FAAS). The results showed that the amount of Na leached from the untreated bottles was higher than the treated bottles around 5 times. It was also found that the quantity of leached Na from the untreated and closed bottles was raised with increasing time after 30 days while the untreated and opened bottles gave a rather constant result.

MR-O-03

Investigation of Fracture Location in Weldments of T22/T91 Dissimilar Welds

Salita Petchsang[a,*], Isaratat Phung-on[b]
[a]*Industrial and Manufacturing Systems Engineering Program, Faculty of Engineering, King Mongkut's University of Technology Thonburi, Bangkok, 10140, Thailand*
[b]*Maintenance Technology Center, ISTRS, King Mongkut's University of Technology Thonburi, Bangkok, 10140, Thailand*
*E-mail: Salita_Raul@hotmail.com

Keywords: Cr-Mo Steel, Failure Mode, Fracture Location, Creep-Rupture Test

Carbon migration problem can be observed in dissimilar welding of Cr-Mo steels across the weld interface during postweld heat treatment (PWHT) due to the activity gradient. This causes the formation of soft zone and hard zone in the lower-Cr side and higher-Cr side at the weld interface, respectively. The metallurgical discontinuity of these regions could lead to premature failure during service exposure. Failure mode occurred could be due to stress rupture (overload) or creep rupture. The objective of this study is to investigate the effect of failure mode on the location of fracture of weldments using various filler metals in T22/T91 dissimilar joining by GTAW process. In this work, four configurations of welding procedures are performed: the first form employs only ER90S-B3, the second utilizes only ER90S-B9, the third applies ER308L as butter layer and followed by ER90S-B9, and the last used ERNiCr-3 as butter layer and followed by ER90S-B9. Postweld heat treatment is carried out at 760°C for 30 minutes. The experiments are divided into two sections; hot tensile test and creep-rupture test. Hot tensile test (or stress-rupture test) is performed in order to determine the fracture location as the tested sample gets overload at high temperature. Moreover, the other data obtained from this tested is the elevated temperature tensile yield strength of each tested sample. For creep-rupture testing, the test is conducted with constant load (90% Yield Strength as residual stress) in order to find out the fracture location of each weldment. Both tests are performed at 550, 650, and 750°C using High-Temperature Tensile Machine (HTTM). Specimen microstructures and fracture surface are characterized by the Optical Microscope (OM) and Scanning Electron Microscope (SEM). The Energy Dispersive Spectroscopy (EDS) are used to acquire chemical analysis of the weldments. The results could show the understanding of the failure mode and the location of failure as the major concern for a life assessment of the weld joints.

MR-O-04

Failure Analysis of a Ductile Iron Roll of Intermediate Rolling Mill Stand

Saneh Boonrampai [a], Samroeng Netpu [b]

[a]Division of Industrial Engineering, Faculty of Engineering and Architecture Rajamangala University of Technology Isan, Muang, Nakhon Ratchasima 30000, Thailand,

[b]S.H.K. Engineering Co., Ltd, Phrapradaeng, Samutprakarn, 10130, Thailand

E-mail: [a] boon.sane@gmail.com

Keywords: Failure Analysis, Ductile Iron Roll, Hot Steel Rolling, Fire Crack, Roll Failure

This paper reports the failure analysis of a ductile iron roll in a hot rolling mill in Medan, Indonesia. The roll failed prematurely after only 3,500 tons of service instead of the normal service life of about 65,000-70,000 tons. Standard procedures for failure analysis were employed in the investigation. It was found that the failure of the roll was due to excessive heat led to causing numerous fire cracks being created very high stress resulting from inadequate water cooling of the roll. Heat cracks around the fracture surface were clearly visible. Therefore, the root cause of the failure is inadequate designs of the roll and associated equipment. Alternative designs are suggested to prevent or minimize similar failures in the future, and to avoid the losses resulting from such failures.

MR-O-05

Thermal Fatigue and Creep of Radiant Coil used in High Temperature Application

Siriwan Ouampan[a,*], Siam kaewkumsai[a], Namurata Palsson[a], Ekkarut Viyanit[a]
[a]National Metal and Materials Technology Center, Klong 1, Klong Luang, Phathumthani, 12120, Thailand
*E-mail address: siriwano@mtec.or.th

Keywords: Radiant Coil, Thermal Fatigue, Creep Voids, High Temperature Failure

Radiant coil used in cracking furnace was observed to be damaged after two years of service. The tube was made of two different centrifugal casted heat resistant alloys, 35Cr41NiNb and 24Cr37NiNb, joined together by welding process. Temperature of the hydrocarbon gas inside the tube was kept at approximately 850ºC with a pressure of 0.6 kscg. The outer surface was subjected to flue gas at a temperature of 1080ºC with a pressure of 15 mmH_2O.

The circumferential crack was observed at heat affected zone, where diameter of the tube was varied. Longitudinal analyses of the failed sample at a macro-scale showed that the cracks initiated within the material and propagated along precipitations towards the surface of the tube. Characterization by means of scanning electron microscopy equipped with energy dispersive spectroscopy technique revealed voids at interfaces of matrix and chromium-rich phase.

The results suggested that the tube failed due to carbon diffusion into the bulk material through localized defect of the oxide scale as a result of rapid thermal change during coking/decoking process. Such carbon penetration led to excessive carbide precipitation which impairs strength of tube, particularly at the heat affected zone. Voids observed at grain boundaries indicated failure due to creep. Moreover, microstructure of the two materials was found to be dissimilar which advised that they were experienced different service temperature.

MR-O-06

Evaluation of Stress Corrosion Cracking Resistance of Welded Stainless Steels in Ethanol

Piya Khamsuk*, Witsanupong Khonraeng, Sikharin Sorachot, Ekkarut Viyanit, Amnuaysak Chianpairot

National Metal and Materials Technology Center, Pathumthani, 12120, Thailand

*piyak@mtec.or.th

Keywords: Stress corrosion cracking, stainless steels, potentiokinetic reactivation, ethanol.

Increasing use of ethanol for biofuel has spurred the need for materials resisting ethanol stress corrosion cracking (SCC) for fabrication of fuel grade ethanol containers. Commercially available stainless steel grades AISI 304, AISI 202, AISI 430 were selected as materials of investigation for potential use as ethanol vessels. In this regard, their SCC resistance was investigated. The three grades of stainless were welded at different welding currents under Ar shielding gas containing varied N_2 contents. After welding, these stainless steels were bent into U-Bend specimens and immersed in ethanol for 2000 h, according to ASTM G30 and G31 standards, to evaluate their ethanol SCC resistance. After 2000-h immersion in ethanol, no evidence of cracking was found on any specimens, indicating satisfactory ethanol SCC resistance of these stainless steels. To further assess the relative ethanol SCC resistance among these stainless steels, double loop potentiokinetic reactivation (DLEPR) technique, following ASTM G108 standard, was employed. The results show that ethanol SCC resistance could be ranked from high to low in the following order: 430 > 304 > 202.

MR-O-07

Evaluation of Stress Corrosion Cracking Resistance of Welded Stainless Steels by Accelerated Immersion Tests

Amnuaysak Chianpairot*, Piya Khamsuk, Witsanupong Khonraeng, Sikharin Sorachot, Ekkarut Viyanit
National Metal and Materials Technology Center, Pathumthani, 12120, Thailand
*amnuaysc@mtec.or.th

Keywords: Stress corrosion cracking, stainless steels, weld, immersion tests.

Conventional U-Bend immersion tests, following ASTM G30 and G31 standards, have shown that welded stainless steel grades AISI 304, AISI 202, AISI 430 are resistant to ethanol stress corrosion cracking (SCC), marking them as potential materials for ethanol containing vessels. The ethanol SCC resistance of these stainless steels was, however, indistinguishable by conventional U-Bend immersion tests because none of these materials cracked after 2000-h immersion in fuel grade ethanol. To distinguish ethanol SCC resistance of these stainless steels, two accelerated immersion test methods were employed. The first accelerated method involved attaching PTFE gaskets to the weld of U-Bend specimens before immersing the specimens in fuel grade ethanol at 50°C. During immersion, the crevices formed between PTFE gaskets and the weld increased localized corrosion susceptibility at the weld, thus facilitating the initiation of SCC cracks. The second accelerated test involved changing the test environment from fuel grade ethanol at 50°C to boiling 37 wt.% $MgCl_2$ solution.

The results from the first accelerated tests showed that AISI 304, AISI 202 and AISI 430 exhibited little, moderate and significant corrosion damage after 1,410-h immersion, respectively. No cracking was observed in all specimens. Furthermore, the accelerated tests in boiling $MgCl_2$ solution showed that times to cracking of AISI 202 and AISI 304 were 122 h and 478 h, respectively. For AISI 430, although it did not crack after 1,098-h immersion in boiling $MgCl_2$ solution, it underwent noticeable pitting corrosion.

MR-O-08

Sulfide Stress Cracking of Welded High Carbon Low Alloy Steel

Namurata Palsson[a,*], Pattima Rattanatrakool[b], Jutaporn Chaichalerm[c]

[a]*National Metal and Materials Technology Center, Klong 1, Klong Luang, Phathumthani, 12120, Thailand*

[b]*Foster Wheeler (Thailand) Limited, Talaythong Tower, Sukhumvit Rd., Thungsukla, Sriracha, Chonburi, 20230, Thailand*

[c]*IS Industrie (Thailand) Ltd., Thai-French Innovation Institute Bld., King Mongkut's University of Technology North Bangkok, Wongsawang, Bangsue, Bangkok, 10800, Thailand*

*E-mail address: namurats@mtec.or.th

Keywords: Sulfide Stress Cracking, Sour Environments, Brittle Fracture, Ductile Fracture

Carbon-manganese and low alloy steels may be susceptible to cracking failure when subjected to aqueous environments containing hydrogen sulfide (H_2S). Such cracking failure is generally termed sulfide stress cracking (SSC) when operate at room temperature and stress corrosion cracking (SCC) when high temperature service is of interest. SSC is an embrittlement phenomenon in which failure can take place under stress below yield strength of the material. A combined process which play important role in SSC are (1) H_2S corrosion leading to metal dissolution, pit formation and evolution of hydrogen atoms and (2) migration of hydrogen atoms into the material causing embrittlement of the metal.

This work aimed to investigate SSC of welded high carbon low alloy steel by means of constant load tensile testing under uniaxial tension in the environment of 0.2% H_2S and 99.8% CO_2 for 720 hr. The specimens were pre-deformed under tensile stresses at 0.2% offset yield strength prior to testing. The results showed no sign of metal dissolution and pitting corrosion. Ultrasonic immersion testing revealed no hydrogen blistering in the material. Longitudinal section of the failed specimens suggested that the main failure mode was SSC which propagated perpendicular to the applied stress. The crack kept on growing until the specimens could not withstand the apply load. Eventually, the final fracture was found to be of ductile mode. Microstructural analysis of the specimen after tensile loading was also discussed.

MR-O-09

Corrosion Evaluation of Zinc-Plated Underhood Automotive Fasteners using Salt Spray Test

Astuty Amrin(presenter)[a,*], Dalila Syairah Mohamad Zubir[b], Liza Mohd Anuar [b] and Abdul Rahim Ishak[b]

[a]*UTM Razak School of Engineering & Advanced Technology, Universiti Teknologi Malaysia Kuala Lumpur,* Jalan Semarak, 54100 Kuala Lumpur, Malaysia.

[b]*Perusahan Otomobil Nasional Sdn. Bhd., HICOM Industrial Estate, Batu 3, P.O. Box 7100, 40918 Shah Alam, Selangor Darul Ehsan, Malaysia*

*E-mail address: astuty@utm.my, syairamz@proton.com

Keywords: Automotive underhood fasteners, Zn-Ni plating, zinc-flake plating, rating number (RN)

Mechanical fasteners such as screws, nuts and bolts are integral components in a vehicle. Rust or corrosion mechanisms of fasteners in the automotive industry is complex and may probably due to many factors includes temperature, pH, ion concentrations, coatings compositions as well as fastener geometry. Most of underhood fasteners used by Malaysia car manufacturer are Zinc coated fasteners. The industry requires interior fasteners are coated to a minimum of 5 µm, while exterior fasteners are of 8 µm minimum thickness. There is a need to understand the corrosion performance of such fasteners in order to improve cosmetic and functional performances of these fasteners. The main objective of this study is to evaluate corrosion performance of three different compositions of Zinc-coated underhood fasteners using laboratory test. Samples were subjected to salt spray test with 5% NaCl for specific periods of time, in accordance ASTM B117- 90 and JIS Z 2371:2000 conforming to their corrosion resistance requirements based on coating type and thickness. Results of the study revealed that Zn-Ni and Zinc-flake platings exhibit superior corrosion resistance characteristics with rating number (RN) of 10 compared to conventional 8 µm hexavalent-chrome free plated fasteners.

MR-O-10

Effects of Heat Treatment on Microstructure and Corrosion Resistance of Boronized Austenitic Stainless Steel AISI 304

Patcharin Naemjan[a], Patiphan Juijerm[a,b,*]

[a]*Department of Materials Engineering – Metals Research Group, Faculty of Engineering, Kasetsart University, Bangkok, 10900, Thailand*

[b]*Residual stress and Fatigue Excellent Center (ReFEC), Iron and Steel Institute of Thailand (ISIT), Bankok, 10110, Thailand*

*E-mail: juijerm@gmail.com, juijerm@isit.or.th

Keywords: Stainless steel, Boriding, Heat treatment, Corrosion

In many industries, austenitic stainless steels are chosen due to their advantaged properties, e.g. good formability with high corrosion resistance. The austenitic stainless steel AISI 304 is widely and extensively used especially in petrochemical industries, where the corrosion problems are always concerned issues. The corrosion resistance of the austenitic stainless steel AISI 304 can be certainly expected for the designed use condition. However, in recent years, many applications are very complicated and in many cases related with surface contact and wear. Therefore, many surface treatments are mentioned and applied to the austenitic stainless steel AISI 304 to protect the surface from wear and corrosion at the same time. The boronizing process is a one of the most well known thermochemical surface treatments possessing many advantaged properties, especially against wear and oxidation. Due to high alloying elements in the stainless steels, the double phase boride layers, FeB (outer) and Fe_2B (inner) are normally observed. The FeB is brittle phase and shall be eliminated before service. The conventional heat treatment is an alternative and simply method to eliminate as well as reduce the FeB phase. Nevertheless, there are still many questions about the corrosion resistance of the boronized stainless steels, especially of the boronized austenitic stainless steel AISI 304. Moreover, the corrosion resistance behaviors of the boronized stainless steels are inconsiderably seen in literatures and still not clarified.

Therefore, in this research, the effects of the heat treatment on microstructure and corrosion behavior of boronized austenitic stainless steel AISI 304 will be investigated. The boronized austenitic stainless steel AISI 304 was heat treated in a temperature range of 800 – 900 °C with soaking time of 2 hr. Afterwards, the phase transformation and the corrosion resistance behavior of the boride layer are addressed. It was found that the double phase boride layer could be transformed to the single phase Fe_2B boride layer after the heat treatment at a temperature of 900 °C with soaking time of 2 hr. Moreover, the corrosion rate of the single phase Fe_2B boride layer is lower than that of the original and boronized austenitic stainless steel AISI 304. After heat treatments at temperatures of 800 and 850 °C, the double phase boride layers were still detected and corrosion rates were high as compared to the original and boronized ones.

Material Reliability Session

POSTER PRESENTATIONS

MR-P-01

Resistive Switching Behavior of Ti/ZnO/Mo Thin Films Structure for Nonvolatile Memory Applications

Rachsak Sakdanuphab[a,*], Aparporn Sakulkalavek[b]
[a]*College of Data Storage Innovation, King Mongkut's Institute of Technology Ladkrabang, Bangkok, 10520, Thailand*
[b]*Department of Physics, Faculty of Science, King Mongkut's Institute of Technology Ladkrabang, Bangkok, 10520, Thailand*
*ksrachsa@kmitl.ac.th

Keywords: resistive switching, nonvolatile memory, RRAM

In this work, we study the resistive switching behavior of a new model metal/insulator/metal (MIM) junction. The MIM junction consists of titanium front electrode, zinc oxide insulation layer, and molybdenum back electrode thin films. The Ti/ZnO/Mo structure was prepared on 3x3 cm^2 soda lime glass substrates using dc magnetron sputtering for metal electrodes and rf magnetron sputtering for ZnO layer. The thicknesses of Ti, ZnO and Mo films were controlled at 200nm, 50nm and 500nm, respectively. The crystalline structure and microstructure of the films were characterized by X-ray diffraction and atomic force microscopy. The current-voltage (I-V) characteristics of the device cells were obtained by using dc voltage sweep mode. The XRD spectra of the devices shows Mo(100) and ZnO(002) preferred orientations. The Mo and ZnO film surfaces exhibit dense crystallized grains with the root mean square roughness (RMS) of 1.0 and 1.4 nm, respectively. The device cells behave a unipolar resistive switching characteristic with reversible, controllable and reliability within 150 cycles. The difference between high resistive state (HRS) and low resistive state (LRS) is about 103 times. A low operating voltage range of 0.50-0.60 V is obtained for switching from HRS to LRS at a current compliance of 10 mA. The new MIM structure was demonstrated and indicated a potential to use as nonvolatile memory application.

MR-P-02

Changes in Structural, Morphological, and Corrosion Properties of CrN Thin Film Effected by Varying N_2 Pressure in the Sputtering Process

Wichuda Wongtanasarasin[a,*], Rachsak Sakdanuphab[b]

[a] *Faculty of Science, KingMongkut's Institute of Technology LadkrabangChalongkrung Rd. LadkrabangBangkok 10520, THAILAND*

[b] *College of Data Storage Innovation, King Mongkut's Institute of Technology LadkrabangChalongkrung Rd. LadkrabangBangkok 10520, THAILAND*

wichuda.wongt@gmail.com, *ksaparpo@kmitl.ac.th

Keywords: CrN thin film, DC reactive magnetron sputtering, Corrosion

The objective of this study was to investigate a facet of the fabrication process of chromium nitride (CrN) film intended as a protective coating for pineapple blades. In this study, CrN thin films were deposited on unpolished silicon wafer substrates by DC reactive magnetron sputtering in $Ar+N_2$. In principle, the proportion of nitrogen pressure to the total pressure in the sputtering process should have considerable effects on the CrN film's deposition rate, its crystal structure, and its corrosion rate. We tested this supposition out by using several different nitrogen partial pressures in the sputtering process and observed the films deposited. The coatings were deposited at four different Nitrogen partial pressures of $4x10^{-4}$ mbar, $8x10^{-4}$ mbar, $1.2x10^{-3}$ mbar and $1.6x10^{-3}$ mbar were used to achieve 2-µm thick CrN films. The films were analysed by several analytical methods, and the following findings were observed. The XRD spectra of the films showed face-centered cubic structure with (111) and (200) preferred orientations, positively identifying them as CrN thin films. The calculated d-spacing and lattice parameter of the CrN films increased with increasing nitrogen partial pressure; the ranges were 2.0550 – 2.9017 Å and 4.1101 – 4.1803 Å, respectively, exhibiting the effect of varying stress and strain in the films. The films corrosion potential, an indicator of their corrosion property, varied from -0.2 to -0.06 volts with varying nitrogen partial pressures. The most corrosion resistant film, exhibiting the highest corrosion potential and the lowest corrosion current, was the one fabricated at $1.2x10^{-3}$ mbar.

MR-P-03

The Influence of N_2 Partial Pressure on Color, Mechanical, and Corrosion Properties of TiN Thin Films deposited by DC Reactive Magnetron Sputtering

Pisitpat Nimnual[a,*], Aparporn Sakulkalavek[a], Rachsak Sakdanuphab[b],
[a]*Faculty of Science, King Mongkut's Institute of Technology Ladkrabang, Bangkok 10520, THAILAND*
[b]*College of Data Storage Innovation, King Mongkut's Institute of Technology Ladkrabang, Bangkok 10520, THAILAND*
*pisispat@gmail.com

Keywords: Titanium nitride, dc reactive magnetron sputtering, corrosion.

Abstract: Multi-functional thin films have gained increasing importance in a decorative application. Among the available material, TiN thin film is interested due to its golden color and mechanical resistance. Beside their properties, the corrosion property of TiN films is mainly considered in order to extend to the decorative application. In this work, the TiN thin films were deposited on 3x3 cm^2 Si(100) substrates by dc reactive magnetron sputtering technique. The effects of N_2 partial pressure on deposited film properties such as microstructure, surface morphology, color, mechanical and corrosion properties were investigated. The deposited films with different N_2 partial pressures were characterized, using X-ray diffraction (XRD), optical camera, atomic force microscopy (AFM), nanoindentation testing and potentiostat/galvanostat measurement. We found that the XRD spectra of the films exhibit the (111) and (200) preferred orientation of TiN crystal structures. The color of TiN films change from golden-yellow to gold-red colors by increasing of N_2 partial pressure that corresponds to the plasma frequency of Ti-N films by using Drude model. The TiN films have smooth surface and the surface is smoother when the N_2 partial pressure increases. Standard corrosion tests in 0.1wt% NaCl solution show the corrosion potential (E_{corr}) in the range between -0.5 to -0.4 volts and the polarization resistance increases with increasing of N_2 partial pressure. The highest hardness of the film is approximately 40 GPa with elastic modulus of 340 GPa, achieved by using N_2 partial pressure of 50%. We conclude that the TiN films would be enhanced mechanical property and corrosion resistance by deposited with high N_2 partial pressure, but the color would be dropped off to gold-red color.

MR-P-04

Failure Analysis of Hydrocarbon Transfer Tube used for High Temperature Service

Siriwan Ouampan[a,*], Kosit Wongpinkaew[a], Siam kaewkumsai[a], Namurata Palsson[a]
[a]*National Metal and Materials Technology Center, Klong 1, Klong Luang, Phathumthani, 12120, Thailand*
*E-mail address: siriwano@mtec.or.th

Keywords: Stainless Steel, Thermal Fatigue, Creep, Intergranular Cracking

The fractured hydrocarbon transfer line made of stainless steel grade AISI 321 used in a naphtha cracking furnace was investigated in this study. The tube was attached to padding and lug, which made of stainless steel grade AISI 304, to minimize vibration and stress during high temperature service. Temperature of the hydrocarbon gas inside the tube was designed for 600ºC with a pressure of 3.1 kscg. The damage was noticed due to an ignition during operation.

Visual inspection indicated circumferential cracks beneath the padding adjacent to the welding of the tube and padding. Macrostructural examination revealed single-type cracks with blunt tip and oxide scale covered densely at the joint between the tube and padding. Microstructural characterization revealed oxide scale formed on the fracture surface and inside the cracks, in which the cracks were propagated from the outer wall of the tube. Cross-sectional analyses of the tube beneath the padding suggested intergranular oxidation. Scanning electron microscopy equipped with energy dispersive spectroscopy examination of the samples showed that the oxide scale covered on the other surface was of porous form. Characterization at the bulk material indicated internal oxidation, precipitation and voids at grain boundaries.

From the results obtained by combination of techniques, it can be concluded that the tube have possibly experienced the service temperature in the range of sensitization (400-800ºC). Intergranular oxidation and precipitation at grain boundaries may lead to intergranular cracking under high pressure and thermal cyclic operation. Single-type with blunt tip cracks covered with oxide scale and voids at grain boundaries suggested failure mode of fatigue at high temperature and creep, respectively.

MR-P-05

Effect of Soil Properties on Corrosion of Hot Dip Galvanized Steel for Underground Application

Namurata Palsson[a,*], **Sikharin Sorachot**[a], **Wanida Pongsaksawad**[a], **Ekkarut Viyanit**[a]
[a]*National Metal and Materials Technology Center, Klong 1, Klong Luang, Phathumthani, 12120, Thailand*
*E-mail address: namurats@mtec.or.th

Keywords: Hot dip galvanized steel, Soil Corrosion, Potentiodynamic Test

Hot dip galvanized steel has been widely used for underground application, for example as ground rods and screw piles. Due to complexity of soil environments, e.g. soil composition, soil resistivity, soil pH, leakage current from surroundings, etc., buried structures are generally susceptible to corrosion.

This study aimed to understand the effect of soil environments on corrosion of hop dip galvanized steel by means of immersion testing and electrochemical techniques according to ASTM G5. Carbon steel grade JIS SS400 samples were coated with zinc through hot dip galvanizing process to achieve a thickness of approximately 80 micron. Potentiodynamic tests were performed in soil with addition of 1 and 2 percent by weight of sodium chloride to represent saline soil environment. Three-electrode corrosion cell was used with copper/copper sulfate and graphite as reference and auxiliary electrodes, respectively. Moreover, the samples were immersed in soil with different sodium chloride concentration (1 and 2 percent by weight) under applied direct and alternating current of 5, 10 and 15 mA to evaluate the effect of leakage current from surroundings. Soil resistivity and pH were controlled for both experiments using de-ionized water.

The results indicated that concentration of sodium chloride exhibited no effect on corrosion of galvanized steel samples when soil resistivity and pH were controlled. Increasing applied direct current accelerated corrosion of the samples. Alternating current showed insignificant impact on corrosion when compared to direct current. Field exposure of galvanized steel ground rods for up to 15 years in different regions in Thailand was also discussed.

Metals, Alloys and Intermetallic Compounds Session

ORAL PRESENTATIONS

MT-O-01

The Effect of Ag and Sc Alloying Additions to the Casting Microstructure of A356 Aluminium Alloy

Phanuphak Seensattayawong[a], Chindanai Chaorainak[a], Patipat Ketpotong[a], Supparerk Boontein[a], Dimitrios Bakavos[a*] and Chaowalit Limmaneevichitr[a]
[a]Department of Production Engineering, King Mongkut's University of Technology Thonburi, 126 Pracha Uthit Rd., Bangmod Thungkhru, Bangkok 10140.
*dimitrios.bakavos@gmail.com,

Keywords: Porosity, alloying, cooling rate, Al

Aluminium cast alloys of the Al-Si system are widely used for shape castings. The low coefficient of thermal expansion, high wear resistance and fluidity enable them to be a suitable material in aerospace and automotive industries. Additions of scandium in A356 aluminium alloys can achieve both α-Al grain refinement and modification of eutectic Si resulting in an improvement to the mechanical strength of hypoeutectic cast components. Further attempts of improving their mechanical properties could be obtained by the addition of alloying elements–copper and manganese–followed by solution heat treated and artificial ageing. Ag addition has been proposed as an important alloying element in Al-Cu-Mg wrought alloys, due to its influence on the enhancement of the ageing kinetics and improvement of strength via the promotion of the omega Ω (Al_2Cu) equilibrium phase on the $(111)_{Al}$ aluminium habit planes. In addition, there are published evidence that in hypoeutectic Al-Si-Mg alloys, alloying additions could alter the solidification characteristics and affect the porosity formation in terms of density, distribution and size which possibly affect the mechanical properties of the cast part.

In this study, the effect of Ag and Sc interactions on the eutectic silicon phase and eutectic grain size along with porosity formation by means of optical scanning electron microscopy have been investigated. Moreover, the effect of cooling rate onto the previously mentioned has also been studied. Two mold types have been used: a graphite mold with higher and a steel mold with lower cooling rate respectively. Finally the effect of the alloying element additions on the strength of the casts has been identified by the aid of Brinell hardness and mechanical testing. The results suggest that the Ag additions show a subtle effect in refining the Si eutectic, and not significant effect to the grain size when compared to the alloy containing Sc. Moreover, evidence of a slight increase in hardness in the Ag, Sc, Ag+Sc modified alloys and a decrease in the porosity size present at low cooling rates (0.5 C/sec) are observed. It suggests that there is an interaction of Ag and Sc tduring nucleation and growth of α-Al. Furthermore, the porosity is finer in size and more uniform in its distribution when both Ag and Sc have been added. The mechanical properties of the A356 alloys with Ag and Sc additions have increased by 15-25 MPa compared to the A356 base alloy. Therefore, beyond doubt the findings suggest that the A356 alloys with Ag, Sc or Ag and Sc additions have improved in terms of strength at the cast condition without further heat treatment.

MT-O-02

Sintered Frictional Fe-based Materials

Monnapas Morakotjinda, Nattaya Tosanthum, and Ruangdaj Tongsri*
Powder Metallurgy Research and Development Unit (PM_RDU),
National Metal and Materials Technology Center, 114 Paholyothin Road, Khlong Nueng,
Khlong Luang, Pathum Thani 12120 Thailand
*ruangdt@mtec.or.th

Keywords: Sintered frictional materials, wear, friction coefficient, wear mechanism.

Sintered frictional materials with high friction coefficient values (≥ 0.80) were produced from mixtures of base powders (Fe-6Cu-3C) and varied contents of reinforced silicon oxide (SiO_2) particles using conventional powder metallurgical route. Dry sliding tests using a pin-on-disc showed that high friction coefficient and high mass loss could be obtained in the sintered Fe-6Cu-3C materials with SiO_2 contents ≤ 10 wt. %. The mass loss was reduced with increasing SiO_2 contents, associated with slight drops of friction coefficient values. Without SiO_2 addition, the sintered Fe-6Cu-3C materials showed accumulation of worn particles on the worn surfaces and particulate-like wear debris. With SiO_2 addition, the sintered composites showed less accumulation of worn particles but the flaky wear debris indicated the formation of compacted layers during thr dry sliding.

MT-O-03

Machined Surface Quality of Pre-sintered Hardenable PM Steel

Thawatchai Khantisitthiporn*, Monnapas Morakotjinda, Bhanu Vetayanugul and Ruangdaj Tongsri
National Metal and Materials Technology Center (MTEC), 114 Paholyothin, Khlong Nueng, Khlong Luang, Pathum Thani, 12120 Thailand
*thawatt@mtec.or.th

Keywords: Powder metallurgy (PM), sinter hardenable PM steel, pre-sintering, pre-sintered machining.

To produce complicated PM parts with undercut and assembled components, additional operation by machining process is still necessary and important because of the limitation of the press and sinter technology. The benefit of pre-sintered machining is to avoid machining difficulty inherited from high hardness of sintered parts especially hardenable PM steels. The hardenable PM steels usually show high hardness microstructures such as bainite and martensite phases so special cutting tool materials are required. Pre-sintering treatment of green PM part at temperatures lower than the normal sintering temperature results in green strength improvement high enough for clamping by a machining holder and the high hardness microstructures are not able to form at the pre-sintering temperatures. Beside of green density and machining conditions, pre-sintering temperature is the most important parameter to achieve machined surface quality. Thus, before applying pre-sintered machining in PM production, the relationship between pre-sintering temperature and machined surface quality should be considered and understood. In this study, the influences of various pre-sintering temperatures, such as at 700, 800, 900 and 1,000°C, lower than the normal sintering temperature of 1120°C in hydrogen atmosphere with holding time of 120 min and several machining conditions on machined surface quality of the pre-sintered PM sample were investigated. All of pre-sintered samples were machined by turning process with carbide cutting insert with varied cutting speeds at a fixed feed rate and depth of cut without cutting lubricant. Chromium alloyed PM steel powder (Astaloy® CrM) samples with (0.5 wt. %C) and without graphite additions (0 wt. %C) mixed with 1 wt. % of zinc stearate were prepared as green parts by cold compaction in cylinder die with a diameter of 30 mm. Green density was about 7.00 g/cm^3 and thickness of each sample was controlled by hydraulic pressure and powder weight of 80 g/sample. All of green samples were treated by pre-sintering treatment before machining testing. Surface quality of each machined sample was evaluated by average surface roughness and surface texture by SEM analysis including the appearance of outlet edge breakout. The experimental results revealed that the pre-sintered samples with graphite addition showed better surface quality in both of surface roughness and surface texture with lower outlet edge breakout appearance. Moreover, at high pre-sintering temperatures of 900 and 1,000°C, the relations between average surface roughness and turning condition were very similar for both temperatures. The obtained surface textures were better than the cases of lower temperatures of 700 and 800°C. The outlet edge breakout did not occur only with the case of pre-sintering at 1,000°C and with added graphite.

MT-O-04

Sintered Microstructures and Mechanical Properties of Mechanically Alloyed Fe-Cu Powders

Nattaya Tosangthum, Monnapas Morakotjinda, Bhanu Vetayanugul and Ruangdaj Tongsri*

Powder Metallurgy Research and Development Unit (PM_RDU), National Metal and Materials Technology Center, 114 Paholyothin Road, Khlong Nueng, Khlong Luang, Pathum Thani 12120 Thailand

* ruangdt@mtec.or.th

Keywords: Mechanical alloying, sub-micron size powders, sintering, mechanical properties

Solid solublities of iron (Fe) in copper (Cu) and vice versa are very limited at low solute concentrations. Strengthening by solid solution of high alloy Fe-Cu and Cu-Fe materials is thus limited. In high alloy Fe-Cu and Cu-Fe materials, coexitence of body center cubic (bcc) Fe and face centered cubic (fcc) Cu is commonly found. Mechanical alloying was proved to be able to produce very fine particles of Fe, Cu and intermetallics. However, there were no works dealing with consolidated products of the mechanically alloyed Fe-Cu powders. In this work, mixed Fe (47 wt. %) and Cu (53 wt. %) powders were mechanically alloyed until the particle size reaching a contant value. The mechanically alloyed powders were compacted into tensile test bars, which were sintered under pure hydrogen at different temperatures, such as 800, 900, 1000 and 1100 ˚C. The sintered Fe-Cu samples made without mechanical alloying were used as references. It was found that microstructures of the sintered materials made from mechanically alloyed powders consisted of fine grains of Fe, Cu and intermetallics. The tensile strengths of the sintered Fe-Cu samples made with and without pre-mechanical alloying increased with increasing sintering temperatures. The strengths of the pre-mechanical alloying materials were double that of the materials without pre-mechanical alloying. However, the sintered materials with fine Fe and Cu grains showed low ductility.

MT-O-05

Sintered Frictional SiC-Reinforced Cu-Base Composites

Jiraporn Damnernsawat[a], Pongpan Kaewtatip[a], Nattaya Tosanthum[b], Bhanu Vetayanugul[b], Pongsak Wila[b] and Ruangdaj Tongsri[b]*

[a]Department of Mechanical Engineering, Faculty of Engineering, King Mongkut's University of Technology Thonburi, 126 Pracha Uthit Rd., Bang Mod, Thung Khru, Bangkok 10140 Thailand

[b]Powder Metallurgy Research and Development Unit (PM_RDU), National Metal and Materials Technology Center, 114 Paholyothin Road, Khlong Nueng, Khlong Luang, Pathum Thani 12120 Thailand

* ruangdt@mtec.or.th

Keywords: Sintered frictional materials, microstructures, mechanical property, friction coefficient

Lead-free frictional materials are important components in safety and power transmission parts of automobiles. In order to avoid using lead-containing friction modifiers, non-toxic ceramic particles are considered to be used as reinforcements. In this research work, copper-based friction materials have been developed by using press and sinter method. Pre-alloyed bronze (Cu-10Sn) powder was admixed with iron (Fe), graphite (C) and varied amounts of silicon carbide (SiC) powders. The admixed powders were compacted into disc-shape samples, which were then sintered at different temperatures in the range of 800-950 ˚C. It was found that sintered density and hardness of the sintered copper-based friction materials reduced with increasing SiC content. Microstructures of the sintered materials showed inhomogeneity due to uneven distribution of coarse Fe and SiC particles. The coarse SiC particles also prohibited bonding between metal powder particles. However, the sintered materials showed high room-temperature friction coefficients, which were in the range of 0.50-0.85, particularly the materials containing ≥ 4 wt. % of SiC particles.

MT-O-06

Effects of Cooling Rates and Alloy Compositions on Solidification of Cu-Sn Powders

Amornsak Rengsomboon, Rungtip Krataitong, Thanyaporn Yotkaew, Autcharaporn Sri-on, Pennapa Muthitamongkol, Nattaya Tosangthum, and Ruangdaj Tongsri*

Powder Metallurgy Research and Development Unit (PM_RDU), National Metal and Materials Technology Center, 114 Paholyothin, Khlong Nueng, Khlong Luang, Pathum Thani 12120 Thailand

*ruangdt@mtec.or.th

Keywords: Solidification microstructure, cooling rate, composition, atomized Cu-Sn powders

Solidification microstructures of gas- and water-atomized Cu-Sn alloys were investigated in this work. Gas atomization was conducted with 3 alloy compositions, such as Cu-51 wt. % Sn, Cu-61 wt. % Sn and Cu-71 wt. % Sn whereas water atomization was performed only with the Cu-61 wt. % Sn alloy. In general, all the as-atomized Cu-Sn powders, investigated under this work, showed similar solidification microstructures consisting of hexagonal $Cu_{6.25}Sn_5$ (η), $Cu_{3.02}Sn_{0.98}$ (ε) and Sn (β) phases. Typical lamellar structures of ε phase formed first as the primary phase, which was followed by peritectic reaction (liquid + ε → η) yielding the peritectic η phase enclosed the ε phase. In the gas-atomized Cu-Sn powders, the volume fractions of the β-Sn phase indicated by X-ray diffraction peak intensity increased with nominal Sn content. For the water-atomized Cu-61 wt. % Sn powders, increase of cooling rates resulted in decrease of β-Sn phase volume fraction. Formation of the ε phase was also suppressed in very fine particles of water-atomized Cu-61 wt. % Sn alloy powders.

MT-O-07

Nondestructive Evaluation for Duplex Stainless Steel Tube using Multi-frequencies Remote Field Testing

Cherdpong Jomdecha[a,*] and Sorrawut Sancharoen[b]
[a] *Maintenance Technology Center, King Mongkut's University of Technology Thonburi, Bangmod, Tungkru, Bangkok, 10140, Thailand*
[b] *Static Equipment Inspection Service, PTT Maintenance and Engineering Company Limited, Map ta phut, Maung, Rayong, 21150, Thailand*
*axlrosez13@hotmail.com

Keywords: Duplex stainless steel, tube, remote field testing, multi-frequencies.

As a difficult testing by conventional non-destructive testing for two-phase structure (ferritic and austenitic) of the duplex stainless steel tube, this paper presents the multi-frequencies technique of remote field testing (RFT) based on eddy current through transmission generation to quantify flaws and wall losses of duplex stainless steel tube grade ASME/ASTM SA 789. The tube specimen dimensions of 25.4 mm outside diameter, and thickness of 1.65 mm with the different artificial flaws was prepared for the experiments. A dual- pickup coils type of RFT probe was employed to inspect the specimen by inserting a probe within the tube specimen. Range of inspection frequency which was different than those inspection frequencies of general steel tube was determined. Then, four different frequencies were simultaneously generated from the oscillator to the RFT probe for detecting the flaws of the tube specimen. The inspection signals were specifically shown in function of voltage and impedance planes to identify the flaw characters. The results showed that the multi-frequencies RFT can be utilized to quantify the wall loss levels of duplex stainless-steel tube. Amplitude and phase of inspection signals were used to evaluate the different depths of the flaws. Consequently, the sensitivity of RFT can be shown the performance for detecting the wall loss at minimum 20% of tube thickness. In addition, the testing results of in-serviced tubes installed in heat-exchanger were described and compared with the tube specimen.

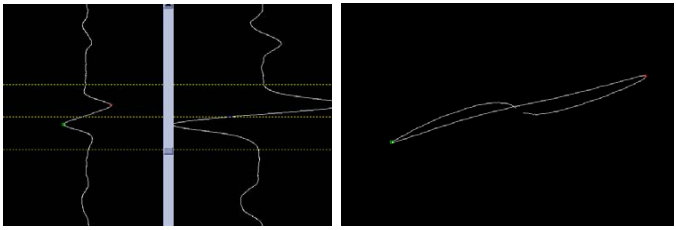

(a) (b)

Fig 1. RFT Inspection signals of 20% wall loss for duplex stainless steel tube (a) voltage plane, (b) Impedance plane.

MT-O-08

The Comparison of Acoustic Emission Activities between Material Integrity and Leakage during CNG Cylinder Testing

Chalermkiat Jirarungsatian[a,*], Cherdpong Jomdecha[a], Rangsan Kenok[a] and Palakorn Homsawat[a]
[a] *Institute for Scientific and Technological Research and Services (ISTRS) King Mongkut's University of Technology Thonburi, Thung-kru, Bangkok, 10140, Thailand*
*chalermkiat.jir@kmutt.ac.th

Keywords: CNG Cylinder, Material Integrity, Leakage, Acoustic Emission

The objective of this paper is to study the different acoustic emission (AE) activities from material integrity and leakage which were obtained from CNG steel cylinder during pressurization. CNG type I cylinders were employed to test by hydrostatic stressing. The pressure was continuously increased to 1.1 time of operating pressure or leakage occurrences. AE sensors, resonance frequency of 150 kHz, were mounted on the outside cylinder wall to detect the AE activities throughout the testing. AE activities were compared between AE of material integrity and leakage by amount of AE signals detected then analyzed by AE parameters. AE parameters including Amplitude, Count, Energy (MARSE), Duration and Rise time were analyzed to distinguish the AE data. Additionally, the location of AE sources were located by the calculation the arriving differenced time of 2 or more sensors to indicate the position of cylinder faults. The results can be shown that the AE signals of material integrity were randomly detected throughout the pressurization while the leakage signals were increased periodically until leakage occurrences. AE parameters of Count and Energy can be significantly assessed the difference between material integrity and leakage.

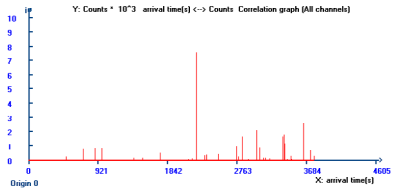

Fig 1 AE activity of material integrity

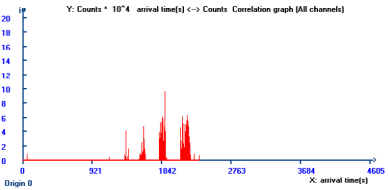

Fig 2 AE activity of leakage

MT-O-09

Correlation of Acoustic Emission with Corrosion of Lacquer Coatings on Tin-Free Steel

Pornsak Srisungsitthisunti[a*], Siriporn Daopiset[a,b] and Noparat Kanjanaprayut[b]
[a]*Production Engineering Department, Faculty of Engineering,*
King Mongkut's Universityof Technology North Bangkok, Bangkok, 1080 Thailand
[b]*Corrosion Technolog Laboratory, Thai – French Innovation Institute,*
King Mongkut's University of Technology North Bangkok, Bangkok, 1080 Thailand
*pornsaks@kmutnb.ac.th

Keywords: Corrosion, Acoustic Emission, Electrochemical Spectroscopy.

Acoustic emission (AE) is a non-destructive technique, and well known for crack monitoring and erosion of metallic structures, and also used for detecting corrosion damage on metallic structures. In this study, AE technique is applied for quick monitoring of corrosion resistance of lacquer coatings on tin free steel and laminated steel for food can-packaging. There are three types of coatings: (A) BPA-NI lacquer, (B) BPA-complied lacquer, and (C) PET lamination. These coatings were investigated in flat-sheet and in deformed sheet. Cathodic disbonding (CD) technique was carried out to cause separation between the coating and the metal substrate and initialize corrosion damage. AE signals can be detected immediately with potential excitation, and showed good correlation with coating corrosion resistance during corrosion development. AE count signal matched with resulting current during CD, and proportional to corroded areas. In addition, coatings properties were measured before and after the CD process by electrochemical impedance spectroscopy (EIS). The AE and CD techniques combination offers a real-time non-destructive corrosion monitoring of coating quality before and during delamination development, and useful for can-packaging testing.

MT-O-10

Analysis of Eddy-Current Measurement System for Residual Stress Assessment in Stainless Steel Grade 304

Cherdpong Jomdecha[a,*] **and Isaratat Phung-On**[a]

[a] *Maintenance Technology Center, King Mongkut's University of Technology Thonburi, Bangmod, Tungkru, Bangkok, 10140, Thailand*

*axlrosez13@hotmail.com

Keywords: Measurement system analysis, Eddy current, Residual stress, Stainless steel.

This paper deals with an analysis of statistical discreteness and measurement capability of the nondestructive eddy-current measurement system for residual stress assessment in stainless steel Grade 304 (SS304). The cylindrical specimens with 50 mm in diameter and 12 mm thickness were prepared to generate residual stress by Resistance Spot Welding technique (RSW) at which the welding currents were set at 12, 14, and 16 kA. The eddy-current measurement system was including a probe with frequency range of 0.1 to 3 MHz and an eddy current flaw detector. They were performed by contacting the probe on the specimen, regardless of coupling material to measure the changed probe impedance caused by the levels of internal residual stress in the specimens. In order to determine the results of the residual stress measurement, the calibration curves between static tensile stress and eddy current impedance at various frequencies were accomplished. The Measurement System Analysis (MSA) was utilized to evaluate the changed eddy-current probe impedance from residual stress. The results showed that using eddy current technique at 1 MHz for residual stress measurement was the most efficient. It can be achieved the Gauge Repeatability & Reproducibility (GR&R) at 172.86 MPa with %GR&R at 16.61479 and Number of Distinct Categories (NDC) at 8. As applied on actual butt welded joint, it could yield the uncertainty of ± 58 MPa at 95 % (U_{ISO}).

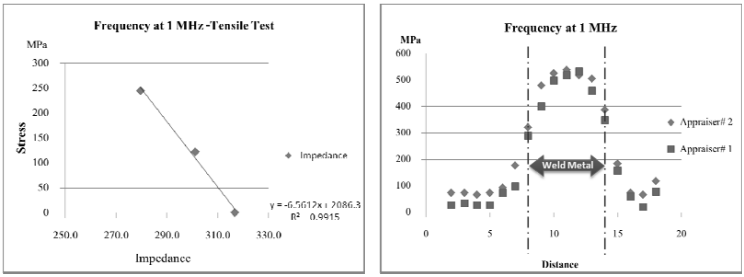

(a) (b)

Fig 1. (a) Calibration curve between stress and the impedance of 1MHz eddy current probe, (b) Residual stress measurement of butt-welded joint specimen.

MT-O-11

Influence of Nitrogen in Shielding Gas on Sensitisation of PCGTAW Austenitic Stainless Steels

Narueporn Vaneesorn[a, c*], Namurata Sathirachinda Pålsson[a], Ekkarut Viyanit[a], John Thomas Harry Pearce[a] and Torranin Chairuangsri[b]

[a]*National Metal and Materials Technology Center, Thailand Science Park, Pathum Thani, 12120, Thailand*

[b]*Department of Industrial Chemistry, Faculty of Science, Chiang Mai University, Chiang Mai, 50200, Thailand*

[c]*Department of Physics and Materials Science, Faculty of Science, Chiang Mai University, Chiang Mai, 50200, Thailand*

* naruepv@mtec.or.th

Keywords: Shielding gas, Sensitisation, PCGTAW, Austenitic Stainless Steels

To reduce alloy costs new commercial low nickel content austenitic stainless steels (ASSs) have been introduced as an alternative to the 300 series. Nickel has been substituted by other austenite stabilisers, notably manganese, copper and nitrogen, with added molybdenum for additional corrosion resistance. There are concerns that the lower Ni content may have detrimental effects on corrosion behaviour after welding operations, especially intergranular corrosion cracking (IGC), which can be observed via the degree of sensitisation (DOS) test. However, such problems may be avoided by appropriate control of welding process parameters, particularly the type of shielding gas.

Pulsed current tungsten arc welding (PCGTAW) is widely employed for the fabrication of stainless steel plates. Using this process plates of AISI 304, AISI 304L and AISI 202 ASS were used for comparison with Mn-substituted 201-2M ASS. Shielding gas was mixed in volume ratio of argon (Ar) and nitrogen (N_2) at 100:0, 95:5 and 90:0. Welding currents were set at 130 and 160 Amp, respectively. Welded plates were cut into coupon shape, polished and used as the working electrode. Saturated calomel electrode (SCE) and platinum (Pt) steckbar were selected as reference- and counter electrodes. Each test coupon was immersed in mixture of 0.5 M sulfuric acid (H_2SO_4) and 0.01 M potassium thiocyanate (KSCN) in the flat cell. Double loop electrochemical potentiokinetic reactivation (DLEPR) was selected to perform the sensitisation test inside a Faraday cage. Each specimen was cathodically cleaned at -500 mV_{SCE} for 60 sec before open loop circuit running for 30 minutes. Later, the anodic polarisation scan was applied from -500 mV_{SCE} to passive potential at +500 mV_{SCE} with scan rate of 1.67 mV/sec to obtain the activation current peak (I_a). Finally, cathodic polarisation was reversely applied with the similar potential range to -500 mV_{SCE} to obtain the reactivation current peak (I_r). DOS was calculated to compare susceptibility to sensitisation among all test specimens.

Optimum welding current for PCGTAW process with the ASSs in this work should be at 130 Amp to maintain good corrosion resistance. Lowest susceptibility to sensitisation was achieved with PCGTAW 201-2M ASS under mixed shielding gas ratio of Ar:N_2 at 95:5 and was comparable to that observed for PCGTAW AISI 304 and AISI 304L ASSs. All welding parameters in this work were not suitable for PCGTAW joining of AISI 202 since this alloy was found to have the highest susceptibility to sensitisation.

MT-O-12

Fe-Sn Intermetallics Synthesized via Mechanical Alloying-Sintering and Mechanical Alloying-Thermal Spraying

Pinya Meesa-Ard[a], Vitoon Uthaisangsuk[a], Nattaya Tosangthum[b], Panadda Sheppard[b], Pongsak Wila[b] and Ruangdaj Tongsri[b]*

[a]Department of Mechanical Engineering, Faculty of Engineering, King Mongkut's University of Technology Thonburi, 126 Pracha Uthit Rd., Bang Mod, Thung Khru, Bangkok 10140 Thailand

[b]Powder Metallurgy Research and Development Unit (PM_RDU), National Metal and Materials Technology Center, 114 Paholyothin Road, Khlong Nueng, Khlong Luang, Pathum Thani 12120 Thailand

* ruangdt@mtec.or.th

Keywords: Fe-Sn intermetallics, mechanical alloying, sintering, plasma spraying

Iron (Fe)-tin (Sn) intermetallics are promising materials for electrochimcal applications, such as a rechargeable battery negative electrode allowing intercalation and deintercation of lithium ion. The cycling performance of $FeSn_2$ intermetallic is constant over 50 cycle numbers at specific capacity of higher than 400 $mAhg^{-1}$. The specific capacity is higher for the $FeSn_2$/graphene composite electrode. Because of its potential applications, the $FeSn_2$ intermetallic was synthesized using two different routes. These two routes had a common synthesis step, in which Fe powder (19 wt. %) was mechanically alloyed with Sn powder (81 wt. %) for 25 h under argon atmosphere. The mechanically alloyed powders were then treated with different heating routes. In the first route, the compacts of the mechanically alloyed powders were sintered at different temperatures for different times. It was found that the $FeSn_2$ content increased with increasing temperature and time. There were small traces of Fe, Sn and FeSn found in the sintered materials. In the second route, the mechanically alloyed powders were plasma-sprayed using different currents of 300, 400 and 500 A. It was found that the porous coatings produced by plasma sprayng consisted of mixed Fe, Sn, $FeSn_2$, SnO, Fe_3O_4 and FeO for all employed currents.

MT-O-13

Synthesis and Characterization of Ni-Co-Si_3N_4 Nanocomposite Coating

Yusrini Marita[a,*], Ridwan[b], Nurdin[c]

[a,b]*Department of Chemical Engineering, Lhokseumawe State Polytechnic, Lhokseumawe, Aceh, 24301, Indonesia*

[c]*Department of Mechanical Engineering, Lhokseumawe State Polytechnic, Lhokseumawe, Aceh, 24301, Indonesia*

*yusrinimarita@yahoo.com

Keywords: Nanocomposite, nickel-cobalt, silicon nitride, coating.

Nanocomposites of a metallic matrix containing dispersion of second phase particles usually display a variety of novel properties. The presence of a second phase particles in a codeposited film offers a variety of benefits on physical and mechanical properties compared to pure metal coatings, such as increased microhardness and improved wear resistance. Generally, nanocomposites containing like Si_3N_4 are preferred for high wear resistance along with increased hardness. The mechanical property of the nanocomposite material is improved due to extremely fine microstructure of the materials. In the present work, Ni-Co- Si_3N_4 nanocomposite coating were prepared by electrodeposition technique. The deposition was performed at 50 mA cm^{-2} on copper substrate. The working temperature of electrodeposition was constant at 50^0C in an acidic environment of pH 4. The effect of silicon nitride dispersion was observed. Morphological studies of Ni-Co- Si_3N_4 nanocomposite coating were carried out with scanning electron microscopy, energy dispersive X-ray spectroscopy was used to determined the composition and the phase present in the Ni-Co-Si_3N_4 were examined with an X-ray diffraction analysis. The addition of Si_3N_4 particles give lower composition of nickel in the nickel-cobalt-silicon nitride nanocomposites coating as compared to the nickel-cobalt alloy coating. Hardness of the Ni-Co- Si_3N_4 nanocomposite coating was measured by a Vickers indentation technique. From elemental mapping procedure, Si_3N_4 nanoparticles were uniformly distributed in the Ni-Co composite coating, indicating good dispersion of Si_3N_4 and contributed in increasing the microhardness of coating.

MT-O-14

Composition Dependence of Morphological and Magnetic Properties of $Co_{100-x}Cu_x$ Film Prepared by RF-Sputtering

G. Chaloeipote[a] and W. Rattanasakulthong[a*]

[a]Department of Physics, Faculty of Science, Kasetsart University,50 Ngam Wong Wan Ladyaow, Chatuchak, Bangkok, 10900,Thailand

* fsciwrr@ku.ac.th

Keywords: Co-Cu film, Sputter deposition, Chemical composition, Magnetic property

Granular $Co_{100-x}Cu_x$ films with the different compositions of x = 19, 40, 54, 65 and 76 were deposited on glass substrates by sputter deposition. Co (HCP) and Cu (FCC) phases were observed in all deposited Co-Cu films. Film thickness was increased with increasing Cu-composition. The minimum and maximum values of electrical resistance measured by four-point probe were observed on the $Co_{24}Cu_{76}$ and $Co_{46}Cu_{54}$ films, respectively. It confirms that electrical property of the films is as a function of the film thickness and composition. Morphological and magnetic properties of all deposited films were clearly depended on film composition. AFM result confirms dependence of surface morphology and magnetic properties on the film composition because of the difference of the deposition rate between Co and Cu atoms during sputtering process. VSM results show that all films show ferromagnetic phase when the magnetic field was applied in perpendicular direction to the film plane. All results confirm that the desired morphological, electrical and magnetic properties of Co-Cu granular film can be achieved by distinction of its chemical composition.

MT-O-15

Microstructural and Phase Analysis of Service-exposed Ni-Cr Alloy Turbine Blade

Nuzul Hazwani Mohamad Hanafi*, **Astuty Amrin and Ayad Omran Abdalla**
UTM Razak School of Engineering & Advanced Technology,
Universiti Teknologi Malaysia Kuala Lumpur, Jalan Semarak,
541000 Kuala Lumpur, Malaysia
* nuzulhazwani@gmail.com

Keywords: Nickel-based superalloy, gas turbine blade, microstructure, service-exposed

Gas turbines are one of the most widely used in the present day for power generating technologies. Nickel-based superalloys are extensively utilized in manufacturing gas turbine components such as disks and blades, which required excellent microstructural stability and mechanical properties at elevated temperatures. Ni-Cr superalloy has commonly used in turbomachinery equipments. Gas turbine blade made from Ni-Cr superalloy experienced the effect of high temperature and stress during the service, which certainly causes various microstructural changed. This study primarily aimed to investigate the microstructural changes at various locations of turbine blade which had been exposed to service conditions. It is found that the formation of spheroidal ɤ' phase replacing the cuboidal ɤ' phase and also the formation of $M_{23}C_6$ along the grain boundaries. Numerous previous studies has been conducted and shown that the microstructure of the turbine blade was being modified by service. The study involved assessing changes in blade microstructure and mechanical properties as a function of service time.

MT-O-16

Phase Equilibria of Bi-Se-Te Thermoelectric Materials at 250 °C

Cheng-Lin Tsai[a,*] and Wojciech Gierlotka[a]

Department of Materials Science and Engineering, National Dong Hwa University, Hualien, 97401, Taiwan

sen79202@gmail.com[a,]

Keywords: Alloy, Bi-Se-Te, Thermoelectric cooler

The Ternary Bi-Se-Te system has a great attention to the thermoelectric coolers due to its excellent thermal conductivity at relatively higher temperature soldering. However, only a limited number of phase equilibrium information is available in the literature with in consistency. The 250 °C isothermal section of the ternary Bi-Se-Te system is experimentally determined in this study. Sample alloys were prepared as selected compositions by annealing at 250 °C for two month. OM and EDS examined the equilibrated alloys microstructures micro-graphically and quantitatively and the isothermal section of a phase diagram was constructed.

MT-O-17

The Effect of CSL Boundary on Carbon Nanostructure Synthesis

Sitthichok Chamnan-arsa[a], Onuma Santawitee[b], Anchalee Manonukul[b], Winadda Wongwiriyapan[c], Panya Kansuwan[a,*]

[a]*Department of Mechanical Engineering, Faculty of Engineering, King Mongkut's Institute of Technology Ladkrabang, Bangkok, Thailand 10520*

[b]*National Metal and Materials Technology Center, Pathumthani, Thailand 12120*

[c]*College of Nanotechnology, King Mongkut's Institute of technology Ladkrabang, Bangkok, Thailand 10520*

*kkpanya@kmitl.ac.th

Keywords: Carbon nanotubes, Coincidence site lattice, Nickel, Chemical vapor deposition

The effect of surface crystallographic orientation on the formation of carbon nanotubes was investigated. Chemical vapor deposition (CVD), having ethanol as carbon source under the atmospheric pressure in argon, was the method to synthesize carbon nanotubes (CNTs) directly on Ni substrates of grade N1000. The substrates were first grain boundary engineered to achieve two different proportions of ∑3-∑27 CSLBs at 45% for H-CSL and 25% for L-CSL samples. EBSD technique was used to evaluate the proportion. The analysis of synthesized products revealed a good accumulation of carbon as well as the growth of CNTs within the early 10 minutes on the H-CSL specimen. There was also a discovery of CNTs on the substrate within merely 1 minute of the synthesis time. The different factors of the proportion of CSLs which collectively represented surface crystal orientation other than surface texture could affect the role of Ni substrate to the decomposition rate of carbon containing gas or the absorption rate of decomposed carbon atoms; thus, controlled the kinetics of CNT formation.

MT-O-18

Application of the Calphad Method to the Nano-systems Calculation.

Wojciech Gierlotka

National Dong-Hwa University, Materials Science and Engineering Department, No. 1, Sec. 2, Da Hsueh Rd., Shoufeng, Hualien 97401, Taiwan, R.O.C.

wojtek@mail.ndhu.edu.tw

Keywords: nano-system calculations, Calphad method.

The Calphad method works great for calculation of the phase diagram and thermodynamic properties for more than 20 years. Recently, the nano-technology started to be one of the most important ways for improving materials properties or even develops materials with new properties. The classical Calphad method works great for bulk materials but for nano-materials it is necessary to extend the Gibbs energy and add the term connected to the surface tension. Theoretical background of application of the Calphad method to nano-system as well as calculation of bismuth-lead nano-system is shown in this presentation.

Metals, Alloys and Intermetallic Compounds Session

POSTER PRESENTATIONS

MT-P-01

Low Cost Synthesis of Superhydrophobic Aluminum Alloy for Self-Cleaning Applications

Pat Sooksaen[a, b]*, Onnuch Chulasinont [a], Wilaiwan Thovasakul [a] and Paradee Janmat [a]

[a] *Department of Materials Science and Engineering, Faculty of Engineering and Industrial Technology, Silpakorn University, Nakhon Pathom 73000 Thailand*

[b] *Center of Excellence for Petroleum, Petrochemicals and Advanced Materials, Chulalongkorn University, Bangkok, 10330, Thailand*

* *pat@su.ac.th*

Keywords: Superhydrophobic, aluminum, anodization, microstructure, absorption

This research fabricated superhydrophobic surfaces of aluminum alloy using chemical treatment methods. The procedures consisted of electrochemical anodization in 10-15 wt% sulpuric acid using 6 to 12 V DC applied voltage. Anodization produced stable oxide layer on the surface. Aluminum alloy formed porous oxide structures with pore diameter ranging from few nanometers to several micrometers. The thickness of the porous layer was affected by the anodizing conditions. The porous structure affected the dye absorption characteristics in which the dyes filled up the pore due to capillary force. In this study, the surface for further chemical treatment can be either non-colored or colored using commercially available inkjet printing inks. The later step, dichloro methylsilane was diluted using hexane or chloroform in the correct concentrations (0.1-0.5 molar) to obtain diluted solutions which had excellent absorption characteristics on the porous oxide layer by capillary effect. The aluminum alloy surfaces either non-colored or colored from the first anodization step which contained enough pore spaces and correct pore structures were then dipped coated into the silane-based solution for 10-60 min. After washing the treated surfaces with soap for many times, superhydrophobic surfaces were obtained with the wetting angle greater than 100 degrees. Water drops of any sizes or running water did not wet the surfaces at all. The treated surface can be used in self-cleaning and anti-icing applications.

MT-P-02

Corrosion Inhibition Efficiency of Pineapple Leaves for Mild Steel in Natural Water

Jatuporn Puttachaiyong[a], Kunapat Pitpanyachut[b] and Manthana Jariyaboon[a,b,c,*]
[a]Department of Chemistry, Faculty of Science, Mahidol University, Bangkok, 10400, Thailand
[b]Materials Science and Engineering Programme, Faculty of Science, Mahidol University, Bangkok 10400, Thailand
[c]Center for Surface Science and Engineering, Faculty of Science, Mahidol University, Nakhon Pathom 73170, Thailand
* manthana.jar@mahidol.ac.th

Keywords: Corrosion inhibitor; Natural extract; Mild steel; Corrosion.

This article describes a corrosion inhibition efficiency of a pineapple leaves extract on a mild steel (SS400) in natural water used for cooling system. Three different concentrations of 0.5, 1.0, and 1.5 g/L pineapple leaves extract were investigated using weight loss measurement and potentiodynamic polarisation technique. Surface morphology was investigated by optical microscope (OM) and scanning electron microscope (SEM). The pineapple leaves extract showed a capability to reduce corrosion rate of the mild steel. Adding the extract with concentrations of 0.5, 1.0 and 1.5 g/L gave a significant reduction in corrosion rate. At 1.0 g/L, it revealed the maximum corrosion inhibition. The corrosion rates were decreased from 12.55 mpy to 4.45, 3.58, and 4.60 mpy corresponding to percent inhibition efficiencies of 64.56%, 71.47%, and 63.36%, respectively. Potentiodynamic polarisation curves indicated that the extract retarded an oxidation process which could be noticed by a reduction in anodic current density associated with a shift in corrosion potential to more positive values. Thus, the extract could be identified as an anodic inhibitor. Furthermore, an increase in immersion time to 6 hours resulted that passivation region with current density was lower by 10 times compared to that of 15 minutes. A uniform corrosion could be seen on mild steel in case of without extract, whereas filiform corrosion was observed in a presence of the extract.

MT-P-03

Effect of Annealing Temperature on Mechanical Properties of Enameled Copper Wires

Somboon Otarawanna[a,*] and Bhanu Vetayanugul[a]
[a]*National Metal and Materials Technology Center (MTEC), Pathumthani 12120, Thailand*
*somboono@mtec.or.th

Keywords: magnet copper wire, wire drawing, work hardening, annealing temperature

Enameled wires are commonly made of copper or aluminum wires coated with a very thin layer of insulation. They are commonly used in the construction of electrical equipment requiring tight coils of wire, e.g. motors, transformers and speakers. In manufacturing plants of enameled copper wires, the production process usually starts with cold drawing of copper rods into wires. The copper wires are further drawn through series of dies until the desired wire diameter is reached. After wire drawing, the number of dislocations and the total length of dislocations per unit volume of crystal increase dramatically. This leads to a sharp rise in the wire's stiffness and tensile strength, and a sudden fall in its ductility. Therefore, annealing is carried out after each drawing step to restore the wire's ductility which is necessary for its drawability in subsequent drawing steps. After the final drawing and annealing pass, the bare wires are coated with polymer film insulation to provide a tough, continuous insulating layer. The coating procedure involves applying liquid polymer into bare wires and baking the polymer coating at relatively high temperature.

One of the major quality concerns of enameled wires is their stiffness. Excessively-stiff wires are not desirable because they cannot be easily wound into tight coils. Annealing temperature is one of the main factors affecting stiffness of enameled wires produced. Therefore, the effect of annealing temperature on mechanical properties of enameled copper wires was studied in this work. The research was conducted on enameled copper wires industrially produced in an enameled wire factory. Wire specimens at four stages during the manufacturing process were used for mechanical testing. The four stages are: 1) before the final drawing step, 2) after the final drawing step, 3) after the final annealing step and 4) after the enamel baking. The experimental results show that wire's ductility loss and stiffness gain during drawing could not be recovered by the normal annealing conditions used at the factory. As a result, increased annealing temperature was experimented. It has been found that the higher annealing temperature implemented could recover wire's ductility loss and stiffness gain during drawing. Furthermore, the increased annealing temperature produced enameled copper wires with less stiffness compared to the normal annealing temperature.

Polymer-based Materials Session

ORAL PRESENTATIONS

PM-O-01

Intumescent Coating on Polyester Fabric via Layer-by-layer Assembly

Warunee Wattanatanom, Pranut Potiyaraj, Sireerat Charuchinda*
Department of Materials Science, Faculty of Science, Chulalongkorn University, Bangkok, 10330, Thailand
*sireeratc@gmail.com

Keywords: layer-by-layer, intumescent, flame retardant, polyester fabric

Poly(ethylene terephthalate) or polyester (PET) fiber has been used widely for many applications in textile industries such as garments, sport wears, barrier fabrics, upholstery textiles or technical textiles. However, polyester fiber might not be safe in the case of fire incident when it melts at 249-290°C. Such molten PET could lead to serious melt dripping during combustion. The melt drips of polyester could be harmful on human skin. Furthermore, heat from this melt drips could ignite flammable materials at nearby areas rapidly. The intumescent coating is one of the most effective methods of protecting polyester fabric or its blend from fire. When heated, they form a thick, porous carbonaceous char layer. This provides an insulation of the fabric surface against an excessive increase in temperature and oxygen accessibility, thus preventing pyrolysis which plays an important role in retarding the combustion. Layer-by-Layer technique (LbL) could generate thin film on substrate by repeating an adsorption different reagent several times. It is expected that the handle touch of LBL polyester fabric could be softer than the conventional coating using binder. In this study, an intumescent coating of polyelectrolyte polyethylenimine and polyphosphate was elaborated through LbL assembly technique in order to improve the fire performance of polyester fabric. Scanning electron microscopy was used to characterize the char layer during combustion and the char residue of coated fabrics. The flame retardancy and melt dripping of LBL coated polyester fabric were also determined by vertical burning test (UL-94V).

PM-O-02

Effect of Annealed Temperature on the Preparation of Polypropylene Hollow Fiber Membrane by Melt Spinning and Stretching Method

Sang Yong Nam*, Seung Moon Woo, Deuk Ju Kim
Department of Materials Engineering and Convergence Technology, Engineering Research Institute, Jin Ju, Gyeongsangnam-do, 660-701, Korea
*walden@gnu.ac.kr

Keywords: melt spinning, stretching method, hollow fiber membrane, porous structure

In this study, microporous hollow fiber membranes were prepared by dry process. Dry process consists of three steps; first extrusion, second annealing and stretching. We spun hollow fiber precursors using semi crystalline polymer, like polypropylene (PP). The hollow fiber precursors were extruded through a single screw extruder equipped with tube-in-orifice structure spinneret. Hollow fiber precursor can be successfully obtained by controlled take-up speeds. The hollow fiber precursors were annealed in oven at 100, 120 and 140 ℃ respectively. And then stretching of annealed hollow fiber precursor was performed by various methods such as cold stretching, hot stretching and cold/hot stretching. Morphology of surface and cross section of membrane were measured by field emission scanning electron microscope (FE-SEM). The optimized preparation condition for the microporous hollow fiber membrane was confirmed through measurement of various take up speed, annealing and stretching condition.

PM-O-03

Effect of Fiber Surface Modification on Properties of Artificial Leather from Leather Fiber Filled Natural Rubber Composites

Jutaporn Sakmat, Azizon Kaesaman*, Natinee Lopattananon
Rubber Technology and Polymer Science Department, Faculty of Science and Technology, Prince of Songkla University, Pattani Campus, Pattani 94000, Thailand.
*kazizon@bunga.pn.psu.ac.th

Keywords: Leather fiber, Natural rubber, Composite, Neutralizing agent

Artificial leather based on natural rubber (NR) filled with leather fibers was prepared using a hot pressing process. The leather fiber was obtained by shredding chrome-tanned leather into fibers with the sizes of 20-mesh. Three different modifying agents (i.e., 1% aqueous solutions of sodium hydroxide, urea, and sodium bicarbonate) were used in the modified of leather fibers. Mechanical properties of NR composites filled with 100 phr of modified or unmodified leather fibers were then investigated. The results showed that cure characteristics, tensile properties, tear strength and abrasion resistance of the composite combined with the modified leather fibers were clearly improved, compared to those of the simple unmodified leather fiber composite. Furthermore, interfacial adhesion between the leather fiber and natural rubber was found to improve. From this study, the result suggested that the urea solution provided the best property improvement when the other modifying agents were compared with.

PM-O-04

Characterizations of Silicon Carbide Whisker-Filled in Benzoxazine-Epoxy Shape Memory Polymers

Chutiwat Likitaporn, Sarawut Rimdusit*

Polymer Engineering Laboratory, Department of Chemical Engineering, Faculty of Engineering, Chulalongkorn University, Bangkok, 10330, THAILAND.

*E-mail: sarawut.r@chula.ac.th

Keywords: Shape memory polymer, Benzoxazine, Epoxy, Silicon carbide whisker

Shape memory polymers (SMPs) are polymer materials that can fix the temporary shape and then recover to their original permanent shape by external stimulation, i.e. apply heat. In this research, shape memory polymer composites (SMPCs) from benzoxazine (BA-a)-epoxy binary systems reinforced with adamantine silicon carbide whisker (SiC_w) are investigated. The SiC_w contents are controlled to be in range of 0 to 20 % by weight. All specimens were fabricated by compression molding technique. The results revealed that the shape memory polymer composites showed higher glassy state storage modulus with increasing amount of the whisker suggesting substantial reinforcement effect of the whisker used. The glass transition temperature was also improved from 102ºC of the based polymer to the value about 122ºC with the addition of about 15% by weight of the silicon carbide whisker. The shape fixity determined from the modulus ratio of the sample is nearly 98% for all the composite samples. Finally, the shape recovery ratios tended to decrease from the value of about 99% of the unfilled polymer matrix to the value about 91% with an addition of 5% by weight of the silicon carbide whisker. The enhancement on recovery stress is also expected from the modification and will be reported in this work.

PM-O-05

Improvement of Structure and Properties of Nanocomposite Foams based on Ethylene-Vinyl Acetate (EVA)/Natural Rubber (NR)/Nanoclay: Effect of NR Addition

Juthapat Julyanon[1], Azizon Kaesaman[1], Tadamoto Sakai[2] and Natinee Lopattananon[1*]
[1] *Department of Rubber Technology and Polymer Science, Faculty of Science and Technology, Prince of Songkla University, Pattani 94000, Thailand*
[2] *Tokyo office, Shizuoka University, 3-3-6 Shibaura, Minato, Tokyo, 108-0023, Japan*
*Inatinee@bunga.pn.psu.ac.th

Keywords: Ethylene-vinyl acetate; Natural rubber; Nanocomposite; Foam

Nanocomposite foams made of ethylene-vinyl acetate (EVA), natural rubber (NR) and nanoclay were fabricated by mean of melt mixing in an internal mixer, and later foaming using azodicarbonamide through compression molding. Effect of NR addition (10-40 phr) into the EVA nanocomposite foam was studied. Characterizations by using Oscillating disk rheometer, X-ray diffraction (XRD), scanning electron microscopy (SEM) and mechanical tests were performed. The XRD analysis showed that the clay was mainly intercalated by the rubber. The SEM analysis revealed that the EVA/NR nanocomposite foams had closed-cell structures. Foaming EVA/clay led to low cell density and large cell size. The EVA nanocomposite foam also had low tensile strength, low compressive strength and low elastic recovery. However, the foam cell structure, i.e., greater cell density and smaller cell size, was obtained with addition of NR. Moreover, the strength and elastic recovery of the EVA nanocomposite foam were improved when the NR was added, and the improvement level was increased with increasing NR content.

PM-O-06

Effect of Electric Field on Conductive Network Formation in Polyvinylidene Fluoride/Carbon Nanotube Composites

Rungsima Yeetsorn[a,b*], **Noppavan Chanunpanich**[a,b]
[a]*Department of Industrial Chemistry, Faculty of Applied Science, King Mongkut's University of Technology North Bangkok, Bangkok 10800, Thailand*
[b]*Integrated Nanoscience Research Center, King Mongkut's University of Technology North Bangkok, Bangkok 10800, Thailand*
*rmy@kmutnb.ac.th and ryeetsorn@hotmail.com

Keywords: Polyvinylidene fluoride composite, Conductive Network, Fiber alignment, Electric field

This work demonstrates how the electric field can assist electrically conductive network forming. Static dissipative films of polyvinylidene fluoride /multiwall carbon nanotube composites were prepared via solution casting under an electrical field. The volume and surface electrical conductivity of the composite films were 10^3 and 10^2 times greater than the values of the film prepared without an electric field. This improvement has been rationalized in terms of multiwall carbon nanotube movement and alignment into the polyvinylidene fluoride matrix along the direction of an electric field. The parameters such as viscosity of polyvinylidene fluoride solution, field strength (or voltage) and MWCNTs loading, which are important for a desired composite film fabrication, were varied. During the film casting period the movement of carbon nanotubes was monitored, and the result showed that carbon nanotubes could rotate and connect to adjacent carbon nanotubes. The connecting of the carbon nanotubes became the fiber network called the electrically conductive network. Composite films' electrical conductivity of both volume and surface conductivity indicated that DC field caused significantly higher electrical conductivity values than non-electric fields. Furthermore, the electrical conductivity of the composite film could be enhanced with increasing an applied voltage. The polyvinylidene fluoride /multiwall carbon nanotube composite film with 1.5 wt% of carbon nanotube loading, under an electric field of 600 V/cm exhibited volume and surface conductivity of 1.3×10^{-7} S/cm and 1.01×10^{-7} S/cm, respectively. The composite is promising to be a static dissipative material for an electronic packing production. The results of this research provide an initial understanding of how electric fields can be applied to control the electrically conductive network creation.

PM-O-07

Photocatalytic Activity and Properties of Nanotitanium Dioxide-filled Natural Rubber in the Presence of Coupling Agents

Pornsiri Toh-ae[a,*], Banja Junhasavasdikul[b], Natinee Lopattananon[a] and Kannika Sahakaro[a]

[a]*Department of Rubber Technology and Polymer Science, Faculty of Science and Technology, Prince of Songkla University, Pattani Campus, Pattani, 94000 Thailand*

[b]*Research and Development Center, Innovation Group (Thailand) Company Limited, Bangkok, 10240 Thailand*

*skannika@bunga.pn.psu.ac.th

Keywords: NR compound, Titanium dioxide nanoparticles, Coupling agent

For rubber compounds, titanium dioxide (TiO_2) is normally used as a white pigment and inorganic filler for an improvement of thermal property. TiO_2 is also known to have an outstanding photocatalytic activity. This work investigates the properties of natural rubber (NR) compounds filled with 5 phr of nanosize TiO_2 (n-TiO_2). The n-TiO_2 was prepared by ultrasonication and their particle sizes were characterized by laser light scattering particle size analyzer. Since the direct incorporation of n-TiO_2 into NR encounters incompatibility problem, two types of coupling agent (i.e. bis-(3-triethoxysilylpropyl) tetrasulfide (TESPT) and isopropyl trioleyl titanate (ITT)) were used. The coupling agent loading was varied in a range of 0-20 wt% relative to n-TiO_2. The filled NR compounds were tested for their Mooney viscosities, cure characteristics, tensile properties and photocatalytic activity by means of a degradation of methyl orange solution. Mooney viscosities and minimum cure torque (M_L) of the compounds increase with increasing coupling agent content and the ones with ITT show higher viscosity than the mixes with TESPT. The use of TESPT leads to shorter optimum cure time and higher torque difference compared to the use of ITT, but the increase of loading causes only small changes. The addition of n-TiO_2 results in the improved modulus, reinforcing index and tensile strength compared to the unfilled vulcanizate. The NR with n-TiO_2/ITT shows higher 300% modulus and reinforcing index, but lower tensile strength and elongation at break compared to the compound with TESPT. The compounds with ITT show optimum 300% modulus and tensile strength at 10 wt% relative to TiO_2, whereas the increase of TESPT content gradually increase the 300% modulus and level off the tensile strength after reaching 10 wt% relative to TiO_2. On comparing to the n-TiO_2 filled NR vulcanizates without coupling agent, the presence of both TESPT and ITT significantly reduces a photodegradation efficiency. The increase of ITT content causes no further reduction but the increase of TESPT content remarkably decreases the photodegradation efficiency. The difference in both properties and photocatalytic activity of n-TiO_2 filled NR having TESPT and ITT as coupling agent indicates their possible different level of dispersion and interactions at the interphases.

PM-O-08

Organomodification of Clay and its Influence on the Thermal, Mechanical and Fire behavior of Clay/Fire additives/Vinylester Composites

K R Vishnu Mahesh*[a], H N Narasimha Murthy[b], B E Kumara Swamy[c] Raghavendra[b], M Krishna[b], H P Nagaswarupa[d]

[a] *Department of Chemistry, ACS College of Engineering Mysore Road, Bangalore-560074, Karnataka, India*

[b] *Department of Mechanical Engineering R V College of Engineering, Bangalore -560059, Karnataka, India*

[c] *Department of P.G Studies and Research in Industrial Chemistry Kuvempu University, Shankaraghatta, Shimoga-577451, Karnataka, India*

[d] *Department of Science, Research center, East West Institute of Technology Bangalore - 560091, Karnataka, India*

***Email:** vishnumaheshkr@gmail.com

Keywords: Nanocomposites, Fire additives, Nanoclay, Vinylester.

Some customers are reluctant to change, because the commercial available organomodified clays are may have higher cost. This is one of the reasons that the in-house modification of clays is always the subject for researchers to pursue. In the current study the low cost clays are collected locally (Indian Bentonite) is not susceptible to polymer due to its organophilic character and low basal spacing. The primary objective of this study was to improve clay platelets separation by organically modifying it with a cation exchanges using Cetyl Trimethyl Ammonium Bromide (CTAB). The basal spacing, presence of functional groups, Zeta-potential with particle size analysis and thermal stability of the Organomodified clay were characterized using XRD, FTIR, Zeta-potential analyzer and TGA respectively. The twin screw extrusion was used to disperse modified clay along with fire additives (Aluminium Tri Hydroxide (ATH) and Magnesium Hydroxide (MH)) in to Vinylester resine and further studied the degree of dispersion using XRD TEM and AFM. The organomodified clay in vinylester composite exhibited exfoliation and distribution of clay platelets which were superior to that of unmodified clay in vinylester composite. The thermal decomposition, glass transition temperature, fire retardation behaviour and micro hardness of the unmodified and modified clay dispersed vinylester composite were studied using DSC, TGA, VBR, HBR, LOI and vicker's hardness test. The synergistic effect of organomodified clay and 30 % ATH increased the glass transition temperature by 18 % and reduced thermal degradation by 47 %. The VBR was improved by 51 %, HBR by 68 %, and LOI by 52 % when compared with that of bare vinylester composites. The increase in micro hardness for 4 wt% organomodified clay/30%ATH/vinylester was up to 85 % compared to that of unmodified clay/fire fire additive/vinylester composite. Further studied the mechanical properties like UTS, FS, ILSS and Impact strength for the glass fibre reinforced organomodified clay/vinylester FRP composites. At the high filler levels, a marked deterioration in mechanical properties and significant viscosity increases, can limit the mechanical performance and their selection for more demanding applications. Hence, reducing filler level without compromising fire retardancy is needed. The uses of fire additives acting in a synergistic manner are the most promising ways to achieve this goal. The modified clay role and synergistic mechanism has been discussed in the paper in terms of the barrier mechanism in the condensed phase and interfacial bond strength.

PM-O-09

Biaxially-Stretched Poly(lactic) Acid (PLA) and Rubber-Toughened PLA Films:Tensile and Physical Properties

Lalintip Boonthamjinda [a], Nawadon Petchwatana [b], Wannee Chinsirikul [c], Noppadon Kerddonfag [c], Sirijutaratana Covavisaruch[a]*

[a] *Department of Chemical Engineering, Faculty of Engineering, Chulalongkorn University, Bangkok, 10330, Thailand*

[b] *Faculty of Agricultural Product Innovation and Technology, Srinakharinwirot University, Bangkok, 10110, Thailand*

[c] *Polymer Research Unit, National Metal and Materials Technology Center(MTEC), Pathum Thani, 12120, Thailand*

*E-mail address corresponding author: sirijutratana.c@chula.ac.th

Keywords: Polylactic acid, Biaxial stretching, Rubber toughening, Bioplastic

Bio-based plastic such as polylactic acid (PLA) is gaining more interest as a substitute of petroleum-based plastics. Despite its growing application in packaging, PLA is still rather brittle. So its weakness has become a major challenge for research endeavors. The objective of this study is to investigate the influences of the biaxial stretching conditions namely the stretch temperature and the stretch ratio of neat PLA film as well as the rubber-toughened ones. A series of the PLA films toughened with core-shell rubber (CSR) in the range of 0 to 10 wt% was prepared by extrusion casting through a slit die to form precursor films and sheets with 30, 270 and 480 μm in thickness. The 270 and 470 μm sheets were simultaneously stretched biaxially at the stretch ratio of 3x3 and 4x4 under the controlled temperatures of 75°C and 80°C. Differential scanning calorimetry (DSC) results revealed the degree of crystallinity of all the as-cast films to be around 1-2%; those of the 3x3/75°C, 3x3/80°C and 4x4/80°C films jumped to 20%, 27% and 25% respectively regardless of the rubber content, implying that greater stretch ratio and elevated temperature induced higher degree of crystallinity. Mechanical tests in terms of tensile properties showed that the modulus of all the as-cast and the biaxially-stretched films remained relatively unchanged at around 3 GPa. Rather significant increment was seen in the tensile strength; that of the 3x3/75°C films and the 3x3/80°C films increased by 1.8 and 2.0 times respectively, while the tensile strength of the 4x4/80°C films did by 2.3 to 2.5 times in both machine direction (MD) and transverse direction (TD) as compare to the as-cast films. All the stretched films endured greater tensile strength as a result of enhanced crystallinity along with higher orientation in the stretched directions. However, an increase in the rubber content led to a drop in the tensile strength from around 90 MPa in the 3x3/80°C neat PLA film to 50 MPa in the 3x3/80°C with 10 wt% CSR film. For as-cast films, an addition of only 1 wt% CSR was found to effectively elevate the elongation at break of the toughened PLA as-cast to 17% from 5% of the neat PLA as-cast. The elongation at break of the biaxially-stretched films was raised with greater CSR content. Having been stretched at 3x3/75°C, 3x3/80°C and 4x4/80°C the films with 10% CSR content exhibited greater elongation than the as-cast

film by 70%, 100% and 50% respectively. The elongation at break of the 3x3/80°C neat PLA film was 70 % while that of the 3x3/80°C with 10 wt% CSR film was 80%. Subsequent test for tear strength showed that the tear resistance of the 3x3/75°C, 3x3/80°C and 4x4/80°C films with 10% CSR also jumped from 200 N/m in both directions of the as-cast films to 500 N/m for both the 3x3/75°C and the3x3/80°C films, and to only 300 N/m for the 4x4/80°C films. The stretch temperature seemed to have no significant influence on the tear strength, which was found to decline upon further stretching. Physical properties important for packaging applications were tested in terms of water vapor permeation and transparency. Biaxial stretching diminished water vapor permeation in all the stretched films regardless of the stretch ratio, the stretch temperature and the rubber contents. Both the neat PLA and the CSR toughened 3x3/80°C films were found to have the lowest water vapor permeation of only 200 g.mil/(m^2.day) compared with the maximum permeation of 350 g.mil/(m^2.day) found in the as-cast film with 10 wt% CSR due to an increase in crystallinity and polymer chain orientation upon stretching. All of the biaxially-stretched films were visibly more transparent than the as-cast one; this was verified by the decline of the haze measurements to 25.2 of the 4x4/80°C with 10 wt% CSR film from 51.4 of the as-cast with 10 wt% CSR film. Increasing the rubber content strengthened the impact resistance of the as-cast film and the elongation at break but weakened the tensile strength, tear resistance and the clarity of the films. Raising the stretch temperature tended to decrease the water vapor permeation. Increasing the stretch ratio enhanced the tensile strength and elongation at break but weakened the tear resistance.

PM-O-10

Thermal Properties of Banana Starch Nanocrystals Prepared by Acid Hydrolysis as Reinforcing Filler

Jittiporn Saeng-on, Duangdao Aht-Ong*
Department of Materials Science, Faculty of Science, Chulalongkorn University, Bangkok, 10330, Thailand
Center of Excellence on Petrochemical and Materials Technology, Bangkok, 10330, Thailand
*duangdao.a@chula.ac.th

Keywords: Banana, Starch Nanocrystal, Acid Hydrolysis, Thermal Properties

Banana is one of the most important tropical fruits in Thailand. It is available throughout the year, i.e., not have a growing season resulting to the low cost. All parts of banana plant can be used, particularly its fruit has several multipurposes in term of how to eat it. However, banana is ripe and perishable easily. Therefore, it is considered as a potential resource that can be utilized and developed in order to add more value of raw materials. In this work, green banana fruits were used as a raw material for preparing a starch nanocrystal reinforcing filler in bio-nanocomposites. The green banana was extracted as banana starch by using 0.05N sodium hydroxide solution. The composition of the obtained banana starch contained 90.61% of starch, 18.82% of amylose, 0.19% of protein, 0.11% of ash, and 0.03% of lipid. The banana starch composition exhibited low contents of protein, ash, and lipid (<0.5%) indicating that the obtained banana starch was pure enough to be used. After that, starch nanocrystal (SNC) was prepared from banana starch by acid hydrolysis with 3.5 M sulfuric acid and 3.0 M hydrochloric acid at 40^{o}C for 5 hours. The obtained banana SNC showed an increase of degree of crystallinity from 28.03% of native banana starch to 45.13% and 40.15% of banana SNC with sulfuric acid and hydrochloric acid hydrolysis, respectively. Furthermore, the thermal properties of banana SNC were investigated by differential scanning calorimeter (DSC) and thermogravimetric analyzer (TGA) in order to assess thermal stability of banana SNC for using as reinforcing filler in bio-nanocomposite. The decomposition temperature of native banana starch and SNC was in the range of 310-345^{o}C. The gelatinization temperature of banana SNC increased as a result of the increment of its degree of crystallinity when comparing with native starch.

PM-O-11

Influences of Starch Types on Reactive Dye Removal Efficiency of Eggshell Powder/Thermoplastic Starch Foam Bio-Composites

Supitcha Yaisun[a], Nuttawan Pramanpol[b], Tatiya Trongsatitkul[a,*]

[a]*School of Polymer Engineering , Suranaree University of Technology, Muang District Nakhon Ratchasima, 30000, Thailand*

[b]*Synchrotron Light Research Institute, Muang District Nakhon Ratchasima, 30000, Thailand*

*E-mail: tatiya@sut.ac.th

Keywords: thermoplastic starch, bio-composite, eggshell-powder, adsorption

This study described the use of eggshell powder (ESP)/thermoplastic starch foam bio-composites for the removal of reactive dye model (Reactive blue 171) from aqueous solutions. Three thermoplastic starch foams were prepared with three different types of starch i.e. cationic, cross-linked, and native starch using twin screw extruder. 20 phr of water and 20 phr of glycerol were used as a blowing agent and a plasticizer, respectively. The investigation of dye removal efficiency of the thermoplastic starch foams was performed using UV-Vis spectrophotometry and revealed that cationic thermoplastic starch foam had the maximum removal efficiency of Reactive blue 171 from aqueous solution at equilibrium (24 h). Scanning electron microscopy showed that the cell structure and morphology of the thermoplastic starch foams were slightly different indicating that the difference in removal efficiency was mainly due to the chemical composition of the starch. ESP 20 wt.% was incorporated into the thermoplastic starch foams to increase their adsorption capability. SEM micrograph showed that the presence of ESP improved porous uniformity of all foams. The dye removal efficiency was also increased in all three bio-composite foams (6-13%) due to an increased surface area introduced to the foams by ESP. The aim of this study is to fabricate fully bio-composite foams that may be environmentally-friendly utilized in waste water treatment of garment/textile industry.

PM-O-12

Fabrication and Application of Nanostructures using gas-assisted Hot Embossing and Self-Assembled Nanospheres

Rong-Hong Hong, Nai-Wen Chang, To-Chung Shu, Sen-Yeu Yang *
Department of Mechanical Engineering, National Taiwan University, Taipei 106, Taiwan
*E-mail syyang@ntu.edu.tw

Keywords: Antireflective, Self-assemble, Nanospheres, Electroforming, Gas-assisted hot embossing.

We develop a simple and competitive fabrication of antireflective (AR) films with high-ordered nanostructures arrays on polycarbonate (PC) substrate by using gas-assisted hot embossing and self-assembled technique. In this method, a self-assembled monolayer of polystyrene (PS) nanospheres is well-patterned on glass substrates as the first template. Subsequently, we use the plasma sputtering to deposit conductive layer onto the surface of nanospheres patterned substrates, and then electroforming is applied to fabricate a nickle mold with inverse shape of nanosphere. In the last step, the unique glass transition specific is utilized to duplicate nanostructures on PC films via gas-assisted hot embossing. Not only in visible light but in near inferred, the optical properties of this AR film are similar or better than other methods. This fabrication process also has great potential in industry, such as simple, large-area but low-cost.

PM-O-13

Microscopic Configuration of Energy Donor-Acceptor Pairs in Organic Thin Films Studied by Selectively Excited Photoluminescence

T. Otake*, **Y. Ishimaru, N. Kamata, and T. Fukuda** *Department of Functional Materials Science, Saitama University, Shimo-Ohkubo, Sakura-ku, Saitama, 338-8570, Japan*
*s13mp202@mail.saitama-u.ac.jp (T.Otake)

Keywords: resonant energy transfer, $Ir(ppy)_3$, Rhodamine B, phosphorescence.

Resonant energy transfer between donor (D) and acceptor (A) molecules has widely utilized for organic light-emitting diodes, phosphors and biosensors etc. The light emission efficiency is governed not only by the energy transfer rate determined by the intermolecular distance $r_{D\text{-}A}$, but energy migration and resultant quenching due to molecular stacking or precipitates, whose degree is schematically represented by $r_{D\text{-}D}$ and $r_{A\text{-}A}$ (Fig. 1). We have shown a clear difference in such microscopic configuration of organic thin films with the same composition but different fabrication processes by studying selectively excited photoluminescence (PL) at room temperature.

We chose *tris*-(2-phenylpyridinato)iridium(III) ($Ir(ppy)_3$) and Rhodamine B (RhB) as an energy donor-acceptor pair, added them into polymethylmethacrylate (PMMA) which was dissolved in 1, 2-dichloroethane. The solution was then spin-coated (samples S) or sprayed by electrostatic spray deposition (ESD) method (samples E) onto a pre-cleaned quartz glass substrate with varying layer thicknesses from 100nm to 1,100nm.

In PL measurements, donor excitation (376nm) was used to obtain the intensity ratio between A and D emissions I_A/I_D (Fig. 2) as a result of the resonant energy transfer. The intensity ratio of samples S showed higher I_A/I_D for the region thicker than 400nm, reflecting smaller $r_{D\text{-}A}$ and higher resonant energy transfer rate. The peak wavelength shift of the acceptor emission under the acceptor excitation (520nm) showed a degree of π-π stacking in RhB (Fig. 3). A smaller peak wavelength shift of samples S below 600nm thickness, which implies less contribution of molecular stacking (smaller $r_{A\text{-}A}$), is consistent with the results of the I_A/I_D.

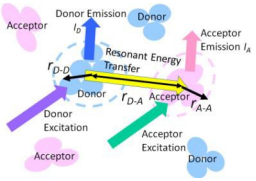

Fig. 1. A schematic representation of molecular configuration.

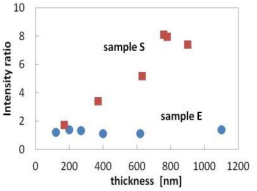

Fig. 2. Thickness dependence of the PL intensity ratio I_A/I_D.

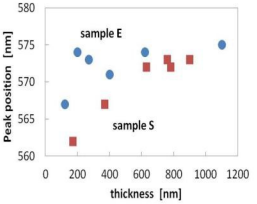

Fig. 3. The peak position of the acceptor emission.

The systematic study on PL by selective excitation reveals a different microscopic configuration of energy donor-acceptor molecules with the same macroscopic composition, which can be utilized for optimizing thin film processes as well as thin film devices.

PM-O-14

Polycarbonate Track-Etched Membranes by Nuclear Fission Reaction: Preparation and Characterization

Suwimol Jetawattana[a,*], Roppon Picha, Pipat Pichestapong, Wichian Ratanatongchai
[a]*Research & Development Group, Thailand Institute of Nuclear Technology (Public Organization), Ongkharak, Nakhon Nayok, 26120, Thailand*
*sjetawattana@hotmail.com

Keywords: track-etched membrane, polycarbonate, nuclear fission products

Track-etched polymer microporous membranes are being used in a wide range of industries such as biotechnology, pharmaceutical, cosmetic, food processing, electronic circuitry including the treatment of waste water and fluids. We prepared uniformly-sized and cylindrical pores on polycarbonate thin film using the nuclear fission reaction (nf) and chemical etching methods. A uranium oxide-coated plate was attached to 6-μm-thick commercial polycarbonate sheets before being bombarded with thermal neutrons (flux of 8.9×10^9 n cm^{-2} s^{-1}) from the thermal column of Thai Research Reactor-1/Modification-1 (TRR-1/M1) for 15 min. The paths of nuclear fission products were collimated to perpendicularly impact the membrane surface by an interlaid 5-mm-thick particle screener. The latent tracked membrane was then chemically etched with sodium hydroxide solution at 6 N, 60°C for 60 min. The monodisperse porous membrane obtained has average pore density 1.04 x 10^6 pore/cm^2 with average pore diameter 1.68 μm as determined by scanning electron microscope (SEM). The density and size of the pores on the membranes can be effectively varied by adjusting the time of exposure and etching conditions. The physical properties such as fluid (water and air) flow rates, molecular weight cutoff, and mechanical properties were also analyzed. The successfully prepared polycarbonate track-etched membranes by nuclear fission reaction will be beneficial in providing low-cost, locally manufactured membranes for various applications.

PM-O-15

Thermal and Mechanical Properties of Acrylonitrile-butadiene Rubber Modified Polybenzoxazine as Frictional Materials

Jakkrit Jantaramaha, Sarawut Rimdusit*
Polymer Engineering Laboratory, Department of Chemical Engineering,
Faculty of Engineering, Chulalongkorn University, Bangkok, 10330, THAILAND.
*E-mail: sarawut.r@chula.ac.th

Keywords: Polybenzoxazine, Acrylonitrile butadiene rubber, Frictional composite

Frictional composites of polybenzoxazine (BA-a) and acrylonitrile butadiene rubber (NBR) are developed in this study. Mechanical and thermal properties of the BA-a/NBR composites were evaluated. The composites with 0, 2, 5, 10, 15 and 20 wt.% of NBR powder were prepared by compounding in an internal mixer at 110°C for 1 hour and shaping in a compression molder at 200°C for 2 hours. Curing behaviors of the NBR-benzoxazine molding compounds were detected by differential scanning calorimetry to show an onset temperature of about 185°C compared with the value of 195°C of the benzoxazine resin suggesting curing acceleration of the resin due to the presence of the NBR particles. The storage modulus of the NBR-filled polybenzoxazine was observed to systematically decrease from the value of 5.9 GPa of the neat polymer to the value of about 3 GPa with an addition of 10% by weight of the rubber powder. Glass transition temperature (T_g) evaluated by dynamic mechanical analysis was determined to be 184°C for BA-a and was observed to increase to the value of about 190°C with an addition of 10% by weight of the NBR. Effect of the rubber particles on thermogravimetric properties as well as friction coefficients of the composites will also be evaluated and reported in this study.

PM-O-16

Influence of Processing Oil Based on Modified Epoxidized Vegetable Oil with N-Phenyl-*p*-Phenylenediamine (PPD) on Extrusion Process Behaviors of Natural Rubber Compounds

Chalida Moojea-te*, Adisai Rungvichaniwat, Kannika Sahakaro
Department of Rubber Technology and Polymer Science, Faculty of Science and Technology, Prince of Songkla University, Pattani Campus, Pattani 94000, Thailand
*E-mail: chalida.moo@gmail.com

Keywords: aromatic oil, extrudability, modified epoxidized vegetable oil, processing oil

Rubber processing oil based on modified epoxidized vegetable oils (m-EVO) was prepared by a reaction of epoxidized palm oil (EPO) or epoxidized soybean oil (ESBO) with N-Phenyl-p-phenylenediamine (PPD) at a mole ratio of 1: 0.5. The comparison of m-EVO with aromatic oil (Treated distillate aromatic extract, TDAE) on extrusion process behaviors (output rate, extrusion rate, screw efficiency, heat generation, die swell, extrudate appearance) of carbon black (N330) filled natural rubber (NR) compound was made. It was found that the m-EVO based NR compounds showed higher Mooney viscosity (ML(1+4)100°C: m-ESBO 65.5±0.7; m-EPO 59.7±0.2; TDAE 56.5±1.0) leading to lower output rate (g/min: m-ESBO 191.0±0.6; m-EPO 191.2±0.4; TDAE 195.5±0.6), extrusion rate (cm^3/min: m-ESBO 179.6±0.6; m-EPO 183.2±0.4; TDAE 186.4±0.6) and screw efficiency (%: m-ESBO 30.8±0.6; m-EPO 31.4±0.4; TDAE 32.0±0.6) when compared with the TDAE based NR compound. However, the values of extrusion process behaviors of the m-EVO based NR compounds were slightly lower than those of TDAE compound. On comparing the influence of the modified epoxidized palm oil (m-EPO) and the modified epoxidized soybean oil (m-ESBO) on NR compound extrusion process behaviors, it was found that the m-ESBO based NR compound showed higher Mooney viscosity leading to lower output rate, extrusion rate and screw efficiency when compared with the m-EPO based NR compound. Heat generation (°C: m-ESBO 61.0±0.8; m-EPO 62.1±0.4; TDAE 63.1±1.0) and die swell (%: m-ESBO 11.0±0.7; m-EPO 11.0±0.5; TDAE 12.7±0.3) of the m-EVO based NR compounds were lower than those of the TDAE based NR compound. The heat generation, die swell and extrudate appearance of the m-EPO and the m-ESBO based NR compounds were not significantly different. Consequently, the m-EVO can be used to replace the petroleum-based aromatic processing oil, in which the m-EPO is more interesting than the m-ESBO due to its greater plasticizing efficiency.

PM-O-17

Effect of Various Extracted Solvents on DPPH Radical Scavenging Activity of Natural Rubber

Suwimon Siriwong*, Adisai Rungvichaniwat, Pairote Klinpituksa
Department of Rubber Technology and Polymer Science, Faculty of Science and Technology, Prince of Songkla University, Pattani campus, Pattani, 94000, Thailand
Phone: +66-81767-6903, Fax : +66-7333-1099,
*E-mail: suwimonsiriwong@yahoo.com

Keywords: Natural Rubber, DPPH scavenging activity, Oxicount Antioxidant kit test, Plasticity retention index

Four types of extracted solvents i.e. mixtures of chloroform : acetone, chloroform : methanol, cyclohexane : acetone and cyclohexane : methanol, in the ratio of 4:1 were used to dissolve the natural rubber. Two grades of natural rubber i.e. air dry sheet (ADS) and ribbed smoked sheet No.3 (RSS3) were investigated. The rubber solution was purified by separated the rubber out with methanol. The non-rubber solution was then quantitative analyzed to verify DPPH radical scavenging activity using Oxicount Antioxidant kit test and also calculated the term half maximal effective concentration (EC50). The plasticity retention index (PRI) of ADS and RSS3 were also investigated in order to compare the ageing properties of the rubber and antioxidant activity results. Furthermore, various rubbers i.e. ADS, RSS3 and standard thai rubber 20 (STR20) was collected during early period of tapping seasons (May, June and July) to analyze the %DPPH radical scavenging activity and EC50. It was found that the mixture of cyclohexane and methanol showed the highest %DPPH radical scavenging activity and lowest EC50. Moreover, RSS3 showed higher %DPPH radical scavenging activity than that of ADS which the higher antioxidant activity also display the higher PRI values. It also found that during the early stage of tapping, the rubber samples which are extracted by mixture of cyclohexane and methanol, showed very little different of %DPPH radical scavenging activity and EC50 in the three months period of sampling. In addition, it also confirmed that RSS3 showed higher %DPPH radical scavenging activity than that of ADS and STR20, respectively.

PM-O-18

Properties of Deproteinized Natural Rubber Latex/Gelatinized Starch Blended Films

Rungtiwa Waiprib[a], Wiwat Pichayakorn[a,b,*], Prapaporn Boonme[a], Wirach Taweepreda[b,c] and Jirapornchai Suksaeree[d]

[a]*Department of Pharmaceutical Technology, Faculty of Pharmaceutical Sciences,*
[b]*Medical Products Innovations from Polymers in Clinical Use Research Unit,*
[c]*Department of Materials Science and Technology, Faculty of Science,*
Prince of Songkla University, Songkhla 90112, Thailand
[d]*Department of Pharmaceutical Analysis Chemistry, Faculty of Pharmacy,*
Rangsit University, Pathum Thani 12000, Thailand
[*]E-mail address corresponding author: wiwat.p@psu.ac.th

Keywords: Deproteinized natural rubber latex, Gelatinized starch, Blend, Film

Natural rubber latex has been wildly used to produce many types of products because of excellent physicomechanical properties. Gelatinized starch is the modified starch that improves property of native starch. This research aimed to study the compatibility and properties of deproteinized natural rubber latex (DNRL)/gelatinized starch blended films for use as transdermal patches. Various starches were previously gelatinized by heat treatment. Then, the DNRL/gelatinized starch blended films were prepared by simple mixing of DNRL with gelatinized starch and then dried at 50ºC. The various parameters such as types (potato, sago, bean, corn, tapioca, rice and glutinous starches), amounts (5, 10, 15 and 20 part per hundred of rubber (phr)) and concentrations of gelatinized starch pastes (5, 10, 20 and 50%) were evaluated. It was found that all starch types could be blended as a homogeneous mixture with DNRL only in 5 phr. Bean starch also provided the good mixture in 10 and 15 phr. Rice and corn starches in the concentrations up to 20 phr could also be blended. Higher concentration of gelatinized starch pastes obtained the higher viscous liquids that were difficult to blend as a homogeneous mixture with DNRL, and provided inhomogeneous blended films. The dried films of all homogeneous DNRL/gelatinized starch mixtures were slightly yellowish transparent with good physical appearances. The tensile strength, swelling and erosion of these blended films increased when increasing amounts of gelatinized starch, but their elasticity was not different comparing to the DNRL itself. Their compatibilities were observed by differential scanning calorimetry, scanning electron microscopy and Fourier transform infrared spectroscopy. However, their elasticities should be further improved by adding some plasticizers. Moreover, these homogeneous film formulations were further loaded with lidocaine for transdermal delivery.

PM-O-19

Fabrication of Novel Polyhydroxybutyrate-co-Hydroxyvalerate (PHBV) Mixed with Natural Rubber Latex

Karndarthip Kuntanoo[a,*], Sarunya Promkotra[b], Pakawadee Kaewkannetra[c]

[a]*Graduate School of Khon Kaen University, Khon Kaen, 40002 Thailand*

[b]*Department of Geotechnology, Faculty of Technology, Khon Kaen University, Khon Kaen 40002 Thailand*

[c]*Department of Biotechnology, Faculty of Technology, Khon Kaen University, Khon Kaen 40002 Thailand*

*thip_kk@hotmail.com

Keywords: Polyhydroxybutyrate-co-hydroxyvalerate (PHBV), Natural rubber latex, Natural rubber (NR), Biopolymer

Polyhydroxybutyrate-co-hydroxyvalerate (PHBV) was mixed with natural rubber latex to make better the material. The various ratios between PHBV and natural rubber latex were examined to improve their mechanical properties. The PHBV are solid, easily broken while natural rubber (NR) is excessive elastic materials. Concentrations of the PHBV solution employed were 1%, 2% and 3% (w/v). The PHBV solution and natural rubber latex mixtures of their three different ratios of 4:6, 5:5 and 6:4 respectively were fabricated into films. They films were characterized using electron microscope (SEM), universal testing machine (UTM) and differential scanning calorimetry (DSC). The SEM photographs of the mixed films and the unmixed PHBV yielded the void distribution around 12-14% and 19-21%, respectively. For mechanical properties, the averaged elastic moduli of 1%, 2% and 3% (w/v) PHBV mixed films were 773, 956 and 1,007 kPa, respectively. The tensile strengths of the mixed increased with the increasing concentrations of PHBV. Similar trend was also found in elastic modulus. The crystallization and melting behavior of pure PHBV and the mixed were examined by DSC. Melting transition temperatures (Tm) of the pure PHBV exhibited two melting peak at 154°C and 173°C. In addition, the melting peaks of the mixed were in the range of 152-156°C and 168-171°C, respectively. According to morphology of the mixed, the void distribution reduced twice, compared to that of unmixed PHBV. The results of mechanical properties and thermal analysis indicated that the mixed PHBV can be improved in their properties with more resilient and wide range of temperature than usual.

PM-O-20

Characterizations of Fluorine-Containing Polybenzoxazine Prepared by Solventless Procedure

Patcharat Pattharasiriwong, Sarawut Rimdusit*
Polymer Engineering Laboratory, Department of Chemical Engineering,
Faculty of Engineering, Chulalongkorn University, Bangkok, 10330, THAILAND.
*E-mail: sarawut.r@chula.ac.th

Keywords: Polybenzoxazine, FTIR, Thermal property, Fluorine-containing polymer.

A fluorine-containing benzoxazine monomer (BAF-4fa) from 4-(trifluoromethyl)aniline, 4,4′-(Hexafluoroisopropylidene)diphenol or bisphenol-AF and paraformaldehyde was synthesized using solventless method at temperature of 110ºC without any catalyst. Chemical structure and thermal properties of as-synthesized benzoxazine resin were investigated and compared with fluorine-containing benzoxazine resin as well as with traditional benzoxazine resin from bisphenol-A and aniline (BA-a) system. From Fourier transform infrared spectrum of BAF-4fa monomer, absorption band at 1243 cm^{-1} which assigned to C-O-C stretching mode of oxazine ring and band around 1505 cm^{-1} and 951 cm^{-1} which attributed to tri-substitutued benzene ring from the oxazine ring moieties were observed. The result is in good agreement with the BA-a monomer, indicating successful preparation of fluorine-containing benzoxazine monomer via solventless technology. The obtained fluorine-containing resin also exhibits thermal curing ability which is a signature of benzoxazine resin. The exothermic heat of reaction of BAF-4fa was found to be less than that of BA-a as observed by a differential scanning calorimeter. The BAF-4fa monomer was step-cured at 150°C for 1 hour, 170°C for 1 hour, 190°C, 210°C and 230°C for 2 hours at each temperature followed by 240°C for 1 hour to achieved its fully cured stage. The glass transition temperature of BAF-4fa from loss modulus of dynamic mechanical analysis was found to be much higher than that of BA-a i.e. 212ºC vs 170ºC. From thermogravimetric analysis, thermal degradation at 5% weight loss of BAF-4fa was found to be 255ºC compared to the value of 315ºC while the char yield was 53% vs 30% of the BA-a polymer. The incorporation of fluorine into polybenzoxazine is able to improve various thermal stability of the polymer which could be applied as high temperature resistance materials such as electronic packaging, thermal resistance coating.

PM-O-21

Investigation of Synthesis Parameters for Modification of Chitosan with Enrofloxacin

Saniwan Srithongkham, Piyawadee Sutcharee, Amornrat Lertworasirikul*

Department of Materials Engineering, Faculty of Engineering, Kasetsart University, Bangkok, 10900, Thailand

*E-mail: fengarl@ku.ac.th

Keywords: Chitosan, Enrofloxacin, Water-Soluble Carbodiimide, N-Hydroxysuccinimide

This research aims to investigate synthesis parameters for modification of chitosan with enrofloxacin. Most modifications of chitosan are concentrated on amino group. Thereare many methods for modification of chitosan, for example, conjugation of amino group with carboxylic group by coupling agents. 1-Ethyl-3-(3-(dimethylamino) propyl) carbodiimide hydrochloride (WSC) and N-hydroxysuccinimide (NHS) are widely used coupling agents for amide formation under mild conditions. In this study, those two coupling agents were applied. Ratio of coupling agents, amount of enrofloxacin and reaction times were investigated. The chemical structures were characterized by proton nuclear magnetic resonance spectroscopy (^{1}H-NMR) and Fourier transform infrared spectroscopy (FT-IR). The amount of enrofloxacin in the modified chitosan was examined by UV-VIS. This modified chitosan can be crosslinked by using glutaraldehyde. The obtained bead gel and rectangular gel are expected to be useful for controlled-release drug delivery system and wound dressing application.

PM-O-22

Thermo-responsive Biocompatible Membranes Based on Poly (ethylene-co-vinyl alcohol) For Biomolecule Separations

Sujith Athiyanathil[*], **Riyasudheen Nechikkattu**
Materials Research Laboratory, Department of Chemistry, National Institute of Technology Calicut, Kozhikode, Kerala-673601, India
*sujith@nitc.ac.in

Keywords: Poly (ethylene-co-vinyl alcohol), surface-initiated atom transfer radical polymerization, poly (N-isopropylacrylamide), water flux, protein adsorption.

Hydrophilic poly (ethylene-co-vinyl alcohol) (EVAL) asymmetric membrane has been modified with surface-initiated atom transfer radical polymerization (SI-ATRP) of N-isopropylacrylamide (NIPAAm). Chemical changes of the membrane surface were characterized by attenuated total reflectance Fourier transform infrared spectroscopy (ATR/FT-IR) and the results revealed that NIPAAm has been successfully grafted on EVAL membrane surface. Surface morphology of the membrane was studied by scanning electron microscopy (SEM) and atomic force microscopy (AFM). The surface stimulus responsive properties of membranes were characterized by water contact angle and protein adsorption measurements at different temperatures. The water contact angles of the membranes were switched to higher value above a certain temperature (~31°C), which was corresponding to the lower critical solution temperature (LCST) of pNIPAAm, 32°C. It is observed that below the LCST membrane, a lesser amount of proteins is adsorbed, whereas above the LCST it adsorbed a larger amount of proteins. The water flux and protein rejection at different temperatures were also determined for modified and unmodified membranes. The permeation results showed an obvious increase in the water flux in the temperature range 31-34 °C for the modified membranes due to LCST of pNIPAAm. Rejection of proteins is found to be switched when the temperature is changed through LCST of grafted pNIPAAm.

Polymer-based Materials Session

POSTER PRESENTATIONS

PM-P-01

Surfactant Treatment and Leaching Processes for Preparation of Deproteinized Natural Rubber Latex

Wiwat Pichayakorn[a,b,*], Prapaporn Boonme[a], Wirach Taweepreda[b,c] and Jirapornchai Suksaeree[d]

[a]*Department of Pharmaceutical Technology, Faculty of Pharmaceutical Sciences,*
[b]*Medical Products Innovations from Polymers in Clinical Use Research Unit,*
[c]*Department of Materials Science and Technology, Faculty of Science,*
Prince of Songkla University, Songkhla 90112, Thailand
[d]*Department of Pharmaceutical Analysis Chemistry, Faculty of Pharmacy,*
Rangsit University, Pathum Thani 12000, Thailand
[*]E-mail address corresponding author: wiwat.p@psu.ac.th

Keywords: Surfactant, Leaching, Deproteinization, Deproteinized natural rubber latex

Several types of protein in natural rubber latex (NRL) have been identified as allergens in human immunogenic responses that are the important limitation to develop many products for human uses. Many researchers have developed the several methods to reduce these proteins from NRL such as enzyme treatment, centrifugation, creaming, simple or ultrasonic leaching, and chlorination. Our group has successfully developed the combination of enzyme treatment and leaching processes to deproteinize fresh NRL. However, the production cost of both added enzyme and processing time is high that is not appropriate to commercialize in industrial scale. Therefore, this study aimed to improve the efficacy of protein removal from fresh NRL and decrease the production cost by using surfactant treatment and leaching processes. The 0.5-3% anionic surfactants, i.e. sodium dodecyl sulfate or sodium lauryl ether sulfate, nonionic Tween80 surfactant, or an amphoteric cocamidopropyl betaine surfactant was used in surfactant treatment process. Moreover, water, aqueous surfactant solutions, and/or 1-5% organic solvents (i.e. ethanol, isopropanol and/or acetone) were then used in leaching process. In stead of NRL stabilization by ammonia addition, the fresh NRL was preserved with parabens in the presence of surfactant at ambient temperature for 20-120 minutes, and then centrifuged. This could prevent the skin irritation of deproteinized NRL (DNRL) caused by ammonia. The upper rubber mass was then leached for up to three times with leaching solvents, and then finally re-dispersed in distilled water. The milk-like DNRLs were obtained by these processes. Their dry rubber contents were 41-47% that could be adjusted. Their viscosities were 9-13 centipoises with the pH of 6.00-7.00. The protein residues in these DNRLs were 0.0000-0.3244% which was lower than that of fresh NRL (1.2428%). These indicated the efficacy of studied deproteinization process for 73.90-100.0%. Types and concentrations of surfactant, incubation times, leaching solvents, and number of leaching process affected the efficacy of deproteinization process. Moreover, the properties of these dried films were not different from that of fresh NR film. This DNRL could be further used for several applications including medical skin products.

PM-P-02

Improvement of Octadecane Latent Heats in Polymer Microcapsule by Pickering Emulsion

Sayrung Noppalit [a], Masayoshi Okubo [a, b], Amorn Chaiyasat [a], Preeyaporn Chaiyasat [a*]

[a]*Department of Chemistry, Faculty of Science and Technology, Rajamangala University of Technology Thanyaburi, Klong 6, Thanyaburi, Pathumthani 12110, Thailand*

[b]*Department of Chemical Science and Engineering, Graduate School of Engineering, Kobe University, Kobe 657-8501, Japan*

*E-mail: p_chaiyasat@mail.rmutt.ac.th

Keywords: Polymer microcapsule, Heat storage material, Octadecane, Pickering emulsion

In this research, the preparation of polymer microcapsule encapsulated octadecane (OD) as heat storage material by pickering emulsion was studied. Poly(styrene-*co*-methacrylic acid) (P(S-MAA)) nanoparticles was firstly prepared by emulsifier-free emulsion polymerization. The prepared particles were spherical having diameter about 200 nm and negative charge about -43 millivolts at the surface derived from sulfate group of initiator and carboxyl group of methacrylic acid. After that, the preparation of P(S-MAA)/OD microcapsules by pickering emulsion was studied by mixing of P(S-MAA) and OD at various weight ratios of OD:P(S-MAA). The optimum condition was OD:P(S-MAA) at 1:1 and pH at 7. The prepared microcapsules were closed packed rough-spherical covered with the polymeric particles. The heats of melting and crystallization of the encapsulated OD were about 200-220 J/g-OD. They were closer to the unencapsulated OD (about 240 J/g) than OD droplet stabilized with polyvinyl alcohol (137-187 J/g-OD). Therefore, the preparation of P(S-MAA)/OD microcapsules by pickering emulsion can improve thermal properties of OD closing to the pure ones.

PM-P-03

Mechanical Properties of All-microcrystalline Cellulose Composites

Supachok Tanpichai[a,*], Jatuphorn Wootthikanokkhan[b]
[a]*Learning Institute, King Mongkut's University of Technology Thonburi,*
126 Pracha Uthit road, Bangmod, Thung khru, Bangkok, 10140, Thailand.
[b]*Division of Materials Technology, School of Energy, Environment and Materials*
King Mongkut's University of Technology Thonburi,
126 Pracha Uthit road, Bangmod, Thung khru, Bangkok 10140, Thailand.
*supachok.tan@kmutt.ac.th

Keywords: Microcrystalline cellulose, mechanical properties, all-cellulose composite

All-cellulose nanocomposites were prepared using microcrystalline cellulose as both matrix and reinforcement. Microcrystalline cellulose was dissolved in a solution of lithium chloride/N,N-dimethylacetamide for 7 days. Microcrystalline cellulose with weight fractions of 0.05, 0.10, 0.15 and 0.20 respectively was mixed with the dissolved cellulose. The transparent nanocomposite films with superior mechanical properties were obtained. The effect of the microcrystalline content in the all-cellulose composites was studied. Mechanical properties of the films were characterized by tensile tests. Higher mechanical properties can be obtained from all-cellulose composites reinforced with microcrystalline cellulose.

PM-P-04

Preparation of Poly(Lactic Acid) Acrylate for UV-Curable Coating Applications

Apinya Musidang[a,*], Nantana Jiratumnukul[a]
[a]*Faculty of Science, Chulalongkorn University, Pathumwan, Bangkok, 10330, Thailand*
*E-mail: ple_ladyship@hotmail.com
E-mail: nantanaj@gmail.com

Keywords: UV-curable coating, Poly(lactic acid), Photopolymerization, Glycolysis

UV-curable process is widely used for paints, inks and adhesives due to its rapid curing, low energy consumption, high efficiency and low volatile organic compounds (VOCs). This objective of this research is to prepare poly(lactic acid) (PLA) based UV-curable coating. PLA was glycolyzed by ethylene glycol (EG) at 190ºC for 90 minutes. The obtained glycolyzed PLA reacted with methacrylic anhydride (MAAH) to provide PLA acrylate oligomer. The PLA acrylate oligomer was used in coating formulations with various types and amounts of reactive diluents. Physical properties of cured coating film were investigated such as pencil hardness, gloss, chemical resistance and haze. The results showed that the UV-curable coating can be prepared from bio-base materials for environmental friendly concern. In addition, the coating film showed good physical properties.

PM-P-05

Nitroxide Mediated Radical Polymerization of Styrene-divinylbenzene Copolymer Containing Pendant Group for Pervaporation Membrane Preparation

Sirinard Jearanai [a], Sayrung Noppalit [a], Warayuth Sajomsang [b], Preeyaporn Chaiyasat [a], Amorn Chaiyasat [a*]

[a]*Department of Chemistry, Faculty of Science and Technology, Rajamangala University of Technology Thanyaburi, Klong 6, Thanyaburi, Pathumthani 12110, Thailand*

[b]*National Nanotechnology Center, National Science and Technology Development Agency 130 Thailand Science Park, Paholyothin Rd., Klong Luang Pathumthani 12120, Thailand*

*E-mail: a_chaiyasat@mail.rmutt.ac.th

Keywords: Pervaporation membrane; Nitroxide mediated polymerization

The research focuses on the preparation of pervaporation membrane of poly(styrene-divinylbenzene)/polydimethylsiloxane [P(S-DVB)/PDMS] to remove the volatile organic compounds (VOCs) from water samples. PS macroinitiator was firstly prepared by Nitroxide mediated radical polymerization using 2,2,6,6-tetramethylpiperidinyl-1-oxy as a mediator in bulk system. The narrow molecular weight distribution (MWD; M_w/M_n = 1.06) was obtained. Secondly, P(S-DVB) was polymerized with various mol% of DVB initiated by the prepared PS macroinitiator. The concentration of DVB at 1 and 2.5 mol% represented homogeneous network formation (containing pendant reactivities) without microgel. The obtained copolymers gave narrow MWD which were 1.44 and 1.13 for 1 and 2.5 mol%, respectively. Finally, P(S-DVB)/PDMS was prepared using Pt-catalyst in xylene solution before film casting in teflon coated paper mold. The optimum ratio of P(S-DVB) and PDMS was 1:2 (2.5 mol% of DVB) resulting in soft and strength film. The obtained film was implemented in pervaporation system to remove VOCs from the synthetic water samples contained benzene, toluene and xylene. The polymeric membrane removed approximately 60-100% VOCs within 2 h.

PM-P-06

Synthesis and Characterization of PolyHIPEs Composites with Silica and Iron Oxide Nanoparticles

Panpailin Seeharaj*, Eakkasit Thasirisap, Tanthip Eamsa-ard
Advanced Materials Research Unit, Department of Chemistry, Faculty of Science, King Mongkut's Institute of Technology Ladkrabang, Bangkok, 10520, Thailand
*kspanpai@kmitl.ac.th

Keywords: PolyHIPEs, high internal phase emulsions, composites, nanoparticles.

Poly high internal phase emulsions (polyHIPEs) are low density, high open porosity, high degree of connectivity and high surface area polymer foams that can be used in many applications such as filtration, water purification, chromatography, tissue engineering and sensor technology. This study investigated the synthesis and modifying the properties of polyHIPEs by incorporating additives into the polymer matrices *i.e.* silica (SiO_2) nanoparticles (1 wt.%) to improve the physical and mechanical properties and iron oxide (Fe_3O_4) nanoparticles (5, 10 and 15 wt.%) to induce the magnetic property. The polyHIPEs composites were prepared in water in oil emulsion system using an organic phase consisted of styrene and divinylbenzene (DVB) as monomers, azo-bis-isobutyronitrile (AIBN) as an initiator and Span 80 as a surfactant. An aqueous phase was a solution of 0.34 g/mol (M) calcium chloride ($CaCl_2.2H_2O$). The ratio of the organic phase to the aqueous phase was 20 to 80 vol.%. The effects of the synthesis parameters on the physical, mechanical, magnetic and adsorption properties were examined by scanning electron microscopy (SEM), Brunauer Emmett Teller (BET) surface analysis, universal testing machine in compression mode, vibrating sample magnetometry (VSM) and atomic absorption spectroscopy (AAS). The polyHIPEs composites with 1 wt.% SiO_2 and 5 wt.% Fe_3O_4 showed high specific surface area of 1287.0 m^2/g, Young's modulus of 3.35 ±0.36 MPa and saturated magnetization of 3.58 emu/g (the surface area and the Young's modulus of polyHIPEs without the additives were 68.9 m^2/g and 4.28 ±0.06 MPa, respectively). The mechanical strength and the surface area of the composites were found to decrease with increasing the Fe_3O_4 contents from 5 to 15 wt.% while the magnetic property increased with increasing the Fe_3O_4. The composites with 1 wt.% SiO_2 and 15 wt.% Fe_3O_4 exhibited the highest saturated magnetization at 12.87 emu/g. The adsorption test showed that the polyHIPEs composites with SiO_2 and Fe_3O_4 nanoparticles could be used for adsorption of iron ions (Fe^{3+}) in iron(III) sulfate ($Fe_2(SO_4)_3.9H_2O$) solution with 98.3 % adsorption at equilibrium.

PM-P-07

Influence of Proteins on Thermal-Oxidative Degradation of Peroxide Cross-Linked Natural Rubber as Revealed by ^{1}H Double-Quantum NMR

Adun Nimpaiboon[a], Juan L. Valentin[b], Jitladda Sakdapipanich[a,c*]
[a]*Department of Chemistry and Center of Excellence for Innovation in Chemistry, Faculty of Science, Mahidol University, Bangkok, 10400, Thailand*
[b]*Instituo de Ciencia y Tecnología de Polímeros (CSIC), Madrid, 28006, Spain*
[c]*Institute of Molecular Biosciences, Mahidol University at Salaya Campus, Nakornpathom, 73170, Thailand*
*jitladda.sak@mahidol.ac.th

Keywords: Natural rubber, Proteins, Degradation, ^{1}H double-quantum NMR

The role of proteins on thermal-oxidative degradation of peroxide cross-linked natural rubber (NR) was investigated by ^{1}H double-quantum (DQ) NMR at low field, which is quantitative and reliable method for measuring weak residual dipolar couplings. A comparative study of NR and deproteinized NR (DPNR) was carried out using the DQ NMR experiment to reveal network chain density the spatial crosslink distribution during aging at 100°C under air atmosphere at 0, 6, 24, 48 h. The result of network chain density showed that network chain density of NR decreased larger and faster than that of DPNR during aging process. The in-depth details of how networks are degraded were observed by spatial distribution of cross-links. It was found that spatial cross-link distribution for aged NR was only shifted towards lower crosslink density, while distribution for aged DPNR was widened to lower and higher cross-link densities. Consequently, proteins in NR can be proved as a pro-oxidant molecule that actively affected the degradation behavior of peroxide cross-linked NR. The pro-oxidant activity of protein was supported by the model study of extracted protein generating hydroperoxide during aging process.

PM-P-08

Improved Thermal Properties of Biodegradable Polyester through Mechanochemical Grafting with Maleic Anhydride

Rattikarn Khankrua[a,*], Sommai Pivsa-Art[b], Hamada Hiroyuki[c] and Supakij Suttiruengwong[a,*]

[a]Department of Materials Science and Engineering, Faculty of Engineering and Industrial Technology, Silpakorn University, Sanamchandra Palace Campus, NakhonPathom, 73000,
[b]Department of Material and Metallurgical Engineering, Faculty of Engineering, Rajamangala University of Technology Thanyaburi, Klong 6, Thanyaburi, Pathumthani 12110, Thailand
[c]Kyoto Institute of Technology, Hashigami-cho, Matsugasaki, Kyoto City 606-8585, Japan
*E-mail:k.rattikarn_su@hotmail.com, supakij@su.ac.th

Keywords: Biodegradable polyester, Thermal properties, Mechanochemical grafting, Ball milling.

The degradation of biodegradable polyester at elevated temperatures can cause the random chain scission (cis-elimination) reaction and progresses via cyclic rupture of polymer molecules. However, the thermal degradation of biodegradable polyester can be retarded by grafting various unsaturated chemicals, or alternatively changing chemical structures. Mechanochemical reaction has been recognized as an easy method in many aspects. Several advantages include –no need for external heat supply, very high efficient of mixing and solvent-free for the reaction. Therefore, the aim of this work was to prepare biodegradable polyester; PHBV, PBS and PLA grafted with maleic anhydride (MA) through the free radical grafting via the ball-milling technique. Polymer powder was first prepared and mixed with MA and benzoyl peroxide (BPO) as an initiator. The concentration of MA was 3 and 5 phr. The ratio between MA and BPO was fixed at 2:1.The reaction was carried out through the high speed ball-mill with rotation speed of around 325 rpm at ambient temperature. All samples were characterized and examined for FT-IR spectroscopy, NMR spectroscopy, degree of grafting, contact angle and thermal properties compared with its pure polymer. The results showed that the graft of MA onto PHBV, PBS and PLA were successively achieved which confirmed by NMR results. % grafting were 0.40, 0.39 and 0.45% for PHBV, PBS and PLA respectively for condition of grafting with MA 3 phr for 6 hours. The degree of grafting of MA onto all polymers was comparable even increasing of MA content and duration time of milling. MA grafted biodegradable polyester exhibited more hydrophilic characteristic when compared to its pure polymer. For the thermal properties, MA grafted polymers showed the improvement of thermal stability as indicated by increasing of onset and inflection temperature when compared to its pure polymers, specially, more pronounced in the case of MA grafted PHBV. β-C–H bond of PHBV could be activated by the neighboring carbonyl group [1] easier than in case of PLA and PBS. The introduction of MA remarkably increased the steric hindrance of polymer chain and inhibited the formation of a six-membered ring on the chains.Therefore the improvement of thermal properties by grafting for PHBV was more evidently observed.

Reference

[1] H. Abe, Macromol. Biosci., 6 (2006) 469-486.

PM-P-09

Mechanical and Thermal Properties of Hemp Fiber Reinforced High Density Polyethylene Composites.

Tawat Soitong[a],* and Napatchon Intarakumnerd[a]
Program of Material Science, Faculty of Science, Maejo University, Chiang Mai, Thailand
*E-mail: stawat@gmail.com

Keywords: Mechanical properties**,** Hemp fibers**,** Composites**,** High density polyethylene

Abstract

Hemp fiber reinforced composites was prepared using high density polyethylene (HDPE). Hemp fiber is a cellulosic fiber. It is used as reinforcement in thermoplastic matrix composite requires knowledge of their morphology and structure. In this paper, mechanical properties of chemically treated fiber reinforced HDPE composites were investigated over range of fiber content (0-50 wt%). The hemp fiber was alkali treated with 1-10 wt% to remove waxes and non-cellulosic surface components and triethoxyvinyl silane treated with 0.5-3 wt% to improve a better fiber-matrix interface. Fiber/matrix adhesion was assured by the use of use of polyethylene-graft-maleic anhydride (PE-g-MA) as a compatibilizer. Scanning electron microscopy (SEM), Fourier transforms infrared spectroscopy (FTIR), Differential scanning calorimetry (DSC), X-Ray Diffraction (XRD) and tensile tests were carried out for hemp fibers high density polyethylene composite. Findings indicate that a 5 wt% NaOH treatment effectively improved the fiber-matrix interface resulting in improved mechanical properties. All 40 wt% alkali treated fiber reinforced HDPE composites displayed higher young's modulus and lower elongation at break as compared to neat HDPE, compatibilization with PE-g-MA resulted in an increased young modulus of the composites as consequence of an improved fiber-matrix interfacial adhesion.

PM-P-10

Photo Degradation of Polypropylene-Vitamin C-TiO_2 Composite Film.

Wipawanee Seekorn[a,*] and Tawat Soitong[a]
Program of Material Science, Faculty of Science, Maejo University, Chiang Mai, Thailand
*E-mail: wipawaneesk@gmail.com

Keywords: TiO_2, Vitamin C, Polypropylene, Photo-degradation

Abstract

Photo-oxidative degradation of polypropylene (PP) films with TiO_2 nanoparticles incorporated was studied. The nano-TiO_2 photocatalyst was modified by vitamin C (ascorbic acid or VC). Composite of PP-VC-TiO_2 were prepared with 1.0 and 2.0 wt% of TiO_2. The mixture of components was performed using a two roll mills and forming a thin film using a compression molding. The solid-phase photocatalytic degradation behavior of PP-VC-TiO_2 nano-composite film under UV light irradiation was investigated and compared with those of the PP-TiO_2 film and the neat PP, with the aid of Fourier Transform Infrared (FT-IR), UV-Vis spectroscopy, scanning electron microscopy (SEM), weight loss monitoring, and X-ray diffraction spectra (XRD). It was found that the degradation rate of PP-VC-TiO_2 film was higher than that of PP-TiO_2 film and neat PP film. The PP–VC–TiO_2 composite was a potential environment-friendly photodegradable polymer material.

PM-P-11

Effect of Particle Sizes on Film Formation Behavior of *Hevea brasiliensis* Natural Rubber Latex

NutChurinthorn[a], Adun Nimpaiboon[a], Jitladda Sakdapipanich[b,*]
[a]*Department of Chemistry and Center of Excellence for Innovation in Chemistry, Faculty of Science, Mahidol University, Bangkok, 10400, Thailand*
[b]*Insitute of Molecular Biosciences,Mahidol University, Nakornpathom, 73170, Thailand*
*E-mail jitladda.sak@mahidol.ac.th

Keywords: Natural rubber, Film formation, particle size, Large rubber particle, Small rubber particle.

Natural rubber (NR) latex obtained from *Heveabrasiliensis* contains a wide rubber particle size distribution. The aim of this study is to investigate the effect of small rubber particles (SPR) and large rubber particles (LPR) on the characteristics of film formation. The rubber particle with different mean diameters can be separated by centrifugation at various speeds to prepare SRP and LRP latex. The average sizes of SRP and LRP were characterized by light scattering technique to show that the size of SRP was in the rage of 200 to 667 nm, while that of LRP was in the range of 750 to 1,100 nm. SRP and LRP latex were dried at room temperature to study the film formation behaviors. The results showed that the film compaction time increased with increasing the particle size of NR. Furthermore, the rubber films were aged at room temperature for 3 weeks in order to observe the surface morphology using atomic forced microscopy (AFM) by tapping mode. The AFM images showed that SRP readily formed a coalescence film, while LRP showed individual particles on the film surface at 24 h of aging time. However, both SRP and LRP films became a smooth surface after 3 weeks of aging time.

PM-P-12

Functionalization of Styrene Butadiene Rubber and Skim Latex by Photo-Catalytic Reaction Using Nanometric TiO_2 Film as a Photocatalyst

Supinya Nijpanich[a], Sirirat Kumarn[b], Jitladda Sakdapipanich[b,*]

[a]*Department of Chemistry and Center of Excellence for Innovation in Chemistry, Faculty of Science, Mahidol University, Bangkok 10400, Thailand*

[b]*Institute of Molecular Biosciences, Mahidol University at Salaya Campus, Nakhonpathom 73170, Thailand*

*E-mail jitladda.sak@mahidol.ac.th

Keywords: Photo-catalytic reaction, TiO_2, Styrene butadiene rubber, natural rubber.

Functionalization of rubber latex is used to improve some weak properties. One method of functionalization is chemical modification by a photo-catalytic reaction. In this work, the functionalization of styrene butadiene rubber (SBR) and skim latex were carried out under UV irradiation in the presence of TiO_2 film, which was spin-coated twice on a petri-dish and then calcined at 550°C. The structural characterization of functionalized rubber latex was analyzed by FT-IR and NMR techniques. In the case of SBR latex, the hydroxyl group was observed after exposure to 80 W of UV irradiation for 3 h in the presence of H_2O_2 at concentration of 20% by weight of dry rubber. However, the gel formation derived from crosslinking as a side reaction obstructed the further characterization of microstructure and limited the applications of latex and solid rubber. Moreover, the effect of radical scavengers (NOCRAC and BHT) was also investigated. FT-IR and UV/Vis spectra confirmed that the radical scavengers cannot successfully attach to the rubber chain. In the case of skim latex. The effect of pH, H_2O_2 concentration and UV irradiation time were studied. It was found that the functionalization was successful after exposure to low power of UV-irradiation for 1 h in the presence of H_2O_2 at concentration of 5-10% by weight of dry rubber. The weight-average molecular-weight slightly decreased from $2x10^6$ to $1x10^6$ g/mol.

PM-P-13

Improvement of Filler-Rubber Interaction by Grafting of Acrylamide onto Saponified Natural Rubber under Ultraviolet Radiation as a Continuous Process

Nattanee Dechnarong[a], Jitladda Sakdapipanich[b,*]
[a]*Department of Chemistry and Center of Excellence for Innovation in Chemistry, Faculty of Science, Mahidol University, Bangkok, 10400, Thailand*
[b]*Insitute of Molecular Biosciences, Mahidol University at Salaya Campus, Nakhonpathom, 73170, Thailand*
*E-mail jitladda.sak@mahidol.ac.th

Keywords: Natural rubber, Grafting by UV radiation, Silica, Rubber-filler interaction

Silica and carbon black have been widely used as the main reinforcing fillers for improving properties of natural rubber (NR). In the silica-filled rubber compound, it is known that the low compatibility between NR and silica affects mechanical properties of rubber products. In order to overcome this drawback, the saponified functionalized NR (SFNR) was carried out by grafting acrylamide (AM) onto the saponified NR under UV radiation as a continuous process. It was revealed that bound rubber content and Mooney viscosity increased with increasing AM content. Storage modulus at low strain amplitude of the silica-filled SFNR was lower than that of the raw NR. In addition, SEM micrographs showed the good dispersion of silica in SFNR. These confirmatory evidences indicates the improvement of rubber-filler interaction and the reduction of filler-filler interaction by functionalization under UV radiation, leading to the good mechanical properties, *i.e.*, tensile strength and elongation at break of the SFNR.

PM-P-14

More Values of L-Quebrachitol from Skim Natural Rubber Latex

Teerawan Wannuch[a], Sirirat Kuman[b], Jitladda Sakdapipanich[b,*]

[a]*Department of Chemistry and Center of Excellence for Innovation in Chemistry, Faculty of Science, Mahidol University, Bangkok, 10400, Thailand*

[b]*Insitute of Molecular Biosciences, Mahidol University, Nakornpathom, 73170, Thailand*

*E-mail jitladda.sak@mahidol.ac.th

Keywords: Natural rubber, L-Quebrachitol, Skim latex.

Natural rubber (NR) latex collected from *Hevea brasiliensis* rubber tree exists as a colloidal suspension with 30% dry rubber content (DRC). For convenient use and transportation, the latex is normally concentrated by centrifugation process. Through this process, the 60% DRC concentrated NR latex and 5% DRC skim latex as a by-product were produced. After using acid coagulation of skim latex, the skim rubber is obtained to use for low grade application due to high amount of non-rubber components as impurities. The water portion remaining after the coagulation of skim rubber consists of various water-soluble materials such as sugar, lipid, protein and minerals, which can cause the water pollution if serum is directly discharged into the environment without proper treatment. However, 1.5% of L-quebrachitol were found in skim latex. It can be used in many applications such as a starting material for the synthesis of bioactive materials and inositol pharmacy. Thus, this work is an attempt to investigate the most effective extraction method of L-quebrachitol from skim latex. It was found that the appropriate solvent for extraction L-quebrachitol at high-temperature and for recrystallization at low temperature is ethanol. The yield of L-quebracchitol about 2-3% by weight of solid serum were obtained. In addition, a sweetness and antibacterial activity were also studied for its further applications. It was found that the sweetness of L-quebrachitol was twice than that of sucrose. However, antibacterial activity of L-quebrachitol against *Staphylococcus aureus* and *Streptococcus mutans* was found.

PM-P-15

Using of LLDPE/coir Materials as a Reinforcement for Natural Rubber Composite

Manit kaewduang[a], Ekrachan Chaichana[a], Adisak Jaturapiree[ab*]
[a]*Division of Chemistry, Faculty of Science and Technology, Nakhon Pathom Rajabhat University, Muang, Nakhon Pathom, 73000, Thailand*
[b]*Research Unit of Agriculture Residue Products and Biomaterials, Nakhon Pathom Rajabhat University, Muang, Nakhon Pathom, 73000, Thailand*
*E-mail: adisak_ja@hotmail.com

Keywords: natural rubber composite, cellulose reinforcement, LLDPE/coir materials

Cellulose based fibers such as sisal, jute and coir are ones of the most frequently used reinforcing fillers for composite materials including natural rubber composites. Generally, the purpose of using coir fiber as the reinforcement in natural rubber is to improve the mechanical properties of natural rubber. However, the main disadvantages of these composites are the poor compatibility between the fiber surface and the host matrices, mainly due to the highly hydrophilic character of the fibers and the hydrophobic character of the host materials. Therefore, in this research, coir had been modified with linear low-density polyethylene (LLDPE) prior to introducing into the natural rubber composites. The LLDPE/coir was synthesized by *in situ* polymerization with MAO/metallocene catalyst, named as modified coir. The unmodified coir and modified coir were then blended with natural rubber latex to prepare natural rubber composites. The morphology and thermal dynamic mechanical properties of the composites were measured by scanning electron microscopy (SEM), and dynamic mechanical analysis (DMA), respectively. The composites blended with the modified coir showed the better compatibility between the coir and the natural rubber than those with the unmodified coir. In addition, they also showed the lower storage modulus and tan delta than the unmodified counterpart and the pure natural rubber without the reinforcement.

PM-P-16

Effect of Polypropylene-*g*-maleic anhydride Compatibilizer on Thermal and Mechanical Properties of Polypropylene/Poly(lactic acid) Blends

Thiraphong Chamkhum [a], Tatiya Thongsatitkul[a,*]
[a]*School of Polymer Engineering , Suranaree University of Technology, Muang District Nakhon Ratchasima, 30000, Thailand*
*E-mail: tatiya@sut.ac.th

Keywords: polypropylene (PP), poly(lactic acid) (PLA), polypropylene-*g*-maleic anhydride (PP-*g*-MA), thermal mechanical properties

In this study, the effects of polypropylene (PP), and polypropylene-*g*-maleic anhydride (PP-*g*-MA, compatibilizer) contents on thermal and mechanical properties of PP/PLA blends were investigated. PP contents of 10, 25, and 50 % wt were incorporated into PLA via melt blending using twin screw extrusion. Tensile test results showed that PP/PLA blend prepared at the ratio of 25/75 exhibited optimum tensile strength and elongation at break. Heat distortion temperature (HDT) increased with PP content and was highest at 70 °C in 50/50 PP/PLA blend. PP-*g*-MA compatibilizer was added to 25/75 PP/PLA blend to improve the compatibility between the two phases. Three different concentrations of PP-*g*-MA (2, 5, and 8 phr) were compared. It was found that the presence of PP-*g*-MA improved mechanical properties of the blend whereas little or no change was observed on HDT. PP-*g*-MA concentration of 5 phr showed the maximum improvement in mechanical properties and thermal stability. Differential scanning calorimetry results indicated that PP-*g*-MA addition enhanced the compatibility of the blend which was well agreed with the mechanical property results as well as the morphologies of the blend observed via scanning electron microscopy. This study provides the fundamental understanding of the material properties and behavior which can be beneficial in further development of fully bio-based blend and composite in the future.

PM-P-17

Morphology and Mechanical Properties of Polyoxymethylene and Acrylonitrile-Butadiene-Styrene Blends with Compatibilizer

Sirirat Wacharawichanant*, Parida Amorncharoen, Ratiwan Wannasirichoke
Department of Chemical Engineering, Faculty of Engineering and Industrial Technology
Silpakorn University, Nakhon Pathom 73000, Thailand
*sirirat.che@gmail.com

Keywords: Acrylonitrile-Butadiene-Styrene, Polyoxymethylene, Compatibilizer, Morphology.

The effects of polypropylene-graft-maleic anhydride (PP-g-MA) compatibilizers on the morphology and mechanical properties of polyoxymethylene (POM)/acrylonitrile-butadiene-styrene (ABS) blends were investigated. Two types of compatibilizers, PP-g-MA with maleic anhydride 0.50 wt% (PP-g-MA1) and PP-g-MA with maleic anhydride 1.31 wt% (PP-g-MA2) were used to study the interfacial adhesion of POM and ABS. POM/ABS blends with and without PP-g-MA compatibilizer were prepared by an internal mixer and molded by compression molding. Scanning electron microscope (SEM) was used to investigate the morphology of ABS phase in POM matrix. The results found that POM/ABS blends clearly demonstrated a two phase separation of dispersed ABS phase and the POM matrix phase, and ABS phase dispersed as spherical domains in POM matrix in a range of ABS 10-30 wt% and the blends containing ABS more than 30 wt% showed the elongated structure of ABS phase. The addition of PP-g-MA could improve the interfacial adhesion of POM/ABS blends due to the domain size of ABS phase decreased after adding PP-g-MA. The mechanical properties showed that the impact strength of POM/ABS blends decreased in a range of 10-20 wt% and did not change after 20 wt%. The addition of PP-g-MA did not change the impact strength of POM/ABS blends. The Young's modulus of POM/ABS blends increased up to 30 wt% of ABS and then decreased. While the blends showed the decrease of tensile strength and percent strain at break with increasing ABS content. The addition of PP-g-MA increased the tensile strength of POM/ABS blends in a range of 30-40 wt% of ABS. The above results indicated that the morphology had an effect on the mechanical properties of polymer blends.

PM-P-18

Properties Study of Thermoplastics Starch/Poly (ethylene-co-methylacrylate) Blends Film

Poonsub Threepopnatkul[a,*], Wipawan Assawatongkorn[a], Wisit Detdecha[a], Weerayut Thongsong[a] and Chanin Kulsetthanchalee[b]

[a]*Department of Material Science and Engineering, Faculty of Engineering and Industrial Technology, Silpakorn University, Nakhon Phatom 73000, Thailand.*

[b]*Faculty of Science and Technology, Suan Dusit Rajabhat University, Bangkok 10300, Thailand*

*E-mail address corresponding author: poonsubt@yahoo.com

Keywords: Thermoplastic starch, Poly(ethylene-co-methylacrylate), Antioxidant

The objective was to study the effect of poly(ethylene-co-methyl acrylate) (EMA) at 10, 30 and 50 wt% on mechanical property and biodegradability of thermoplastic starch (TPS). Urea and formamide were used as plasticizer (30 wt%). In addition, the effect of antioxidants namely, 3,5-di-tert-butyl-4-hydroxyhydrocinnamate (DTBH), butylated hydroxytoluene (BHT) and bis(octadecyl)hydroxylamine (BOH) at 1 wt% were investigated on mechanical property and biodegradability of TPS/EMA films. Films were produced by compression molding machine and tested by Universal testing machine. The characterization studies were also performed by thermo gravimetric analysis, scanning electron microscropy, and water vapor permeability measurement. From the results, it was found that the increment of EMA contents blended with TPS could improve mechanical property, thermal property and biodegradable property of TPS films. Regarding the antioxidant effect, tensile modulus and tensile strength of TPS/EMA films containing DTBH were higher than the ones of BOH and BHT, respectively. However, it had no effect on thermal property and biodegradable property of TPS.

PM-P-19

Effects of Small Rubber Particle on the Green Properties of Natural Rubber

Manus Sriring[a], Adun Nimpaiboon[a], Jitladda Sakdapipanich[b,*], Shigeyuki Toki[c]
[a]*Department of Chemistry and Center of Excellence for Innovation in Chemistry, Faculty of Science, Mahidol University, Bangkok, 10400, Thailand*
[b]*Insitute of Molecular Biosciences, , Mahidol University at Salaya campus, Nakornpathom, 73170, Thailand*
[c]*National Metal and Materials Technology center (MTEC) Pathum thani 12120, Thailand*
*E-mail jitladda.sak@mahidol.ac.th

Keywords: Centrifuged natural rubber, Small rubber particle, Green properties

Natural rubber (NR) latex is composed of large rubber particle (LRP) and small rubber particle (SRP). SRP and LRP showed differences in chemical structure. It is expected that SRP may contribute to the properties of NR. In this work, the effects of SRP on green mechanical properties of NR were investigated. The green strength and elongation at break of specimen increases with amount of SRP below the SRP content 10%. The amount of SRP from 10% to 50 % show significant decrease of the green strength and elongation at break. Thus, the green strength was improved by the addition of proper amount of SRP. On the other hand, the green mechanical properties are decreased by the excess amount of SRP. It may be caused by the non-rubber components of NR, especially proteins. The presence of proteins was confirmed by the nitrogen analysis Moreover, non-rubber components were the main factor affecting to color index of sample sheets.

PM-P-20

Preparation and Characterization of Natural Rubber/Chitosan Films

Kansiree Paoribut[a,*], Kanoktip Boonkerd[a], Wirach Taweepreda[b]
[a]*Faculty of Science, Chulalongkorn University, Bangkok, 10300, Thailand*
[b]*Faculty of Science, Prince of Songkla University, Hatyai, Songkhla, 90112, Thailand*
*E-mail k.paoribut@gmail.com

Keywords: Natural rubber latex, Chitosan, Thermal aging, Tensile strength.

Natural rubber/chitosan (NR/CS) films at various NR/CS ratios were prepared here from the mixture of natural rubber latex (NRL) and chitosan solution using a solution casting method. The NRLs with and without curing agents were used. The NR/CS films were obtained after heating at 50°C for 24 hours. The NR/CS films prepared from the NRL with curing agents were further heated at 120°C for 30 min to acquire the NR networks. From swelling testing, it was found that incorporation of CS into the NR matrix gave the films with higher solvent resistance. The swelling index reduced proportionally with the increased CS loadings. Additionally, the solvent resistance of the NR/CS films was improved more once the NR was crosslinked. In general, for every NR/CS ratio, the tensile strengths of the cured NR/CS films were higher than those of the uncured NR/CS films. After thermal aging, it was found that the tensile strength of the pure NR films was decreased. However, for both cured and uncured NR/CS films, their tensile strengths were increased after thermal aging.

PM-P-21

Morphologies and Tensile Properties of Biodegradable Blends of Wheat Gluten and Poly(butylene succinate)

Onuma Santawitee[a,*], Sudsiri Hemsri[b], Chanchai Thongpin[b], Warunee Borwornkiatkaew[a]

[a]National Metal and Materials Technology Center, Pathumthani 12120, Thailand
[b]Department of Materials Science and Technology, Faculty of Engineering and Industrial Technology, Silpakorn University, Nakornpathom, 73000, Thailand
*onumas@mtec.or.th

Keywords: wheat gluten, poly(butylene succinate), morphology, tensile property

Wheat gluten (WG) is an inexpensive biodegradable protein derived from wheat and has been investigated for potential use in non-food applications. However, WG has poor processibility and the plastic made from WG are quite brittle. Blending WG with ductile polymers is one approach to improve WG properties. This research has focused on the study morphology and mechanical properties of blending WG with poly(butylene succinate) (PBS). The WG/PBS blends were prepared in an internal mixer and then were compression-molded. The WG contents in the blends were varied from 70 to 30 % by weight. Scanning electron microscopy (SEM) was used to investigate both surface and cross-sectional morphologies of the blends. The SEM images of all ratios of the blends showed a two-phase morphology with WG phase dispersed in continuous phase of PBS. Young's modulus of the WG/PBS blends decreased with an increase in PBS content. This result was expected since PBS has lower rigidity than WG. Maximum tensile strength of pure WG and PBS were higher than those of the WG/PBS blends due to poor compatibility between WG and PBS. However, maximum tensile strength and elongation at break of the WG/PBS blends were improved with an increasing amount of PBS.

PM-P-22

Preparation and Characterization of Polyurethane Foams from Bio-Based Succinate Polyols

Tatcha Sonjui[a], Nantana Jiratumnukul[b,*]
[a] *Department of Materials Science, Faculty of science, Chulalongkorn University, Bangkok, Thailand 10330*
[b] *Research Unit of Advanced Ceramic and Polymeric Materials, National Center of Excellence for Petroleum, Petrochemicals and Advanced Materials, Chulalongkorn University, Bangkok, Thailand 10330*
Department of Materials Science, Faculty of science, Chulalongkorn University, Bangkok, Thailand 10330
*E-mail: nantanaj@gmail.com

Keywords: Bio-based Polyurethane, Polyurethane foam, Succinic acid, Bio-based Succinate Polyol

Polyurethane foams or PU foams are among the most important materials with widely used in many fields. Recently, intensive interest has been paid to the synthesis of PU foams starting from natural resources due to their important availability, sustainability, biodegradability and added values. Succinic acid (SA) from fermentation of sugars, is one of the most important value added chemicals from biomass due to its going to be abundance and inexpensive feed stock. In this research, the feasibility of using SA as bio-based polyols for bio-based PU foams preparation was studied. Bio-based succinate polyols were synthesized by condensation reaction using SA and various types of glycols. The chemical structures, molecular weights, functionality and viscosity of bio-based succinate polyols were characterized. Bio-based PU foams were prepared by using the synthesized bio-based succinate polyols with isocyanate. Physical and chemical properties of prepared PU foams were taken relatively to PU foams obtained from commercial polyol.

PM-P-23

Effects of Particles Size of Nanosilica on Properties of Polybenzoxazine Nanocomposites

Nutthaphon Liawthanyarat, Sarawut Rimdusit*
Polymer Engineering Laboratory, Department of Chemical Engineering, Faculty of Engineering, Chulalongkorn University, Bangkok, 10330, Thailand.
*E-mail: sarawut.r@chula.ac.th

Keywords: Polybenzoxazine, Nanocomposites, Nanosilica, Thermomechanical Property.

Polybenzoxazine nanocomposites filled with four different sizes of silica nanoparticles are investigated for their mechanical and thermal properties. In this research, silica nanoparticles with primary particle sizes of 7, 14, 20 and 40 nm were incorporated in polybenzoxazine matrix at a fixed content of 3% by weight. From the experimental results, the storage modulus of the polybenzoxazine nanocomposite was found to systematically increase with decreasing the particle sizes of the nanosilica suggesting better reinforcement of the smaller particles. Glass transition temperature was found to slight increase with the addition of the silica nanoparticles. The uniformity of the composite samples were also evaluated by thermogravimentric analysis to show good dispersion of the silica nanoparticles in the composite samples as a result of high processability of the benzoxazine resin used i.e. low A-stage viscosity with good wetting behaviors. Degradation temperature at 5% weight loss ($T_{d,5}$) of polybenzoxazine nanocomposites filled with different particle sizes of silica nanoparticles was found to increase from the value of 325^{o}C of the neat polybenzoxazine to the maximum value of about 340.3^{o}C with an addition of the nanosilica of the smallest particle size. Finally, the smaller nanosilica particle size was also found to show more pronounced effect on $T_{d,5}$ enhancement of the composite sample as a result of greater barrier effect from larger surface area of the smaller particles.

PM-P-24

Mechanical and Thermal properties of Silane Treated Pineapple Leaf Fiber Reinforced Polylactic Acid Composites

Supatra Pratumshat[a,b]* Phutthachat Soison[a], Sukunya Ross[a]

[a]*Department of Chemistry, Faculty of Science, Naresuan University, Phitsanulok, 65000, Thailand*

[b]*Research Center for Academic Excellent in Petroleum, Petrochemicals and Advanced Materials, Naresuan University, Phitsanulok, 65000, Thailand*

**E-mail: supatraw@nu.ac.th*

Keywords: Pineapple leaf fiber (PALF) composite/ Polylactic acid (PLA)/ Silane treatment/ fiber surface modification

In this work, the mechanical and thermal properties of pineapple leaf fiber (PALF)/poly(lactic acid) (PLA) composites were studied. Pineapple leaf fibers were pretreated with 4 %wt sodium hydroxide solution followed by various silane solutions i.e. γ-(aminopropyl) trimethoxy silane (APS), γ-methacrylate propyl trimethoxy (A174) and bis[3-(triethoxysilyl)propyl] tetrasulfide (Si69). The FTIR results show a significant functional groups of C=O and C=C of methacrylic group, NH_2 group and Si-O which are the characteristic of these silane coupling agents. SEM micrographs of pretreated PALF with sodium hydroxide solution showed a rough surface while untreated and silane treated PALF revealed less roughness. The mechanical properties of the composites were determined using tensile and impact testing. It was found that the tensile strength at break of PLA is 56 MPa and tensile strength of composites decreased when fiber content increased. The tensile modulus of all silane treated PALF/PLA composites were higher than PLA, whereas their impact strength were similar to PLA. Si69 treated PALF showed lower impact strength compared to the others silanes treated fiber which indicates more phase separation between fiber and matrix. This is related to high percentage of crystallinity of composite from Si69 treated fiber. It was also found that the addition of PALF did not change the glass transition temperature and melting temperature of PLA while the percentage of crystallinity increases as the fiber content increased. In addition WAXS study of composite from Si69 treated fiber reveals sharp crystalline peaks of PLA while the others silane treatments show amorphous characteristic of PLA.

PM-P-25

Alkaline Extraction of Hemicelluloses from Bagasse and Structure Modification by Arabinofuranosidases

Chaiyaporn Pomchaitaward[a,*], Chakrit Tachaapaikoon[b,c], Patthra Pason [b,c], Rattiya Weanukul[b,c], Khanok Ratanakhanokchai[c]

[a]*National Metal and Materials Technology Center (MTEC), 111 Thailand Science Park, Thanon Phahonyothin, Tambol Klong Nueng, Amphoe Khlong Luang, Pathum Thani 12120, Thailand*

[b]*Pilot Plant Development and Training Institute (PDTI), King Mongkut's University of Technology Thonburi (KMUTT), Bangkhunthian, Bangkok, 10150, Thailand*

[c]*School of Bioresources and Technology, King Mongkut's University of Technology Thonburi (KMUTT), Bangkok, 10150, Thailand*

*chaiyapp@mtec.or.th

Keywords: Alkaline cooking, Modification, Arabinofuranosidase, Bagasse, Xylan

The biorefinery of plant cell wall polysaccharides have received considerable attention in recent years to produce chemicals, represents a more sustainable path. Generally the biorefinery of plants gives three main components: cellulose, lignin and hemicelluloses. In this study, we focused on hemicelluloses isolated from bagasse using hot alkaline. Hemicelluloses represent a type of hetero-polysaccharide with complex structure containing glucose, xylose, mannose, galactose, arabinose, rhamnose, glucuronic acid, and galacturonic acid in various amounts, depending on the source. For this work, the conditions promoting a compromise between the yield and the structure and minimizing the thermal degradation of the fractions extracted from bagasse were found as following: (1) extraction at 100°C, to remove the sugar mixed with water-soluble lignin-xylan complex; (2) Suspension of the residue left in aqueous 12% NaOH and treated at 55°C; (3) subsequent purification by 95% ethanol precipitation at 4°C and washing with 70% ethanol. Using this sequential procedure, the yield of hemicelluloses was about 100 mg/g dry bagasse. The obtained powdered hemicelluloses were analyzed by attenuated total reflection-Fourier transform infrared spectroscopy (ATR-FTIR) and solid-state nuclear magnetic resonance spectroscopy (Solid-state ^{13}C NMR). The spectrum results showed that the hemicellulose fractions were strongly enriched in xylose-containing polysaccharide. In order to enhance functionality of this hemicellulose comprised mainly xylan, the selective removal of arabinose side chains via enzymatic hydrolysis was carried out to increase both crystallinity and the hydrophobic interaction capacities. The releasing activity of the purified alpha-L-Arabinofuranosidases (Xar CalH produced in house) were used to release arabinose side chains from xylan, compared with that of commercial one (E-AFAM2® Megazyme International Ltd.). The amount of arabinose was measured via high-performance liquid chromatography using Aminex® HPX-87P column.

PM-P-26

Photo-induced Polymerization of PVA/aniline and PEG/aniline Composite

Thanaphon Kansa-ard[a,*], Somtop Santibenchakul[b,c] Wanichaya Mekprasart[a] and Wisanu Pechrapa [a]

[a]College of Nanotechnology Ladkrabang, King Mongkut's Institute of Technology Ladkrabang, Bangkok, 10520, Thailand

[b]Faculty of Science, King Mongkut' Institute of Technalogy Ladkrabang, Bangkok, 10520, Thailand

[c]Faculty of Science and technology, Rajmangala University of Technology Tawan-Ok, Chonburi 20110, Thailand

*tkansaard@gmail.com

Keywords: Photo-induced polymerization, Photopolymerization, Aniline, PVA and PEG

This article represents the preparation of polyaniline (PANI) by photo-induced polymerization method under UV-irradiation. Photo-polymerized composite polymers based on polyaniline were initially prepared from aniline monomer. Polyvinyl alcohol (PVA) and polyethylene glycol (PEG) were used to synthesize the composite polymers. The morphologies of composite polymers were characterized by scanning electron microscope (SEM). Results of UV-visible, Raman and FT-IR spectroscopy suggested that the polymerization of PANI were carried outwith photopolymerization method. Thermal gravimetric analyzer (TGA) was utilized to characterize the composite polymer thermal properties. The significant difference of morphologies and relevant properties of both composite polymers are observed and scrutinized.

PM-P-27

Effect of Components on the Electrical Property of Stretchable Carbon Black Electrode

Tae-Won Lee, Min-Hee Hong, Hae-Noo-Ree Jung, Hyung-Ho Park*
Department of Materials Science and Engineering, Yonsei University, Yonsei-ro 50, Seodaemun-gu, Seoul 120-749, Korea
*E-mail address corresponding author: hhpark@yonsei.ac.kr

Keywords: Carbon black, Stretchable electrode, Electrical property

Today, demands for stretchable devices are emerging because types of electronic goods change. To realize these devices, stretchable electrode is essential which prevents rapid increase of electrical resistivity when it is deformed. We have fabricated stretchable carbon electrode by using easy and low cost process. In fact 3 main components were needed to make this composite. First carbon black was used as conductive filler because of good electrical conductivity, low prices and easy processing. And dispersant was used to distribute carbon particles uniformly which show an agglomeration due to complex structure and high surface area. Finally water based acrylic emulsion was used as binder which gives adhesion between electrode and substrates. Electrical resistance of this electrode was not increased drastically when it is stretched, even resistivity was decreased. And amount of dispersant and binder, carbon filler had effect on the electrical conductivity and stretchability of electrode. In this study, the electrical resistivity was measured by using Hall measurement. Surface and cross section of electrode were visualized by scanning electron microscope. Functional groups which were attached to surface of filler were investigated by Fourier transform infrared spectroscopy. Through these analyses, the effect of component on the electrical property of stretchable carbon black electrode could be evaluated.

References

1. T. Yamada, Y. Hayamizu, Y. Yamamoto, Y. Yomogida, A. Izadi-Najafabadi, D. N. Futaba, K. Hata, Nat. Nanotechnol., 6, 296 (2011)
2. J. A. Rogers, T. Someya, Y. G. Huang, Science, 327, 1603 (2010)
3. D. J. Lipomi, B. C. K. Tee, M. Vosgueritchian, Z. N. Bao, Adv. Mater., 23, 1771 (2011)
4. Y. Li, S. F. Wang, Y. Zhang, Y. X. Zhang, J. Appl. Polym. Sci., 99, 461 (2006)
5. J. Yu, L. Q. Zhang, M. Rogunova, J. Summers, A. Hiltner, E. Baer, J. Appl. Polym. Sci., 98, 1799 (2005)
6. L. Flandin, A. Chang, S. Nazarenko, A. Hiltner, E. Baer, J. Appl. Polym. Sci., 76, 894 (2000)
7. L. Bokobza, M. Rahmani, C. Belin, J. –L. Bruneel, N.-E. E. Bounia, J. Polym. Sci. Pol. Phys, 46, 1939 (2008)

PM-P-28

The Modification of Polyethersulfone Membrane with 2- (Methacryloyloxy)Ethyl Phosphoryl Chloline Polymer in N-Methyl-2-Pyrrolidone

Nasrul Arahman*, Sri Aprilia, Teuku Maimun
Chemical Engineering Department, Syiah Kuala University. Jl. Syeh Abdurrauf, No. 7 Darussalam Banda Aceh
*E-mail: nasrular@unsyiah.ac.id

Keyword: Hydrophobic polymer, hydrophilic membrane, membrane modifying agent, membrane preparation.

Membrane technology has been widely adopted in a variety of industrial applications. Membrane has become an attractive option for separation of natural organic matter in water purification processes. Membrane has also been widely used for gas separation and for the production of vegetable oil. To be applicable in those specific industries, the membrane should be qualified by specific criteria in accordance with the properties of materials. The recent study on membrane technology was focused on selection of polymer material, modification of polymer solution, and optimization of membrane preparation condition. In this work, the hydrophobic polyethersulfone membrane was modified to be a hydrophilic porous polymeric membrane Hydrophilic polymer 2-(methacryloyloxy)ethyl phosphoryl chloline (MPC) were used as a membrane modifying agent (MMA) in order to improve the hydrophilicity of PES membrane. The effect of addition of MPC on the morphology and ultrafiltration performance of resulted PES membrane were studied systematically. Cloud point experiment was performed to investigate the non-solvent amount necessary for induced phase separation of polymer system. Scanning electron microscopy was used to confirm the morphology changes of fabricated membrane. Single sheet module of hollow fiber membrane was conducted to clarify the ultrafiltration performance of the original and the modified membrane. In summary, the MPC was useful additive as MMA to improve the hydrophilicity and the performance of hydrophobic membrane.

PM-P-29

Properties of Thermoplastic Elastomer Composites Prepared from Para Rubber Wood Sawdust Filled-polypropylene/natural Rubber Blends

Rattiya Phakdee* and Ploenpit Boochathum
Department of Chemistry, Faculty of Science King Mongkut's University of Technolygy Thonburi, 126 Pracha-utis Road, Bangmod, Toongkru, Bankok 10140, Thailand
**E-mail: ploenpit.boo@kmutt.ac.th*

Keywords: Thermoplastic elastomer composites, Natural rubber (STR5L), Para rubber wood sawdust, Mechanical properties

Thermoplastic elastomer composites (TEC) based on blending of polypropylene (PP) and natural rubber (STR5L) filled with Para rubber wood sawdust were prepared by melting polypropylene at 180°C in the internal mixer followed by adding STR5L and subsequently Para rubber wood sawdust. The size of Para rubber wood sawdust used were less than 800 μm. Thermoplastic elastomer composite compounds were compression molded at 180°C for 13 min. for specimen preparation. The effect of blend ratios and Para rubber wood sawdust loading on the mechanical and physical properties of TEC were investigated. It was found that tensile strength, Young's modulus, hardness and flexural strength of TEC decreased with STR5L and Para rubber wood sawdust loading, whereas the impact strength increased with increasing STR5L. It was obvious that loading of Para rubber wood sawdust didn't change impact resistance and hardness of TEC. Furthermore, it was clarified that TEC (PP:STR5L:Sawdust) with the weight ratios of 90:10:30, 90:10:50, 70:30:30 and 70:30:50 showed the best mechanical properties. Accordingly, they were selected for further measurements of the water absorption and flexural properties for application to flooring. The water absorption of TEC was determined by immersing the composite samples in distilled water for 24 hr at room temperature. The results showed that water absorption of TEC with the ratios of 70:30:30 and 70:30:50 was 0.25% and 1.64%, respectively, compared to the standard value of ≤ 3.00% for low water absorption ceramic tiles, ≤10.00% for medium absorption ceramic tiles and ≥10% for high water absorption ceramic tiles regarding to Thai Industrial Standards. For flexural properties, all selected TEC showed flexural modulus higher than 700 MPa which was the minimum requirement of Thai Industrial Standard (≥ 700 MPa). However, only TEC with the weight ratio of 90:10:30 gave the modulus strength reach to Thai Industrial Standards value of ≥30 MPa. Morphology of the cracked surface from the notched impact specimens with the weight ratio of 90:10:50 and 70:30:50 was examined by using Scanning Electron Microscopy (SEM). It indicated that the interfacial bonding between Para rubber wood sawdust and the polymer matrix of TEC with 90:10:50 ratio was poorer in comparison with that of 70:30:50 due to the numerous pulled-out sawdust flakes of TEC with 90:10:50 ratio observed much more than TEC with 70:30:50 ratio. This result indicated that adhesion between filler and polymer matrix of TEC with 30% STR5L blending was obvious to be stronger than that with 10% STR5L blending. As a result, it was remarkable that thermoplastic elastomer composites prepared with three immiscible materials showed acceptable mechanical and physical properties for application to flooring product with the economical process.

PM-P-30

In-situ Reinforcement of PLA using Nylon 6 in PLA/Nylon 6 Extrudate Blend via Twin-screw Extrusion

Chanchai Thongpin[a,*], Kullanith Chaemprasith [a], Jakapan Teeralertpanich [a] and Parisara Saensuk [a]

[a] *Department of Materials Science and Engineering, Faculty of Engineering and Industrial Technology, Silpakorn University, Sanamchandra Palace Campus, Nakornpathom, 73000 Thailand.*

*E-mail address corresponding author: chanchai@su.ac.th, cmaterials@hotmail.com

Keywords: In-situ reinforcement, Elongates Nylon 6 in PLA/Nylon 6 extrudate, Twin screw extrusion.

This research was aimed to study the possibility of in-situ reinforcement of PLA by elongated Nylon 6 in PLA/Nylon 6 blend during elongating of PLA/Nylon extrusion. PLA was melt blending with Nylon 6 in a twin screw extruder with various compositions i.e. 5, 10, 15 and 20 % of Nylon 6. The extrudate was drawn after leaving extrusion orifice die of 3 mm in diameter, with the pulling speed of 12 cycles per minute. The extrudate gauge length of 5, 10 and 15 cm were used to perform tension test in order to investigate both length effect and tensile properties. The blending between PLA and Nylon 6 with 11 phr of benzene sulfonamide (BSA), based on Nylon 6, as a plasticizer was also investigated at the same PLA/Nylon 6 blend ratio. The extrusion conditions were also the same. Tension was also performed onto the extrudates with the gauge length of 5, 10 and 15 cm. Thermal properties of the blends i.e. crystallization using DSC, thermal degradation using TGA, were also investigated. The SEM micrographs of blends in the longitudinal direction of PLA/Nylon 6 extrudate showed elongated of Nylon 6 in PLA matrix phase. The elongated of Nylon 6 phase in PLA matrix phase was found very clear in the plasticized blends. This phenomenon clearly occurred for the blends composition of both 95/5 and 90/10, with and without plasticizer. The results also showed that Young's modulus of the blends with 5 % Nylon 6 was increased about 10 % whereas at 10 % nylon 6, the modulus was not significantly different from neat PLA, i.e. Young's modulus was found to be increased about 25 %. With the addition of plasticizer, nylon 6 was elongated more than the un-plasticized blends. Due to the lack in interfacial adhesion, shown by SEM micrograph, tensile strength was found to be decreased. As expected, the elongation at break under tension was increased with the content of nylon 6. This was due to the toughening effect of elongated Nylon 6. DSC results clearly showed no interaction between PLA and nylon 6 as T_g, T_{cc} and T_m of PLA in the blends did not seem to be changed. Thermal stability, notified by degradation temperature of PLA, maximum T_d, was found to be improved. This was due to the high thermal stability of nylon 6. The results from the research can inform that the elongated nylon 6 phase in PLA matrix can perform as fibrous reinforcement. At high content of nylon 6, i.e. 15 and 20 %, the elongation of nylon 6 was rather difficult due to the less matrix phase and low shearing between PLA and nylon 6. Phase compatibility improvement could be the factor to improve the in-situ reinforcement.

PM-P-31

Preparation of Microfibrillated Cellulose via Dissolution/Precipitation Technique and Its Nucleation Effect on the Crystallization Behavior of Polypropylene

Sarit Thanomchat[a,b], Alois K. Schlarb[b,c,d], Kawee Srikulkit[b,e,*]
[a]*Department of Materials Science, Faculty of Science, Chulalongkorn University, 10330, Thailand*
[b]*Chair of Composite Engineering, University of Kaiserslautern, Kaiserslautern, 67663, Germany*
[c]*Research Center OPTIMAS,University of Kaiserslautern, Kaiserslautern, 67663, Germany*
[d]*INM-Leibniz Institute for New Materials, Saarbrucken, D-66123, Germany*
[e]*Center of Excellent on Petrochemical and Materials Technology, Chulalongkorn University, 10330, Thailand*
*kawee@sc.chula.ac.th

Keywords: Microfibrillated Cellulose, Hydrophobic surface treatment, Nucleation, Polypropylene

Microfibrillated cellulose (MFC) was prepared by controlled precipitation of NaOH/Urea solubilized microcrystalline cellulose/starch solution in an HCl bath followed by hydrophobic surface modification via silanization with an organosilane to enhance the hydrophobicity of MFC. The MFC was melt mixed with polypropylene powder (PP) as matrix via twin screw extrusion. The behavior of PP in the presence of MFC particularly crystallization was investigated. The MFC exhibited an extraordinarily high water retention due to its small size with high surface area, resulting in its presence in gel-like form when compared to powder form of microcrystalline cellulose (MCC). The morphology of MFC exhibits a web-like structure with a diameter in the range of 10-20 nm. The XRD pattern of MFC showed the partially amorphous structure arising from the imperfect orientation of a cellulose chain obstructed by a starch molecule during precipitation process. The surface modification of MFC was carried out using an organosilane. The morphology, the functional groups and the crystallinity of organosilane treated MFC were characterized by SEM, FT-IR and XRD, respectively.

The MFC/PP compound was prepared by twin screw extrusion. The thermal properties of nanocomposites were characterized by DSC. The results indicated that the organosilane treated MFC can act as a nucleating agent for PP as observed by an increase in crystallization temperature from 111 to 118 °C and a slight increase in % crystallinity. The crystallinity of nanocomposites was also confirmed again by XRD which illustrated the strong beta crystal peak of PP at $2\theta = 16.1°$. In addition, the non-isothermal crystallization behavior of nanocomposites by an optical microscope was presented.

PM-P-32

Spectroscopic and Thermo–Mechanical Studies of Liquid Crystal Elastomer

Rita A. Gharde [a,*], Santosh A. Mani [a,b,*], Jessy P. J [a], Jyoti R. Amare [a], Patrick Keller [c]

[a] *Department of Physics, University of Mumbai, Mumbai 400 098, INDIA*

[b] *K. J. Somaiya College of Engineering, Vidyavihar (E), Mumbai 400 077, INDIA*

[c] *Institut Curie, Centre de Recherche, CRNS UMR 168, Paris Cedex 05, FRANCE*

*samphy2013@gmail.com

Keywords: Liquid Crystal Elastomers (LCEs), Raman Spectroscopy (RS), Fourier Transform Infrared (FTIR) Spectroscopy and Polarizing Microscopy Studies (PMS).

The structure and influence of temperature on mechanical deformation of Liquid Crystal Elastomers (LCEs) were studied using various techniques like Raman Spectroscopy (RS), Fourier Transform Infrared (FTIR) Spectroscopy and Polarizing Microscopy Studies (PMS) etc. The spectroscopic studies confirmed the presence of functional group attached to the sample. The shrinkage in length was observed while heating whereas material returns to its original length on cooling which revealed the correlation of mechanical behavior of Liquid Crystal Elastomers with temperature. This spontaneous shape changing property indicates that LCE material plays an important role in biological applications.

PM-P-33

Microfluidic Device Based on Nanocomposite Micro Hydrogels Composed of Clinoptilolite and Poly(methacrylamide-co-Potassium methacrylate)

Aboulfazl Barati[a,*], **Taghi Miri**[a]
[a]*Chemical Engineering Department, Faculty of Engineering, Arak University, Arak, 38156-8-8349, Iran*
*E-mail: a-barati@araku.ac.ir

Keywords: Nanocomposite, Micro hydrogel, pH-sensitivity, Microfluidic device.

pH sensitive nanocomposite micro hydrogels based on nano sized particles of natural zeolite (clinoptilolite) and polymer matrix composed of poly(methacrylamide-co-potassium methacrylate) were synthesized by micro emulsion copolymerization in the presence of N,N'-methylene bisacrylamide (Bis) as a cross-linking agent. The micro hydrogels formed were characterized by Fourier transform infrared spectroscopy to confirm the physical entanglement, hydrogen bonds and chemical crosslinking, scanning and transmission electron microscopy to understand the surface morphology and thermo gravimetric analysis and X-ray diffraction to confirm a uniform distribution of the nano sized particles in the polymer matrix. The effect of methacrylamide, potassium methacrylate, clinoptilolite, initiator and cross-linking concentration on the swelling behavior of micro hydrogel was investigated by equilibrium and dynamic swelling measurement freely and under load. pH sensitivity of the resultant micro hydrogels were highly dependent on the composition of the hydrogels as well pH of the local medium. These hydrogel materials are desirable for potential applications as smart pump for microfluidic systems.

Simulation, Design and Manufacturing Session

ORAL PRESENTATIONS

SD-O-01

Multi-scale Multi-physics Modelling of Fusion Welding: Materials, Process and Mechanisms

C. Panwisawas*, Y. Sovani, R.P. Turner, J.W. Brooks, H.C. Basoalto
School of Metallurgy and Materials, University of Birmingham, Birmingham B15 2TT, UK
E-mail address: c.panwisawas@bham.ac.uk

Keywords: Multi-scale modelling, Fusion welding, Aerospace materials, Titanium alloys

Integrated computational materials engineering (ICME) is a methodology in which all computational modelling across length scales is integrated with experimental validation to be beneficial for achieving efficient materials, process design and manufacturing improvement. During the operation of fusion welding especially in aerospace materials, when a high energy heat source interacts with the materials, it can create a deep penetration weld to join two parts together. To determine the weld integrity, one needs to ensure that the quality of the weld is good, e.g. zero-defect and no distortion. In this work, a novel technique of multi-scale multi-physics approach is presented in an ICME framework to model fusion welding in two-phase titanium alloys. This is in order to establish a physics-based model that fully describes the phenomenon in-depth and to provide a predictive capability for component design and process improvement. Computational fluid dynamics (CFD) programmed in the C++ OpenFOAM source code is used to calculate fluid flow and heat transfer during fusion welding. The resulting temperature history and weld geometry are to be linked with a cellular automaton (CA) - finite element calculation implemented in the CA module in commercial ProCAST software package. Grain microstructure along with texture information and grain distribution is then predicted and exported to provide a representative grain structure for a two-phase alloy which is constructed using Neper open source code. The effective grain structure is then used to simulate the location specific mechanical response via a dislocation-density based crystal plasticity model implemented in a user materials subroutine of the Abaqus/standard finite element code. Representative volume elements are used to obtain the mean behavior, i.e. yield stress in this work. The modelling results are critically compared with experimental information.

SD-O-02

A Block Algorithm and Its Optimal Block Size for Cholesky Decomposition of Finite Element Matrices in 3D Free Vibration Analysis

Wassamon Phusakulkajorn[a,*], **Atipong Malathip**[a], **Somboon Otarawanna**[a]
[a]*CAD/CAE Laboratory, Design and Engineering Research Unit, National Metal and Materials Technology Center (MTEC), Pathumthani 12120, Thailand*
E-mail: wassamon.phu@mtec.or.th

Keywords: algorithm-by-blocks, optimal block size, block Cholesky factorization, eigenvalue problem

Free vibration analysis is essentially about determining natural frequencies and mode shapes of a mechanical structure which is prone to mechanical resonance. When mechanical resonance occurs, the structure oscillates with a dramatically higher amplitude than it does at other frequencies. This leads to unwanted violent motions and possibly a failure in the structure. In order to investigate the resonance behavior in 3D complex structures, finite element method (FEM) is commonly used for free vibration analysis.

In free vibration analysis without damping by FEM, a common computational step is the Cholesky decomposition of the mass matrix into a lower triangular matrix and its transpose. This is done to transform the finite element equation into the standard form of eigenvalue problems. This step usually concerns with a large mass matrix which cannot be effectively loaded into the cache memory of a computer. Consequently, a block algorithm has been introduced in order to improve the efficiency of memory hierarchies and minimize the computational time. Its idea is based on dividing a large matrix into small blocks of sub-matrices which can be efficiently loaded into the computer's caches.

Regarding a block algorithm, one of the important factors affecting the computational performance is the block size used. In this work, a block algorithm has been implemented for the Cholesky decomposition of the mass matrix and various block sizes have been experimented to find an optimal block size. The numerical experiments show that small-sized matrices do not get benefit from the block algorithm as computational time does not decrease significantly after employing the algorithm. On the other hand, the block algorithm is very beneficial for relatively large matrices as computational time decreases by an order of magnitude compared to the unblock version. Regarding the optimal block size, choosing a block size to be the largest prime factor of the matrix size assures the shortest computational time.

SD-O-03

Effect of Weld Line Formation on Mechanical Properties for 3D-MID Technology

Supakit Chuaping[a], Thomas Mann[b], Rapeephun Dangtungee[a], Suchart Siengchin[a,*]
[a]*Materials and Production Engineering Department, The Sirindhorn International Thai-German Graduate School of Engineering (TGGS), King Mongkut's University of Technology North Bangkok, 1518 Pracharat 1 Road, Bangsue, Bangkok, 10800, Thailand*
[b]*Plexpert GmbH, Pfromaeckerstraße 21, Aalen, 73432, Germany*
E-mail: suchart.s.pe@tggs-bangkok.org

Keywords: Molded interconnect devices (MID); Weld line; Adhesion; Mechanical properties

In recent years, the growing use of 3D Molded Interconnect Devices (3D-MID) in peripheral application, the stresses as climatic mechanical and chemical are increasing on the MID parts. The injection molded part is one of the key successes for MID technology. However, the suited injection molded part for MID has a lack of investigation. Especially the influence of weld lines on the part is not yet described. The topic of this research work is to demonstrate the feasibility of the concept of 3D-MID using injection molding technique and investigates the effects of weld angle on the mechanical properties such as adhesive, tensile and flexural strength. In order to obtain more understanding of the bonds between polymer and metals, two different polymer bases of polyphthalamide (PPA) with the same type and amount of filler content are produced by injection molding with different processing conditions. A mold is designed in such a way that weld and meld line can be produced with different angles by changing inserts inside of the mold. The mechanical properties such as stiffness, tensile strength and flexural strength were determined in tensile and flexural tests, respectively. The preliminary results are in line with the expectation of high reduction in mechanical properties. Result of tensile mechanical characteristics is given in figure 1. It is clearly seen that weld and meld line showed a great influence to tensile properties. The reductions of tensile strength range from 51 % to 67 % according to weld angles. On the other hand, the effect of the injection time on the tensile strength is marginal.

Figure 1:

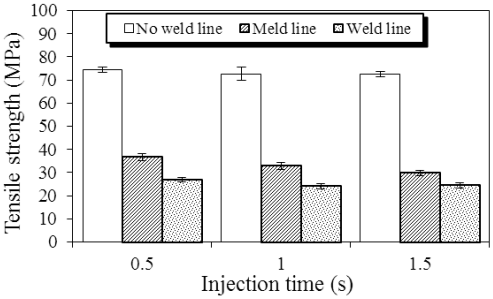

Reference:

[1] T. Leneke, S. Hirsch, B. Schmidt, A multilayer process for the connection of fine-pitch- devices on molded interconnect devices (MIDs), Circuit World 35 (2009) 23-29.

[2] B.Ozcelik, E. Kuram, M. Mustafa Topal, Investigation the effects of obstacle geometries and injection molding parameters on weld line strength using experimental and finite element methods in plastic injection molding, International Communications in Heat and Mass Transfer 39 (2012). p. 275–281.

SD-O-04

Numerical Simulation of Fluid Mixing in Micro-Mixers

Suppasit Prasertlarp, Sompong Putivisutisak*
Department of Mechanical Engineering, Faculty of Engineering, Chulalongkorn University, Pratumwan, Bangkok, 10330, Thailand
*sompong.pu@chula.ac.th, Tel.: +66-2-218-6337

Keywords: micro-mixers, water-ethanol mixture, ultrasound imaging, CFD

A 3-D numerical simulation is performed to study the flow dynamics and mixing characteristics between two different kinds of fluid within T-shaped micro-mixers. Water and ethanol are selected as the mixing fluids due to its application in calibrating the ultrasound imaging equipment. The present work focuses on the effects of inlet velocity and aspect ratio of the mixing channel. The Reynolds number is varied from 0.1 to 300 and the aspect ratio in the range between 0.25 and 1. The flow of interest is laminar, steady and without chemical reaction. It is found that at low Reynolds number, the stratified flow character is presented. As the velocity inlet increases, the mixing efficiency is decreased. However, for the Reynolds number greater than 100 the mixing efficiency is increased due to the buildup vortex structure. Furthermore, when increasing the Reynolds number, the pressure drop significantly increases. Thus, it is seen that both the inlet velocity and aspect ratio significantly affect the mixing efficiency and pressure drop.

SD-O-05

Design of Runner and Gating Systems for the Investment Casting of 431 Stainless Steel Netting Hook through Numerical Simulation

P.Suwankan[a,*], N.Sornsuwit[a], N.Poolthong[b]

[a]*Department of Materials and Production Technology Engineering, Faculty of Engineering, King Mongkut's University of Technology North Bangkok, 10800, Thailand.*

[b]*Division of Materials Technology, School of Energy, Environmental and Materials, King Mongkut's University of Technology Thonburi, Bangkok, 10140, Thailand.*

patrpimols@kmutnb.ac.th

Keywords: Investment casting, simulation, shrinkage porosity, flow behavior

In the production of netting hook which requires wear resistance and long lifetime, enabling the fishing net production with good efficiency. There has been a study to achieve the forming method for high durability and designated smooth surface. The process of investment casting or known "Lost wax casting" is one of production cost to fabricate metal part by the method of casting. Flow behavior of stainless steel grade 431 at the temperature higher than 1600°C is a critical factor in casting mold design of the lost wax process. The CAST-DESINER™ program was used to analyze the flow of liquid metal to clarify solidification of SS431 which cause defects in the product. The unsuitability of heat transfer phenomena and using of the unsuitable mold were the conditions leading to defects in casting such as misruns, cold shuts, shrinkage, pin holes and porosity. Factors affecting casting such as pouring temperature, preheating temperature, preheat time, pouring rate and cooling rate were given by the present production condition. The experimental design technique for simulation analysis of the casting and the gating system has been designed to be consistent and appropriate to the casting part. The cross-sectional design of the runner was 2 types of hexagonal and circular cross-section runner. The angle of gating system was constant at 90 degrees to the runner. As a results of the simulation, shrinkage porosity, filling time as well as solidification time were used to evaluate the cross-sectional design of runners. It was found that a hexagonal cross-section runner led to the shorter filling time than a circular one. Furthermore, there was no remarkable difference of shrinkage porosity in all simulated condition. However, in the terms of filling time, the results depended on the combination of runner design and gating system.

SD-O-06

Study of the Fabrication of Microreactor Made of Stainless Steel AISI Type 304 by Using Laser Beam Welding

Tinna Sorasiri [a,*] , **Bovornchok Poopat** [b]
[a,b]*Department of Production Engineering, Faculty of Engineering,*
King Mongkut's University of Technology Thonburi, Bangkok, 10140, Thailand
s.tinna@hotmail.com

Keywords: Laser Beam Welding, Microreactor, Distortion

Microreactor is a device in which chemical reactions occur in a confinement with typical lateral dimensions below 1 mm. Microreactors offer many advantages over conventional scale reactors, such as vast improvements in energy efficiency, reaction speed and yield, and a much finer degree of process control. Due to the small size of microreactor components, Laser beam welding is one of the suitable processes for microreactor fabrication because it provides the small size weld beads with high accuracy, high precision, low heat input and low distortion. The objectives of this research are to investigate laser beam welding parameters and to develop welding procedures for the fabrication of microreactor made of 1-mm-thick AISI 304 stainless steel sheets. Specimens were prepared as lap joints and welded as partial joint penetration seam welds using a continuous wave 2 kW fiber laser welding system. To evaluate the optimal process parameters, i.e., laser power and weld speed, the weld bead profiles obtained from macro etch tests and the strength of welded joints obtained from tensile peel tests were analyzed. Furthermore, the temperature gradient data were collected during welding to use as the input data for finite element simulations by ANSYS. The simulated distortion results were compared with the experimental results. The comparisons indicated that finite element simulation can be applied to help developing welding procedures for the minimal distortion in microreactor fabrication.

SD-O-07

Effect of Vortex Finder, Inlet and Body Diameter of Hydrocyclone on the Separation Efficiency for Crude Palm Oil Industry

Supachart Pakpooma, Kruakaew Praropb, Swasdisevi Thanita and Wongsarivej Pratarnb,*

[a]*King Mongkut's University of Technology Thonburi, 126 Pracha-utid Road, Bangmod, Toongkru, Bangkok 10140, Thailand*

[b]*National Nanotechnology Center, National Science and Technology Development Agency, 111 Thailand Science Park, Phahonyothin Road, Khlong Nueng, Khlong Luang, Pathumthani 12120, Thailand*

E-mail: pratarn@nanotec.or.th

Keywords: Inlet, Vortex finder, Hydrocyclone, Separation Efficiency

Hydrocyclone is novel optional equipment that can be applied to solid separation in crude palm oil process because of the advantage over the existing one. Hydrocyclone is the continuous tool, cheap and easily to maintenance. The objectives of this research were to investigate the effect of vortex finder, inlet and body diameter of hydrocyclone on separation efficiency of palm meal from crude palm oil by using pvc resin as the solid phase and biodiesel B5 as the liquid phase. All parameters were studied with simulation using computational fluid dynamic, CFD while the inlet diameters were additionally tested experiment. The various feed flow rates in both of simulation and experiment were 4, 6, 8, 10, 12 and 14 L/min at the flow ratio of 0.2 and 2 wt% of pvc resin. The designs of experiments were clearly specified. In addition, the vortex finder diameters of 3.8, 4.8 and 5.8 mm were simulated. The simulated inlet diameters were 5, 6 and 7 mm. The three sizes of body diameter of 30, 40 and 50 mm were selected as the example sizes. From the simulation results, the smaller the vortex finder, inlet and body diameter of hydrocyclone revealed the better separation efficiency. That was confirmed by the experimental result, the smaller inlet diameter obtained the better separation efficiency.

SD-O-08

Influence of Spinning Process Parameters on Spinning Deformation, Force and Surface Roughness

Thanapat Sangkharat[a] , Surangsee Dechjarern[a,*]
[a]Production engineering department, Faculty of engineering, King Mongkut's University of Technology North Bangkok, 1518 Pracharat 1 Road, Bangsue, Bangkok, 10800, Thailand
* surdec2000@yahoo.com

Keywords: Metal spinning, Finite element, Force, Roughness

Metal spinning process has been developed in recent years and widely used in manufacturing many types of components. The advantage of spinning process is that it requires a lower power than other metal forming process, larger deformation with the good surface finish and improved mechanical properties. The aim of this paper is to investigate the influences of spinning process parameters, i.e. roller radius, feed rate and feed depth, on the deformation, spinning force and workpiece surface roughness. Finite element model of the metal spinning process was developed using elastic-plastic material property. The spinning experiments were carried out and the piezoelectric force transducer was used to measure forces in 3 directions. The workpieces were etched to form circle grid on its surface, then the deformation was captured by a camera and the image processing program was developed to calculate strain during spinning process. The finite element prediction was compared with the experimental measurements and the results agreed well. Spinning force and surface finish were studied by varying the roller radius, spinning speed and feed rate.

SD-O-09

Cost Effective Production of a Permanent Mold Gravity Die Cast A356.0 Aluminum Alloy Motorbike Shock Absorber through Casting Simulation.

Muhammad Saqib Qayyum

Foundry Service Centre, Lahore, Punjab, 54890, Pakistan

saqibqayyum786@gmail.com

Keywords: Shock absorbers; Die cast; Computational Methoding; Modeling and Simulation.

Motorbike shock absorbers of gravity die cast aluminum A356.0 alloy were being imported in the as-cast condition and later on machined at local foundries and workshops by sub-vendors to achieve the required dimensions and on many occasions a nearly complete solid block was cast and machined to achieve the desired shape but this process not only lowered the metallic yield but also the high machining costs and time required made it very uneconomical. Motorbike shock absorbers are critical vehicle components which are always under load and must never fail suddenly without warning therefore they need to be free of defects like shrinkage and micro-porosity. The thin wall thickness of 6mm and troublesome nature of cores required makes this component quite difficult for the conventional metal caster. The current research paper deals with the methoding, die designing, modeling and simulation, optimization and finally casting of these components following the data produced by the former. Initially a single piece per mold was suggested but later on considering the economics of the project two pieces i.e. left and right were recommended to be cast from a single sprue in each die with a vertically parted permanent die mold. For the methoding calculations the Thermal modulus has been used instead of the conventional casting modulus and for gating the naturally pressurized system is incorporated. Throughout the simulation process a significant number of iterations were made to achieve the final design which ensured a laminar flow of liquid aluminum below the critical velocity limit; the actual die casting results yielded good comparison with the simulation studies showing shrinkage cavity away from the risers and micro-porosity only in ingates.

Simulation, Design and Manufacturing Session

POSTER PRESENTATIONS

SD-P-01

Effect of Cell Configuration and Size on Strength of Lightweight Structural Cores Sandwich Panels

Passawit Pittayapaisan[a*], Assoc. Prof. Dr. Somchai Norasethasopon[a*]
[a]*Department of Mechanical Engineering, Faculty of Engineering, King Mongkut's Institute of Technology Ladkrabang, Bangkok, Thailand 10520* passawit.mat@gmail.com, n-somchai@hotmail.com

Keyword: Sandwich panel, Honeycomb core, Three-point bending, Impact test,

Bending and failure of lightweight structural cores sandwich panels, Aluminum 1200, were studied and presented in this paper. Five types of the cell configuration of the lightweight structural cores such as triangle, square, parallelogram, hexagonal and waves were tested by set the unit cell equally. Three-point bending and Impact testing were used in this investigation. Finite element simulation was also used for predicting the failure load in Aluminum 1200, the lightweight structural cores sandwich panels. From the results, we found that the parallelogram and hexagonal cell configuration structures were the best of the high strength sandwich panels respectively.

SD-P-02

The Wet Etching Technique to Reduce Pyramidal Hillocks for Anisotropic Silicon Etching in NaOH/IPA Solution

Chupong Pakpum[a,*]

[a]*Program in Materials Science, Faculty of Science, Maejo University, Chiang Mai, 50290, Thailand*

E-mail address: chupong@mju.ac.th

Keywords: NaOH+IPA solution, pyramidal hillocks, silicon(100), ultrasonic agitation

The various methods of silicon wet etching techniques, which utilize ultrasonic agitation to reduce pyramidal hillocks in etched patterns, were evaluated in NaOH+IPA solution. The comparison of the etching methods composed of; 1.) no agitation + sample horizontally orientated, 2.) ultrasonic agitation + sample horizontally orientated, 3.) ultrasonic agitation + sample vertically orientated, and 4.) ultrasonic with rotation agitation + sample vertically orientated. It was found that the percentages of the etched patterns presenting hillocks after etching were 100%, 79.77%, 32.67% and 2.62%, respectively. Ultrasonic coupled with rotation agitation along with the sample vertically orientated is the most powerful etching technique, offering a high yield of smooth etched surface. The difference in etch rate between without agitation and applying ultrasonic agitation was not observed in this experiment, as it was operated in a solution temperature 60-65°C and a 275nm/min etch rate was achieved. The theories that relate to each evaluated method are also discussed.

SD-P-03

Application of Numerical Method and Statistical Analysis in the Integrated Intensity Calculation of the Peaks from the X-Ray Diffraction (XRD) Pattern of α-Iron

Parinya Chakartnarodom[a,c], Nuntaporn Kongkajun[b,*], Payoon Santongkaw[a,c]
[a]*Department of Materials Engineering, Faculty of Engineering, Kasetsart University, Chatuchak, Bangkok, 10900, Thailand*
[b]*Department of Physic, Faculty of Science and Technology, Thammasat University, Klong Luang, Prathumthani, 12121, Thailand*
[c]*Materials Innovation Center, Faculty of Engineering, Kasetsart University, Chatuchak, Bangkok, 10900, Thailand*
* n-kongkj@tu.ac.th (corresponding author)

Keywords: numerical method, statistical analysis, integrated intensity, x-ray diffraction

The aim of this work is to analyze the uncertainty of the calculated integrated intensity of the x-ray peaks of α-iron (Fe) powder from x-ray diffraction (XRD) by using the numerical method and the statistical analysis. The α-Fe powder was analyzed by the x-ray diffractometer at step size 0.03° 2θ and preset time from 0.1 to 3.5 s. The integrated intensity of the x-ray peaks and their uncertainty were calculated using numerical method. The correlation between the uncertainty (ΔI_{int}) of calculated integrated intensity (I_{int}) and the preset time (t) were analyzed by the statistical analysis methods which are linear regression and statistical hypothesis testing. The results from the statistical analysis at significance level of 0.05 show that the percent relative uncertainty ($y = (\Delta I_{int} \ I_{int}) \times 100$) correlate with the preset time (t) by $y = a_1 / t^{a_2}$ when a_1 and a_2 are the constants. From the mathematical model, to minimize the relative uncertainty, the preset time should be greater than one second. Moreover, at the same preset time and step size, the lower integrated intensity, the higher percent relative uncertainty.

Surface Engineering and Heat Treatment Session

ORAL PRESENTATIONS

SH-O-01

Evaluation of Surface Roughness of Engineered Wood Composites

Salim Hiziroglu
Department of Natural Resource, Ecology & Management, Oklahoma State University
Stillwater, Oklahoma 75078-6013, U.S.A.
E-mail: salim.hiziroglu @okstate.edu

Keywords: Surface roughness, wood composites, overlays.

Roughness of substrate composite panels is a latent property until they are exposed to high humidity exposure. Therefore it is important to quantify surface roughness of the panel to have a better overlaying of the substrate. In this study, surface characteristics of different types of panels manufactured from wood and non-wood fiber resources were evaluated. Samples in dimensions of 15 cm by 15 cm panels were overlaid with resin impregnated decorative paper. Roughness measurements were randomly taken from the surface of control and overlaid samples using a fine stylus profilometer. Three roughness parameters, namely average roughness (R_a), mean peak-to-valley height (R_z) and, maximum roughness (R_{max}) were used to evaluate surface characteristics of the samples conditioned at 55% and 92% relative humidity levels. Once panels were overlaid with decorative paper samples had an average R_a value of 1.86 µm which is 3.29 times lower than its original surface. Statistical analysis revealed that significant difference was found between roughness values of panels at initial and final conditions. When the samples were exposed to 92 % relative humidity they all had significantly higher values of R_a, R_z and R_{max} than those of measurements taken at 55 % relative humidity. It appears that stylus method is able to detect differences in surface roughness of overlaid panels that can occur due to changes in environmental conditions. Initial findings of this study suggest that surface quality of composite panels made from wood and non-wood under-utilized species can be quantified subjectively by stylus technique to provide numerical data so that such panels can be used for manufacture of further value added products more effectively.

SH-O-02

Comparison Study of TiO_2, Ni-B and Thiourea doped TiO_2 Synthesized by Sol-gel Process at Low Temperature.

Kumthorn Tangwongsirikul[a], Vishnu Rachphet[a,*], Lek Sikong[a]
Department of Mining and Materials, Faculty of Engineering, Prince of Songkla University, Hat Yai, Songkla, 90112, Thailand
*E-mail rvishnu@eng.psu.ac.th

Keywords: TiO_2, Reflux, UV light, Contract angle, Escherichia coli.

Titanium dioxide (TiO_2) film was synthesized by sol - gel process at low temperature, refluxing and drying at 80 °C. The investigation of crystalline structure surface roughness characterized by Scanning electron microscope (SEM), X-Ray diffraction (XRD), X-ray photoelectron spectroscopy (XPS) and Atomic force microscopy (AFM), respectively. Finally, we found that the titanium dioxide (TiO_2) film doped with Thiourea(S-N) has the better rate of degradation of methylene blue (10^{-6} M), it kills all of E.*coli* in only 20 minutes. White, doping with Ni-B make titanium dioxide (TiO_2) film become more hydrophobic surface with the contact angle at 133 degrees.

SH-O-03

The Effects of O_2:N_2 Gas Ratios on Structural, Optical, Electrical Properties of TiO_xN_y Thin Film deposited by Reactive DC Magnetron Sputtering

Tanakorn Khumtong[a,*], Rachsak Sakdanuphab[a]
[a]*College of Data Storage Innovation, King Mongkut's Institute of Technology Ladkrabang, Bangkok 10520 Thailand.*
*TanakornK34@gmail.com

Keywords: Titanium oxynitride, reactive magnetron sputtering, O_2:N_2 gas ratio.

In this work, titanium oxynitride (TiO_xN_y) thin films were deposited on glass slide substrates by using reactive dc magnetron sputtering technique. The reactive gas ratios between O_2 and N_2 were studied in the range of 15-30% with a constant of Ar gas at 110 sccm and a time of 120 minutes. Microstructure, optical, and electrical properties of TiO_xN_y thin films were analysis by using SEM, AFM, GIXRD, UV-VIS spectrophotometer, and 4-point probe measurements. We found that the thickness of the films decreases from 1.0 to 0.8 μm with increasing O_2 gas ratios. The TiO_xN_y thin films have smooth surface related to small nano-grain size. The roughness of the films slightly decreases with increasing O_2 gas ratios. From optical transmission spectra, we observed that the transparent of the films increases with increasing O_2 gas ratio and shifts the band gap from 2.67 to 3.32 eV. The resistivity of the films obviously increases from 3.04 x 10^{-3} Ω-cm to 5.45 Ω-cm by increasing O_2 gas ratio. This result indicates the phase changes of the TiO_xN_y films from metallic to oxide phases. The XRD spectra show poor crystalline TiN (220) and TiO_2 (021) at 15% of O_2 ratio and then the films become amorphous structure when increase O_2 gas ratios. The O_2:N_2 gas ratio affects to the different concentration of oxygen and nitrogen into the TiO_xN_y thin films that lead to the various optical and electrical properties.

SH-O-04

Microstructure and Immersion Behavior of Plasma Sprayed Bi-Layered Ceramic Coatings

S.Sathish[a,*], C.Senthilvel[a], B.Dilip Jerold[a], Mohd.F.Shabir[a]
[a]*Aalim Muhammed Salegh College of Engineering, Avadi IAF,Chennai-600055,India*
*mechhh_er@rediffmail.com

Keywords: Plasma spraying; Bilayered coating; Immersion test

Atmospheric plasma spraying technique was employed to fabricate ZrO_2, Al_2O_3, ZrO_2/Al_2O_3 and Al_2O_3/ZrO_2 coatings on 304 stainless steel substrate. Anodic polarization studies were carried out to measure the corrosion characteristics of the coatings. Immersion test was also performed in 1N HCl. The corrosion potential and the corrosion current density obtained from the coatings were related to the microstructures. The results revealed that there has been a significant enhancement in the corrosion resistance of Al_2O_3/ZrO_2 coating and this is attributed to the dense and compact microstructures with very few porosity. The lowest mass loss was recorded for Al_2O_3/ZrO_2 coating in immersion test depicting that the presence of an intermediate Al_2O_3 layer between the stainless steel and ZrO_2 coating has provided a very effective protection of the substrate against corrosion in HCl solution.

SH-O-05

Use of Scratch Test to Evaluate Cohesive Strength of Mo/NiCrBSi Composite Plasma Sprayed Coating

Hathaipat Koiprasert*, Sirinee Thaiwatthana, Panadda Sheppard
National Metal and Materials Technology Center, Pathumthani, 12120, Thailand
*E-mail: hathaik@mtec.or.th

Keywords: Mo/NiCrBSi, plasma spray, cohesive strength, scratch test.

One limitation in using a scratch test to replace a conventional pull-off test method to evaluate a bond strength of a thermal sprayed coating is that the scratch test performed on a cross-section of the coating demonstrates a cohesive strength of the coating while an adhesive and/or a cohesive strength of the coating can be measured using the pull-off test. This makes the scratch test inappropriate for the evaluation of a bond strength of multilayer coatings. Nevertheless, the scratch test result obtained from the cross-section of the coating is beneficial for comparison of the cohesive bond strength of the composite coating. This method can reduce the testing cost in the long run due to the significant cost reduction in consumables as well as energy and time saving from the curing step. This research concerns the possibility of using the scratch test to measure the cohesive bond strength of Mo and its composite with NiCrBSi. The results from the pull-off test and the scratch test indicate that the cohesive strength obtained from the two techniques exhibit a similar trend. The cohesive bond strength increases with an increase in NiCrBSi percent content.

SH-O-06

Investigation of Abrasive Flow Machining on Aluminum 5083 Mold Polishing

Theerapong Maneepen[a,*]
[a]*Production Technology Education Department,Faculty of Industrial Education and Technology,King Mongkut's University of Technology Thonburi, Bangmod, Thongkru, Bangkok, 10140, Thailand*
* theerapong.man@kmutt.ac.th

Keywords: Abrasive Flow Machining, AFM, Mold Polishing, Aluminum 5083.

The paper presents the effect of pressure and machining time of specimens and media for surface roughness (Ra) of Al 5083 mold that related to the abrasive flow machining (AFM). This research experimented with flat specimens. AFM experiments are performed to identify the improvement surface roughness when applied to the polishing specimens. Specimens were prepared by grinded, and polished with the abrasive flow machining (AFM) and measured an original value of Ra compared with the final value of Ra in the end of process. The process parameters are as follows: an abrasive particle size (Al_2O_3) 0.05 μm in oil-based solution (50 % concentration by weight), hardness force of specimens 500 kg 10 mm was 65, pressure 10 bar, and machining time 5, 15, 25 min consequently. The experimental results show that under these conditions, the average surface roughness of specimens is differenced from an original value of Ra 0.005 μm.

SH-O-07

The Effect of Heat Treatment on Fe^{2+}/Fe^{3+} Ratio in Soda-lime Silicate Glass

Ekarat Meechoowas[a,*], Suwipa Poosrisom[a], Tepiwan Jitwatcharakomol[a]

[a]*Glass Expert Laboratory, Physic and Engineering Program, Department of Science Service, Bangkok, 10400, Thailand*
*ekarat@dss.go.th

Keywords: Soda-lime glass, Sand, Iron oxide, Redox reaction.

The redox reaction of a tableware soda-lime silicate glass contained with 0.04 - 1.00 wt% of iron oxide was investigated by UV-Vis spectroscopy. High purity of raw materials especially sand are require to control the amount of iron oxide as low as possible. Normally tableware glass contain small amount of iron oxide (0.01 - 0.04 wt%) and iron effect (green color) is controlled by adding decolorizing agent. The heat treatment around transition temperature is another method to decolorize iron by using redox reaction. It is believed that the reaction of iron oxide Fe^{2+}(green) $\leftrightarrow$ Fe^{3+}(yellow) still occurred in annealing process. In this study, the glasses were prepared by melting in the platinum crucible. After annealing, were cut glasses to four pieces and heated at 550 560 570 and 580ºC with different times. The result of the transmittance showed no significantly change but the color in CIE L*a*b* system of glasses heat treated at 550 and 560 ºC slightly changed into white shade. According to the result of calculate Fe^{2+}/Fe^{3+} ratio, ratio of this glasses were decreased by 5 and 2.5 % respectively, at this temperature the reaction is $Fe^{2+} \rightarrow Fe^{3+}$. On the contrary, the ratio of glass heated at 580 ºC increased, due to $Fe^{3+} \rightarrow Fe^{2+}$ and the color changed into green. The results proved the kinetic of the redox reaction and possibility to use annealing process as another tool to control flint color of glass.

SH-O-08

Residual Stresses and Fatigue Performance of Modified Mechanical Surface Treated Martensitic Stainless Steel AISI 420

Patiphan Juijerm[a,b,*]

[a]*Department of Materials Engineering – Metals Research Group, Faculty of Engineering, Kasetsart University, Bangkok, 10900, Thailand*

[b]*Residual stress and Fatigue Excellent Center (ReFEC), Iron and Steel Institute of Thailand (ISIT), Bankok, 10110, Thailand*

*E-mail: juijerm@gmail.com, juijerm@isit.or.th

Keywords: Mechanical surface treatment, Residual stress, Fatigue, Stainless steel

Nowadays, mechanical surface treatments, such as shot peening or deep rolling have an important role and are frequently mentioned in automotive industries in Thailand. Many machinery parts concerned the fatigue performances are mechanical surface treated. Generated compressive residual stresses and work hardening layers at the surface, and near-surface regions are the key reasons to inhibit or retard crack initiation, as well as propagation during service in dynamic, as well as cyclic loading. However, the generated compressive residual stresses and work hardening layers can be relaxed (reduced) due to thermal-, mechanical loading, or both, which directly affect the fatigue lifetime of the mechanical surface treated components. That means that if the relaxation process could be retarded, the greater fatigue lifetime and performance should be expected. These relaxation phenomena are associated by dislocation movement and realignment, such as a polygonization in a recovery process. Thus, residual stress relaxation of the mechanical surface treated condition could be slow down if the dislocation movements were hindered. The strain ageing concept is the one of the ways to pin dislocations by solute atoms called Cottrell cloud. Moreover, in some researches, very fine precipitated carbides pinning dislocations are also detected and reported.

To clarify the effects of mechanical surface treatments included static and dynamic strain ageing on the fatigue performance, in this research, the deep rolling (conventional) and its modifications, high temperature deep rolling (dynamic strain ageing) and deep rolling followed by annealing (static strain ageing) were performed on the martensitic stainless steel AISI 420. Residual stress and work hardening (represented by FWHM values) depth profiles were measured using X-Ray Diffraction (XRD) with $\sin^2\psi$ method. Fatigue tests were performed using a rotating bending fatigue machine. It was found that the deep rolling could enhance the fatigue lifetime, as well as performance of the deep rolled martensitic stainless steel AISI 420 through the generated compressive residual stresses and work hardening layers at the surface, and near-surface regions. The fatigue performances of the modified deep rolled (high temperature deep rolling and deep rolling followed by annealing) conditions exhibit the greater fatigue lifetime and performance than that of the conventional one, although some residual stress and work hardening relaxations were observed after the modified deep rolling processes.

SH-O-09

Phase Equilibria of Bi-Se-Sb Thermoelectric Materials at 250C

Hsiung Chin, Chun Wojciech Gierlotka
Dept. of Materials Science and Engineering, National Dong Hwa University
College of Science and Engineering, Hualien, Taiwan
Dong Hwa University, Shoufeng Township, Hualien County 974, Taiwan (R.O.C.);
610222029@ems.ndhu.edu.tw

Keywords: Bi-Se-Sb,Phase diagram,Isothermal section

The Ternary Bi-Se-Sb system hooks a great attention as a promising hydrogen storage material. However, only a limited number of phase equilibrium information is available in the literature. The 250C isothermal section of the ternary Bi-Se-Sb system is experimentally determined in this study. Sample alloys were prepared as selected compositions by arc-melting and after that annealing at 250C for two month. The equilibrated alloys microstructures were examined micro-graphically and quantitatively by OM and EDS, respectively. After the experimental examination an isothermal section of the ternary Bi-Se-Sb system was constructed.

SH-O-10

Investigation and Characterization of Crystalline ZrN Thin Films Deposited by DC Reactive Magnetron Sputtering on Unheated Substrate for Decorative-Coating Applications

Witthawat Wongpisan[a,*], Arunee Lakkham[a], Mati Horprathum[b], Chanunthorn Chananonnawathorn[b], Saksorn Limwichean[b], Viyapol Patthanasettakul[b], Pitak Eiamchai[b]

[a] *Failure Analysis and Surface Technology Laboratory, National Metal and Materials Technology Center, Pathumthani 12120, Thailand*

[b] *Optical Thin-Film Laboratory, National Electronics and Computer Technology Center, Pathumthani 12120, Thailand*

* witthaww@mtec.or.th

Keywords: Zirconium Nitride, Decorative Coating, Sputtering, Unheated Substrate.

Recently, research involving the performance, cost-effective and time-consuming of deposited zirconium nitride (ZrN) film by low-temperature process has gained significant attention for decorative coatings industrial. In this article, crystalline ZrN thin films were successfully deposited by dc reactive magnetron sputtering for decorative-coating applications. Silicon (100) wafers and glass slides were used as substrates without heat treatment and substrate bias. The films were deposited under different time, from 150 to 1,500 s. The obtained films were primarily characterized for crystal structures, morphologies, film compositions, mechanical, and optical properties. The results showed that the ZrN thin films exhibited a cubic closed-packed structure with the (111) plane. The effects of the deposition time was observed and discussed from the changes in morphologies, compositions, adhesion, and optical properties of the films.

SH-O-11

Study of the Influence of Thermal Effects on the Tribological Properties of Element Added-DLC Films

Nutthanun Moolsradoo[a,*], Chavin Jongwannasiri[b], Shuichi Watanabe[b]
[a]*King Mongkut's University of Technology Thonburi, Faculty of Industrial Education and Technology, Bangkok, 10140, Thailand*
[b]*Nippon Institute of Technology, Faculty of Engineering, Saitama, 345-0826, Japan*
*nutthanun.moo@kmutt.ac.th

Keywords: Thermal, Mechanical, Tribological properties, DLC films.

Diamond-like carbon (DLC) coatings are metastable amorphous films that exhibit unique combinations of properties such as high hardness and elastic modulus, low friction coefficients, good wear resistance, and excellent corrosion resistance. Hence, these films are commonly applied as wear resistance protective coatings in magnetic storage, tooling, and biomedical applications. However, DLC films have low thermal stability at higher working temperatures and no sufficient friction coefficient depending on their application environment. The addition of foreign elements during film growth has shown to be especially powerful. This research is to study the influence of thermal effects on the tribological properties of element added-DLC films. The Si-DLC and Si-N-DLC films were deposited from gaseous mixtures of C_2H_2:TMS and C_2H_2:TMS:N_2, at three different ratios, 2:1, 1:2, and 1:4. The bias voltage was set to -5 kV, at an RF power of 300 W. The deposition pressure was set to 2 Pa and total deposited thickness was approximately 500 nm. All films were deposited by Plasma Based Ion Implantation (PBII) technique. Additionally, conventional DLC film was utilized to compare with element added-DLC films. The conventional DLC film was deposited from C_2H_2, with bias voltage of -5 kV, at an RF power of 300 W, and total thickness of 500 nm. The films structure was analyzed by Raman spectroscopy. The relative atomic contents of films was analyzed by Energy dispersive X-ray spectroscopy (EDS). The thermal stability of films was analyzed by Thermaogravimetric and Differential thermal analysis (TG/DTA). The tribological properties of films was measured by a ball-on-disk friction tester. The friction test was performed under ambient air at high temperature, 400°C, 650°C and 900°C. In the friction test, a dry sliding test was carried out using a ball indenter, SUS 440 C under a normal applied load of 3 levels, 3 N, 5 N and 7 N at linear speed of 31.4 mm/s. The area of an abraded cross-section of the wear mark was measured after friction tests to calculate specific wear rate.

SH-O-12

Dissolution of Y and Al during Plasma Spraying of NiCrAlY

P. Sheppard*, C. Sukhonket and K. Ninon
National Science and Technology Development Agency, National Metal and Materials Technology Center, Pathumthani, Thailand.
*Corresponding author: panaddn@mtec.or.th

Keywords: Thermal barrier coating; Yttrium; Reactive element; NiCrAlY.

Aluminium has been added to NiCr alloy to improve its high temperature oxidation resistance via the selective oxidation mechanism. Yttrium as a reactive element has been added to NiCrAl to promote an adhesion of it alumina scale, formed from selective oxidation. This produces NiCrAlY superalloy, a commercial thermal spraying bondcoat powder, used extensively as part of a protective thermal barrier coating (TBC). The exact role of yttrium has received a great deal of attention in recent years. Previous research works have shown that a small amount of the scarce and expensive yttrium, at 1 wt. % or less, can help to increase the adhesion of a thermally-grown oxide scale (TGO) which is formed throughout the TBC service life at high temperature. Yttrium can also act as a gettering element for sulphur which can further enhance the adherence of TGO. Thus the service life of the coating can be lengthened provided that there is a sufficient amount of yttrium in the bondcoat. This work investigates the loss of yttrium and aluminium from NiCrAlY powder particle during its in-flight oxidation. This was achieved by rapidly cooling the NiCrAlY spraying powder in mid-flight using a high pressure argon jet. Thus the microstructure of the powder a moment before the impact with the substrate was preserved. The powder was then characterised using a scanning electron microscope in order to obtain a better understanding of its oxidation behaviour. It was found that yttrium and aluminium dissolution took place during the short flight. Near the center of the plasma plume, a large amount of yttrium-containing oxide phase was found amongst an aluminium-rich oxide. Both oxides were formed in-flight during air plasma spraying. This results in a significant reduction in yttrium concentration in the NiCrAlY splat as it deposits on a substrate forming the bondcoat layer. Further away from the center of the plume however, an increase in yttrium concentration was observed due to the selective evaporation of the superalloy. This results in a sprayed powder of mixed microstructure. The resultant coating inevitably exhibits a heterogeneous structure in terms of aluminium and yttrium distribution.

SH-O-13

Post Weld Heat Treatment Cracking in Heat Resistant Alloy

Kosit Wongpinkaew[a], Siam kaewkumsai[a,*], Siriwan Ouampan[a], Ekkarut Viyanit[a]

[a]*National Metal and Materials Technology Center, Klong 1, Klong Luang, Phathumthani, 12120, Thailand*

*E-mail address: siamk@mtec.or.th

Keywords: Outlet Pigtail Tube, Intergranular Cracking, High Temperature Failure

The petrochemical plant discovered the failure of hydrogen reformer outlet pigtail tube, which is a component of reformer fire heater. It was used for feeding hydrogen gas (~80%) which was cracked from the natural gas and liquid petroleum gas. During operation, the temperature in the outlet pigtail tube was maintained at about 800-850 ºC and the internal pressure was about 30.6 barg. The tube was made of heat resisting alloy grade Incoloy 803. During the scheduled turnaround of the plant, micro-crack and bulging was observed on the outlet pigtails tube. The failed tubes were replaced and subject to subsequent post weld heat treatment (PWHT) for stress relief. PWHT was conducted at the temperature 1150 ºC and soaking for 20 minutes. Unfortunately, during induction heating of one tube, overheating was detected. The temperature was measured about 1250 ºC. Furthermore, when the temperature reaches around 1250 ºC, the heater was out of order. Then, the plant personnel tried heating up again. The second heat treatment was successful. However, after an unspecified period of operation for about 3 weeks, the outlet pigtail tube developed circumferential crack around 10-15 cm far from the weld, resulting to plant shutdown.

The investigation included visual examination, emission spectroscopy, macro- and micro-fractography, metallography, tensile test, and micro-hardness measurement. Six conditions of PWHT simulation were performed for comparison. Analytical results pointed out that the cracking of the outlet pigtail tube was caused by overheating during the post weld heat treatment process in the mode of intergranular cracking. Significant growth of precipitates of carbides both at grain boundaries and within grain interiors was observed in the failed zones. The grain growth, indicative of overheating, was also observed. Overheating during PWHT is primarily responsible for significant degradation in mechanical properties and microstructure in the failed portion of the tubes. Tube bowing promotes cracks. To avoid such overheating, precautions should be taken by improving the PWHT condition. It is necessary to specify the finer grain size before using the alloy in high temperature application.

Surface Engineering and Heat Treatment Session

POSTER PRESENTATIONS

SH-P-01

Effect of Additives and Operating Conditions on the Electroplating Ni-W Alloy

Jiaqian Qin[a,*], Ekachai Srikaen[b], Malay Kumar Das[a] , Yanan Xue[c], Xinyu Zhang[c], Adisak Thueploy[a], Sarintorn Limpanart[a], Yuttanant Boonyongmaneerat[a]

[a]*Metallurgy and Materials Science Research Institute, Chulalongkorn University, Bangkok,10330, Thailand*

[b]*Department of Physics, King Mongkut's University of Technology Thonburi, Bangkok, 10140, Thailand*

[c]*State Key Laboratory of Metastable Materials Science and Technology, Yanshan University, Qinhuangdao 066004, P.R. China*

*E-mail address jiaqianqin@gmail.com, jiaqian.q@chula.ac.th

Keywords: Ni-W alloy, Electrodeposition, Hardness

The interest in electrodeposition of nickel-tungsten (Ni-W) alloys has increased in recent years due to their unique combination of tribological, magnetic, electrical and electro-erosion properties. These alloys exhibit good mechanical properties (e.g., high tensile strength and premium hardness, as well as superior abrasion resistance), good resistance to strong oxidizing acids, and high melting temperature. It is well known that codeposition of nickel and tungsten is very sensitive to changes in operating conditions and the additives (e.g., sodium dodecyl sulfate (SDS), saccharin sodium). However, there are very less of study on the effect of these additives on the chemical compositions, microstructure and mechanical properties of Ni-W alloy coatings. Furthermore, to improve conductivity, sodium bromide (NaBr) is always used in the Ni-W electrolyte, but no detailed investigation of the role of NaBr on the electroplating Ni-W alloys. Thus, the objective of the current work is to study the effect of additives and operating conditions on the Faradaic efficiency, chemical composition, surface morphology, thickness and hardness of Ni-W alloys deposited on carbon steel. The morphology of the deposits was studied by scanning electron microscopy (SEM) as well as optical microscope (OM), and the approximate composition by energy dispersive spectroscopy (EDS). The phase and crystalline size were determined by X-ray diffraction (XRD). Metallographic cross-sections were also analyzed, and microhardness was performed by Vickers hardness tester. EDS results show that saccharin sodium and NaBr can significantly affect the tungsten contents and hardness in deposits. Ni-W alloy with 30 at.% W plated at current density of 0.1 A/cm^2, without NaBr and any additives exhibited the maximum hardness of 784 HV. Ni-W alloy plated at current density of 0.05 A/cm^2, with NaBr 18g/L and saccharin sodium 2 g/L exhibited the lowest tungsten contents of 12.82 at.%. The results are discussed in detail with emphasis on routes to increase the tungsten contents and hardness, while reducing the extent of cracking.

SH-P-02

An XRD Phase Analysis of Al-F Re-deposition Produced from Reactive Ion Etching

Chupong Pakpum[a,*]

[a]*Program in Materials Science, Faculty of Science, Maejo University, Chiang Mai, 50290, Thailand*

*E-mail address: chupong@mju.ac.th

Keywords: AlF_3, Fluorine-based plasma, RIE etching, XRD

This paper reports the analysis of the composition, structure and phase of the re-deposition material that was generated from the reaction from CF_4 plasma etching on the Al_2O_3-TiC substrate. The re-deposition was sputtered from the etching area and deposited on a silicon coupon for analysis. The morphology of the re-deposition was investigated by scanning electron microscope (SEM) and the composite element of the re-deposition was detected by using energy dispersive x-ray spectroscopy (SEM-EDX). X-ray diffraction (XRD) was used to analyze the structure and phase of the re-deposition. The results show that the prepared re-deposition was composed of F and Al atoms, with 51.24 At% and 27.67 AT%, respectively. XRD revealed that this was owing to the chemical formula AlF_3, which has a rhombohedral crystal structure in the most stable alpha phase (α-AlF_3).

SH-P-03

Effect of Electro-polishing Process on Surface Morphology of Anodic Aluminum Oxide in Second Step Anodized

Jameekorn Jadto, Peerawith Sumtong, Pimsuree Choksumlitpol, Chayangkoon Mangkornkarn, Apiluck Eiad-ua*
College of Nanotechnology, King Mongkut's Institute of Technology Ladkrabang, Ladkrabang, Bangkok 10520, Thailand
* keapiluc@kmitl.ac.th

Keywords: Electro-polishing, Anodization, Anodic aluminum oxide.

Electro-polishing is the metal surface cleaning and modified surface of metal by electrical process. In this experiment, aluminum sample was used for study the effect of electro-polishing on morphology of anodic aluminum oxide (AAO). The current research studies the effect the electro-polishing process by applying different conditions of voltage, time and temperature for identifying the best condition for the anodization process. Field Emission Scanning Electron Microscope (FE-SEM) were used to characterize the morphology of AAO. It was also observed that increase voltage decreased the ordered pore. Increasing time, the morphology is no difference with time. Highly ordered pore with low temperature. In addition, the relationship between electro-polishing process and AAO is further discussed.

SH-P-04

Comparative Study of Non-Annealing and Annealing on the Properties of ITO Deposited by RF Magnetron Sputtering

S.Tipawan Khlaybooneme[a,*], Warawoot Thowladda[a]

[a]Surface Physics and Laser Research Laboratory, Department of Physics, Faculty of Science, King Mongkut's Institute of Technology Ladkrabang, Bangkok, 10520, Thailand

*kktipawa@kmitl.ac.th

Keywords: ITO thin films, Optical properties, Electrical properties, Annealing.

Indium tin oxide (ITO) thin films were deposited onto glass substrates by RF magnetron sputtering of ceramic In_2O_3: SnO_2 target (10wt% SnO_2) in pure argon atmosphere at a low base pressure of $3x10^{-6}$ mbar. Two thin films of ITO were studied: one was unannealed and the other was annealed at a temperature of 400 °C for 1 h. The crystalline phase, morphology, lateral structure, elemental composition as well as electrical, optical and hydrophobic properties of the films were characterized by FE-SEM combined with EDX, XRD, Hall effect measurements, UV-Vis transmission and reflectance spectroscopy, FTIR and contact angle measurements. The predominant orientation of the films was (400) and its intensity increased after the film was annealed. The crystallite size increased from 13.1 to 32.5 nm. The structure of the annealed film became reformed in a columnar structure. The annealing treatment was effective in increasing mobility from 7.5 to 27.5 $cm^2.V^{-1}.s^{-1}$ and in decreasing both film resistivity from $2.7x10^{-3}$ to $1.1x10^{-3}$ Ω.cm and carrier density from 3.0 $x10^{20}$ to 2.0 x 10^{20} cm^{-3}. The change in these electrical properties resulted from an increasing tin incorporated in the film. The increasing incorporated tin induced optical energy band gap to increase from 3.36 to 3.46 eV and refractive index to decrease from 2.76 to 2.54. The ITO films are highly transparent in the visible region with transmittance of ~80% for the as-grown film and 85% for the annealed film. The measured contact angle reduced from 95 to 80 degrees. The correlation between the elemental composition of the films and the properties will be discussed.

SH-P-05

Influence of Heat Treatment on Mechanical Properties of Al-Si-Cu-Mg Alloys Produced by Squeeze Casting

Nattawat Pinrath[a,*], Weerachai Arjharn[a], Chakkrist Phongphisutthinan[b], Pongsak Dulyapraphant[b]
[a]*Suranaree University of technology, Nakhonratsima, 30000, Thailand,*
[b]*National Metal and Materials Technology Center, Pathum Thani, 12120, Thailand*
*nattawatpinrath@gmail.com

Keywords: Heat treatment, aluminum alloys, squeeze casting.

Today the automotive industries demand materials with good mechanical properties, environmental friendly and energy efficiency. Aluminum alloys are lightweight materials which can be produced in many products depending on the manufacturing process. Casting is the most common manufacturing process of aluminum alloys. However, the major drawbacks for conventional advanced casting techniques, e.g., high pressure die-casting (HPDC) are the formation of defects such as air entrapment, shrinkage porosity and microporosity.

High strength aluminum alloys can be produced by squeeze casting in order to minimize the defects in the conventional casting process. Squeeze Casting is a combination process of conventional casting and applying pressure. This process requires non turbulence flow which can reduce air entrapment during die filling. Moreover, the squeeze or applying pressure can increase the solidification rate and minimize the porosity during solidification. Therefore, heat treatment can be applied on the squeeze cast product in order to maximize the mechanical properties of the heat treatable cast aluminum alloys.

This research investigated the influence of T4, T5 and T6 heat treatment and natural aging of specimen of Al-Si-Cu-Mg alloys produced by squeeze casting process. Various solution treatments (at 460°C, 480°C, 495°C and 530°C) incorporating with artificial aging (at 180°C) and natural aging were performed. Hardness test (HRB) and tensile test were performed to evaluate the mechanical properties of the heat treated specimens.

The results showed that the squeeze cast specimens are heat treatable at high temperature without blistering. Good improvements of the mechanical properties are achieved by the heat treatment. The maximum hardness value depends on solution temperature and holding time. The peak hardness was found at 495°C because of the presence of Cu. Higher solution temperatures accelerate the peak aging time. Solid solution temperatures also affect the morphologies of the intermetallic compounds. Si phases become more spheroidized depending on the solid solution temperatures. Tensile test results show that the control of both precipitation hardening and spheroidization of Si strongly affect the mechanical properties in strength and elongation. Finally, various combinations of the heat treatment were performed to vary the yield strength, ultimate strength and elongation.

Thailand-Japan Polymer Initiative

TJ-O-01

Nanomatrix Structure and Mechanical Properties of Natural Rubber

Seiichi Kawahara
Department of Materials Science and Technology, Faculty of Engineering, Nagaoka University of Technology, Nagaoka 940-2188, Japan

Nanomatrix structure is a novel phase separated structure for a multi component system, which may provide outstanding mechanical, optical and electrical properties. It is defined to consist of dispersoid of a major component and matrix of a minor component. Here, we form the nanomatrix structure with natural rubber as a dispersoid and polystyrene as a matrix, in which almost all polystyrene links up to natural rubber at an interface. It is proven to be a unique nano-structure by both field-emission scanning electron microscopy equipped with focused ion beam and transmission electron micro-tomography, in which nanomatrix is connected to each other in all directions. A dramatic increase in storage modulus at plateau region is associated with the formation of the nanomatrix structure. This work opens up the creation of novel materials by controlling nano-structure of a minor component as a matrix.

1. INTRODUCTION

Natural rubber has held a unique place in industry as only one naturally occurring rubber (green material), whose annual production is about 10^9 tons/year. It attracts researcher's attention as a carbon neutral resource to reduce a greenhouse effect gas, CO_2; in fact, there is a plan to replace synthetic rubber made from fossil resources with natural rubber. However, there may be a ceiling production of natural rubber due to limited area for plantation of Hevea brasiliensis. In order to keep a balance of demand and supply, it is necessary to develop an innovative technology for natural rubber. We must prepare a high performance rubber from natural rubber through morphology-control.

Nanomatrix structure [1,2] is a novel nano-phase separated structure, which may provide outstanding mechanical, optical and electrical properties. It is defined to consist of dispersoid of a major component and matrix of a minor component, in which the dispersoid of several micrometers in

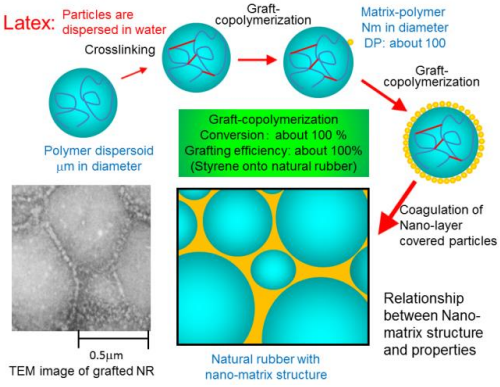

Fig.1 Green process of natural rubber.

TJ-O-02

Functionalized Magnetic Polymeric Nanoparticles for Bioanalytical Applications

P. Tangboriboonrat[a,*], C. Kaewsaneha[a], S. Trungkathan[a], D. Polpanich[b], P. Opaprakasit[c], P. Sreearunothai[c] and K. Jangpatarapongsa[d]

[a]*Department of Chemistry, Faculty of Science, Mahidol University, Phyathai, Bangkok 10400, Thailand*
[b]*National Nanotechnology Center (NANOTEC), Thailand Science Park, Klong Luang, Pathum Thani 12120, Thailand*
[c]*School of Bio-Chemical Engineering and Technology, Sirindhorn International Institute of Technology (SIIT), Thammasat University, Pathum Thani 12120, Thailand*
[d]*Center for Innovation Development and Technology Transfer, and Department of Clinical Microbiology and Applied Technology, Faculty of Medical Technology, Mahidol University, Bangkok 10700, Thailand*
[*] pramuan.tan@mahidol.ac.th

Keywords: Magnetic nanoparticle; Magnetic polymeric particle; Surface functionalization; Fluorescence

Magnetic nanoparticle (MNP) with specially tailored surface functional group has been developed for various purposes. Prussian blue-coated MNPs could effectively remove cesium from contaminated environment whereas the carboxylated MNPs, chemically bound with anti-*P.falciparum* IgG antibodies, were used for enrichment of malaria parasites. In order to prevent the oxidation of MNP and to easy surface functionalization, the magnetic polymeric nanoparticle (MPP) was synthesized via the miniemulsion polymerization of styrene/divinyl benzene/acrylic acid monomers in the presence of MNPs stabilized by oleic acid. The MPPs with > 40 wt% magnetic content were then coated with high molecular weight (300 kDa) chitosan and then immobilized with fluorescein isothiocyanate (FITC) before incubation with cancer cells, i.e., HeLa, Hep G2 and K562. Results showed that the MPPs-chitosan/FITC penetrated inside cells within a few hours, without the toxicity (> 95.3 % of relative cells viability). In parallel, mannose-rhodamine (Rh) conjugate (80% yield) was synthesized and immobilized onto MPPs for *E. coli* detection. TEM images clearly demonstrated that multiple mannose-Rh MPPs could be captured by *E. coli* strain ORN178 which indicated that the functionalized MPPs offer a simple and rapid strategy for bacterial detection.

TJ-O-03

Bromination of Natural Rubber by Anodic Oxidation in Water Process in the Presence of Carbon Dioxide

Yoshimasa Yamamoto[a,] , Yudai Yamamura[a] and Seiichi Kawahara[b, *]
[a]*Tokyo National College of Technology, 1220-2, Kunugida-machi, Hachioji, Tokyo 193-0997, Japan*
[b]*Nagaoka University of Technology, 1603-1, Kamitomioka-machi, Nagaoka, Niigata 940-2188, Japan*
*kawahara@mst.nagaokaut.ac.jp

Keywords: Natural rubber, Bromination, Anodic Oxidation, Carbon Dioxide

Anodic oxidation may have a potential to open a new field of natural rubber chemistry, since it is performed in aqueous medium to be an environmentally friendly water process. In the anodic oxidation, natural rubber latex, isolated from *Hevea brasiliensis*, is able to be used, as it stands, in which natural rubber particle of about 1 μm in diameter is dispersed in water. It is quite important to increase an affinity between the natural rubber particle and hydrophilic active species generated by the anodic oxidation in latex stage, since natural rubber latex is a biphasic reaction system of water and natural rubber particles. For instance, bromination of natural rubber in latex stage may proceed by transportation of a hydrophilic bromocation generated on the anode into the natural rubber particle with carrier component, on the basis of a bromination of low-molecular-weight aliphatic alkenes through anodic oxidation. In this regard, carbon dioxide may be one of the most effective carrier component, since it is attracted with natural rubber and water as an inert molecule.

In this study, bromination of natural rubber through anodic oxidation in latex stage was investigated in the presence of carbon dioxide. The resulting products were characterized by ^{1}H-NMR spectroscopy. After the anodic oxidation, new signals appeared at 1.9 and 4.2 ppm in ^{1}H-NMR spectrum, indicating electrophilic attack of bromocation to carbon-carbon double bond of *cis*-1,4-isoprene unit. The bromination of natural rubber in the presence of carbon dioxide occurred at an olefinic position, while that in the absence of carbon dioxide did not at all. The conversion and bromination efficiency of the anodic oxidation depended on supplied electricity and dry rubber content. These results indicate that the reaction between natural rubber and bromocation, generated by anodic oxidation of sodium bromide in latex stage, is promoted with carbon dioxide.

TJ-O-04

Development of Nano-chitosan for Biomedical Applications via Water-based Reaction System

Suwabun Chirachanchai[a, b, c*], Sutima Chatrabhuti[a], Patomporn Chantarasataporn[a], Jatesuda Jirawutthiwongchai[a], Chutamart Pitakchatwong[a], Visuta Engkakul[a]

[a]*The Petroleum and Petrochemical College, Chulalongkorn University, Bangkok 10330, Thailand.*

[b]*Center of Innovation Nanomaterial, Chulalongkorn University, Bangkok 10300, Thailand*

[c]*Center for Petroleum, Petrochemicals and Advanced Materials, Chulalongkorn University, Bangkok 10330, Thailand.*

* csuwabun@chula.ac.th

Keywords: chitin-chitosan, water-based system, nanoparticle, chitosan whisker

Chitin-chitosan is the second most natural abundant polysaccharide with attractive properties in terms of biocompatibility, biodegradability, and non-toxicity. Regarding to the chemical structure, chitosan is also unique as it has two different reactive functional groups, i.e. hydroxyl and amino groups to expect for various derivatizations. However, the chemical reaction of chitosan is rather difficult due to the strong inter- and intra-molecular hydrogen bond networks until it is soluble only in acid solvents. This obstructs not only the chemical modification but also the general fabrication of chitosan to materials, especially when we consider the acid free condition. On this viewpoint, our group focuses on the reaction of chitosan in water and develops the water-based chitosan chemistry. The presentation will review a series of our chitosan nanoparticles obtained from the water-based reaction conditions. The ring opening reaction of caprolactone by using chitosan whisker leads us to the wide range of morphologies, from nanoparticles to rod-like and to gel. Water soluble chitosan-hydroxybenzotriazole (chitosan-HOBt)[1] provides the successful conjugation with phenylalanine and polyethylene glycol to result in the nanoparticles which enable us to extend the study on allergen delivery system. In similar concept, water-soluble chitosan-*N*-hydroxysuccinimide (chitosan-NHS) can be decorated with poly(N-isopropyl acrylamide) and the material obtained shows thermoresponsive properties to capture-release nanopaticles, especially magnetic nanoparticles. The chitosan-HOBt also enables the conjugation on magnetic nanoparticles by coupling with epoxysilane resulting in pH responsive magnetic nanoparticles[2]. Chitosan-polyethylene glycol obtained from conjugating reaction in water effectively performs copper-free Click chemistry by the use of oxanorbornadiene[3] to obtain chitosan-gold nanoparticles which shows the potential application as the novel type of rapid antigen detection kit[4]. Lactic acid favors the solubility of chitosan whisker in water and allows polycondensation on chitosan to be chitosan-PLA in the form of nanoparticles.

[1] Macromolecular Rapid Communications (2006), 27, 1039−1046.
[2] Carbohydrate Polymers (2013), 97, 441-450.
[3] ACS Macro Letters, (2013), 2, 177−180.
[4] Macromolecular Rapid Communications (2014), 35, 1204-10.

TJ-O-05

Controlled Polymerization of Terpene as Renewable Vinyl Monomer for Novel Bio-based Polymers

Kotaro Satoh[a,b,*] **and Masami Kamigaito**[a]
[a]*Department of Applied Chemistry, Graduate School of Engineering, Nagoya University, 464-8603 Nagoya, Japan*
[b]*Precursory Research for Embryonic Science and Technology (PRESTO), Japan Science and Technology Agency, Japan*
*satoh@apchem.nagoya-u.ac.jp

Keywords: Terpene/Bio-Based Polymer/Precision Polymerization/Cycloolefin

Bio-based polymer materials from renewable resources have recently been attracting much attention from the viewpoint of environmentally benign and sustainable chemistry. In this study, we examined controlled/living radical and cationic polymerization and copolymerization of a series of naturally-occurring terpenes, such as beta-pinene and limonene, as alternatives for those from traditional petrochemical products. Beta-pinene was cationically polymerized as alicyclic hydrocarbon monomers in a controlled fashion to result in a promising novel bio-based cycloolefin polymer. The radical copolymerization of limonene with maleimide derivatives underwent unprecedented 1:2 alternating fashion. Furthermore, the combination with a reversible addition-fragmentation chain transfer (RAFT) agent via the controlled/living radical polymerization resulted in end-to-end sequence-regulated copolymers with both highly-sequenced chain ends and main-chain repeating units as well as controlled molecular weights.

TJ-O-06

Synthesis of Cyclic Polyesters: The Catalyst Design

Khamphee Phomphrai*

Center for Catalysis, Department of Chemistry and Center of Excellence for Innovation in Chemistry, Faculty of Science, Mahidol University, Rama 6 Road, Bangkok, 10400, Thailand

* khamphee.pho@mahidol.ac.th

Keywords: Polylactide, Biodegradable polymers, Catalysis, Cyclic polyesters.

Recently, polymers derived from cyclic esters such as lactide, glycolide, and ε-caprolactone are of interest and widely used in pharmaceutical industries due to their biocompatibility and biodegradability. These polymers are synthesized from the ring-opening polymerization (ROP) of cyclic esters using ligated metal complexes as catalysts. Most polymers are linear in nature. Only recently cyclic structures are gaining more interest due to their potentials in drug delivery over the linear counterpart. In this work, novel tin(II) complexes derived from Schiff's base ligands were successfully synthesized and structurally characterized. They were active for the melt polymerization of lactide and ε-caprolactone at 110 °C. The resulting polymers were shown to have cyclic and/or linear structures depending on the ligand structures and the polymerization conditions. Results have shown that long reaction time promoted the formation of cyclic polymer for ε-caprolactone but not with lactide.

TJ-O-07

Synthesis and Properties of Aliphatic Polycarbonates from Epoxides and CO_2

Koji Nakano *
Tokyo University of Agriculture and Technology, Koganei, Tokyo 184-8588, Japan
*k_nakano@cc.tuat.ac.jp

Keywords: Carbon dioxide, Epoxide, Copolymerization, Polycarbonate

The alternating copolymerization of epoxides with carbon dioxide (CO_2) is one of the most promising processes for CO_2 utilization.[1] Since the first report by Inoue and co-workers with Et_2Zn/H_2O as a catalyst in the late 1960s,[2] numerous efforts have been devoted to develop high performance metal catalysts. We have also developed a variety of novel catalyst systems. For example, the cobalt-salen complex with tertiary ammonium groups can suppress the formation of cyclic carbonate (by-product), which is an incident problem for the copolymerization, to give the desired alternating copolymer selectively.[3] The cobalt complex copolymerizes propylene oxide (PO) in regio- and enantiomer-selective manners, giving poly(propylene carbonate) (PPC) with a stereogradient structure. The obtained stereogradient PPC demonstrates higher thermal degradation temperature because of its unique stereo-sequence. The first active catalysts based on metal(IV) species were also developed.[4] In particular, iron(IV)-corrole complexes were found to copolymerize PO with CO_2, which was first successful PO/CO_2 copolymerization by using iron complexes. Control of properties of epoxide/CO_2 copolymers and their applications as functional materials will be discussed.

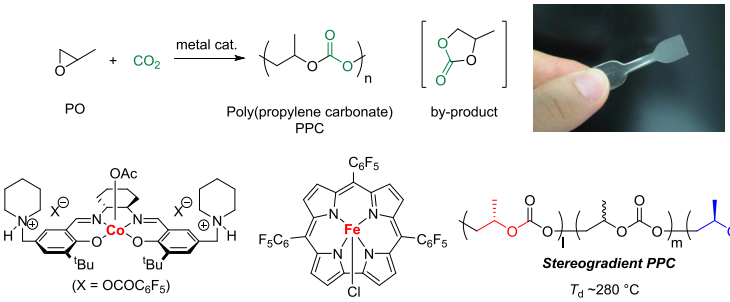

References: (1) (a) Nakano, K.; Kosaka, N.; Hiyama, T.; Nozaki, K. *Dalton Trans.* **2003**, 4039. (b) Coates, G. W.; Moore, D. R. *Angew. Chem. Int. Ed.* **2004**, *43*, 6618. (c) Darensbourg, D. J. *Chem. Rev.* **2007**, 107, 2388. (2) Inoue, S.; Koinuma, H.; Tsuruta, T. *J. Polym. Sci., Part B: Polym. Lett.* **1969**, *7*, 287. (3) Nakano, K.; Hashimoto, S.; Nakamura, M.; Kamada, T.; Nozaki, K. *Angew. Chem. Int. Ed.* **2011**, *50*, 4868. (4) (a) Nakano, K.; Kobayashi, K.; Nozaki, K. *J. Am. Chem. Soc.* **2011**, *133*, 10720. (b) Nakano, K.; Kobayashi, T.; Ohkawara, H.; Imoto, H.; Nozaki, K. *J. Am. Chem. Soc.* **2013**, *135*, 8456.

TJ-O-08

Polymer Nanostructures observed by Electron Microscopy

Hiroshi Jinnai[a,*]

[a]*Institute of Materials Chmistry and Engineering (IMCE), Kyushu University, 744 Motooka, Nishi-ku, Fukuoka, 819-0935, Japan*

* hjinnai@cstf.kyushu-u.ac.jp

Keywords: Fuel cells, rubber nano-composite, electron tomography

The three-dimensional (3D) morphology of particulate fillers embedded in a rubbery matrix (hereafter called a rubber nano-composite) and fuel cell electrodes were examined by transmission electron microtomography (electron tomography for short, ET).

In the rubber nano-composite, two types of nano-fillers, i.e., carbon black (CB) and silica (Si) nano-particles, were used as the nano-fillers. Although the CB and Si nano-particles were difficult to distinguish by conventional transmission electron microscopy (TEM), they appeared different by ET; the CB and Si nano-particles appeared to be hollow and solid particles in the cross-sectional images of the TEMT 3D reconstruction, respectively, demonstrating that ET itself provided a unique particle-discriminative function. The nano-particles were found to form aggregates in the matrix. It is intriguing that each aggregate was made of only one species; not a single aggregate contained both the CB and Si nano-particles [1]. A 3D image of the rubber nano-composite can be used together with a computer simulation method, the finite element analysis, to estimate the mechanical property of the material [2].

In the fuel cell electrodes, ET was used to locate Pt catalytic particles with respect to the carbon substrate, i.e., whether the particles are inside or on the surface of the substrate. A considerable amount of Pt particles were found to be inside the substrate [3]. Structural changes of the fuel cell electrodes in the course of the durability test have been examined by ET, from which the external Pt particles tend to aggregate more extensively than the internal ones. Performance loss of the fuel cells will be discussed from the morphological viewpoints.

References

[1] H. Jinnai *et al.*, *Macromolecules*, **40**, 6758-6764 (2007).
[2] K. Akutagawa *et al.*, *Rubber Chem. Tech.*, **81**, 182-189 (2008).
[3] T. Ito *et al.*, *Electrochemistry*, **79**, 374-376 (2010).

TJ-O-09

Starch-based Rheology Modifiers in Structuring Health Foods

Asira Fuongfuchat[a,*], Thidarat Makmoon[a], Nispa Seetapan[a], Pawadee Methacanon[a] and Chaiwut Gamonpilas[a]

[a] *National Metal and Materials Technology Center (MTEC),National Science and Technology Development Agency (NSTDA), Pathumthani, 12120 Thailand*

* asira.fuongfuchat@nstda.or.th

Keywords: Crosslinked Tapioca Starch, Rheology Modifier, Food Structuring

Many types of foods, semi-solid food in particular, are in the form of dispersions. Rheology modifiers used in these foods should thus provide dispersion characteristics in order to retain the original texture. Gelatinized starch in dispersion form, i.e. dispersion of swollen starch granules in low-viscous aqueous solution, is a promising one. The gelatinized starch dispersions at different volume fraction regimes exhibited rheological behavior ranging from viscous liquid to soft gel. Rheological behavior, including viscoelasticity, of starch dispersions is strongly dependent on volume fraction and state of the granules, similarly to that of other non-colloidal systems. The rheological parameters, e.g. viscosity, yield stress and storage modulus, of the starch dispersions are essentially correlated to volume fraction following classic phenomenological models (Krieger & Dougherty, Quemada, and Maron-Pierce-Kitano). Especially in the case of crosslinked tapioca starch, its intact granules with a limited swelling power yielded the rheological parameters that closely followed those models. Structure-related "large amplitude oscillatory shear (LAOS)" behavior of the gelatinized starch dispersions showed "local" shear softening. Mixture of the starch and certain types of polysaccharides, on the other hand, exhibited synergistic effect in rheological properties and "local" shear stiffening in LAOS. From microscopic observations, micro-scale spatial arrangement in gelatinized starch dispersions and their mixtures with different polysaccharides was in good agreement with the observed rheological properties. Consequently, the structure – rheology relationship of these particular systems would play a crucial role in "creating" and "engineering" food texture based on the "food materials science" approach. Potential applications of gelatinized starch dispersions and their polysaccharide mixtures in structuring health foods were subsequently evaluated.

TJ-O-10

Effect of Mechanical Instability at Polymer Surface on Cell Adhesion

Keiji Tanaka*, Shinichiro Shimomura and Hisao Matsuno
Kyushu University, Fukuoka 819-0373, Japan
* k-tanaka@cstf.kyushu-u.ac.jp

Keywords: Surface, Segmental dynamics, Cell adhesion.

The adhesion of fibroblast on polymer bilayers composed of a glassy polystyrene (PS) prepared on top of a rubbery polyisoprene (PI) was studied. Since the top PS layer is not build on a glassy, or firm, foundation, the system becomes mechanically unstable with decreasing thickness of the PS layer. When the PS film was thinner than 25 nm, the number of cells adhered to the surface decreased and the cells could not spread well. On a parallel experiment, the same cell adhesion behavior was observed on plasma-treated PS/PI bilayer films, where in this case, the surface was more hydrophilic than that of the intact films. In addition, the fluorescence microscopic observations revealed that the formation of F-actin filaments in fibroblasts attached to the thicker PS/PI bilayer films was greater than those using the thinner PS/PI bilayer films. On the other hand, the thickness dependence of the cell adhesion behavior was not observed for the PS monolayer films. Taking into account that the amount of adsorbed protein molecules evaluated by a quartz crystal microbalance method was independent of the PS layer thickness of the bilayer films, our results indicate that cells, unlike protein molecules, could sense a mechanical instability of the scaffold.

TJ-O-11

Polymers for New Generation Solar Cells

J. Wootthikanokkhan*, N. Seeponkai, P. Khunsriya and O. Pongchumpon
Nanotec-KMUTT Center of Excellence on Hybrid Nanomaterials for Alternative Energy.
King Mongkut's University of Technology Thonburi, Bangkok, 10140, Thailand
*Jatuphorn.woo@kmutt.ac.th

Keywords: Organic photovoltaic, dye sensitized solar cells, Fullerene, Electrolyte.

There has been a considerable interest in the developments of some alternative solar cells such as organic photovoltaic (OPV), dye sensitized solar cells (DSSC), perovski cells, and the quantum dot cells during the past several years. These types of solar cells are sometime known as emerging photovoltaic cells. Some advantages of these new generation solar cells include their flexibility, lower cost for the fabrication process, and a possibility to enlarge the production scale by using the existing roll-to-roll printing technology. On the other hand, material cost, durability, and performance of the solar cells have yet to be further improved before their commercial uses can be realized. In this talk, fundamental concepts of the organic solar cell and the dye sensitized solar cells were introduced. Roles of polymeric materials in these devices were also pointed out. Then, two case studies concerning the development of polymers for new generation solar cells were presented in more details. The first one is a development of fullerene functionalized polymers for use as an electron acceptor for OPV. This work was based on the assumption that by dispersing the fullerene groups along the polymer chains, an aggregation of the material can be suppressed and a better photovoltaic performance of the OPV can be expected. The fullerene functionlized polymer was prepared by carrying out chemical modifications of poly(vinyl chloride) via dehydrochlorination and atom transfer radical addition mechanism. Chemical structures, thermal behaviors, and electrical properties of the polymers were characterized and tested. The second case is a development of gel electrolyte based on PVDF nanofiber composite for DSSC. In this work, attempts were made to enhance the duablity of the cell containing polymeric gel electrolyte by preparing the polymer in a form of nanofiber via an electrospinning process. It was assumed that by increasing porosity of the material, electrolyte uptake, power conversion efficiency and durability of the cell can be compromised. Photovoltaic performance of these solar cells containing the modified polymer was determined and compared with those of the conventional cells using standard materials. The results were discussed in light of structure-properties relationships of the developed materials.

TJ-O-12

Biobased Furan Polymers with Self-healing Ability and Shape Memory

Naoko Yoshie
Institute of Industrial Science, The University of Tokyo
Komaba, Meguro-ku, Tokyo 153-8505, Japan
yoshie@iis.u-tokyo.ac.jp

Keywords: Provide a maximum of four keywords.

Based on growing demand for environmentally friendly materials, a number of novel platform chemicals and polymer materials are derived from biomass. Among them, 5-hydroxymethylfurfural (HMF) is promising owing to its rich chemistry and potential availability from carbohydrates. HMF is converted easily into various compounds including monomers for valuable polymer designs.

In this study, bio-based polyester, PFS, were prepared by a condensation of bis(hydroxymethyl)furan (BHF), a reduction product of HMF, and succinic acid (SA), which is also available from biomass by microbial fermentation. This polyester has furan rings in the main chain, allowing the formation of reversible cross-links by means of DA reactions with bis-maleimides (M_2) such as 1,8-bis(maleimido)triethylene glycol. Through the control of the amount of M_2, the networked furan polymers, PFS/M, with a wide variety of properties were obtained. They include relatively hard materials with a yield point and flexible elastic ones. Introduction of 1,4-butanediol into PFS as a comonomer further widen the variation of the properties. Among the networked furan polymers, the elastic ones had good self-healing ability: when it broke, their surfaces could be rejoined without any external stimulus at room temperature. For PFS/M with furan-to-maleimide ratio of 6/1 recovered as much as 74% of the toughness of the original sample by self-healing. Healing was more effective when the broken surfaces were activated by a solvent (chloroform) or by an M_2 solution. Further, the network polymers show unique multi-shape memory controlled by local glass transition temperature. Local glass transition temperatures of a PFS/M film were changed by immersing sections of the film in M_2 solutions with different concentrations. Each section memorizes a temporary shape, which recovers its permanent shape at a different recovery temperature depending on the local glass transition temperature.

Acknowledgement: This work was supported in part by a Grant-in-Aid for Scientific Research (no. 25288080) from Japan Society for the Promotion of Science.

TJ-O-13

Biodegradable Nanocomposite Blown Films Based on Poly(lactic acid) Containing Silver-Loaded Kaolinite

Winita Punyodom[a,*], Sutinee Girdthep[a], Patnarin Worajittiphon[a], Robert Molloy[a,b], Saisamorn Lumyong[c] and Thanawadee Leejarkpai[d]

[a] *Polymer Research Laboratory, Department of Chemistry, Faculty of Science, Chiang Mai University, Chiang Mai, 50200, Thailand*

[b] *Materials Science Research Center, Faculty of Science, Chiang Mai University, Chiang Mai, 50200, Thailand*

[c] *Department of Biology, Faculty of Science, Chiang Mai University, Chiang Mai, 50200, Thailand*

[d] *National Metal and Materials Technology Center, National Science and Technology Development Agency, Pathum Thani, 12120, Thailand*

* winitacmu@gmail.com

Keywords: Polymer-clay nanocomposite, Barrier properties, Shelf life prediction, dried longan

Novel biodegradable polymer nanocomposites blown films have been developed in this study as materials for use as a model package for dried longan. Poly(lactic acid) (PLA) was the main component of the nanocomposites with poly(butylene adipate-co-terephthalate) (PBAT) as flexibility enhancer. Tetrabutyl titanate (TBT) was also added as a compatibilizer to enhance the interfacial affinity between PLA and PBAT by inducing the formation of some PLA/PBAT via transesterification during the melt blending process, thereby improving the mechanical properties of the blends. Silver-loaded kaolinite (AgKT) synthesized via chemical reduction was also incorporated into the compatibilized blends for property improvement. Additionally, controlled silver release which provides long-term antibacterial activity is attributed to AgKT's layered structure. The amount of released silver ions herein also complies with migration levels specified by the standard for food-contact plastic packages. Dried longan shelf lives as eventually predicted by experimental moisture sorption isotherm and by Peleg model are almost identical (~308 days) for the nanocomposite films being over two folds of that obtained from the compatibilized blend package at ambient condition. On the basis of these properties, the developed nanocomposites are considered to be promising candidates for use in bio-packaging applications to replace non-biodegradable and petro-based plastics.

TJ-O-14

Enzymatic Synthesis and Functionalization of Multiphase Cellulose Materials

Takeshi Serizawa
Department of Organic and Polymeric Materials, Tokyo Institute of Technology, 2-12-1 Ookayama, Meguro-ku, Tokyo 152-8550, Japan
serizawa@polymer.titech.ac.jp

Keywords: Cellulose, Enzyme, Nanosheet, Hydrogel

Cellulose composed of ß-1,4-linked anhydro-D-glucose repeating units is the most abundant biopolymer in the biosphere, and has drawn considerable attention as a sustainable raw material used for industrial products. In nature, crystalline fibrils are formed during biosynthesis, and are hierarchically assembled into larger fibers with other biopolymers such as lignin, heteropolysaccharides, and proteins. In the fibrils, cellulose chains adopt parallel configurations, which are stabilized by intra- and inter-molecular hydrogen-bonding networks.
In order to obtain pure and well-defined cellulose, its chemical synthesis has been investigated so far. Ring-opening polymerization of adequate monomers is one of the potential synthetic methods; however, it is normally difficult to precisely control polymerization degree, morphologies, and crystal structures. On the other hand, in vitro synthesis of cellulose using enzymes such as cellulase has also been investigated so far. Enzymatic reactions are attractive because they are preceded in aqueous phase under mild conditions.

Previously, crystalline cellulose nanosheets have been synthesized by reverse reactions of cellodextrin phosphorylase (CDP), in which α-glucose-1-phosphate and D-glucose are used as monomer and primer, respectively.[1,2] We hypothesized that other primers such as D-glucose derivatives were applicable to the enzymatic synthesis of cellulose, when the specificity of CDP for primer structures was not so high. In this study, multiphase cellulose materials with nanosheet, hydrogel, and mosaic structures were synthesized by using different primers for the enzymatic synthesis, and were functionalized by introduction of functional molecules.

References

1. E. Samein *et al.*, *Carbohydr. Res.* **1995**, *271*, 217.
2. M. Hiraishi *et al.*, *Carbohydr. Res.* **2009**, *344*, 2468.

TJ-O-15

Waste to Value - Production of Pectin from Pomelo Peel

Pawadee Methacanon[a,*], Chaiwut Gamonpilas[a], Jaruwan Krongsin[a], Ratana Teeklee[a] and Suk Meng Goh[b]
[a]*National Metal and Materials Technology Center, NSTDA, 114 Paholyothin Rd., Klong 1, Klong Luang, Pathum Thani 12120 Thailand*
[b]*Singapore Institute of Technology, 10 Dover Drive, 138683, Singapore*
* pawadeem@mtec.or.th

Keywords: pomelo pectin, extraction, properties, food applications

In modern lifestyle, consumers demand and enjoy foods that are healthy, delicious, convenient, and affordable. Natural food additives such as pectin and advances in technological have made it possible to achieve this. Pectin is a complex polysaccharide, which consists mainly of methylated ester of poly 1,4-linked α-D-galacturonic acid. It is used extensively in many food industries as a thickener, a gelling agent, or a stabiliser. Although pectin exists in many higher plant cell walls, commercial pectins are extracted from only a few sources, namely, citrus peel and apple pomace. In this work, an alternative source of pectin extraction was explored. Polemo (*Citrus maxima Merr.*), which is another kind of citrus fruits largely cultivated in Thailand, has been sought as an alternative source of pectin extraction due to the large amount of its peel disposal as waste. The extraction was performed using nitric acid at pH 2 and at 90°C for 90 min. Such condition resulted in pectin yield of approximately 23.2±2.8% which was comparable with commercial pectins. Moreover, the average molecular weight (MW) and degree of esterification (DE) were found to be 353±78 kDa and 57.9±0.6%, respectively. With DE > 50%, the extracted pectin was therefore classified as high methoxy pectin. Furthermore, the molecular structure of pectin was examined using a high-performance anion-exchange chromatography. The results showed that the extracted pectin was largely composed of galacturonic acid with branching chains that was predominantly arabinose. More interestingly, this finding contradicts with those of commercial pectins which branches are dominated by galactose. Rheological properties of pomelo pectin dispersions were also examined. It was found that they formed gel at the concentration above 0.8% w/v and exhibited shear thinning behaviour. Furthermore, they possessed calcium sensitiveness which enhanced their rheological properties when small amount of Ca^{2+} was added. Since the pectin is high methoxy, the acid-induced gelation property was also investigated. It was shown that, for the same concentration, the gel strength and elasticity of pomelo pectin gel samples were much superior to those prepared from a commercial pectin with similar MW and DE. To further explore the application of pomelo pectin, acidified soy milk samples with and without calcium fortification were prepared for stability study. It was noticeable that samples without pectin addition showed protein aggregation after acidification to pH 3.8 while samples with added pomelo pectin still showed good stability without phase separation throughout 15 days storage at 4°C. Additionally, to better understand the complex structure formed between soy proteins and pectin under acidified and calcium fortified conditions, confocal laser scanning microscopy analysis was performed. The result revealed the differences in microstructure of soy proteins, which was dependent on pectin and calcium concentrations. Apart from pectin, the residue obtained after pectin recovery was also processed and used as a fat replacer in low-fat foods. Overall, it could be concluded that pomelo peels are a promising source of pectin extraction. The pilot-scale extraction is also being presently investigated.

Thai Parkerizing Co., Ltd.

Leading in Surface Treatment Field

Products & Services:

Surface Treatment Chemicals

- Paint base coating
- Degreasing & Washing
- Al coating
- Wear resistant
- Coat for cold Forming

Rust Preventive products

- Oil & Wax
- Rust preventive film

Heat & Surface Treatment Processing

- Tufftride Treatment
- Phosphate Treatment
- Gas Heat Treatment
- Pallube Treatment

Address : 570 Moo 4 Bangpoo Industrial Estate Soi 12 Sukhumvit Rd. Prakasa, Muang, Samutprakarn 10280 Tel:0-2324-6600 Fax: 0-2324-6637

Website : www.thaiparker.com

HEAT TREATMENT
SERVICE COMPANY

THAI TOHKEN THERMO CO.,LTD .

"Let's Contribute to the Society through our Heat Treatment Expertise"

Austempering	Gas Carburizing
Quenching Tempering	Vacuum Quenching
Normalizing	Vacuum Tempering
Annealing	Vacuum Carburizing
Isothermal Annealing	PVD (CrN, TiN) Coating
Gas Sulphur Nitriding	DLC Coating
Gas Nitrocarburizing	Induction Annealing
Gas Cabonitriding	Induction Quenching Etc.

Amata Nakorn Industrial Estate 700/314 Moo 6, Bangna -Trad Road Km.57
Tambon Don Hua Roh, Amphur Muang , Chonburi 20000, Thailand.
Tel: 038-214-417 ~ 20 Fax: 038-214-421 E-mail: salesservice@thaitohken.co.th

posco THAINOX

โพสโค-ไทยน๊อคซ์ แบรนด์เนมแห่งสเตนเลสคุณภาพชั้นเยี่ยม

คุณภาพ-เทคโนโลยี-บริการ-และคุณค่า
คือความแตกต่างของโพสโค-ไทยน๊อคซ์จากสเตนเลสนำเข้าอื่นๆในประเทศ

เทคโนโลยี
สเตนเลสโพสโค-ไทยน๊อคผลิตจาก กระบวนการผลิตระดับโลก สอดคล้องทั้งมาตรฐาน เอเชีย (JIS) อเมริกา (ASTM) และยุโรป (EN)

คุณภาพ
การรับรอง มอก.เหล็กกล้าไร้สนิม แห่งเดียวในประเทศไทย และคุณภาพ ครบวงจรจากนานาชาติ สเตนเลส โพสโค-ไทยน๊อคซ์จึงได้การตอบรับ สูงสุดทั้งในประเทศและตลาดโลก

คุณค่า
บูรณาการคุณค่าเพื่อสเตนเลสในการ ใช้งานระดับครัวเรือนและภาคอุตสาหกรรม ของประเทศ ช่วยให้ลูกค้าและผู้ใช้งานใน อุตสาหกรรมสามารถบริหาร สต๊อค การขาย และการผลิต ได้อย่างมีประสิทธิภาพ

บริการ
บริการเทคนิคและการเผยแพร่ องค์ความรู้เกี่ยวกับสเตนเลสก่อน และหลังการขาย ทำให้แบรนด์เนม 'โพสโค-ไทยน๊อคซ์' ได้รับความ วางใจตลอดกว่า 20 ปี ในประเทศไทย

มอก. 1378-2539 | ISO / IEC 17025 : 2005 | PED | RoHS | REACH | ISO 9001 ISO 14001 OHSAS 18001 BUREAU VERITAS Certification

มาตรฐานผลิตภัณฑ์อุตสาหกรรม มอก.1378-2539
มาตรฐานความปลอดภัยด้านการจำกัดสารพิษปนเปื้อน

มาตรฐานการทดสอบในห้องปฏิบัติการ ISO/IEC 17025:2005
มาตรฐานความปลอดภัยด้านการใช้สารเคมีในการผลิต

มาตรฐานระบบจัดการอุตสาหกรรม ISO 9001:2008, ISO 14001:2004, OHSAS 18001:2007
มาตรฐานความปลอดภัยเกี่ยวกับแรงดัน PED 97/23 EC

บริษัท โพสโค-ไทยน๊อคซ์ จำกัด (มหาชน)

สำนักงานกรุงเทพฯ :
ชั้น 31 ยูนิต 3101-3 อาคารซีอาร์ซีทาวเวอร์ 87/2 ออลซีซั่นส์เพลส ถนนวิทยุ แขวงลุมพินี เขตปทุมวัน กรุงเทพฯ 10330
โทรศัพท์ : +66 (0) 2250 7622-32
โทรสาร : +66 (0) 2250 7633
ติดต่อ :
sales@poscothainox.com ; ต่อ 314
export@poscothainox.com ; ต่อ 306
technical@poscothainox.com ; ต่อ 310

โรงงานระยอง :
324 หมู่ 8 ถนนทางหลวงหมายเลข 3191 ตำบลมาบข่า อำเภอนิคมพัฒนา จังหวัดระยอง 21180
โทรศัพท์ : +66 (0) 38 636 125-32
โทรสาร : +66 (0) 38 636 099
ติดต่อ :
technical@poscothainox.com ; ต่อ 473

ศูนย์บริการโพส-ทีเอสพีซี :
700/453 นิคมอุตสาหกรรมอมตะนคร หมู่ 7 ตำบลดอนหัวฬ่อ อำเภอเมือง จังหวัดชลบุรี 20000
โทรศัพท์ : +66 (0) 38 454 141-3
โทรสาร : +66 (0) 38 454 179
ติดต่อ :
sales-tspc@poscothainox.com
qc-tspc@poscothainox.com

ผู้ผลิตสเตนเลสรีดเย็นคุณภาพชั้นเยี่ยมแห่งเดียวในประเทศไทย... และหนึ่งในเครือข่ายโกลบอลโพสโค ผู้นำอุตสาหกรรมเหล็กของโลก www.poscothainox.com

Every step

for a sustainable energy future

No matter how far the journey or how treacherous the path, PTTEP is ready to take the next step forward with an unwavering commitment to provide a secure source of energy for the future while ensuring the well-being of our communities and preserving the environment.

www.pttep.com

PTTEP

Integrating All the Great Businesses

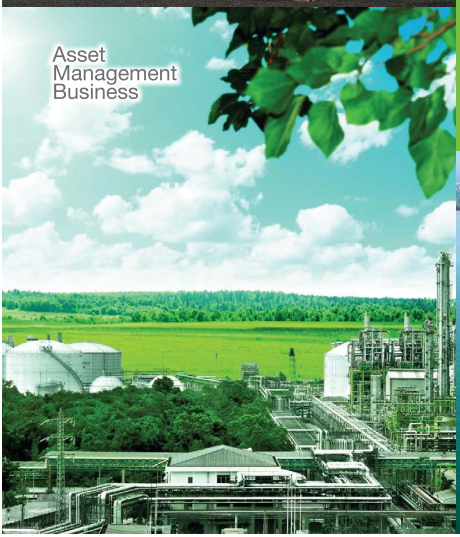

Petroleum Business
The third biggest oil refinery in Thailand with a refining capacity of 215,000 barrels per day

Petrochemical Business
The leader in petrochemical and plastic industries which cover all product categories and innovations which are friendly to the environment and the communities to answer all lifestyles in the future without limits

Port Business
Deep-Sea Port in Rayong province, equipped with complete online technology and a complete range of facilities for goods transfers

Asset Management Business
The sustainable land development project to develop the green industrial estate in Rayong province to be a prosperous green industrial estate

www.irpc.co.th

IRPC

SSI

ASEAN's largest fully-integrated flat steel producer

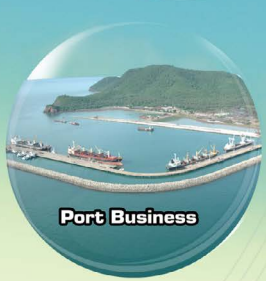

SSI

innovate · strength

Sahaviriya Steel Industries Public Company Limited (SSI)

"Innovate premium value steel products and services for customers; generate consistent profit and sustainable value for stakeholders."

www.ssi-steel.com

Gold Sponsors

THAI PARKERIZING CO., LTD.

THAI TOHKEN THERMO

posco THAINOX

Silver Sponsors

PTTEP

IRPC Public Company Limited

100 YEARS SCG

SSI

Bronze Sponsors

SYS SIAM YAMATO STEEL

EDAX AMETEK MATERIALS ANALYSIS DIVISION

COAX

WD Western Digital

Supporters

TCEB THAILAND CONVENTION & EXHIBITION BUREAU

BETAGRO

National Metal and Materials Technology Center (MTEC)
114 Thailand Science Park, Phahonyothin Road,
Khlong Nueng, Khlong Luang, Pathum Thani 12120, Thailand
Tel: 66 2564 6500 Fax: 66 2564 6501-5